University of Sussex

Quantum Chaos and the Emergence of Statistical Physics

Charlie Nation

Submitted for the degree of Doctor of Philosophy

University of Sussex

March 2020

For Judith

Declaration

I hereby declare that this thesis has not been and will not be submitted in whole or in part to another University for the award of any other degree.

This thesis is based on the publications

- *Off-diagonal observable elements from random matrix theory: distributions, fluctuations, and eigenstate thermalization*, C. Nation, D. Porras, New Journal of Physics, 20 (10), 103003 (2018). I contributed both mathematical and numerical aspects of this paper, and wrote the manuscript, under supervision of D. Porras.

- *Quantum chaotic fluctuation-dissipation theorem: Effective Brownian motion in closed quantum systems* C. Nation, D. Porras, Physical Review E, 99 (5), 052139 (2019). I contributed both mathematical and numerical aspects of this paper, and wrote the manuscript, under supervision of D. Porras.

- *Ergodicity probes: using time-fluctuations to measure the Hilbert space dimension*, C. Nation, D. Porras, Quantum 3, 207, (2019). I contributed both mathematical and numerical aspects of this paper, and wrote the manuscript, under supervision of D. Porras.

In each of these publications D. Porras contributed significant edits to the final form of the manuscript. This thesis further includes sections adapted from,

- *Taking snapshots of a quantum thermalization process: emergent classicality in quantum jump trajectories* C. Nation, D. Porras, Arχiv:2003.08425

Signature:

Charlie Nation

UNIVERSITY OF SUSSEX

Charlie Nation, Doctor of Philosophy

Quantum Chaos and the Emergence of Statistical Physics

Summary

The question of how statistical physics can be seen to emerge from unitary quantum dynamics goes back to Schrödinger and von Neumann, however has been reaffirmed as a topic of importance due to recent advances in experimental capabilities, allowing the observation of the unitary evolution of many-particle systems over long periods of time. Understanding why such a system evolves to the specific thermal equilibrium state, *effectively* described by a relevant thermodynamic ensemble, has thus seen significantly more interest in recent years. Furthermore, observations of the dynamics of such systems open questions on the route to equilibrium, and subsequent fluctuations. In this thesis I will develop an approach to this problem, taking as a starting point the non-integrability of the system under study, which leads to a generic model in terms of random matrix theory (RMT), and more generally, chaotic wavefunctions.

In the formulation of these methods, special attention is paid to the form of local observables of quantum systems, and an approach to their description is developed in terms of correlation functions of chaotic wavefunctions. From this approach a key conjecture in the understanding of thermalization, the eigenstate thermalization hypothesis (ETH), is derived in full, and the dynamical behaviour of such observables is obtained analytically. Further, I will show that emergent classical behaviour can be observed in the form of a fluctuation-dissipation theorem (FDT) of Brownian processes. This is exploited to develop an experimental proposal to measure the 'complexity' of a quantum device, by experimentally obtaining its effective Hilbert space dimension in terms of a fully connected system. Finally, quantum jump trajectories, describing stroboscopic projective measurements of local observables are studied, and shown to display classical Brownian dynamics in the form of a Markov process. Throughout this thesis, exact diagonalization calculations of realistic quantum spin systems are used to confirm analytical results.

Acknowledgements

Firstly, and most importantly, I am delighted to thank Diego Porras for giving me the opportunity to undertake this PhD, and for supervising me during my time at Sussex. He has been a patient and kind teacher, taking time and effort to help me not only with physics, but with career guidance and support. He has consistently astounded me with his vision for interesting and novel physics, and his knowledge of many pertinent fields. I sincerely could not have hoped for a better supervisor and mentor during these years.

I would additionally like to thank Juan Garrahan and Jacob Dunningham for taking the time to examine this work, and for a deeply enjoyable conversation in my viva.

Sussex is a wonderful, vibrant university, and I have deeply enjoyed my time here. I would like to thank those who have helped make my PhD such an amazing experience - Michail, Jesús, Pedro, Sam, Alex, and Mitch. I have also been lucky enough to spend a lot of time during my PhD in Madrid, and would like to thank those at CSIC who have been so welcoming, made my stays in Madrid entertaining, and shown me around a beautiful new city. Further, I would like to thank Luis Pedro Garcia-Pintos, and Alvaro Alhambra for some useful and inspiring discussions.

I must also thank my family, to whom I owe so much. Mum, John, Nan, Lucy, Juice, and little Kenzie; as well as Dad, Abi, and Jack. You have all been so supportive and understanding, and I will always be grateful.

Brighton will always be a special place to me. It has a wonderful charm, and an inspiring culture of inclusion and kindness. A warm thanks goes to those who made my time here so memorable: Guillaume, Abdul, Gizem, Connor, Jacob, Sana, and Marco.

I am lucky enough to have a list of people too long to reasonably mention who mean the world to me, particularly those from back home in Cornwall, Exeter, and London; I can only thank you all for being there, and hope you forgive my neglect over the years it took me to write this. Individual thanks are owed to Lachlan, who kindly took the time to proofread this thesis, and whose encouragement and friendship have been invaluable to me, to Tegen, who despite my distance has always been there when I have needed her support.

Jesús Rubio Jiménez, Mitch Peaks, and Abdul Afzal were kind enough to proofread parts of this thesis, and I am very grateful for their time and effort.

Finally, I would like to thank Judith, to whom this thesis is dedicated. Her tireless love and support through these years have been so important to me. She is the most wonderful person I have ever known, and I am lucky to share this time with her.

Contents

List of Figures

Chapter 1

A Modern Approach to Statistical Physics

1.1 Introduction

> "It is the only physical theory of universal content, which I am convinced, that within the framework of applicability of its basic concepts will never be overthrown."
>
> - - Albert Einstein, on thermodynamics [1]

Despite being one of the most successful theories in all of science, statistical physics remains lacking a concrete theoretical foundation from realistic physical principles. These foundational principles have been the subject of a large body of work, beginning with Clausius, Maxwell, Boltzmann, and Gibbs [2], and extended to quantum systems as early as von Neumann and Schrödinger [3, 4]. Since then, statistical mechanics has become an incredibly useful tool in nearly all areas of science. Despite this, a truly satisfying understanding of why generic systems tend to a thermal equilibrium, in a manner essentially independently of their interactions or constituents, remains elusive. The evolution in time to a thermal equilibrium state from a non-thermal one is called *thermalization*, and understanding the mechanism and conditions under which it occurs is the principal question of statistical physics.

Statistical physics is the attempt to describe systems composed of large numbers, N, of particles. Typically, in a macroscopic system, N is of the order $\sim 10^{23}$, and thus an attempt at exactly solving the interacting dynamics of each of the constituent particles is essentially futile, leading to the necessity of statistical assumptions. In quantum systems, however, N may be significantly smaller and a statistical description may still be justified, as the number of degrees of freedom in a quantum system grows exponentially in N.

The key feature, then, of statistical physics, is that an attempt at describing the system on the level of exact states of the system, the *microstates*, is abandoned. It is instead generally assumed that collections of microstates may be treated as indistinguishable, and hence a probabilistic treatment of distributions of microstates may be formulated to

obtain the generic behaviour of their observable features, represented by *macrostates*. The property of a system that links the macro- and micro- worlds is the Boltzmann entropy,

$$S_B = k_B \ln \Omega, \tag{1.1}$$

where k_B is the Boltzmann constant, and Ω is the number of indistinguishable microstates consistent with a given observed macrostate (defined in more detail below). This equation links a thermodynamic property, the entropy, to the microscopic Ω.

Characteristic properties of thermalization may be represented by the features and dynamical qualities of the observed macrostate. Namely, we expect that at equilibrium the system is in a state of maximum entropy, that the entropy is non-decreasing in time[1], and that we observe irreversible dynamics towards thermal equilibrium. Simply put, the system evolves from a state that is less probable (small Ω) to one that is more probable (large Ω). These are empirical statements about our observations of reality, and the probabilistic treatment is largely justified by agreement to these statements. However, a sound justification from the underlying fundamental description is still lacking. Whilst there remains a large amount of discussion on such a justification from classical physics, our universe is fundamentally quantum, and thus the topic of this thesis is on a route to quantum foundations for the thermalization of generic systems.

Understanding statistical physics in detail has obvious difficulties: its theoretical domain lies precisely in the regime of incredibly complicated systems of many interacting constituents. Yet, astoundingly, statistical physics 'works' - making predictions that are confirmed by experiment. Until recently, the question of the underlying fundamentals of this statistical behaviour was entirely academic, with no real application or natural experimental testbed. That is, until quantum technologies have allowed the study and manipulation of many-body quantum systems on a microscopic level, leading to a resurgence in the relevance of foundational principles of statistical physics.

Such technologies, in recent years, have attempted to realise Feynman's vision [5] of simulating quantum systems in the laboratory. These pioneering experiments are leading to new regimes for the study of quantum systems. These systems have enabled observations of such phenomena as quantum phase transitions [6], quantum magnetism [7], and many-body localization [8], requiring ever more precise control over the individual constituents of many-body quantum systems.

Such experiments are thus enabling the study of the limits and regimes of quantum statistical physics, probing the conditions under which it arises as an effective theory. For example, the incredible 'Quantum Newton's Cradle' experiment by Kinoshita et. al [9], where in a system of ultracold atoms, thermalization was emphatically *not* observed in a many-body quantum system. This is understood to be a consequence of the integrability of the model, and indeed, when integrability breaking interactions are introduced, thermalization was observed as expected [10]. From this we can see that not all quantum systems can be expected to reach a thermal equilibrium, however it is generally expected that *non-integrable* models should, with the exception of many-body localising systems,

[1] Except for rare revival times in finite systems

which themselves may be understood in a similar manner to integrable systems [11].

Further experiments, as well as many numerical works, have indeed confirmed this expectation. Implementation of thermalization dynamics has been performed on various platforms, including trapped ions [12], superconducting qubits [13], and ultracold atoms [8, 10, 14, 15]. Such physical and numerical experiments provide a useful testbed for the fundamental assumption of statistical physics. Initialised in a pure state, a quantum system has zero entropy, the state is known, and thus $\Omega = 1$. In a closed system, the state evolves under unitary dynamics, and thus total entropy is conserved. Nonetheless, a physical[2] observable of the (non-integrable) system acts as if it were in contact with a bath, and thermalizes to a finite temperature described by an effective maximum entropy state. The system thus acts as its own heat bath, where local areas are described by an effective temperature, yet the global state remains pure. The fundamental problem, then, is how and under what conditions this behaviour emerges from unitary dynamics.

In this thesis, I will develop a dynamical approach to statistical physics based on a description of the thermalization of closed, non-integrable quantum systems. The theory will make use of ideas from quantum chaos theory, and exploit a random matrix theoretic model for explicit calculations. The aim of this approach is to provide a useful dynamical theory of non-integrable many-body quantum systems, which may be used as a tool to calculate generic features of such models. We will see that from this approach the dynamics of thermalization can be described for pure and mixed initial states. This dynamics equilibrates to the expected thermal state, and further, reproduces *classical* dynamics and fluctuation relations in the expected regime, both under unitary dynamics, and continuous measurement. A further theme of this thesis will be the application of the developed theory to quantum devices and their characterisation.

This thesis is arranged as a 'thesis by publications'. In the remainder of this introductory chapter, I will give a brief introduction to statistical physics, quantum devices, and quantum thermalization. In Chapter 2 I will give a theoretical overview of recent work on the thermalization of closed quantum systems. Particular focus will be paid to the role of quantum chaos and random matrix theory, which will become the basis for the work in later chapters. I will also discuss some other important results, such as typicality, and equilibration timescales. Chapter 3 will give a detailed description of the theoretical framework to be developed, focussing on the required assumptions for random matrix theory to be applied to a realistic system, on the structure of local observables, and on the physical conditions under which the main assumptions hold. Chapter 4 will give a non-technical outline of the key results, which will then be presented in Chapters 5, 6, 7, and 8. Of these, Chapters 5, 6, and 7 will be presented in paper format, and are the works of Refs. [16], [17] and [18] respectively. These chapters are thus self-contained, and thus some information is repeated between them. Footnotes are added to allow the reader to skip these sections if they choose. Chapter 8 is based on Ref. [19]. I will finally give a conclusion and outlook in Chapter 9.

[2] Typically a local observable to some subsection

1.2 Classical Statistical Physics: A Brief Review

Classical statistical physics has seen multiple attempts at physical justification. These broadly separate into two schools of thought: Boltzmann, and Gibbs; individualist, or ensemblist [20]. These approaches will be outlined in brief in this section. Of course, we are ultimately looking for a quantum theory of statistical physics, and thus a formulation based on classical laws will never be satisfactory. The aim here is thus not to go into details of classical approaches, but rather to grasp their key attributes for application and reference to a quantum formulation. For those interested in more detailed accounts of classical statistical physics see e.g. [2, 21–23].

A classical system of N particles may be described entirely by a phase space point $\mathbf{X}(t) = (\mathbf{q}(t), \mathbf{p}(t))$, with $\mathbf{q}(t) = \{\mathbf{q}_1(t), \cdots, \mathbf{q}_N(t)\}$ and $\mathbf{p}(t) = \{\mathbf{p}_1(t), \cdots, \mathbf{p}_N(t)\}$, where $\mathbf{q}_i(t), \mathbf{p}_i(t)$ are the generalised position and momentum coordinates, in 3 dimensions, of the i^{th} particle at time t, respectively. For a macroscopic system of particles N is roughly of order $\sim 10^{23}$. As alluded to above, solving Hamilton's equations for the entire system is beyond our capability, and a solution would be beyond useful comprehension; an exact approach is thus abandoned, in favour of a statistical method. The essential question, then, is how to define and interpret the necessary probability distributions in such a theory.

Perhaps the most important modern development in classical statistical physics is that of ergodic theory [24, 25]. A classical system is ergodic if, for a smooth function $f(\mathbf{X}(t))$, the time-average value of f, given by

$$\overline{f(\mathbf{X}(t))} := \lim_{T\to\infty} \frac{1}{T} \int_0^T dt f(\mathbf{X}(t)), \tag{1.2}$$

is equal to the phase space average

$$\langle f \rangle_E := \frac{1}{\Omega(E)} \int D\mathbf{X} \delta(H(\mathbf{X}(t)) - E) f(\mathbf{X}(t)) \tag{1.3}$$

over an energy hypersurface $H(\mathbf{X}(t)) = E$, where H is the Hamiltonian of the system. The integral in Eq. (1.3) is over the entire phase space, and $\Omega(E) = \int d\mathbf{X} \delta(H(\mathbf{X}(t)) - E)$. If a system is ergodic, then, the fraction of time it spends in a given region R_E of phase space is proportional to its volume $\Omega(R_E)$ in phase space, and thus the fraction of time spent in this region is given by the ratio $\frac{\Omega(R_E)}{\Omega(E)}$.

In Boltzmann's approach, the phase space is split into 'macrospaces', R_i, representing distinct macrostates of the system, and a statistical theory is formulated by interpreting the probability of finding a system in a given macrospace as the fraction of time spent in said macrospace. As we have seen, ergodicity implies that the proportion of time a system should spend in i^{th} macrostate is $\frac{\Omega(R_i)}{\Omega(E)}$. We can thus write down the probability density on the energy hypersurface as:

$$\rho_E(\mathbf{X}) = \frac{1}{\Omega(E)}, \tag{1.4}$$

which is known as the microcanonical distribution. The key source of controversy in the foundations of classical statistical physics can be traced to interpretation of this distribu-

tion.

Letting $W = \Omega(R_{eq})$ be equal to the phase space volume of the equilibrium subspace R_{eq}, such that $W \geq \Omega(R_i)\,\forall\, i$, with the equality saturated only for $i = eq$, we have the associated Boltzmann entropy of the equilibrium subspace

$$S_B = k_B \ln W, \tag{1.5}$$

which is the maximal entropy over all subspaces. Boltzmann's 'law' [22] is the statement that this entropy increases monotonically in time, and thus the system tends to the equilibrium state.

A further assumption to ergodicity, that of *mixing*, is often employed to explain the evolution to equilibrium in such systems. Briefly stated, mixing requires, for any f and g, that $\overline{\langle f(\mathbf{X})g(\mathbf{X})\rangle_E} = \langle f(\mathbf{X})\rangle_E \langle g(\mathbf{X})\rangle_E$. Mixing implies that for a distribution $f(\mathbf{X}(t))$, as $t \to \infty$ the time-average is not only equal to the phase space average over the entire energy hypersurface, but over any region of the hypersurface of non-zero measure. The time average over such a region can be expressed by writing $g(\mathbf{X}) = \frac{1}{\Omega(R_i)}\rho(\mathbf{X} \in R_i)$, and thus mixing implies the time average of $f(\mathbf{X})$ over the region R_i is equal to $\langle f(\mathbf{X})\rangle_E$. Mixing thus implies ergodicity, but not *vice versa*, and further ensures that even non-equilibrium initial distributions are indistinguishable from the microcanonical average at late times.

Much of the discussion [2, 22] around the validity of the Boltzmann approach thus rests on the ergodic hypothesis, which, aside from other criticisms [22] has only been proven for a small number of systems. Importantly for our current application, it is not obvious how these arguments extend to the quantum regime. Ergodicity of the phase space trajectory in classical systems is justified on the grounds of chaotic dynamics, which relies on the non-linearity of the equations of motion. For a closed quantum system, this equation is the Schrödinger equation, which is manifestly linear, and does not admit chaotic motion in this manner. This motivates a fundamental question for quantum objects: What does it mean for quantum dynamics to be chaotic, or ergodic?

An alternative approach to the foundation of statistical physics, due to Gibbs, takes as its starting position an *ensemble* of systems characterised by a probability density $\rho_G(\mathbf{X})$. Observable quantities then directly correspond to phase space averages of phase functions f, as in Eq. (1.3), without appeal to ergodicity or time averages.

A major appeal of this approach is that the Gibbs entropy S_G, which is defined as

$$S_G := -k_B \int d\mathbf{X} \rho_G(\mathbf{X}) \ln \rho_G(\mathbf{X}), \tag{1.6}$$

has an evident connection to the information theory of Shannon [26], and can be seen to be maximised and equal to that of Boltzmann for the microcanonical distribution over the relevant subspace. This approach is often phrased in terms of a postulate of equal *a priori* probabilities, stating as a starting point that each state congruent with the energetic restrictions on the system is equally likely, i.e. taking $\rho_G(\mathbf{X})$ as equal to Eq. (1.4). This leads to an equilibrium macrostate, which is that with the largest volume in phase space,

and the equilibrium value is the ensemble average.

The Gibbs approach, however, obviously has no physical meaning when one is in fact concerned with the behaviour of a single realisation of a system, as probability is defined by taking the distribution over an ensemble. Indeed, there has been much confusion over what the physical interpretation of Gibbsian statistical mechanics is, if any can be made at all [20, 27].

A common interpretation of the ensemblist perspective, initially formulated by Jaynes [28, 29], is an information theoretic formulation, where the postulate of equal *a priori* probabilities is obtained assuming a principle of 'least bias'. That is, if one does not know any details of the system state, just, say, its energy, then it is natural to start from a position that allows for all possible states, and treats them equally. This is, however, not a description of the physical system, but a problem of statistical inference.

Both the Gibbs and Boltzmann approaches above lead us to the same intuition that the statistical behaviour of large numbers of particles emerges due to the fact that the overwhelming majority of the possible (micro)states of the system lead to the same observable outcome - the equilibrium macrostate has the largest volume in phase space, and is thus overwhelmingly likely. Whilst this intuition is certainly valid, we have seen that these classical formulations of statistical physics can have perplexing interpretations as physical theories: Gibbs' formulation relies on imaginary ensembles, and Boltzmannian probabilities have a debatable physical meaning [21, 22], relying on the ergodic hypothesis, which is difficult to prove for a given system, and has no clear quantum limit.

1.3 Quantum Statistical Physics

We now turn to the statistical physics of macroscopic *quantum* systems, which has historically looked to understand the equilibrium properties of a quantum system in contact with an environment, which acts as a heat bath. As with the classical formulation, the framework of quantum statistical physics does not attempt to solve the full dynamics of each particle, which would require solving the Schrödinger equation for some $\sim 10^{23}$ interacting particles. Instead, the system is treated statistically. In this section, we outline a generic approach to quantum statistical physics, as in e.g. Refs. [30, 31].

In the quantum regime, rather than a set of generalised co-ordinates in phase space, we have a state $|\psi\rangle$ in a Hilbert space $\mathcal{H}$. The precise eigenstates, $|\psi_\mu\rangle$ of the Hamiltonian H of the quantum system (which we take here to include the environment) may be extraordinarily complicated to calculate in practise. Even defining the specific state of the system is incredibly complicated, and not achievable in generic large systems.

The assumption made is then similar to the classical Gibbs approach, that of *equal a priori probabilities*. To formulate this we take a subset $\mathcal{H}_E \in \mathcal{H}$ of the total system + bath Hilbert space, called an energy shell, which spans microstates with energies $[E, E + \delta E]$ around some energy E. The shell energy width δE is chosen to be large enough such that many states lie within the energy shell, however negligible on macroscopic scales.

The postulate of equal a priori probabilities states that every state in the energy shell $\mathcal{H}_E$ is equiprobable. To get to a microcanonical ensemble requires a further assumption

in the quantum case, that of *random phases* [32]. Together, these assumptions allow one to imagine the microcanonical ensemble as a collection of systems in the states $|\psi\rangle = \sum_\alpha c_\mu |\psi_\mu\rangle$, where $|c_\mu|^2$ is constant for $E_\mu \in [E, E+\delta E]$, and zero otherwise, where the phases of the complex valued c_α are random numbers - each member of the ensemble is in an effective incoherent superposition.

The state may thus be written as a *mixed state*

$$\begin{aligned} \rho_{\mathrm{ME}}(E) &= \frac{1}{d_E} P_E \\ &= \frac{1}{d_E} \sum_{E_\mu \in [E, E+\delta E]} |\psi_\mu\rangle\langle\psi_\mu|, \end{aligned} \tag{1.7}$$

where P_E is the projector onto the energy shell $\mathcal{H}_E$, with $d_E = \dim(\mathcal{H}_E)$. Eq. (1.7) defines the microcanonical ensemble for a quantum system. The equilibrium value of an observable O is then

$$O_{\mathrm{ME}}(E) = \mathrm{Tr}(\rho_{\mathrm{ME}}(E) O), \tag{1.8}$$

which we label the microcanonical average of O.

Continuing, we write the total Hamiltonian as $H = H_S \otimes \mathbb{1}_B + \mathbb{1}_S \otimes H_B + H_{SB}$, where H_S and H_B are the (sub)system and bath Hamiltonians, and $\mathbb{1}_{S(B)}$ is the identity on the system (bath) Hilbert space $\mathcal{H}_{S(B)}$. We assume that $d_S := \dim(\mathcal{H}_S) \ll d_B := \dim(\mathcal{H}_B)$, and further, the coupling H_{SB} is assumed to be weak. We denote eigenstates of $H_0 = H_S \otimes \mathbb{1}_B + \mathbb{1}_S \otimes H_B$ by $|\phi_\alpha\rangle = |s(\alpha)\rangle |\phi^{(B)}_{\alpha_B(\alpha)}\rangle$, where $|s(\alpha)\rangle \in \mathcal{H}_S$ and $|\phi^{(B)}_{\alpha_B(\alpha)}\rangle \in \mathcal{H}_B$ are system and bath eigenstates with energies $\epsilon_{s(\alpha)}$ and $E^{(B)}_{\alpha_B(\alpha)}$ respectively.

Due to the assumption of weak coupling, the states $|\phi_\alpha\rangle$ can be used as approximate eigenstates of the total system, the microcanonical state reads

$$\rho_{\mathrm{ME}}(E) \approx \frac{1}{d_E} \sum_{E_\alpha \in [E, E+\delta E]} |s(\alpha)\rangle\langle s(\alpha)| \otimes |\phi^{(B)}_{\alpha_B(\alpha)}\rangle\langle\phi^{(B)}_{\alpha_B(\alpha)}|. \tag{1.9}$$

To obtain the state of the system ρ_S alone, we then trace out the bath degrees of freedom, obtaining

$$\rho_S = \frac{1}{d_B} \sum_s^{d_S} d_{B,s} |s\rangle\langle s|, \tag{1.10}$$

where $d_{B,s} = \dim(\mathcal{H}_{B,[E-\epsilon_s, E-\epsilon_s+\delta E]})$ is the number of bath states congruent with the initial energy condition. This can be expressed as an entropy in a similar manner to the Boltzmann entropy above [23], writing $S_{qB}(E-\epsilon_s) = \ln d_{B,s}$ (where we have set $k_B = 1$),

$$d_{B,\alpha} = e^{S_{qB}(E-\epsilon_s)} \approx e^{S_{qB}(E) - \frac{dS_{qB}(E)}{DE}\epsilon_s}, \tag{1.11}$$

where we have assumed $\epsilon_s \ll E$. Thus, we finally obtain

$$\rho_S = \frac{1}{Z} \sum_s^{d_S} e^{-\beta\epsilon_s} |s\rangle\langle s|, \tag{1.12}$$

where $\beta = \frac{dS_B(E)}{dE}$ is the thermodynamic inverse temperature of the bath. This is known as the *canonical ensemble*, and is written as

$$\rho_\beta = \frac{1}{Z} e^{-\beta H}, \tag{1.13}$$

and thus expectation values of observables O_S on the system Hilbert space $\mathcal{H}_S$ in equilibrium are given by

$$\langle O \rangle_\beta = \mathrm{Tr}(\rho_\beta O). \tag{1.14}$$

We thus observe that the microcanonical state of a total system + bath Hilbert space taken at a given energy is locally equivalent to a canonical ensemble at a given temperature.

It should be stressed that the assumptions made in justifying the description of the quantum system in terms of a microcanonical ensemble are far from satisfactory. The key issue is the starting point of the principle of equal a priori probabilities, requiring a Gibbsian definition of probability via an ensemble of all possible states in an energy shell. For a single isolated system, initialised in a pure quantum state, evolving under unitary dynamics, this assumption is obviously invalid, however. It is precisely this situation that modern quantum devices have enabled the direct study of in the laboratory, as will be discussed in the next section.

The fundamental question of equilibrium statistical physics, then, is to justify the equivalence

$$\langle O(t \to \infty) \rangle \leftrightarrow \langle O \rangle_{\mathrm{ME}} \approx \mathrm{Tr}(\rho_\beta O), \tag{1.15}$$

that is, the equivalence of the expectation value of an observable after a suitably long time to an ensemble average, either microcanonical $\langle O \rangle_{MC}$, or canonical $\mathrm{Tr}(\rho_\beta O)$. To obtain a satisfying theory of statistical physics, then, we must be able to explain the approach to thermal equilibrium without the appeal to unphysical probability distributions, that is, taking as our starting point a single quantum state $|\psi(0)\rangle$, and showing the thermalization of physical local observables in the sense of (1.15).

Further, additional questions on *dynamical* features of equilibration arise: what is the route to equilibrium from a given non-equilibrium condition? How long does a system take to reach equilibrium? Each of these questions is left embarrassingly un-answerable in the standard formulations of the theory. As we will see in the next section, these are precisely the questions raised by modern experimental approaches in quantum simulator devices.

1.4 Quantum Devices

The idea of using one quantum system to mimic the dynamics of another, more difficult to probe, quantum system is attributed to Richard Feynman [5], and we now call this quantum simulation. In recent years, this has gone from a concept to a reality, and further, more ambitious exploitations of quantum dynamics, such as quantum computers, have been brought into the realm of possibility. Platforms for quantum devices, including trapped ions [7, 33–37], superconducting qubits [38–41], and ultracold atoms in optical

lattices [42–46] have developed rapidly over recent years, and each aim at surpassing classical computational abilities in some way. In the following, we will focus on applications of quantum simulator devices, however many of the ideas carry over to quantum computers, and other devices such as quantum annealers [47], etc.

The distinction made here between a quantum computer and a quantum simulator is that the latter is capable only of a restricted set of quantum operations. That is, a quantum computer requires access to a universal set of high fidelity quantum gates, and a host of further criteria [48] that are some way from being achieved experimentally. These criteria are not all required for a quantum simulation; instead, analogue simulators may work simply by mimicking the desired interactions, and simulating the quantum evolution via unitary evolution rather than a set of quantum gates. This is advantageous for near term devices with difficulty in scaling, readout, and individual control of qubits [49–51], as well as avoiding the difficult task of error correction required for a universal quantum computer [52]. Even restricting to quantum simulation, quantum devices offer a new paradigm of study for problems in many fields, including high-temperature superconductors, quantum chemistry, and even applications in high energy physics and cosmology [49, 50, 53], offering the ability to perform calculations that are not feasible classically.

The main barrier for the efficient simulation of quantum systems on classical computers is the exponentially growing Hilbert space dimension required to fully define a Hamiltonian of the system in question. For example, if we have a system of spin-$\frac{1}{2}$ particles, from here on *qubits*, each with a local Hilbert space dimension of 2, the total Hilbert space dimension of N qubits grows as 2^N. In many cases the $2^N \times 2^N$ Hamiltonian has a simple sparse structure, and thus does not need to be held in its entirety in memory, however the state of the system consists of 2^N independent numbers, requiring approximately 4TB of memory to store the state of 40 qubits [50].

Computational methods that avoid the requirement to store the entire exponentially increasing state have been formulated, for example matrix product state methods [54], which exploit the locality of interactions to reduce the required number of degrees of freedom of a realistic model. These, however, are limited to certain regimes, such as ground state calculations. Quantum simulators have provided a new paradigm to perform calculations of quantum systems, and are currently pushing the limits of classical capabilities, without the limitation caused by exponential memory requirements. Such devices thus raise natural questions on whether or not a given 'calculation' could, in principle, be performed on a current classical computer. Demonstration to the contrary is labelled 'quantum supremacy', and has been recently claimed in Ref. [55]. The characterisation of the complexity of a quantum device via its dynamics for such a comparison is an important application, to which will return in the following chapters.

Vital for our application, the construction of quantum simulator devices has enabled the study of many-body closed quantum systems over long periods of time. This has allowed for the further study of the thermalization of quantum systems, initialised in both pure and mixed states [10, 12, 13, 15, 56], as well as its breakdown at the onset of many-body localization [8, 45] (MBL). Such experiments motivate a more detailed description

of statistical physics, and pose theoretical questions on the precise conditions required for quantum thermalization to occur. These experiments contradict the approach of Gibbs - assuming a probabilistic treatment of the state of the system, by reducing uncertainty in this initial state via precise control of the initial microstate - thus eliminating any justification for a postulate of equal a priori probabilities[3]. We must thus look for an approach that explains thermalization for a given state, based on assumptions about properties of the system itself, as Boltzmann inspired via the ergodic hypothesis.

1.5 Pure State Statistical Mechanics

Above, we have seen that the standard approach to statistical physics has some fundamental limitations in its justification from a microscopic theory. The main assumption, taking the microcanonical ensemble as a starting point via the assumption of equal *a priori* probabilities, is simply not valid for application to modern quantum devices, which, in principle, can have a known initial *microstate*. We thus wish to obtain a theory of the thermalization of closed quantum systems in terms of the unitary dynamics of a pure state alone. In this section, I will outline the setting for a dynamical approach to thermal equilibrium in a closed quantum system, and describe the key quantities of interest for such a theory.

Concretely, then, we define quantum thermalization as the occurrence of two simultaneous conditions on an observable of a quantum system:

1. Equality of time average and microcanonical average: $\overline{\langle O(t)\rangle} \approx O_{\mathrm{MC}}(E)$
2. Vanishing fluctuations around time average: $\delta_O^2(\infty) \sim \mathcal{O}(e^{-N})$,

where N is the number of particles in the quantum system. These conditions describe the core predictions of equilibrium statistical physics, and thus efforts towards their justification from a general initial pure state that has been labelled 'pure state statistical mechanics' [58].

If 1) is not satisfied, yet a different (or undefined) observable value is obtained in the long time limit, with small fluctuations in the sense of 2), then the system is said to have *equilibrated* rather than thermalized.

The time average observable value and time-average fluctuations can be cast simply in terms of properties of eigenstates as follows. We define (as will be the notation throughout this thesis) a state of a system at time t by $|\psi(t)\rangle$, which evolves in time under a Hamiltonian H with eigenstates $\{|\psi_\mu\rangle\}$. In many scenarios the Hamiltonian may be written as $H = H_0 + V$, where H_0 is some non-interacting Hamiltonian (which may itself be integrable or non-integrable), and V represents a coupling between regions of interest.

[3]Of course, there is necessarily some experimental uncertainty, which one may attempt to exploit to formulate a statistical theory based on the mixed initial state due to this. Indeed, there have been suggestions along these lines for large systems based on estimates of experimental errors [57], which are very well justified for macroscopic quantum systems, and perhaps also for many current quantum devices. Even so, a classical computer simulation of a pure state evolving under the Schrödinger equation still thermalizes, and in such an ideal case the error is zero. We thus see the underlying mechanism should not be a probabilistic treatment of the initial state as an ensemble.

For example, we may consider a lattice where H_0 describes the local on-site energies, and V describes interactions between lattice sites. We will represent the eigenbasis of H_0 by $\{|\phi_\alpha\rangle\}$, which we refer to as the non-interacting basis. Observables O have matrix elements $O_{\alpha\beta} := \langle\phi_\alpha|O|\phi_\beta\rangle$ and $O_{\mu\nu} := \langle\psi_\mu|O|\psi_\nu\rangle$, where we reserve the indices α, β for the non-interacting basis, and μ, ν for the interacting basis, $\{|\psi_\mu\rangle\}$.

Some key intuition for quantum thermalization may be easily understood with very few assumptions by considering the time evolution, long time average, and fluctuations around equilibrium of an arbitrary observable. Indeed, much of our discussion below will be based around these three quantities.

In general, the time evolution of an arbitrary initial pure state may be written as

$$|\psi(t)\rangle = \sum_\mu c_\mu e^{-iE_\mu t}|\psi_\mu\rangle, \tag{1.16}$$

with $c_\mu := \langle\psi_\mu|\psi(0)\rangle$. Relating this to the time evolution of an observable O, we see that

$$\langle O(t)\rangle := \langle\psi(t)|O|\psi(t)\rangle = \sum_{\mu\nu} c_\mu c_\nu O_{\mu\nu} e^{i(E_\mu - E_\nu)t}. \tag{1.17}$$

The time average $\overline{\langle O(t)\rangle}$, defined in Eq. (1.2), may be written as,

$$\begin{aligned}\overline{\langle O(t)\rangle} &= \lim_{T\to\infty}\frac{1}{T}\int_0^t dt \sum_{\mu\nu} c_\mu c_\nu^* O_{\mu\nu} e^{i(E_\mu - E_\nu)t} \\ &= \sum_\mu |c_\mu|^2 O_{\mu\mu},\end{aligned} \tag{1.18}$$

assuming that there are no degenerate energy levels, such that $E_\mu - E_\nu = 0$ implies $\mu = \nu$, and thus $\lim_{T\to\infty}\frac{1}{T}\int_0^T dt e^{-i(E_\mu - E_\nu)t} = \delta_{\mu\nu}$.

We describe the time-averaged fluctuations of observables by,

$$\delta_O(\infty) := \lim_{T\to\infty}\frac{1}{T}\int_0^T dt(\langle O(t)\rangle^2 - \overline{\langle O(t)\rangle}^2), \tag{1.19}$$

which, assuming that also there are no degenerate energy gaps, such that $E_\mu - E_\nu = E_{\mu'} - E_{\nu'}$ implies $\mu(\nu) = \mu'(\nu')$, leads to

$$\delta_O(\infty) = \sum_{\substack{\mu\nu \\ \mu\neq\nu}} |c_\mu|^2|c_\nu|^2|O_{\mu\nu}|^2, \tag{1.20}$$

which we can see relies entirely on the off-diagonal elements of the observable.

From this we can make two important observations on the time average properties of O:

1. The time average value depends on diagonal elements of the observable $O_{\mu\mu}$.

2. Fluctuations from equilibration depend on off-diagonal elements $O_{\mu\nu}$.

Eqs. (1.18) and (1.20) are known as the 'diagonal ensemble' descriptions of the observable and observable fluctuations, respectively. This term is used as they reproduce the

result of the diagonal ensemble density matrix ρ_{DE}, defined by

$$\rho_{\mathrm{DE}} = \sum_{\mu} |\psi_\mu\rangle\langle\psi_\mu|\rho|\psi_\mu\rangle\langle\psi_\mu|, \tag{1.21}$$

where ρ is the initial density matrix of the state, which for the pure state case above is simply $\rho = |\psi(0)\rangle\langle\psi(0)|$. ρ_{DE} can be seen to be the effective time-average density matrix $\overline{\rho}$, as the diagonal elements are those that survive the time average, as above.

It should be noted that, under unitary evolution, a quantum system may never reach a stationary state from a non-stationary one, ρ_{DE} is thus not a physical state that one would ever expect to occur in a real system. It is rather a purely a theoretical construct, indicating the time-averaged behaviour of the system. In reality, a system will evolve to a state close to ρ_{DE}, and continually fluctuate in time. Equilibration, then, is when fluctuations around this state are small, as discussed above.

Furthermore, for a system with a discrete energy spectrum, revivals are inevitable. That is, if we were to wait long enough, the system would return arbitrarily close to its initial state. Thus we see that equilibration can only be defined on average. In the context of closed quantum systems, then, when we refer to equilibration or thermalization in the following, we mean that a system is close to its equilibrium state *for most* times, except for these rare revival times.

There are further caveats to the notion of thermalization in a quantum system. Indeed, for any quantum system one may specially choose states such that thermalization never occurs. A trivial example is if the system were prepared in an eigenstate of H. In this case, the system is in a steady state, and cannot evolve in time. In fact, this acknowledgement renders thermalization itself a rather surprising phenomenon from the perspective of quantum theory, as any state may be expressed simply as a linear superposition of eigenstates, each simply with a time evolution described by an oscillating phase factor

$$|\psi(t)\rangle = \sum_{\mu} c_\mu e^{-iE_\mu t}|\psi_\mu\rangle. \tag{1.22}$$

This has motivated statements on the fundamental mechanism of thermalization in terms of the dephasing of these eigenstate components [59, 60]. This further gives an intuitive picture of revival processes as the complete or partial rephasing of such components.

Further, one may always design an observable O that never thermalizes. An example would be a projector onto a single eigenstate, which again is necessarily constant in time. As we will discuss in detail in this thesis, the form of observables is very important, and it is expected that observables that are 'physical' in some manner, should be those that thermalize.

Chapter 2

Theoretical Overview

After Schrödinger and von Neumann, the problem of quantum thermalization saw relatively little attention. In fact, von Neumann's work on the topic was largely disregarded, for reasons we now understand to be tenuous [61, 62]. It was not until the early 90's that the beginning of the modern approaches to the topic would make significant progress, with the seminal works of Srednicki [63], and Deutsch [64, 65], who developed the Eigenstate Thermalization Hypothesis (ETH) from arguments from quantum chaos and random matrix theory. The ETH later gained significant attention after numerical works showing its broad validity in many systems [66], pioneered by Rigol et. al. [67].

Other approaches to foundational arguments have attempted to establish thermalization via properties of 'typical' states in high dimensional Hilbert spaces, and thus may avoid the assumptions of quantum chaos. We will see that this approach has been very successful in rigorously establishing equilibrium properties of quantum systems, however is unable to explain equilibration from an initial 'atypical' state. I will summarise some such approaches below, and argue that the ETH approach is, in-fact, a preferable and realistic mechanism for thermalization in closed quantum systems.

The focus of this chapter will thus be an introduction to the ETH. I will begin by discussing the quantum theory of chaotic systems, and their description in terms of random matrix theory (RMT). I will discuss two approaches to justification of the ETH, the first due to Srednicki [63] via a conjecture due to Michael Berry [68] on the structure of eigenstates of chaotic quantum systems, and the second a more general RMT approach initially due to Deutsch [64]. We will see that each of these approaches is very similar in the fundamental underlying assumptions. I will then introduce the full ETH itself, in the form of an ansatz by Srednicki [69, 70]. We will then see that fulfilment of Srednicki's ansatz is sufficient for thermalization to be guaranteed. A further section is devoted to other approaches to statistical physics, with a focus on typicality. We will here also see that equilibration can be shown on far more general grounds, and discuss bounds on timescales of equilibration.

This chapter will aim to provide the necessary background to understand the ETH, its key consequences, and its justifications in terms of chaotic wavefunctions; however for a more comprehensive review we point the reader to Ref. [66]. For an accessible introduction of greater detail than will be discussed below, I recommend Ref. [71]. Further, the review

Ref. [72] focusses in more detail on quantum chaos and RMT, and their relation to physical systems such as spin chains. In the latter part of this chapter, typicality methods and equilibration conditions will be discussed, which are reviewed in Ref. [73]. It will be the aim throughout this chapter to provide an intuitive overview of these broad topics in order to motivate the current work. This motivation will be discussed explicitly at the end of this chapter.

2.1 Eigenstate Thermalization

2.1.1 Quantum Chaos

The appeal to ergodicity in classical statistical physics relies on a particular feature of a system in order for thermalization to occur. That is, in a hand-waving way, the system should be sufficiently 'complicated' such that trajectories are not dominated by closed loops, as they would be for an integrable or (finite) near integrable models. This intuition extends to the quantum regime, as, indeed, integrable models cannot be expected to thermalize to the thermodynamic ensembles discussed in the previous chapter. Rather, integrable models, characterised by their extensive number of conserved quantities, equilibrate instead to a *generalised Gibbs ensemble* (GGE) [74, 75], which must explicitly account for these conserved quantities.

We thus expect thermalization to occur only in non-integrable systems[1]. Whilst 'true' chaos, in the sense of exponentially divergent trajectories in phase space, cannot exist in quantum systems [77, 78], quantum chaos is instead characterised in terms of properties of eigenfunctions, and energy spectra [72] of a chaotic Hamiltonian. In the chaotic regime, these are related to those of random matrix ensembles, as we will see below.

Berry's Conjecture

The study of quantum chaos began with the study of the semi-classical quantization [79, 80] of one-body classically chaotic models [81–83], such as chaotic billiards. It was observed that the eigenstates of such models had a particularly complicated structure. This observation motivated a conjecture due to Berry [68]: the wavefunctions $\psi(\mathbf{x})$ at position $\mathbf{x}$ of quantum systems whose classical counterpart is chaotic, and that are not close to the ground state, are made up of a random superposition of plane waves. Thus $\psi(\mathbf{x})$ is selected from a Gaussian distribution, with a two-point correlation function

$$\left\langle \psi^* \left(\mathbf{x} - \frac{\mathbf{s}}{2}\right) \psi \left(\mathbf{x} + \frac{\mathbf{s}}{2}\right) \right\rangle = \frac{1}{\Omega} \int d\mathbf{p} e^{\frac{i}{\hbar}\mathbf{p}\cdot\mathbf{x}} \delta(E - H(\mathbf{x}, \mathbf{p})), \tag{2.1}$$

where $\mathbf{p}$ is the canonical momentum, $H(\mathbf{x}, \mathbf{p})$ is the classical Hamiltonian, E is the eigenstate energy, and $\Omega = \int d\mathbf{x} d\mathbf{p} \delta(E - H(\mathbf{x}, \mathbf{p}))$.

Interestingly, Berry's conjecture may actually be derived from a principle of least bias

[1] There is a caveat here, in which the chaotic features of a model may also be introduced through an initial state that is, say, an eigenstate of a non-integrable model, yet the system evolves under an integrable one [76]. This can be seen to have equivalent chaotic dynamics.

[84], via a random matrix theoretic framework detailed in Ref. [85]. Thus, an approach to quantum thermalization based on this conjecture then constitutes both an information theoretic approach in the same spirit as Jaynes, as well as a physical condition on a property of chaotic systems.

Berry's conjecture was exploited by Srednicki [63] to formulate the ETH. Indeed, it can be seen to lead to 'eigenstate thermalization' in the sense that *individual eigenstates* exhibit thermal behaviour, yielding the correct thermal statistics for a given symmetry property (that is, Maxwell-Boltzman, Bose-Einstein, or Fermi-Dirac distributions depending on the eigenstate symmetries). More importantly for our discussion, eigenstate expectation values of observables are approximately thermal expectation values given by a microcanonical ensemble [63]. The key feature of Berry's conjecture that leads to such behaviour is the fact that the Wigner distribution of the wavefunction $\psi(\mathbf{x})$, which is given by,

$$W_E(\psi(\mathbf{x})) = \frac{1}{(2\pi\hbar)^D}\int d\mathbf{s}\psi^*\left(\mathbf{x}-\frac{\mathbf{s}}{2}\right)\psi\left(\mathbf{x}+\frac{\mathbf{s}}{2}\right)e^{-\frac{i}{\hbar}\mathbf{p}\cdot\mathbf{x}}, \tag{2.2}$$

where D is the dimensionality of the system, is given by a microcanonical distribution after taking the ensemble average over eigenstates (equivalent a smoothing process in the $\mathbf{x}$ coordinate) [63]. This can be easily seen by taking the Fourier transform of Eq. (2.1) to obtain

$$W_E(\psi(\mathbf{x})) \approx \frac{1}{\Omega}\delta(E - H(\mathbf{x},\mathbf{p})). \tag{2.3}$$

Here the $\approx$ sign indicates that we have used the ensemble average.

This may be exploited to obtain the expectation value of an observable O in the state $\psi(\mathbf{x})$, which can be written as

$$\langle O\rangle = \int\int d\mathbf{x}d\mathbf{p}W_E(\psi(\mathbf{x}))\tilde{O}(\mathbf{x},\mathbf{p}), \tag{2.4}$$

where $\tilde{O}(\mathbf{x},\mathbf{p})$ is the Weyl transform of O, defined by

$$\tilde{O}(\mathbf{x},\mathbf{p}) := \int d\mathbf{s}e^{-\frac{i}{\hbar}\mathbf{p}\cdot\mathbf{s}}\left\langle\mathbf{x}+\frac{\mathbf{s}}{2}|O|\mathbf{x}-\frac{\mathbf{s}}{2}\right\rangle. \tag{2.5}$$

Thus, we have

$$\langle O\rangle \approx \frac{1}{\Omega}\int\int dxdp\delta(E - H(\mathbf{x},\mathbf{p}))\tilde{O}(\mathbf{x},\mathbf{p}), \tag{2.6}$$

which can be seen to be a microcanonical average. We thus have, assuming Berry's conjecture, that the expectation value of an observable O (suitably coarse grained) in a high energy eigenstate is equal to its microcanonical average. This is the essential statement behind the ETH, as will be seen below.

Random Matrix Theory

The study of chaotic quantum systems via random matrix theoretic models dates back to Wigner, who employed such methods in the study of heavy nuclei [86, 87]. Since then, RMT has become the key tool in descriptions of many-body quantum chaos [72, 88–93].

There are two distinctive properties of quantum chaotic systems that we will describe in this section, which may be understood in terms of random matrix theory. Firstly, the energy level statistics of neighbouring eigenstates, and secondly, the distribution of (chaotic) wavefunctions.

In order to build a picture of many-body chaos in quantum systems we begin with an integrable Hamiltonian H_0[2], with eigenstates $|\phi_\alpha\rangle$ and eigenenergies $E_\alpha^{(0)}$. Integrable systems are characterised by an extensive number of conserved quantities O_i, and thus a large number of degenerate energy levels [78]. Indeed, the generic indicator of integrability [66] is the energy-level statistics - which for integrable systems follow the Berry-Tabor conjecture [94]. This is the statement that for integrable models the energy level statistics follow a Poissonian distribution,

$$P_{\mathrm{P}}(s) = e^{-s}, \tag{2.7}$$

where s is the spacing of neighbouring energy levels. The energy levels are thus effectively uncorrelated.

Upon introduction of an integrability breaking perturbation V the energy level statistics of non-integrable models follow the Wigner-Dyson distribution - that of a random matrix with the appropriate symmetry conditions. For a time-reversal symmetric Hamiltonian this is the Gaussian Orthogonal Ensemble (GOE), which is made up of Gaussian distributed real values, and will be discussed in more detail below. The Wigner-Dyson distribution for the GOE takes the form,

$$P_{\mathrm{WD}}(s) = \frac{\pi}{2} s e^{(-\frac{\pi s^2}{4})}. \tag{2.8}$$

The key feature to note about Eq. (2.8) is that it displays energy level repulsion, that is, the probability of finding degenerate states $P_{\mathrm{WD}}(s \to 0)$ vanishes. Such an integrability breaking perturbation V can thus be seen to reduce the number of conserved quantities to the energy alone. This can be observed as, due to the level repulsion, the full non-integrable Hamiltonian H now has non-degenerate energy levels. Noting that if a quantity O_i is conserved it has the same eigenstates as H, if all energies are non-degenerate, eigenvalues of the observable must be determined by energy alone. Thus, any conserved quantity $O_i = f(H)$ is a function of the Hamiltonian.

The Berry-Tabor to Wigner-Dyson transition is the key marker of the crossover between integrability and non-integrability [90, 95], however it is not the most important attribute in defining quantum chaos in our discussion. That role is played by the wavefunction distribution [72]. The resulting chaotic eigenstates are the fundamental feature of many-body quantum chaos [96].

After perturbing a non-interacting system described by H_0 with a sufficient interaction V, we have a new set of eigenstates $|\psi_\mu\rangle$ of the total Hamiltonian $H = H_0 + V$. The key intuition here is that for energies sufficiently far from the ground state with high energy level densities, even small perturbations cause the many-body eigenstates $|\psi_\mu\rangle$ to be made up of a large number of independent frequencies and phases contributing to

[2]Note that in later chapters H_0 will not necessarily be integrable

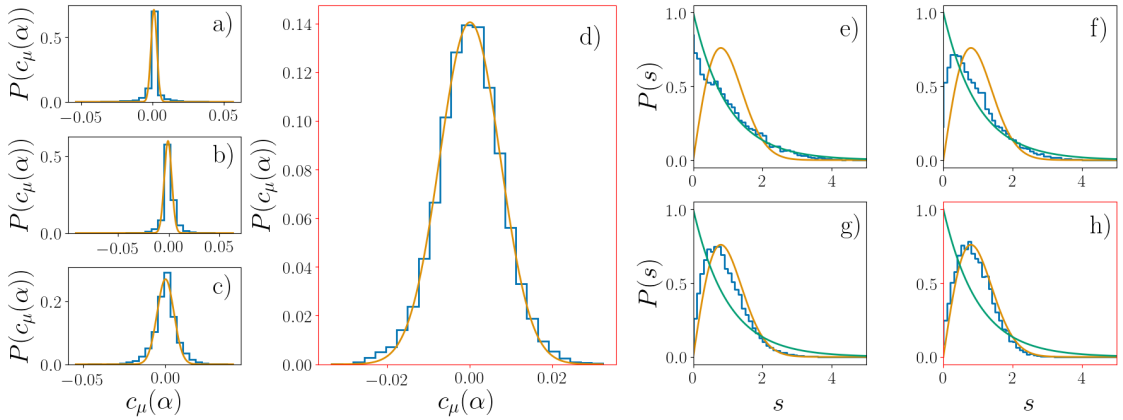

Figure 2.1: Comparison of distributions of a realistic spin-chain (Hamiltonian in Eq. (5.60)) system with quantum chaos and RMT as integrability is broken. Red bordered plots indicate fully chaotic regime. a)-d) Show probability distribution of a mid-energy wavefunction (blue), with a Gaussian fit (yellow), showing the Gaussian ansatz for chaotic wavefunctions of Eq. (2.9). d)-g) Shows the energy level statistics of spin-chain (blue), Wigner-Dyson distribution (yellow), and Poissonian distribution (green). Both the Berry-Tabor conjecture and Berry's conjecture are seen to hold, as in the integrable limit (a), e)) energy level statistics are Poissonian, as integrability breaking parameter is increased, wavefunctions become Gaussian distributed and level statistics become Wigner-Dyson. Parameters: $N = 14, B_x^{(S)} = B_z^{(B)} = 0, B_z^{(S)} = 0.8, B_x^{(B)} = 0.3, J_z^{(B)} = 0.3, J_z^{(S)} = 0.2, J_x^{(B)} = 1., J_x^{(S)} = 0$ (a), e)), 0.15 (b), f)), 0.25 (c), g)), 0.5 (d), h)).

the resulting eigenstate distribution $c_\mu(\alpha) = \langle \phi_\alpha | \psi_\mu \rangle$ expressed in the basis of H_0. This motivates a Gaussian ansatz on the form of such chaotic wavefunctions reminiscent of Berry's conjecture, with

$$P(c_\mu(\alpha)) \propto e^{-\frac{c_\mu(\alpha)^2}{2\Lambda(\mu,\alpha)}}, \tag{2.9}$$

for some $\Lambda(\mu, \alpha)$ defining the shape of the chaotic wavefunction. The function $\Lambda(\mu, \alpha)$ is very similar to the 'strength function' or local density of states (LDOS) exploited in the description of chaotic wavefunctions in e.g. Refs. [72, 91, 96–98], and the key feature for chaotic wavefunctions is that $\Lambda(\mu, \alpha)$ is a smooth function in energies E_μ, E_α. The expression of chaotic eigenstates in terms of a superposition of many independent principal components is the essential mechanism behind chaos in many-body quantum systems. We note that this definition of chaotic wavefunctions is a somewhat weaker restriction than e.g. Ref. [91], where the chaotic wavefunctions are assumed to have a Gaussian form of Λ, as well as probability distribution.

Indeed chaotic wavefunctions have proven a successful tool for application to many-body chaotic systems, and can be seen to underpin many of the ideas of the ETH. We will see in the next section that a similar approach to that of Srednicki above may be used to obtain some key ideas of the ETH from chaotic wavefunctions. Further, works by Flambaum and Izrailev [96, 99] can be seen to provide a foundation for the ideas of the ETH - showing that the Fermi-Dirac distribution may be obtained in an interacting Fermionic system using the structure of chaotic eigenstates.

To demonstrate these ideas, in Fig. 2.1 we show the crossover from Poissonian to

Wigner-Dyson statistics in a spin chain system as an integrability breaking interaction is increased. In Fig. 2.1 we see the transition from integrability to chaos in a spin-chain model (introduced in Chapter 5), and observe that, indeed, there is a crossover from Poissonian to Wigner-Dyson statistics as an integrability breaking perturbation is introduced. Further, there is a corresponding crossover to a Gaussian probability distribution of eigenstates. Indicating that indeed a chaotic wavefunction ansatz of Eq. (2.9) is valid in the non-integrable regime.

In the following, we thus refer to quantum chaotic systems in reference to the conjectured properties of non-integrable[3] models [72, 91]. These include non-degeneracy of energy levels and energy gaps, as well as the form of chaotic wavefunctions in terms of a smooth distribution $\Lambda(\mu, \alpha)$. Note that the specific Gaussian probability distribution will be modified in chapter 5, where we will see that the purely Gaussian form (which we will label the random wavefunction ansatz) is shown to be insufficient. However the underlying ideas are the same.

2.1.2 Deutsch's Random Matrix Theory

A description of chaotic quantum systems in terms of random matrix theory can be exploited using the approach of chaotic wavefunctions in order to describe thermalization and the ETH [64]. This approach utilises a model Hamiltonian given by an $\mathcal{N} \times \mathcal{N}$ matrix of the form,

$$H = H_0 + V, \tag{2.10}$$

where the non-interacting Hamiltonian H_0 has matrix elements $(H_0)_{\alpha\beta} = \delta_{\alpha\beta}\omega_0$, with $\omega_0 = \frac{1}{\mathcal{N}}$. V is a real symmetric random matrix with matrix elements $V_{\alpha\beta} = h_{\alpha\beta}$ with averages $\langle h_{\alpha\beta}\rangle_V = 0$ and $\langle h^2_{\alpha\beta}\rangle_V = \frac{(1+\delta_{\alpha\beta})g^2}{\omega_0\mathcal{N}}$. Here $\langle\cdots\rangle_V$ represents an average taken over realisations of the random matrix V. The perturbation matrix may be written as $V = \frac{g}{\sqrt{\mathcal{N}}}$GOE, where GOE is a random matrix selected from the Gaussian Orthogonal Ensemble, and g is a coupling strength. As above, we denote the eigenstates of H_0 by $|\phi_\alpha\rangle$, and of H by $|\psi_\mu\rangle$.

In Deutsch's approach, the assumption of chaotic wavefunctions of Eq. (2.9) is made on the wavefunction $c_\mu(\alpha) := \langle\phi_\alpha|\psi_\mu\rangle$. In this case, the probability distribution is taken over realisations of the random interaction Hamiltonian V, and thus $\Lambda(\mu, \alpha) := \langle|c_\mu(\alpha)|^2\rangle_V$.

This model can be solved [16] for large $\mathcal{N}$ and small g , which is shown in Appendix A.1. It can be shown that the chaotic wavefunctions form a Lorentzian distribution,

$$\Lambda(\mu, \alpha) = \frac{\omega_0\Gamma/\pi}{(E_\mu - E_\nu)^2 + \Gamma^2}, \tag{2.11}$$

with $\Gamma = \frac{\pi g^2}{\mathcal{N}\omega_0}$ setting an energy scale that describes the width of a single chaotic wavefunction.

This model will become the basis for much of the work in later chapters, and we delay further discussion of many of its properties and relation to physical systems until then,

[3] and non-many-body localising

except to summarise the work by Deutsch [64, 65], as it applies to the ETH.

One may immediately note from Eq. (2.11) that the chaotic wavefunctions can be seen to form an effective microcanonical ensemble, in the sense that they take non-zero values over some width Γ from the central energy E_μ. This can be seen to lead to a similar conclusion as Srednicki's approach above: the diagonal observable matrix elements in the interacting basis, or eigenstate expectation values, $O_{\mu\mu}$, of the model are equal to,

$$\langle O_{\mu\mu}\rangle_V = \sum_\alpha \Lambda(\mu,\alpha) O_{\alpha\alpha}. \tag{2.12}$$

Thereby, one may observe that the eigenstate expectation values are given by a microcanonical average defined over a width Γ around the eigenstate energy E_μ.

Further important properties of this model were revealed by Reimann [100], who demonstrated that eigenstate expectation values vary smoothly between eigenstates in the sense that,

$$|\langle O_{\mu\mu}\rangle_V - \langle O_{\nu\nu}\rangle_V| \leq |\mu-\nu|\Delta O \frac{\omega_0}{4\pi\Gamma}, \tag{2.13}$$

where $\Delta O = O_{max} - O_{min}$ is the difference between the largest and smallest values of the observable. Secondly, Reimann showed that the off-diagonal elements $O_{\mu\nu}$ for $\mu \neq \nu$ can be observed to be vanishing for large systems.

Further random matrix models have been exploited to describe even dynamical features of the decay of the initial state as measured by the survival probability $P(t) := |\langle\psi(0)|\psi(t)\rangle|^2$. This has been obtained by analysis of a full random matrix Hamiltonian, and shown to resemble the decay of realistic physical models in Refs. [72, 89, 101], however, this is limited by certain non-physical features of full-random matrix Hamiltonians, such as the Wigner semicircle law [87] for the density of states, which differs from the Gaussian density of states expected for generic spin-chain systems. This has the effect of the decay to equilibrium taking the form of a Bessel function, rather than an exponential, or Gaussian decay, as would be expected in a realistic spin-chain model. Further, the survival probability is a non-physical observable, as it is a projector onto a single state. In fact, it has been shown to display behaviour that deviates from typical physical observables as expected by the ETH [18, 102].

There are a further multitude of random matrix models in the literature, which generally aim to capture some relevant property of real systems missed by the GOE. For example, the two-body-random ensemble is a random matrix approach applying random values only to matrix elements corresponding to two-body interactions [72, 103, 104], and is thus able to recreate the sparsity of a realistic model represented in a computational basis [105]. Further, models have been developed to describe non-integrable systems that do not thermalize due to on-site disorder leading to MBL effects [106, 107]. In general, however, detailed analysis of such models are limited to numerical computations.

2.1.3 Srednicki's Ansatz and General Formulation

We have seen thus far that 'eigenstate thermalization' may be justified in the sense of the resemblance of individual chaotic eigenstates to a microcanonical distribution, and the

approximate equality of eigenstate expectation values with microcanonical averages. The latter equality motivates writing the ETH in terms of matrix elements of observables in the basis of eigenstates of the full interacting Hamiltonian H. Indeed, the ETH is usually formulated as an ansatz, initially by Srednicki [69, 70], precisely in this manner:

$$O_{\mu\nu} = O_{\mathrm{ME}}(E)\delta_{\mu\nu} + \frac{1}{\sqrt{D(E)}} f(E,\omega)\mathcal{R}_{\mu\nu}, \tag{2.14}$$

where $O_{\mathrm{ME}}(E)$ is the microcanonical average of Eq. (1.8) at energy $E := \frac{E_\mu + E_\nu}{2}$, f is a smooth function of E and $\omega := E_\mu - E_\nu$, that decays to zero for increasing $|E_\mu - E_\nu|$, $D(E)$ is the density of states, and $\mathcal{R}$ is a stochastic variable with mean zero and unit variance. The factor $\frac{1}{\sqrt{D(E)}}$ is often written instead in terms of the thermodynamic entropy $S(E)$ as $e^{-S(E)/2}$. This can be seen to capture the relevant details seen in the previous sections from RMT and Berry's conjecture: namely, that the eigenstate expectation values ($\mu = \nu$ in Eq. (2.14)) are given by the microcanonical average, and the off-diagonal elements are exponentially small in system size. Note that latter term was not derived or justified through quantum chaos or RMT, rather simply on the grounds that, as we will see in the next section, it guarantees the correct form for observable fluctuations.

We note a key question that remains in the formulation of the ETH. What is O? Generally, it is stated that the ETH should apply to 'physical' observables, that is, those that we observe to thermalize. Thus, the ETH has a reasonable working definition, in the sense that it may be easily applied to a system, however precisely what constitutes a 'physical' observable is unclear. In Chapter 3 we will outline some specific features of local observables, which in Chapter 5 we use to derive the ETH in the form of Eq. (2.14).

2.1.4 Sufficiency for Thermalization

For a particular observable that satisfies the ETH, we may show that the structure of the matrix elements leads directly to the conditions for thermalization described in Section 1.5: The time average of an observable should be equal to the microcanonical average around the initial state energy, and the time-fluctuations should decrease exponentially in system size.

These conditions are trivial to obtain from the diagonal ensemble results from Section 1.5 for the time-averaged observable and time-fluctuations. To see this, first using Eq. (1.18) and the ETH we have that

$$\begin{aligned} \overline{\langle O(t)\rangle} &= \sum_\mu |c_\mu|^2 O_{\mathrm{MC}}(E) \\ &= O_{\mathrm{MC}}(E_0), \end{aligned} \tag{2.15}$$

where we have taken initial states that are not macroscopic superpositions of energies, such that $\mathcal{O}(E)$ is approximately constant over all occupied eigenstates, and thus the microcanonical average at the initial state energy E_0 may be removed from the summation. For a macroscopic superposition state, one simply obtains a weighted average of microcanonical values, which is also what we should expect. It can thus be seen that the ETH guarantees

that the equilibrium state is the expected thermal state.

To describe the fluctuations, we use Eq. (1.20), which can be seen to depend solely on the off diagonal element of O. Using the second term of the ETH, then, for a system of N particles we have,

$$\begin{aligned}\delta_O^2(\infty) &= \sum_{\substack{\mu,\nu \\ \mu\neq\nu}} |c_\mu|^2|c_\nu|^2 \frac{1}{D(E)} f(E,\omega)\mathcal{R}_{\mu\nu} \\ &\leq \sum_{\substack{\mu,\nu \\ \mu\neq\nu}} |c_\mu|^2|c_\nu|^2 \frac{1}{D(E)} f(E,\omega) \\ &\approx \frac{1}{D(\alpha_0)} f(E,0) \\ &\sim \mathcal{O}(e^{-N}),\end{aligned} \tag{2.16}$$

where we have again assumed that the initial state is not in a macroscopic superposition, however, once again, for cases where the initial state does take this form we can still see that $\delta_O^2(\infty)$ would be on the order of the inverse of the density of states weighted by the initial state population, as $f \sim \mathcal{O}(1)$.

Of course, the ETH is not expected to be true for all systems, and thus cannot be proven in general. One would have to show it for given systems, which due to the non-integrability of systems for which it is conjectured to hold, leaves mainly numerical methods for demonstration of the ETH. Such approaches have proven to be a fruitful platform to study the ETH. Indeed, studies of both the diagonal [66, 67, 108, 109], and non-diagonal [66, 110–114] elements of observables in non-integrable quantum systems have proven very useful in showing that the ETH applies to a broad range of non-integrable models. As well as observing the validity of the ETH as the integrability of a system is broken [95, 115], and its breakdown at the onset of MBL [116].

Note that a formulation of quantum statistical physics based on the ETH ansatz is already preferable to standard approaches. This is because the ETH is a physical property of a single system, and does not require an appeal to ensemble averages for justification of thermalization after initialisation in a non-equilibrium initial state. However, the ETH in the form of Eq. (2.14) is still a very strong assumption that is not rigorously justified. One of the key contributions of this thesis will be to establish the full ETH in the form of Eq. (2.14) based on a framework of chaotic wavefunctions.

2.2 Other Approaches to Thermalization

2.2.1 Typicality

We have seen above that thermalization is guaranteed by the ETH, however, that is is a strong assumption to make on a given system. Typicality seeks to avoid such assumptions by attempting instead to find generic properties of large quantum systems. Typicality can be summarised in terms of the behaviour of the 'overwhelming majority' of states, observables and/or Hamiltonians in large dimensional models. The key principle can

be understood from picking a random state of a system. Roughly speaking, typicality asserts that this state is overwhelmingly likely to resemble a canonical thermal state. It is immediately intuitive that this is very similar in spirit to RMT methods, as such randomly selected states are equivalent to eigenstates of random matrices. In this section, we will discuss such typicality approaches. Whilst typicality is not the main focus of this work, it is has been an important development in the understanding of the thermalization of closed quantum systems, and thus we review some of the key successes of the approach, as well as its limitations, below. For an extensive review of typicality approaches see Ref. [73].

There are several approaches to quantum thermalization that may be described in terms of typicality, which we will briefly discuss here. The most prominent is the canonical typicality [117–119]. Typicality approaches have the shared theme of showing that thermalization occurs for 'most' quantum systems due to generic features such as entanglement [73, 120].

The main statement of canonical typicality is as follows: For a random state $|\psi\rangle$ selected from a uniform distribution on the unit sphere, the *reduced state* $\rho_S = \mathrm{Tr}_B\{|\psi\rangle\langle\psi|\}$ on an energy shell $E_{|\psi\rangle} \in [E, E+\delta]$, where Tr_B indicates a trace over the bath degrees of freedom, is overwhelmingly likely to satisfy

$$\rho_S = \mathrm{Tr}_B\{|\psi\rangle\langle\psi|\} \approx \mathrm{Tr}_B\{\rho_{\mathrm{ME}}(E)\} \approx \rho_\beta. \tag{2.17}$$

This is shown in [118] under the very general conditions by application of Levy's lemma, assuming only that the (sub)system is small compared to the bath, and the total Hilbert space is large. Note here that this result gives a uniquely quantum foundation to statistical physics, in the sense that the canonical state emerges as a result of the entanglement between the system and bath in a randomly selected state.

These methods, however, do not remove the need for an arbitrary probability distribution, in the sense that they select states from a predefined distribution - the uniform distribution, or Haar measure over the unit sphere. In this sense they are not far removed from the assumption of equal a priori probabilities from the previous chapter, though take an important additional step of stating that individual states from this ensemble have the required properties, and not just the ensemble itself. The essential proof is that the variance around the average over this distribution is small. Here we see a further relation to random matrix approaches, where a Haar average over random *Hamiltonians* is a common tool, and a 'self-averaging' assumption is often made [121], that the variance in observable dynamics between Hamiltonian realisations is small.

The intuition underpinning canonical typicality - that of the resemblance between a randomly selected state and an equilibrium state can be taken a step further, and even describe the time dependence of a state. *Dynamical typicality* [122] has been shown under similar conditions, and is the statement that two states $|\psi_{1(2)}\rangle$ with the same expectation value of an observable O on a small subspace of the total Hilbert space are likely to have the same expectation value at some later time. Both canonical and dynamical typicality have proven to be useful numerical approximation tools [123–125], allowing the use of a

single state, rather than a density matrix, to describe time evolution, and thus drastically reducing memory cost [125].

Canonical typicality thus gives a rigorous justification to the statement that 'typical' states are in thermal equilibrium with respect to a local observable O, guaranteeing that $\langle\psi|O|\psi\rangle \approx \mathrm{Tr}\{\rho_\beta O\}$ for almost all $|\psi\rangle$. Note that there are also other typicality approaches to thermalization, namely Normal Typicality [61, 62], which shows that typical states of systems thermalize with respect to a 'macroscopic' observable in the sense that a random state $|\psi\rangle$ satisfies $\langle\psi|P_{eq}|\psi\rangle \approx 1$, where P_{eq} is a projector onto an equilibrium subspace $\mathcal{H}_{eq}$. This approach has been further generalised in Ref. [126].

The results shown above from typicality show clearly and conclusively that thermal equilibrium is a property of typical states and/or observables. One may argue, however, that these approaches offer little insight into realistic thermalization dynamics, which takes as its starting point a non-thermal, and thus *atypical* state. If a system initially starts in such an atypical state, should it evolve into a typical state under unitary dynamics? If so, under what conditions? As this central question is left unanswered by the above approaches, they therefore cannot tell the whole story of quantum thermalization. However, typicality nonetheless has provided very useful results, and rigorously confirm an intuition obtained from the classical approaches above - the equilibrium state has essentially the same observable properties as a 'typical' state.

2.2.2 Equilibration

Under general conditions, we have seen that typicality approaches above justify the relation between a typical state of a generic system and a thermal state, however fail to account for non-equilibrium initial states, and cannot show that evolution in time leads to equilibration, or thermalization. Here we will see that equilibration, at least, may in-fact be shown under very general assumptions. The main starting point will be the non-resonance condition, from which we obtained a time average observable value given by Eqs. (1.18). To show equilibration, we are interested in bounding fluctuations Eq. (1.20), which is repeated for convenience:

$$\delta_O(\infty) = \sum_{\substack{\mu\nu \\ \mu\neq\nu}} |c_\mu|^2 |c_\nu|^2 |O_{\mu\nu}|^2. \tag{2.18}$$

If this value is small, at least at some long-time, the observable will reach an equilibrium value, around which fluctuations are small, and equilibration (on average) is realised.

The simplest of these bounds is obtained trivially [73],

$$\delta_O^2(\infty) \leq \max_{\mu\neq\nu} |O_{\mu\nu}|^2, \tag{2.19}$$

which tells us equilibration is guaranteed as long as all off-diagonal observable elements are small. A more illuminating bound is obtained by Reimann [57], who showed for initial states $|\psi(0)\rangle$,

$$\delta_O^2(\infty) \leq (O_{max} - O_{min})^2 \mathrm{IPR}(|\psi(0)\rangle), \tag{2.20}$$

where IPR($|\phi_{\alpha_0}$) is the inverse participation ratio (IPR),

$$\text{IPR}(|\psi(0)\rangle) = \sum_{\mu} |\langle\psi_\mu|\psi(0)\rangle|^4. \tag{2.21}$$

The IPR is sometimes written as $\frac{1}{D_{eff}}$ where D_{eff} is the effective dimension, and can be seen to be a measure of the number of eigenstates that contribute a non-trivial weight to the initial state. Thus, the IPR is expected to be very small for generic initial states (including non-equilibrium states). We thus see that equilibrium on average is expected under quite general conditions. Linden *et. al* [127] obtained a similar bound, on the time-average trace distance between the reduced density matrix and that of the diagonal ensemble [127].

Reimann's result has been further iteratively improved upon, by Short [128], Short and Farrely [129], who notably removed the need for a nonresonance condition, and obtained Eq. (2.20) with the difference that the RHS is multiplied by the number of resonances. Reimann and Kastner then further improved the bound [130], allowing also for the initial state to exhibit a small effective dimension D_{eff}, as long as the second largest populated energy level is small.

We note that these results on equilibrium, as well as the typicality results of the previous section, include, for example, integrable and many-body localising systems, and thus are too general to recover thermalization in full. The ETH is thus still required to complete the picture, and ensure that the equilibrium state is that of a thermal ensemble.

2.2.3 Timescales of Equilibration

An important missing piece to our discussion thus far is the timescale over which the system, initialised in some non-equilibrium state, reaches its equilibrium state, thermal or otherwise. So far we have seen that typical states of large systems are described by thermal states from typicality, and further, that *any* initial state equilibrates under the non-resonance condition if the inverse participation ratio is large. We have also seen that, if the ETH is satisfied, this equilibrium state is described by the microcanonical ensemble. Thus, what naturally remains are questions on timescales, and dynamics.

The first major results of this kind gave unreasonably large timescales [129, 131, 132], which grew with the Hilbert space dimension. Indeed, these timescales were seen to in-fact be tight, as observables can be constructed that saturate the bounds. However, such observables have little physical relevance, as realistic observables are seen to decay in timescales that are independent of bath size. On the other hand, fast thermalization was shown for 'typical' observables in a similar manner to the previous section [132], and even dynamical information was captured by Reimann [133] using an approach reminiscent of RMT. The implied timescales of these bounds is particularly interesting, as it states that the typical dynamical behaviour is close to the fastest possible decay [132], and rare, non-typical observables are those that can be constructed to have excessively large equilibration times.

The first bound to capture information on timescales of *physical* (local) observables was

by Garcia-Pintos [134], who showed that a given observable equilibrates in a 'reasonable time' (that does not scale with the bath dimension), provided some conditions are met on the initial state, off-diagonal observable elements, and the distribution of energy gaps. For pure-state initial states, however, this bound once more appeals to typicality arguments, and the generic bound is valid for a bath in a sufficiently mixed state.

2.3 Motivations for Current Work

We have already seen that the current understanding of the foundations of statistical physics is severely limited. Yet it is one of the most universally accepted theories in all of physics, owing to its predictive power and generality. We have seen in the previous chapter that quantum devices are allowing for the experimental study of the limits of statistical physics. An important question, then, is regarding what precisely the regime of statistical physics is: under what conditions does statistical physics hold?

Indeed, the apparent ubiquity of the conditions under which thermalization is observed may be seen as precisely the motivation to study the problem of thermalization. This leads to interesting questions regarding how thermalization may be *beaten* in search of more exotic behaviour. Examples of quantum synchronisation [135], and other types of non-stationary dynamics [136, 137] - requiring by necessity conditions that avoid the ETH and thermalization.

We have seen above, some rather general approaches to quantum thermalization and its relation to the foundations of statistical physics have already been understood. There are still some major gaps, however, particularly surrounding the issue of timescales of thermalization, and the dynamics itself, as well as the form of observables one expects to thermalize. We have observed that the ETH provides a feasible mechanism for thermalization that has been extensively studied numerically and verified. The ETH, however, is a strong assumption on observable matrix elements that is not currently understood in terms of physical properties of a system. The first major goal of this work is thus to establish the ETH on more physical grounds, in terms of a weaker set of assumptions.

Typical studies of thermalization, as we have seen above, focus on quantities that are beyond experimental reach. An important aim of the work in this thesis will be to obtain analytical results in terms of physical properties of quantum systems that may be realised in current experiments. Such experimental realisation may not only show markers of chaos in quantum systems in terms of observable quantities, but will also prove to be useful in characterisation of the experimental device itself.

There has further been a growing interest in using RMT methods for applications to quantum circuits [55, 138–140], as both a testbed for quantum chaos, and in order to characterise quantum algorithms and near term, noisy, quantum computers. Similar applications are a major motivation for the current work, allowing for application of theories of quantum chaos to quantum simulators and other quantum devices. Along these lines, as we will see in Chapter 7, thermalization dynamics may be exploited to characterise the complexity of a quantum computation in a meaningful sense [18]. Indeed, such applications are an important step in the hunt for quantum supremacy [141], as well as more

ambitious projects, such as quantum machine learning [142]. We thus see that an understanding of the conditions for the thermalization of quantum systems may have many implications on the advancement of quantum technologies.

There are also reasons to be inspired by the problem of thermalization from purely theoretical grounds. Thermalization is a beautiful example of an *emergent* behaviour [143–146], and perhaps the simplest; it is thus an exciting testbed for understanding the greater topic. With concepts such as emergence, it is important to have a clear definition in mind. What is meant here by an emergent theory is the following: A system that is described on some scale by a theoretical description, that when suitably coarse grained can be described by a completely new theoretical framework bearing no resemblance to the more detailed model. For the case of the study of thermalization as outlined above, the end goal of the field is to understand how and under what conditions a quantum system evolving under a microscopic description by the Schrödinger equation can be described by the emergent higher level theory of thermodynamics.

The main aim of this work will be to establish an approach to non-integrable systems that allows for explicit calculation of the thermalization process. The main goal is to develop a useful tool for calculations of non-integrable quantum systems, under some physically justified assumptions. I will endeavour to connect these assumptions to the foundational arguments discussed in this section, but note that the aim is not to obtain a rigorous and totally general model - such an effort seems some way from being obtainable for non-equilibrium physics without a more detailed understanding of chaos in quantum systems [71]. Rather, the goal is to obtain a formulation that captures critical features of non-equilibrium dynamics and equilibration of generic chaotic systems. We will see that, under the assumptions of quantum chaos outlined in the next chapter, we may obtain not only the ETH, but the full thermalization dynamics of physical observables to the thermal state. We will additionally observe the emergence of generic features of classical statistical physics, and connect the results to thermodynamic properties of the system such as entropy growth.

Chapter 3

Random Matrix Theoretic model of Quantum Chaotic Systems

In this Chapter I will introduce the features of chaotic wavefunctions which will be exploited to describe generic chaotic quantum systems via a random matrix theory (RMT) approach. Particular attention will be paid to the key assumptions on physical quantities that allow the application of RMT to real systems. It is the aim here to present a detailed description of the conditions under which one may expect a given physical model to be well described by the chosen RMT model, and, more generally, the theory of chaotic wavefunctions to be developed in later chapters.

This chapter will begin by introducing the form of chaotic wavefunctions that will be used in the following chapters. This form of chaotic wavefunctions will be exploited in Chapter 5 to solve the Deutsch model of the previous chapter, which will become the basis for many further results. I will therefore, in Section 3.1.1, discuss some key features of the model that distinguish it from full random matrix approaches, and make the model a suitable heuristic for realistic quantum systems. In particular, energy scales defined by the chaotic wavefunctions can avoid common issues with random matrix models, such as the restriction to infinite temperatures, non-local interactions, and allowing for changing parameters in energy, such as the density of states. Following this, Section 3.2 will be devoted to obtaining generic features of local observables, and their application to RMT. This is an important feature of the current approach, as analytical RMT methods generally do not allow for physical, local observables. Finally, I will detail the key conditions under which important assumptions are expected to hold. These assumptions are those that allow approximations with chaotic wavefunctions that will be used throughout the text, and thus some time will be spent to cast the required conditions in terms of physical properties of a system. The chapter will conclude with a summary of these conditions.

3.1 Model

As in Sec. 2.1.2 we will us a random matrix Hamiltonian of form $H = H_0 + V$, described in Eq. (2.10). This model can be solved [16] for large $\mathcal{N}$ and small g, which we perform in Appendix A.1. The Gaussian ansatz on the distribution of the matrix c describing

the many-body eigenstates $|\psi_\mu\rangle = \sum_\alpha c_\mu(\alpha)|\phi_\alpha\rangle$, discussed in Chapter 2, will be seen in Chapter 5 to lead to inconsistent results for the off-diagonal elements of observables. Thus a modification is required in order to describe thermalization dynamics and the full ETH. Here we use a modified form for the probability distribution p of the matrix c of eigenstate coefficients $c_\mu(\alpha)$, explicitly accounting for the mutual orthogonality of wavefunctions:

$$p(c,\Lambda) = \frac{1}{Z_p}\exp\left(-\sum_{\mu\alpha}\frac{c_\mu^2(\alpha)}{2\Lambda(E_\mu,E_\alpha)}\right)\prod_{\substack{\mu\nu\\ \mu>\nu}}\delta\left(\sum_\alpha c_\mu(\alpha)c_\nu(\alpha)\right). \tag{3.1}$$

The function $\Lambda(E_\mu,E_\alpha) = \Lambda(\mu,\alpha)$ describes the distribution of the chaotic wavefunction for a given Hamiltonian, and as is shown in Appendix A.1, is described by a Lorentzian,

$$\Lambda(\mu,\alpha) = \frac{\omega_0\Gamma/\pi}{(E_\mu - E_\alpha)^2 + \Gamma^2}, \tag{3.2}$$

with $\Gamma = \frac{\pi g^2}{\mathcal{N}\omega_0}$ setting an energy scale that describes the width of a single chaotic wavefunction. We will see in Chapter 5 that using Eq. (3.1) solves issues that arise when ignoring orthogonality using a purely Gaussian chaotic wavefunction, however focus in this chapter on the physical conditions required to perform calculations with this ansatz.

It is important to note that the approach from chaotic wavefunctions is distinct from the RMT model, in the sense that Eq. (3.1) is valid for generic chaotic systems. For the particular case of Deutsch's RMT model we have that $\Lambda(E_\mu,E_\alpha)$ is described by a Lorentzian. A further simple example is that of full random matrix Hamiltonian, where H is simply selected from the GOE. In this case $\Lambda = \frac{1}{\mathcal{N}}$, with $\mathcal{N}$ the dimension of the random matrix. Further, it is common to assume a Gaussian structure on $\Lambda(E_\mu,E_\alpha)$, which as we will see in Chapter 5, is expected to be valid for strong coupling regimes of quantum spin-chains [91].

We note that chaotic wavefunctions of the form (3.1) can be shown to be *self-averaging*. This means that a single member of the ensemble behaves as the ensemble average, $\langle\langle O(t)\rangle\rangle_V \approx \langle O(t)\rangle$. This justifies the use of the ensemble average for the RMT approach in the following chapters, and is proven, and discussed in more detail, in Appendix C.

3.1.1 Energy Scales

The condition of locality in energy of wavefunctions can be seen from the property, $\Lambda(E_\mu,E_\alpha) \to 0$ for $|E_\mu - E_\alpha| \gg \Gamma$ for some Γ describing the width of a chaotic wavefunction. This is satisfied for the RMT model above, as can be seen by Eq. (3.2), but not the full random matrix Hamiltonian, with $\Lambda(\mu,\alpha) = \frac{1}{\mathcal{N}}$. The energy scale Γ is a very important feature of the RMT model of Eq. (2.10) that distinguishes the current approach from typical full random matrix methods.

The definition of energy scales by chaotic wavefunctions is precisely what prevents the long-range couplings in the random matrix interaction Hamiltonian V from rendering the model unphysical. This can be understood through a condition that is a part of the ETH

in the form of Eq. (2.14): off-diagonal matrix elements $O_{\mu\nu}$ of observables should decay to zero for $|E_\mu - E_\nu| \gg \Gamma$ for some energy scale Γ. If this condition is fulfilled, then states of energy scales much greater than Γ cannot affect one another through the action of O, and are thus irrelevant to the observable dynamics. We will see this is satisfied by the RMT model in Eq. (2.10) in Chapter 5 in deriving the ETH.

Further, we can see it is this property that allows for a natural definition of a microcanonical temperature within the system, which can be seen by recalling Eq. (1.18), and writing for the time average of an observable initialised in the state $|\phi_{\alpha_0}\rangle$,

$$\begin{aligned} \langle\overline{\langle O(t)\rangle}\rangle_V &= \langle\sum_\mu |c_\mu(\alpha_0)|^2 O_{\mu\mu}\rangle_V \\ &= \sum_{\mu\alpha}\langle|c_\mu(\alpha_0)|^2|c_\mu(\alpha)|^2\rangle_V O_{\alpha\alpha}, \end{aligned} \tag{3.3}$$

where for simplicity we have assumed $O_{\alpha\beta} \propto \delta_{\alpha\beta}$. Assuming for now that the chaotic wavefunctions may be taken as purely Gaussian[1], we can write

$$\langle\overline{\langle O(t)\rangle}\rangle_V = \sum_{\mu\alpha}\Lambda(\mu,\alpha_0)\Lambda(\mu,\alpha)O_{\alpha\alpha}, \tag{3.4}$$

which for a full random matrix with $\Lambda(\mu,\alpha) = \frac{1}{\mathcal{N}}$ is just an infinite temperature average $Tr(e^{-\beta H}O)$ with $\beta \to 0$, and thus full random matrix methods are limited to calculations in this limit. If, however, some energy scale is set by $\Lambda(\mu,\alpha)$, we see that the infinite time average above is dictated by the energy of the initial state E_{α_0}, as the other indices are summed over. In Chapter 8 we will see in detail how a finite temperature state can emerge from this property, with $\beta = \beta(E_{\alpha_0})$.

Finally, in applying this model to realistic systems, we will in fact see that the RMT approach is capable of describing systems that have a changing density of states with energy, despite the model itself assuming $D(E) = \frac{1}{\omega_0} = \text{const}$. This apparent contradiction is avoided as the RMT assumption that $D(E) = \text{const}$ must apply over the width of a single chaotic wavefunction, rather than over the entire system. This will be formalised in the discussion of the 'smoothness' condition below, and will become necessary when treating high temperature initial states in Chapter 7.

3.1.2 Microcanonical Averages of Matrix Elements

In the following, a particular form of averages of matrix elements of observables will be used repeatedly, which we will first briefly introduce here. We define, then, the quantity

$$\overline{[O_{\alpha\alpha}]}_\mu = \sum_\alpha \Lambda(\mu,\alpha)O_{\alpha\alpha}, \tag{3.5}$$

which can be seen to be an effective microcanonical average, with a Lorentzian rather than uniform weighting, around the energy μ with a width Γ.

[1] We will see in Chapter 6 that the effective interactions due to the orthogonality condition do not affect the time average value

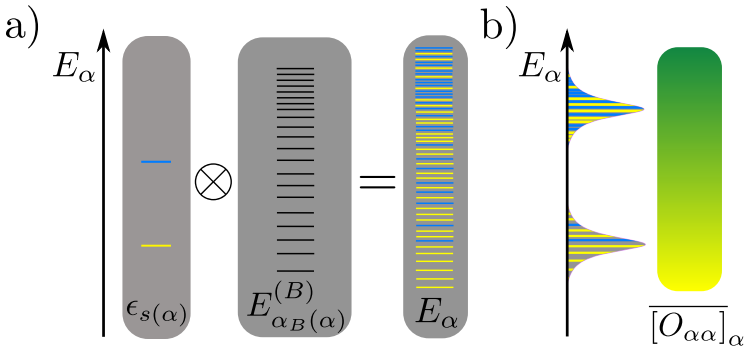

Figure 3.1: a) Energy level diagram. Shown are two system energy levels ϵ_s in distinct colors, the bath energy levels $E^{(B)}_{f(\alpha,s)}$, and the total system + bath energy levels E_α, coloured according to their respective system state. b) Illustration of microcanonical average $\overline{[O_{\alpha\alpha}]}_\alpha$. Each level in the average is weighted by the function Λ, this average is assumed to be made up of many energy levels, and to vary smoothly with energy.

In-fact, we have already seen this average in Eq. (2.12), in the discussion of diagonal elements of observables $O_{\mu\mu}$ from Deutch's approach. Here we saw that this microcanonical average was equal to the ensemble average $\langle O_{\mu\mu}\rangle_V$. In Fig. 3.1 we see a diagram of this averaging process for an observable of the system.

We will also make use of a generalisation of this averaging procedure to off-diagonal elements in $O_{\alpha\beta}$, which may be written as,

$$\overline{[O_{\alpha,\alpha+n}]}_\mu = \sum_\alpha \Lambda(\mu,\alpha) O_{\alpha,\alpha+n}, \tag{3.6}$$

where n defines an offset from the diagonal. We will see below that this form of observable averages emerges naturally for local observables.

3.2 Defining a Local Observable for RMT

A key issue in RMT methods has been to provide a description of physical local observables. Generally, RMT methods use either simple yet non-physical observables such as the survival probability [72], or are concerned with 'typical' observables in the sense of the Haar average [132, 133]. However, due to the specific structure of physical observables (which are generally well-defined in some computational basis), most observables selected are thus atypical, and physical features may thus be missed.

In the following, we will discuss some specific properties of local observables, and exploit these properties in order to perform calculations involving observable matrix elements and chaotic wavefunctions. We will see that a description of local observables in RMT may be achieved via imposing two conditions upon matrix elements $O_{\alpha\beta} := \langle\phi_\alpha|O|\phi_\beta\rangle$ of a Hermitian matrix O.

The first condition, *sparsity*, is derived directly from the assumption of locality of observables. The obtained form for local observables will have a particularly simple structure for the RMT model. The second, *smoothness*, is a more technical condition on microca-

nonical averages of observables. This condition is crucial to the formulation of physical models in terms of RMT, and allows for the calculation of certain relevant summations. The smoothness condition is initially formulated in terms of observable matrix elements, however can be recast into conditions on physical parameters - either formulated in terms of the density of states of a system or a microcanonical temperature. The smoothness condition will be shown to be trivially validated for standard statistical ensembles, and further allows the simpler RMT form of the sparsity condition to be applied to real models.

3.2.1 Sparsity

The first condition one may observe on the matrix elements of observables in the non-interacting basis - *sparsity* - will be shown below as a consequence of the observable acting non-trivially only on a subset $\mathcal{H}_S \in \mathcal{H}$ of the total Hilbert space $\mathcal{H}$. To begin, we separate the non-interacting basis of H_0 into disconnected system + bath parts, $H_0 = H_S \otimes \mathbb{1}_B + \mathbb{1}_S \otimes H_B$, with $\mathbb{1}_{S(B)}$ as the identity matrix on the system (bath) Hilbert space $\mathcal{H}_{S(B)}$, denoted by subscript $S(B)$. We define $d_S := \dim \mathcal{H}_S \ll d_B := \dim \mathcal{H}_B$. The eigenstates $|\phi_\alpha\rangle$ of H_0 may then be written as,

$$|\phi_\alpha\rangle = |s(\alpha)\rangle_S |\phi^{(B)}_{\alpha_B(\alpha)}\rangle_B, \tag{3.7}$$

and have energies $E_\alpha := \langle\phi_\alpha|H_0|\phi_\alpha\rangle$ given by,

$$E_\alpha = {}_B\langle\phi^{(B)}_{\alpha_B(\alpha)}|{}_S\langle s(\alpha)|H_S + H_B|s(\alpha)\rangle_S|\phi^{(B)}_{\alpha_B(\alpha)}\rangle_B = \epsilon_{s(\alpha)} + E^{(B)}_{\alpha_B(\alpha)}. \tag{3.8}$$

Here we have denoted eigenenergies of the system and bath Hamiltonians by $\epsilon_{s(\alpha)}$ and $E^{(B)}_{\alpha_B(\alpha)}$ respectively.

Now, we are interested in the action of a local observable $O = O_S \otimes \mathbb{1}_B$. Noting simply that this action may only cause transitions in the system energy levels, we see that O may only have non-zero matrix elements corresponding to such transitions - local system observables do not act on the bath degrees of freedom - we may thereby observe,

$$O_{\alpha\beta} = {}_B\langle\phi^{(B)}_{\alpha_B(\alpha)}|{}_S\langle s(\alpha)|O|s(\beta)\rangle_S|\phi^{(B)}_{\alpha_B(\beta)}\rangle_B = (O_S)_{s(\alpha)s(\beta)}\delta_{\alpha_B(\alpha)\alpha_B(\beta)}, \tag{3.9}$$

where $(O_S)_{s(\alpha)s(\beta)} := {}_S\langle s(\alpha)|O_S|s(\beta)\rangle_S$. This expression already shows that there can only be as many as $d_S(d_S-1)$ independent non-zero off-diagonal matrix elements $O_{\alpha\beta}|_{\alpha\neq\beta}$ corresponding to system energy transitions, plus d_S possible independent diagonal elements $O_{\alpha\alpha}$. Thus, whilst for a generic system $O_{\alpha\beta}$ is a very large matrix, it is also highly degenerate [147], in the sense that non-zero entries are made up of few repeated values. A simple example is the case of a spin chain, where the system S is a single spin; O_S then has 4 distinct matrix elements, and thus, the non-zero matrix elements of $O_{\alpha\beta}$ may take on a maximum of 4 possible values (plus zeros on elements that do not correspond to system transitions). These values must therefore be repeated in many entries of $O_{\alpha\beta}$.

Continuing, then, Eq. (3.9) can be written as the requirement that transitions induced

by the action of the operator O must obey

$$\begin{aligned} E_\alpha - E_\beta &= \epsilon_{s(\alpha)} - \epsilon_{s(\beta)} \\ &:= \Delta\epsilon_n, \end{aligned} \tag{3.10}$$

where the subscript n lists the possible energy transitions due to O. For example, for a system consisting of two energy levels, $s(\alpha) = \{1, 2\}$, there are two possible distinct transition energies, plus a (doubly degenerate) zero-energy transition from diagonal elements of O_S. Thus, $\Delta\epsilon_n = \{0, \epsilon_1 - \epsilon_2, \epsilon_2 - \epsilon_1\}$.

For the random matrix model, we have that $E_\alpha = \alpha\omega_0$, and thus, the condition for local observable elements $O_{\alpha\beta}$ to be non-zero becomes,

$$\begin{aligned} (\alpha - \beta)\omega_0 &= \Delta\epsilon_n \\ &= n\omega_0, \end{aligned} \tag{3.11}$$

where here n is an integer running through possible values $n\omega_0$ of the system energy gaps. We label this set $\mathcal{N}_\mathcal{O}$, which has length $N_O = d_S(d_S - 1) + 1$. This leads us to the requirement on β for $O_{\alpha\beta}$ to be non-zero: $\beta = \alpha - n$. We see then, that diagonal values in O_S must fill the diagonal values $O_{\alpha\alpha}$, whereas off diagonal elements in O_S fill values in $O_{\alpha\beta}$ corresponding to the relevant energy gap in the system. As n runs over positive and negative integers we can redefine $n \to -n$ (which is the convention used in the following chapters), and thus we have that

$$O_{\alpha\beta} = \sum_{n \in \mathcal{N}_\mathcal{O}} O_{\alpha,\alpha+n}\delta_{\beta,\alpha+n}. \tag{3.12}$$

We note that, in-fact, the above discussion is valid for any observable, not necessarily local. Locality is enforced when we require that $d_S \ll d_B$, and thus we have $N_O \ll \mathcal{N}$. We thus refer to Eq. (3.12) with $N_O \ll \mathcal{N}$ as the *sparsity* condition on matrix elements of observables.

Of course, in realistic physical systems there is not in general a constant energy gap ω_0 between all neighbouring levels. However, we can use similar considerations to write the same condition more generally without this assumption. We are interested in the effect of locality of observables of typical summations required for calculations of observable quantities. For example, we introduce some function F of energy $F(E_\alpha, E_\beta)$, and would wish to be able to evaluate summations of the form,

$$\sum_\beta O_{\alpha\beta} F(E_\alpha, E_\beta). \tag{3.13}$$

Exploiting Eqs. (3.9) and (3.10), we then see that the summation of Eq. (3.13) may be

written as,

$$\begin{aligned}\sum_{\beta} O_{\alpha\beta}F(E_\alpha, E_\beta) &= \sum_{\beta} O_{s(\alpha)s(\beta)}\delta_{\alpha_B(\alpha)\alpha_B(\beta)}F(E_\alpha, E_\beta) \\ &= \sum_{n\in\mathcal{N}_\mathcal{O}} O_{s(\alpha)s(n)}F(E_\alpha, E_\alpha - \Delta\epsilon_n).\end{aligned} \tag{3.14}$$

We thus observe that summations of observables multiplied by functions of energy may be significantly simplified by application of the sparsity condition on $O_{\alpha\beta}$. Notably, the summation has been reduced from a sum over $\mathcal{N}$ elements, to a summation over $d_S(d_S - 1) + 1$ elements.

Finally, it is important to note when we may use the sparsity condition in the RMT form, Eq. (3.12), to describe a summation of the form Eq. (3.13) in a realistic system as we have just described. We can see this is the case where the function F is defined over some width Γ_F, such that $F(E_\alpha, E_\beta)$ for $E_\alpha - E_\beta \gg \Gamma_F$ vanishes. In this case, in order to apply (3.12) we no longer require that all neighbouring energy levels of the non-interacting Hamiltonian are separated by a constant energy ω_0, rather, simply that energy levels within the width Γ_F of can be approximated as such. We thus observe that in a realistic system the average energy spacing ω_0 may change with energy over an energy width wider than Γ_F, and Eq. (3.12) may be applied. We will analyse this requirement in more detail in the next section.

This consideration is important in application of RMT to realistic models. It implies that we do not require the entire Hamiltonian of the physical model to resemble the RMT model described by Eq. (2.10), rather, we require only such a resemblance locally in energy. This important consideration is treated more formally in the next section, where physical conditions are found to justify its application.

3.2.2 Smoothness

Above we have seen that a generic feature of local observables may be understood from consideration of the possible transitions caused by action of a local operator onto a state of the total system in the non-interacting basis. We have observed that this can be applied to summations of the form Eq. (3.13), in order to drastically reduce the number of terms involved in the summation, as only terms that correspond to energy transitions of the system contribute. In this section, we will see that a further condition - *smoothness* - allows for the evaluation of the remaining sum, and we will derive specific conditions on the system and observable that ensure the validity of the smoothness assumption.

Continuing, then, in order to carry out the summation in Eq. (3.13), we will require a further condition on observable matrix elements $O_{\alpha\beta}$. That is, we wish to observe under which conditions we may perform the approximation

$$\sum_{\alpha} O_{\alpha,\alpha+n}F(E_{\alpha_0}, E_\alpha + \Delta\epsilon_n) \approx \mathcal{O}_n(\alpha_0)\sum_{\alpha} F(E_{\alpha_0}, E_\alpha + \Delta\epsilon_n), \tag{3.15}$$

where $\mathcal{O}_n(\alpha_0)$ is a smoothed, or coarse grained[2], version of the observable $\overline{O_{\alpha,\alpha+n}} = \mathcal{O}_n(\alpha_0)$, at an energy E_{α_0}. This approximation will be of particular importance to later chapters, where it will be used to simplify expressions obtained using RMT. We now wish to understand the conditions under which the approximation of Eq. (3.15) is valid, and test if these conditions are reasonable for a typical non-integrable many-body system.

To this end, we consider a the function $F(E_\alpha, E_\beta)$ to be normalized, with a characteristic width Γ_F, such that

$$\begin{aligned} \sum_\alpha F(E_{\alpha_0}, E_\alpha + \Delta\epsilon_n) &= 1, \\ \sum_\alpha F(E_{\alpha_0}, E_\alpha + \Delta\epsilon_n)(E_\alpha - E_{\alpha_0}) &= 0 \\ \sum_\alpha F(E_{\alpha_0}, E_\alpha + \Delta\epsilon_n)(E_\alpha - E_{\alpha_0})^2 &= \Gamma_F^2. \end{aligned} \tag{3.16}$$

We may then calculate the (coarse-grained) variance,

$$\Delta_O^2(\Delta\epsilon_n) = \overline{\left(\sum_\alpha O_{\alpha,\alpha+n} F(E_{\alpha_0}, E_\alpha + \Delta\epsilon_n) - \mathcal{O}_n(\alpha_0)\right)^2}, \tag{3.17}$$

which provides a measure of the deviations from the approximation of Eq. (3.15). We see

[2]This coarse graining procedure could be, for example, a microcanonical or weighted average around the element α, or one could treat the values $O_{\alpha\alpha}$ themselves as random variables with some distribution, in which case the overline would represent an ensemble average over this distribution. For now the specifics of the coarse graining procedure are not important - however later we will use $\overline{O_{\alpha,\alpha+n}O_{\beta,\beta+n}} = \mathcal{O}_n(\alpha)\mathcal{O}_n(\beta)$ for $\alpha \neq \beta$, and thus we limit to procedures congruent with this condition.

that Eq. (3.17) can be expanded to obtain,

$$\begin{aligned}
\Delta_O^2 &= \sum_{\alpha\beta} \overline{O_{\alpha,\alpha+n}O_{\beta\beta+n}} F(E_{\alpha_0}, E_\alpha + \Delta\epsilon_n) F(E_{\alpha_0}, E_\beta + \Delta\epsilon_n) + \mathcal{O}_n(\alpha_0)^2 \\
&\quad - 2\mathcal{O}_n(\alpha_0) \sum_\alpha \overline{O_{\alpha,\alpha+n}} F(E_{\alpha_0}, E_\alpha + \Delta\epsilon_n) \\
&= \sum_{\substack{\alpha\beta \\ \alpha\neq\beta}} \overline{O_{\alpha,\alpha+n}}\,\overline{O_{\beta,\beta+n}} F(E_{\alpha_0}, E_\alpha + \Delta\epsilon_n) F(E_{\alpha_0}, E_\beta + \Delta\epsilon_n) + \mathcal{O}_n(\alpha_0)^2 \\
&\quad + \sum_\alpha \overline{(O_{\alpha\alpha})^2} F(E_{\alpha_0}, E_\alpha + \Delta\epsilon_n)^2 - 2\mathcal{O}_n(\alpha_0) \sum_\alpha \overline{O_{\alpha,\alpha+n}} F(E_{\alpha_0}, E_\alpha + \Delta\epsilon_n) \\
&= \sum_{\alpha\beta} \overline{O_{\alpha,\alpha+n}}\,\overline{O_{\beta,\beta+n}} F(E_{\alpha_0}, E_\alpha + \Delta\epsilon_n) F(E_{\alpha_0}, E_\beta + \Delta\epsilon_n) + \mathcal{O}_n(\alpha_0)^2 \\
&\quad + \sum_\alpha \overline{(O_{\alpha\alpha})^2} F(E_{\alpha_0}, E_\alpha + \Delta\epsilon_n)^2 - 2\mathcal{O}_n(\alpha_0) \sum_\alpha \overline{O_{\alpha,\alpha+n}} F(E_{\alpha_0}, E_\alpha + \Delta\epsilon_n) \\
&\quad - \sum_\alpha \overline{O_{\alpha,\alpha+n}}^2 F(E_{\alpha_0}, E_\alpha + \Delta\epsilon_n)^2 \\
&= \sum_\alpha \left(\overline{(O_{\alpha,\alpha+n})^2} - \mathcal{O}_n(\alpha)^2 \right) F(E_{\alpha_0}, E_\alpha + \Delta\epsilon_n)^2 \\
&\quad + \left(\sum_\alpha \mathcal{O}_n(\alpha) F(E_{\alpha_0}, E_\alpha + \Delta\epsilon_n) - \mathcal{O}_n(\alpha_0) \right)^2 \\
&:= \Delta_{O,1}^2 + \Delta_{O,2}^2,
\end{aligned} \tag{3.18}$$

where to arrive at the third equality we add and subtract the term $\sum_\alpha \overline{O_{\alpha\alpha}}^2 F(E_{\alpha_0}, E_\alpha + \Delta\epsilon_n)^2$, and further, we have used that $\overline{O_{\alpha,\alpha+n}O_{\beta,\beta+n}} = \mathcal{O}_n(\alpha)\mathcal{O}_n(\beta)$ for $\alpha \neq \beta$.

Deviations from the approximation (3.15) therefore come from two terms. The first term, $\Delta_{O,1}^2$, can be seen to depend on the smoothed observable variance,

$$\left(\overline{(O_{\alpha,\alpha+n})^2} - \mathcal{O}_n(\alpha)^2 \right). \tag{3.19}$$

For spin operators this is bounded by 1, and more generally is bounded by $|\max(O_S) - \min(O_S)|$. We thus see that the first contribution is bounded by

$$\Delta_{O,1}^2 \leq |\max(O_S) - \min(O_S)| \sum_\alpha F(E_{\alpha_0}, E_\alpha + \Delta\epsilon_n)^2, \tag{3.20}$$

which is small when

$$\sum_\alpha F(E_{\alpha_0}, E_\alpha + \Delta\epsilon_n)^2 \ll 1. \tag{3.21}$$

The latter condition occurs (noting that F is normalised), when there are many terms contributing to the summation over α. In fact, the summation in Eq. (3.21) can be seen to be of the order $\frac{1}{\Gamma_F D_{\alpha_0}}$, where D_{α_0} is the DOS at energy E_{α_0}.

The second contribution, $\Delta_{O,2}^2$, to the variance (3.17) can be bounded assuming that $\mathcal{O}(\alpha)$ is approximately constant over a width Γ_F around the energy E_α. In this case, we may expand $\mathcal{O}(\alpha)$ in the form of a Taylor series, $\mathcal{O}(\alpha) \approx \mathcal{O}(\alpha_0) + \mathcal{O}'(\alpha_0)(E_\alpha - E_{\alpha_0}) +$

$(1/2)\mathcal{O}''(\alpha_0)(E_\alpha - E_{\alpha_0})^2$, such that

$$\begin{aligned}\Delta_{O,2}^2 \approx &\Big(\mathcal{O}(\alpha_0)\sum_\alpha F(E_{\alpha_0}, E_\alpha + \Delta\epsilon_n) + \mathcal{O}'(\alpha_0)\sum_\alpha F(E_{\alpha_0}, E_\alpha + \Delta\epsilon_n)(E_\alpha - E_{\alpha_0}) \\ &+ \frac{1}{2}\mathcal{O}''(\alpha_0)\sum_\alpha F(E_{\alpha_0}, E_\alpha + \Delta\epsilon_n)(E_\alpha - E_{\alpha_0})^2 - \mathcal{O}(\alpha_0)\Big)^2 \\ = &\frac{1}{4}\mathcal{O}''(\alpha_0)^2\Gamma_F^4.\end{aligned} \tag{3.22}$$

Therefore, we see that $\Delta_{O,2}$ is simply the variation in $\mathcal{O}$ over the width Γ_F. Thus, we recover the following conditions for the Eq. (3.17) to be small, and thus the smoothness approximation to be valid:

$$\begin{aligned}\frac{\Gamma_F}{\omega_0} &\gg 1 \\ \Gamma^2\Big|\frac{d^2}{dE_\alpha^2}\mathcal{O}(\alpha)\Big| &\ll 1.\end{aligned} \tag{3.23}$$

Here we have used that $D(E) = \frac{1}{\omega_0}$, and such the first condition in (3.23) asserts that many states are present in an energy range Γ_F ensuring that $\Delta_{O,1} \ll 1$. The second condition can be understood as the statement that the smoothed observable $\mathcal{O}(\alpha)$ does not vary too quickly over the width Γ_F, and thus assures that $\Delta_{O,2} \ll 1$.

Now, applying these conditions to the chaotic wave functions of Section 3.1, we simply replace $\mathcal{O}_n(\alpha_0) \to \overline{[O_{\alpha,\alpha+n}]}_{\alpha_0}$. We note that in all uses below we will be interested in summations over functions F with a characteristic width on the order of Γ, the width of the chaotic wavefunction. In this case, our conditions (3.23) can be understood as: i) each chaotic eigenstate $|\psi_\mu\rangle$ is formed of many non-interacting states, and ii) the smoothed observable $\overline{[O_{\alpha,\alpha+n}]}_{\alpha_0}$ changes slowly in energy E_{α_0} over the width Γ of a single eigenstate.

One can immediately note that the second condition in (3.23) is precisely the requirement for microcanonical average of observable matrix elements that does not vary too quickly in energy to be defined. These conditions are thus natural and intuitive for application to a realistic model.

In order to complete the discussion of defining local observables in RMT, we may wish to understand the conditions under which the above is fulfilled, that is, recast this second condition in terms of physical parameters. To do so, we begin by rewriting explicitly the expression for $\overline{[O_{\alpha,\alpha+n}]}_{\alpha_0}$:

$$\overline{[O_{\alpha,\alpha+n}]}_{\alpha_0} = \sum_\alpha O_{\alpha,\alpha+n}\frac{1}{D(E_{\alpha_0})}\frac{\Gamma_{\alpha_0}/\pi}{(E_\alpha - E_{\alpha_0})^2 + \Gamma_{\alpha_0}^2}. \tag{3.24}$$

Note that E_{α_0} and E_α can be interchanged in the definition of Λ, since we require that both Γ_α and $D(E_\alpha)$ vary negligibly over energy scales of the order of Γ_α. Under this very approximation, we can change the Lorentzian into a Dirac delta function. Additionally, we work in the continuum limit, such that we may re-express the sum over α_B as an integral

over the bath eigenstates, $\sum_{\alpha_B} \to \int dE_{\alpha_B} D_B(E_{\alpha_B})$, such that

$$\begin{aligned}
\overline{[O_{\alpha,\alpha+n}]}_{\alpha_0} &= \sum_s (O_S)_{ss_n} \sum_{\alpha_B} \frac{1}{D(E_{\alpha_0})} \delta\left(E_\alpha - E_{\alpha_0}\right) \\
&= \sum_s (O_S)_{ss_n} \int dE_{\alpha_B}^{(B)} \frac{D_B(E_{\alpha_B})}{D(E_{\alpha_0})} \delta\left(E_\alpha - E_{\alpha_0}\right) \\
&= \sum_s (O_S)_{ss_n} \int dE_{\alpha_B}^{(B)} \frac{D_B(E_{\alpha_B})}{D(E_{\alpha_0})} \delta\left(\epsilon_s + E_{\alpha_B}^{(B)} - E_{\alpha_0}\right) \\
&= \sum_s (O_S)_{ss_n} D_B(E_{\alpha_0} - \epsilon_s) \frac{1}{D(E_{\alpha_0})} \\
&= \sum_s (O_S)_{ss_n} p_{\alpha_0}(s).
\end{aligned} \tag{3.25}$$

Here s_n indicates that the system observable element contributing to $O_{\alpha,\alpha+n}$, such that $O_{\alpha,\alpha+n} = (O_S)_{ss_n} \delta_{\alpha_B(\alpha)\alpha_B(\alpha+n)}$. We have further defined the probabilities

$$p_{\alpha_0}(s) = \frac{D_B(E_{\alpha_0} - \epsilon_s)}{D(E_{\alpha_0})} = \frac{D_B(E_{\alpha_0} - \epsilon_s)}{\sum_s D_B(E_{\alpha_0} - \epsilon_s)}, \tag{3.26}$$

Here we have used that the density of states may be written in terms of the bath density of states $D_B(E)$ via,

$$D(E_\alpha) = \sum_s D_B(E_\alpha - \epsilon_s), \tag{3.27}$$

which counts the number of states of the bath that matches the energies of the system.

Notice that the expression Eq. (3.25) does not rely on the RMT description, and is a reasonable definition of a microcanonical average assuming only that the density of states changes slowly over the width over which the average is taken. Now, the smoothness condition on observables becomes

$$\Gamma^2 \left| \frac{d^2}{dE_{\alpha_0}^2} \left(\sum_s (O_S)_{ss_n} p_{\alpha_0}(s) \right) \right| \ll 1, \tag{3.28}$$

so, we wish to calculate the second derivative of Eq. (3.25), in order to obtain conditions that lead to its contribution being small. Continuing, then, we note that as $D_B(E)$ is positive, we can define a function $\beta(E)$ such that

$$D_B(E) = e^{\beta(E)E}, \tag{3.29}$$

and thus,

$$\begin{aligned}
p_{\alpha_0}(s) &= \frac{e^{\beta(E_{\alpha_0} - \epsilon_s)(E_{\alpha_0} - \epsilon_s)}}{\sum_{s'} e^{\beta(E_{\alpha_0} - \epsilon_{s'})(E_{\alpha_0} - \epsilon_{s'})}} \\
&= \frac{e^{-\beta(E_{\alpha_0})\epsilon_s}}{\sum_{s'} e^{-\beta(E_{\alpha_0})\epsilon_{s'}}},
\end{aligned} \tag{3.30}$$

where in the second line we have assumed that $\beta(E_{\alpha_0} - \epsilon_s) \approx \beta(E_\alpha) \forall\, s$, as $\epsilon_s \ll E_{\alpha_0}$.

This is a physical condition for our scenario, where the (sub)system S is a small part of a total system, and the bath is initialised in a state that is not close to its ground state. We thus write,

$$\frac{d^2}{dE_{\alpha_0}^2}\sum_s (O_S)_{ss_n} p_{\alpha_0}(s) = \sum_s (O_S)_{ss_n} \frac{d^2}{dE_{\alpha_0}^2} \frac{e^{-\beta(E_{\alpha_0})\epsilon_s}}{\sum_{s'} e^{-\beta(E_{\alpha_0})\epsilon_{s'}}}. \tag{3.31}$$

Now, performing these derivatives leads to the expression,

$$\begin{aligned}\frac{d^2}{dE_{\alpha_0}^2} \frac{e^{-\beta(E_{\alpha_0})\epsilon_s}}{\sum_{s'} e^{-\beta(E_{\alpha_0})\epsilon_{s'}}} &= e^{-\beta(E_{\alpha_0})\epsilon_s}\Bigg[2\beta'(E_{\alpha_0})^2\frac{\langle\epsilon\rangle_S^2}{Z_p} - \beta'(E_{\alpha_0})^2\frac{\langle\epsilon^2\rangle_S}{Z_p} + \beta''(E_{\alpha_0})\frac{\langle\epsilon\rangle_S}{Z_p} \\ &\qquad - 2\epsilon_s\beta'(E_{\alpha_0})^2\frac{\langle\epsilon\rangle_S}{Z_p} + \beta'(E_{\alpha_0})^2\frac{\epsilon_s^2}{Z_p} - \beta''(E_{\alpha_0})\frac{\epsilon_s}{Z_p}\Bigg] \\ &\leq \frac{e^{-\beta(E_{\alpha_0})\epsilon_s}}{Z_p}\Bigg[3\beta'(E_{\alpha_0})^2(\epsilon_{max}^2 - \epsilon_{min}^2) + \beta''(E_{\alpha_0})(\epsilon_{max} - \epsilon_{min})\Bigg],\end{aligned} \tag{3.32}$$

with $Z_p = \sum_s e^{-\beta(E_{\alpha_0})\epsilon_s}$, $\langle\epsilon\rangle_S = \frac{\sum_s \epsilon_s e^{-\beta(E_{\alpha_0})\epsilon_s}}{Z_p}$, $\beta'(E_{\alpha_0}) = \frac{d\beta(E_{\alpha_0})}{dE_{\alpha_0}}$, and $\beta''(E_{\alpha_0}) = \frac{d^2\beta(E_{\alpha_0})}{dE_{\alpha_0}^2}$. We can then define $\Delta\epsilon = \epsilon_{max} - \epsilon_{min}$ and $\Delta\epsilon^2 = \epsilon_{max}^2 - \epsilon_{min}^2$, such that,

$$\frac{d^2}{dE_{\alpha_0}^2}\sum_s (O_S)_{ss_n} p_{\alpha_0}(s) \leq 3||O_S||\Delta\epsilon^2\beta'(E_{\alpha_0}) + ||O_S||\Delta\epsilon\beta''(E_{\alpha_0}), \tag{3.33}$$

where $||O_S||$ is simply the maximum element in O_S. Thus, we arrive at three separate conditions for the fulfilment of the smoothness condition:

$$\begin{aligned}\frac{\Gamma}{\omega_0} &\gg 1 \\ \Gamma^2|\beta'(E_{\alpha_0})^2| &\ll \frac{1}{3||O_S||\Delta\epsilon^2} \\ \Gamma^2|\beta''(E_{\alpha_0})| &\ll \frac{1}{||O_S||\Delta\epsilon}.\end{aligned} \tag{3.34}$$

The first condition is fulfilled when eigenstates $|\psi_\mu\rangle$ of H are made up of many contributing non-interacting eigenstates $|\phi_\alpha\rangle$. Further, for the latter two conditions, we can see that the function $\beta(E)$, defined through the density of states $D_B(E) = e^{\beta(E)E}$, can be understood as a microcanonical inverse temperature. In-fact, for the standard case of statistical physics, where the bath is infinite in size, and at temperature β_B, $D_B(E) = e^{\beta_B E}$, we see that these conditions are trivially fulfilled.

It is also interesting to note that if the density of states is constant in the sense that $D_B(E_{\alpha_0} - \epsilon_S) = D_B(E_{\alpha_0})$ we have, from Eq. (3.26), $p_{\alpha_0}(s) = \frac{1}{d_S}$, and we recover the equal a-priori probabilities, and the smoothness condition is also trivially satisfied.

We therefore observe that above requirements fit into standard quantum statistical physics, and constitute a more general set of assumptions that are fulfilled by, but not limited to, the canonical and microcanonical assumptions of an exponentially increasing

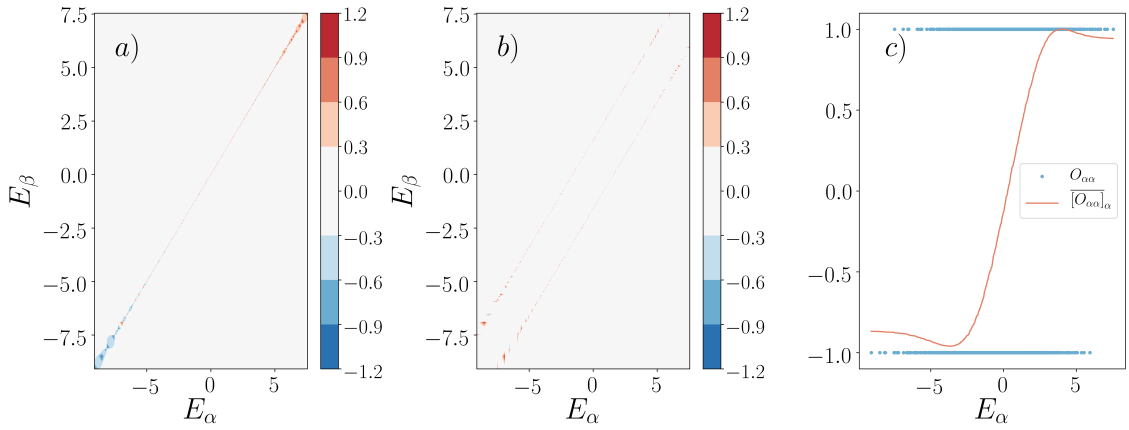

Figure 3.2: Demonstration of sparsity a), b), and smoothness c) of observables of a spin-chain model. a) Plot of $O_{\alpha\beta}$ for $O = \sigma_z$ b) Plot of $O_{\alpha\beta}$ for $O = \sigma_x$ c) Plot diagonal elements $O_{\alpha\alpha}$ and microcanonical average $\overline{[O_{\alpha\alpha}]}_\alpha$ for $O = \sigma_z$. Hamiltonian given in Eq. (5.60), parameters: $N = 10, B_x^{(S)} = B_z^{(B)} = 0, B_z^{(S)} = 0.8, B_x^{(B)} = 0.3, J_z^{(B)} = 0.1, J_z^{(S)} = 0.2, J_x^{(B)} = 1., J_x^{(S)} = 0.4$.

DOS, and constant probability distribution over observable outcomes, respectively. We thus see that the approach based on chaotic wavefunctions is a more general description, which is compatible with the standard formulations of quantum statistical physics in their respective limits.

Finally, we note that it is under these very conditions that the general sparsity condition Eq. (3.14) may be replaced by Eq. (3.15), as the average energy spacing ω_0 is approximately constant over the width Γ.

3.3 Summary of Assumptions

Above we have discussed physical conditions under which we can use RMT approaches to describe realistic quantum systems. The first condition, which derives from a discussion of the locality of observables, enforces that the observable take an ordered and sparse structure in the non-interacting basis. A simpler form can be derived from RMT, which exploits a constant average energy spacing ω_0. This condition is given by Eq. (3.12), which is referred to as the *sparsity* condition.

Additional conditions, referred to as *smoothness*, are required in order to exploit the RMT form of the sparsity condition in a real system, and further to evaluate summations and perform calculations. These conditions are seen in Eq. (3.23) to describe the ability for one to define a microcanonical average of an observable that varies smoothly in energy over a width Γ[3]. This can then be written in terms of physical quantities via Eq. (3.34), which state that the smoothness condition is fulfilled as long as the microcanonical temperature varies sufficiently smoothly with energy, and also that many states lie within an energy

[3]This can thus be seen as a minimal assumption for statistical physics to apply, as without this condition the equilibrium state cannot depend smoothly on the initial state, and thus has sensitive dependence to the initial *microstate*.

range Γ. A demonstration of the smoothness and sparsity conditions is shown in Fig. 3.2. Note that the first form, Eq. (3.23) describes the most general assumption required for the validity of the methods to be developed, whereas Eq. (3.34) has the feature of expressing these conditions in terms of a physical thermodynamics property of a physical system.

Together, the assumptions may be summarised as allowing summations to be calculated along the following outline:

$$\begin{aligned}\sum_{\alpha\beta} O_{\alpha\beta}F(\alpha_0,\alpha,\beta) &\xrightarrow{\text{sparsity}} \sum_{n}^{\mathcal{N}_O}\sum_{\alpha}(O_S)_{\alpha,\alpha(n)}F(\alpha_0,\alpha,\alpha(n)) \\ &\xrightarrow{\text{smoothness}} \sum_{n}^{\mathcal{N}_O}\overline{[O_{\alpha,\alpha+n}]}_{\alpha_o}\sum_{\alpha}F(\alpha_0,\alpha,\alpha+n)\end{aligned} \tag{3.35}$$

for some F, centred on energy E_{α_0}, with some width Γ_F.

In the following chapters, these conditions will be exploited in order to develop a theory of chaotic wavefunctions for application to non-integrable quantum systems. Note that the imposed conditions on observables constitute a far weaker assumption than the ETH itself.

Chapter 4

Main Results: A Non-Technical Overview

In the following chapters I will develop a model of thermalization based on the RMT approach and assumptions on chaotic wavefunctions described in the previous chapter. The algebraic structure of the theory is applicable to local observables of systems with wavefunctions satisfying Eq. (3.1). We will see that a dynamical approach to quantum statistical mechanics can be obtained, and, further, that hints at the emergence of classical behaviour are observed. Particular attention is also paid to applications of the theoretical model to near term quantum devices, and their characterisation. In the following, I will summarise the key results of the remainder of this thesis.

The main result of Chapter 5 is a derivation of the eigenstate thermalization hypothesis (ETH) from chaotic wavefunctions. The method outlined in performing this calculation will be the main tool that is developed through the rest of this text, and applied to more complex calculations. This takes the form of an approach to the calculation of arbitrary correlation functions ,

$$\langle c_\mu(\alpha)c_\nu(\beta)\cdots c_\mu(\alpha')c_\nu(\beta')\rangle_V, \tag{4.1}$$

of chaotic wavefunctions. We will see that, reminiscent of Wick's theorem, summations over these correlation functions may be factorised into possible contractions of interacting and non-interacting indices. However, it will be shown that, as described in the previous chapter, a Gaussian ansatz on chaotic wavefunctions is not sufficient for the description of off-diagonal matrix elements of observables, and an additional factor enforcing the mutual orthogonality of eigenstates is required, as in Eq. (3.1). This effective interaction in the statistical theory of chaotic wavefunctions causes a non-trivial 4-point correlation function, which may not be factorised. This correlation function will become the basis for many calculations throughout this work via a 'self-averaging' property, commonly used in random matrix theory (RMT) approaches, which is discussed and proven in Appendix C.

This theory of correlation functions is exploited to derive the ETH, as well as a form for the long-time fluctuations that will be further elaborated on in Chapter 6. It is thus demonstrated that, under the assumptions of quantum chaos, equilibrium quantum statistical physics may be justified. That is, via derivation of the ETH we see that the time

average of an observable is equal to the microcanonical average, and the time-fluctuations are small. The key focus of Chapter 5 is on observables that are diagonal in the basis of H_0 - results will be extended to the full form implied by the sparsity condition in Chapter 6, and Appendix B.

A further discussion in Chapter 5 is an analysis of when a physical Hamiltonian may be described by the RMT approach. Numerical exact diagonalizations are performed to analyse when a full random matrix interaction Hamiltonian V well describes a realistic interaction Hamiltonian. It is seen that in a low coupling limit, defined by the energy scale of the width of the banded interaction Hamiltonian of the real system, the eigenstates have a form that matches the RMT model. Above this coupling strength the banded nature of the interaction Hamiltonian can be seen to affect the structure of the wavefunctions, and a deviation from a Lorentzian form derived from RMT, to a Gaussian form, is observed. We note that the theory of chaotic wavefunctions is still valid in this high coupling regime, the ETH still holds, and the fluctuations maintain the same form, with a different numerical prefactor. Indeed, a Gaussian ansatz on Λ in this regime matches well with the numerics.

In Chapter 6 a fully dynamical theory of the approach to equilibrium is developed from the statistical theory of correlation functions of Chapter 5. It is shown that after initialisation in a non-equilibrium pure state the expectation value of a local observable decays exponentially to a time average state that is given by a microcanonical average[1]. Further, the form of observable fluctuations obtained in Chapter 5 is investigated in greater detail, which may be understood analogously to a fluctuation-dissipation theorem of classical Brownian motion for time-fluctuations, as the fluctuations can be seen to depend on the rate of decay to equilibrium. We thus label the form of fluctuations the 'quantum chaotic fluctuation-dissipation theorem' (QC-FDT). Numerical analysis will be shown, of both the observable time-dependence and the QC-FDT, for a realistic quantum spin chain.

Chapter 7 will be devoted to an application of the theoretical model to quantum devices. The key problem here is related to proofs of 'quantum supremacy', which aim to show that a particular calculation is infeasible to perform on a classical computer. As discussed in Chapter 1, the main issue with simulating a quantum system on a classical computer is the exponential increase in the memory requirements for increasing size of the quantum system of interest. However, approximation methods are in some cases able to exploit features of the system, such as locality of interactions, to enable calculations of much larger systems than would be possible via exact methods. Thus, due to the fact that quantum devices themselves usually have local connectivity [54], a 'calculation' performed on a device with, say, N qubits, may be executable without storing the 2^N dimensional state in its entirety. The inspiration for Chapter 7 is then to ask the question: given a calculated observable time dependence on a quantum device, what is the minimum Hilbert space dimension required in terms of an *effective* fully connected device? This effective dimension, I claim, is a far better comparison to make between classical computers and quantum devices than simply the Hilbert space dimension in terms of the number of

[1]The exponential decay is a result of the specific RMT model, more generally, for a given chaotic wavefunction distribution Λ, the decay has the form of the Fourier transform of the observable distribution, itself dictated by Λ.

qubits[2].

In order to approach this question I will extend the theoretical model of thermalization dynamics and time-fluctuations to initial finite and infinite temperature states. We will see, then, that the fluctuation-dissipation theorem depends explicitly on the Hilbert space dimension of the random matrix model. Thus, via measurements of the time-fluctuations and decay rate, one may obtain the effective Hilbert space dimension in terms of a fully connected device. The analytical calculations are compared to numerical exact diagonalization calculations, which indeed show that this effective Hilbert space dimension scales exponentially with system size for a non-integrable quantum system.

An important motivation in the study of quantum thermalization is the attempt to understand how the quantum dynamics of an initial pure state leads to the emergence of classical thermodynamic properties. This will be the topic of Chapter 8. In particular, I will discuss the relation of a description of thermalization in terms of chaotic wavefunctions and RMT to classical Brownian motion - a paradigmatic model of classical non-equilibrium statistical physics describing the dynamics of colloidal particles subject to a random noise. We will see that in an appropriate regime, the results of classical Brownian motion are recovered in closed quantum systems, and thus the observable dynamics can be described by an *effective* classical theory.

This emergent classical description can be further observed in more physical scenarios than the observable expectation value dynamics. That is, realistic experiments on quantum systems often cannot access the full dynamics of $\langle O(t)\rangle$, but rather make repeated measurements of a local observable as the system evolves. In such experiments, one acquires a measurement record, or quantum jump trajectory, of measurement outcomes taken at each time step. As the measurement process affects the state of the system, the dynamics as a whole is not unitary; however, in between measurements unitary thermalization dynamics takes place.

In Chapter 8 the approach to the description of Brownian motion in closed quantum systems will be extended to quantum jump trajectories, and thus we will see that classical Brownian motion may be observed in a single system, via repeated quantum measurements. Further, the ability to statistically describe individual quantum trajectories provides a link between quantum chaos and work in stochastic thermodynamics [148, 149]. The latter is the extension of thermodynamic notions such as work, and entropy production to the regime of single classical stochastic trajectories. Here we describe the entropy production, and derive the second law, in the context of quantum jump trajectories.

Further, in Chapter 8, I will derive a fluctuation theorem describing the ratio of quantum fluctuations (the variance of an observable) to the time-averaged fluctuations $\delta^2_O(\infty)$ introduced in Chapter 1. We will see that this fluctuation theorem may be exploited to measure the density of states of a quantum device. This continues the theme of exploiting quantum chaos to characterise such systems.

[2]The latter can be easily seen to be a poor metric by imagining an N dimensional quantum simulator with no connections - the time evolution of any initial state is trivially obtainable, yet the Hilbert space still grows exponentially with N

4.1 Summary

The main contributions of this thesis are thus to develop a theoretical model of the thermalization of closed quantum systems from an ansatz on chaotic wavefunctions of non-integrable models. A dynamical picture of the approach to thermal equilibrium is described for local observables, showing their decay to an equilibrium state given by the microcanonical average. Particular focus is paid to applications on quantum devices, and assumptions are phrased in terms of physical quantities of quantum systems.

The developed theory can be exploited to experimentally measure both the effective Hilbert space dimension of a system, as well as its density of states, and may thus be of use to the experimental community, as well as of theoretical interest to the foundations of statistical physics.

Further, *classical* relations can be shown to emerge in the developed model. That is, for observables with many independent energy levels, the resulting dynamics displays classical Brownian motion, formally identical to an Ornstein-Uhlenbeck process [150] - thus the model has an effective description in terms of a Langevin equation. This effective classical description occurs for the observable expectation value time dependence, but also, more interestingly, from quantum jump trajectories obtained by repeated projective measurements of a local observable. In the latter, we thus observe emergent classical trajectories from a sequence of quantum measurements.

The contributions made by the current work to the field of quantum thermalization are thus important in two clear ways: Firstly, a theoretical model of thermalization dynamics is developed, based only on assumptions on physical properties of a quantum system - namely, quantum chaos, as described above. This theory is extended beyond the usual setting of quantum thermalization, to also to describe a more physical measurement protocol of quantum jump trajectories, where classical Brownian dynamics is observed. Second, this model is applied to the characterisation of realistic quantum devices that may be currently experimentally studied, and shown to allow for the measurement of relevant quantities such as the density of states, and the effective Hilbert space dimension.

Chapter 5

Off-Diagonal Observable Elements from Random Matrix Theory: Distributions, Fluctuations, and Eigenstate Thermalization

5.1 Abstract

We derive the Eigenstate Thermalization Hypothesis (ETH) from a random matrix Hamiltonian by extending the model introduced by J. M. Deutsch [64]. We approximate the coupling between a subsystem and a many-body environment by means of a random Gaussian matrix. We show that a common assumption in the analysis of quantum chaotic systems, namely the treatment of eigenstates as independent random vectors, leads to inconsistent results. However, a consistent approach to the ETH can be developed by introducing an interaction between chaotic wavefunctions that arises as a result of the orthonormality condition. This approach leads to a consistent form for off-diagonal matrix elements of observables. From there we obtain the scaling of time-averaged fluctuations of generic observables with system size for which we calculate an analytic form in terms of the Inverse Participation Ratio. The analytic results are compared to exact diagonalizations of a quantum spin chain for different physical observables in multiple parameter regimes.

5.2 Introduction

The emergence of statistical physics from unitary quantum dynamics has been debated since the early days of quantum theory [3]. It is by now widely accepted that generic non-integrable quantum systems undergo a process known as quantum thermalization, which implies that an initially out-of-equilibrium state of an isolated quantum system will approach thermal equilibrium after some typical relaxation time. The underlying mechanism behind quantum thermalization is still a subject of debate [57–59, 66, 72, 73, 127–129, 151–154]. One of the most successful approaches to this long-standing problem is the

Eigenstate Thermalization Hypothesis (ETH) [63, 64, 67]. According to this conjecture, the many-body eigenstates of a non-integrable Hamiltonian yield the same expectation values of local observables as those calculated with a microcanonical ensemble. Below we will give a more detailed presentation of this conjecture, which can be formulated as an ansatz for the matrix elements of observables in the eigenbasis of a many-body Hamiltonian. To visualise qualitatively the physics behind the ETH, we can consider a quantum lattice system with interactions coupling different sites. If we express a many-body eigenstate in a local basis, we expect that interactions lead to a highly entangled state distributed over the lattice [78, 155]. The ETH assumes that the resulting linear superposition has similar properties to a microcanonical ensemble. Note that this mechanism for thermalization is purely quantum mechanical since the existence of quantum correlations and entanglement are essential ingredients.

The validity of the ETH has been confirmed for a wide range of non-integrable systems by means of exact diagonalizations [95, 109, 112, 156–159]. Still, there are some aspects of quantum thermalization and the ETH that are not completely clear. The conjecture can be qualitatively justified by using the theoretical framework of quantum chaos, however, it has not yet been fully derived mathematically from first principles. A possible direction to address the validity of the ETH is to try to derive it from a more basic or fundamental assumption or set of assumptions. In particular, we know that many-body eigenstates of large systems can be often described by Random Matrix Theory (RMT). The original work by J. Deutsch [64] actually used a Random Matrix Hamiltonian as a toy model to show the emergence of quantum thermalization in isolated quantum systems. In Deutsch's approach, a non-ergodic system is perturbed by a Gaussian random matrix, which results in an approximate description of many-body eigenstates by wavefunctions with uncorrelated random coefficients. This theoretical framework does not by itself prove the occurrence of thermalization in particular many-body systems, however, it proves certain aspects of the process as long as reasonable assumptions on the underlying system are fulfilled.

The quantum thermalization process has two fundamental aspects. Firstly, it involves the equivalence between time-averages of expectation values of observables and microcanonical averages. Secondly, it also involves the equilibration of an initially excited state into a thermal state, that is, we expect that time-fluctuations around thermal averages will be small. Furthermore, those fluctuations should decrease with system size such that statistical mechanics is recovered in the thermodynamic limit. Equilibration is governed by the off-diagonal matrix elements of an observable in the basis of eigenstates of the Hamiltonian. The ETH as formulated by Srednicki [63] includes a condition for off-diagonal matrix elements, which ensures equilibration. Furthermore, it has been proved that a model based on random uncorrelated wavefunctions can be used to qualitatively reproduce the ETH result for time-fluctuations [100]. However, chaotic wavefunction models usually work under the assumption of statistically independent random coefficients, which we label the random wavefunction ansatz. This condition limits the validity of this approach, as we show in the next section.

A deeper understanding of time-fluctuations in the quantum thermalization process

is actually crucial to describe current experiments with microscopic systems. Physical realisations of isolated quantum systems, where the emergence of statistical physics can be investigated, have been made possible only recently due to advances in quantum simulators with atomic and solid-state systems [49, 50, 160]. These include ultracold atoms [45, 161, 162], trapped ions [12, 163], and superconducting qubits [13]. Identifying quantum thermalization would ideally involve a comparison between observed time-averages and microcanonical averages, however computing the latter is a challenge in complex many-body systems. An alternative path to test theoretical ideas such as the ETH is to check predictions made on the time-fluctuations of observables, such as the scaling with system size or interaction strength. For that aim, a deeper understanding of the physics and assumptions underlying the ETH would be required, to obtain quantitative predictions that can be used to identify ergodic phases in experiments.

In this chapter, we present a derivation of the ETH in a random matrix model that yields an approximate description of a quantum non-integrable system under some reasonable assumptions. We build on the theoretical model introduced by J. Deutsch [64], and extend it to the calculation of off-diagonal matrix elements of observables. We show that correlations induced by orthonormality between chaotic wavefunctions must be taken into account to obtain a consistent derivation of the ETH from Random Matrix Theory. Our work cannot be considered as a proof of the validity of the ETH, however, it shows that the conjecture can be fully obtained from a description in terms of chaotic wavefunctions. Our theory can be used to quantify time-fluctuations after a quantum quench, and to predict the scaling of fluctuations with system size, thus yielding predictions that can be compared with experimental results and used to identify ergodic regimes in quantum many-body systems.

This chapter is structured as follows. In Section 5.3 we introduce the ETH ansatz and discuss the limitations of a model of independent random wavefunctions to describe the behaviour of off-diagonal matrix elements of observables. In Section 5.4 we introduce Deutsch's random matrix model consisting of a diagonal Hamiltonian perturbed by a Gaussian random matrix. We extend the original model to account for interactions between chaotic wavefunctions arising from the orthonormality condition. In Section 5.5 we calculate the correlation functions between chaotic wavefunctions. In Section 5.6 we use those correlation functions to calculate the off-diagonal matrix elements of an operator, and show that they take the same form predicted by the ETH. In Sections 5.7 and 5.8 we present a numerical confirmation of our analytical results. Finally, in Section 5.9 we show that our model provides us with a good description of the time-fluctuations in a non-integrable quantum spin chain. We finish with our Conclusions in Section 5.10, where we discuss the range of applicability of our results and their implications.

5.3 Eigenstate Thermalization Hypothesis and the Limitation of the Independent Random Wavefunction Ansatz

In this section, we introduce the ETH and the random wavefunction ansatz. We will show that a description of many-body wavefunctions based on independent random variables does not lead to a consistent description of off-diagonal matrix elements of typical observables.

To focus our discussion, consider a system described by a non-integrable Hamiltonian, H, with eigenvectors and eigenenergies $|\psi_\mu\rangle$ and E_μ, respectively, such that $H|\psi_\mu\rangle = E_\mu|\psi_\mu\rangle$. The system is initially in the state $|\Psi(0)\rangle = \sum_\mu c_\mu|\psi_\mu\rangle$ with mean energy $\bar{E} := \langle\Psi(0)|H|\Psi(0)\rangle$. The equilibration of a closed quantum system into a thermal state implies that (assuming non-degenerate energy levels),

$$\lim_{T\to\infty}\frac{1}{T}\int_0^T\langle O(t)\rangle dt = \sum_\mu |c_\mu|^2 O_{\mu\mu} \approx \langle O\rangle_{\text{micro}}, \tag{5.1}$$

where we have used the definition $O_{\mu\mu} := \langle\psi_\mu|O|\psi_\mu\rangle$. Eq. (5.1) expresses an equivalence between the time-average of $\langle O(t)\rangle$ and the microcanonical average of O taken over an energy shell of eigenstates with energies E_μ close to $\bar{E}$. The ETH for diagonal elements of observables consists of the assumption that $O_{\mu\mu}$ is a smooth function of the energy E_μ, $\mathcal{O}(E_\mu)$,

$$O_{\mu\mu} \underset{\text{ETH}}{=} \mathcal{O}(E_\mu). \tag{5.2}$$

Assuming that probabilities $|c_\mu|^2$ take non-vanishing values close to $\bar{E}$, the ETH ensures that the second term in Eq. (5.1) is equivalent to a microcanonical average.

To understand the relation between the ETH and a random wavefunction ansatz, let us assume that the observable O is a local operator in a quantum lattice model defined on a subsystem S. The rest of the lattice forms a bath, B, and we write the total Hamiltonian like $H = H_S + H_B + H_{SB}$, where H_{SB} is the interaction term. Now we define $H_0 = H_S + H_B$, and the non-interacting energy eigenbasis, $H_0|\phi_\alpha\rangle = E_\alpha|\phi_\alpha\rangle$. To simplify the notation in what follows we will assume that variables with indices μ, ν refer to eigenenergies or eigenstates of the interacting Hamiltonian, whereas indices α, β refer to H_0.

The random wavefunction ansatz consists of the assumption that

$$|\psi_\mu\rangle = \sum_\alpha c_\mu(\alpha)|\phi_\alpha\rangle, \tag{5.3}$$

with $c_\mu(\alpha)$ independent normalized random variables with average

$$\langle c_\mu(\alpha)c_{\mu'}(\alpha')\rangle_V = \delta_{\mu,\mu'}\delta_{\alpha,\alpha'}\Lambda(\mu,\alpha), \tag{5.4}$$

where $\Lambda(\mu,\alpha)$ is a function of $(E_\mu - E_\alpha)$, normalized such that $\sum_\alpha \Lambda(\mu,\alpha) = \sum_\mu \Lambda(\mu,\alpha) = 1$. The average $\langle\cdots\rangle_V$ is taken over realisations of the random wavefunction (this will be more clearly defined in the next section). We assume that the function $\Lambda(\mu,\alpha)$ is smooth,

has a maximum when $E_\mu = E_\alpha$, and vanishes when $E_\mu - E_\alpha \gg \Gamma$, with Γ being a typical energy width. A perturbative calculation, in which $H_{\rm SB}$ was approximated by a random matrix, carried out by Deutsch [65] leads to a random wavefunction model with a Lorentzian,

$$\Lambda(\mu,\alpha) = \frac{\Gamma\omega_0/\pi}{(E_\mu - E_\alpha)^2 + \Gamma^2}, \tag{5.5}$$

where ω_0 is the average spacing between energy levels and we assume for now that both Γ and ω_0 are independent of α, μ. Outside a perturbative regime, however, numerical calculations on non-integrable models have shown that wavefunctions have a Gaussian shape [91, 97, 113, 115, 164].

Diagonal matrix elements in the interacting basis can be approximated under the assumption of self-averaging[1],

$$O_{\mu\mu} = \sum_{\alpha\beta} c_\mu(\alpha)c_\mu(\beta)O_{\alpha\beta} \approx \sum_\alpha \Lambda(\mu,\alpha)O_{\alpha\alpha}, \tag{5.6}$$

where $O_{\alpha\beta} := \langle\phi_\alpha|O|\phi_\beta\rangle$. Eq. (5.6) implies that the coupling induced by $H_{\rm SB}$ leads to the smoothing of the distribution of diagonal matrix elements in the interacting basis and provides us with a justification for the ETH for diagonal elements of observables (5.2) within the random wavefunction model [64, 151], since we can make the identification,

$$\mathcal{O}(E_\mu) = \sum_\alpha \Lambda(\mu,\alpha)O_{\alpha\alpha}, \tag{5.7}$$

which yields a smooth function as long as the sum runs over a sufficiently large number of states.

We also expect that in the thermodynamic limit the average $\langle O(t)\rangle$ does not deviate too much from its mean-value (equilibration aspect of quantum thermalization). The averaged time-fluctuations over an infinite integration time are given by [70],

$$\delta^2_O(\infty) = \sum_{\substack{\mu,\nu \\ \mu\neq\nu}} |O_{\mu\nu}|^2|c_\mu|^2|c_\nu|^2, \tag{5.8}$$

under the assumption of non-degenerate energy gaps. Based on quantum chaos theory, Srednicki [63] introduced the ETH ansatz for the off-diagonal matrix elements $O_{\mu\nu}$,

$$O_{\mu\nu}|_{\mu\neq\nu} \underset{\rm ETH}{=} \frac{1}{\sqrt{D(E)}} f_O(E,\omega)R_{\mu\nu}. \tag{5.9}$$

In this expression $D(E)$ is the density of states (the original expression by Srednicki included an equivalent normalization by using the microcanonical entropy instead), $E = (E_\mu + E_\nu)/2$ and $\omega = E_\nu - E_\mu$. $R_{\mu\nu}$ is a set of random variables with zero average and unit variance. $f_O(E,\omega)$ is a continuous function of E and ω, which we expect to be centred around $\omega = 0$, and take negligible values if the difference between energies ω is larger than a typical energy width.

[1] The self-averaging assumption is proven in Appendix C.2 for the current model.

A natural question is whether a random wavefunction model can be used to justify the ETH ansatz for off-diagonal matrix elements as well. As the off diagonal elements of a typical observable average to zero, it is convenient instead to analyse the squared modulus. To simplify the discussion we restrict our evaluation for now to those observables that are diagonal in the basis of H_0,

$$|O_{\mu\nu}|^2_{\mu\neq\nu} = \sum_{\alpha\beta} c_\mu(\alpha)c_\nu(\alpha)c_\mu(\beta)c_\nu(\beta)O_{\alpha\alpha}O_{\beta\beta}. \tag{5.10}$$

A common assumption that is made here [64, 100] is to treat the coefficients $c_\mu(\alpha)$ as uncorrelated random numbers, the only surviving terms of this sum will then be

$$|O_{\mu\nu}|^2_{\mu\neq\nu} = \sum_{\alpha} |c_\mu(\alpha)|^2|c_\nu(\alpha)|^2O^2_{\alpha\alpha} \approx \sum_{\alpha} \Lambda(\mu,\alpha)\Lambda(\nu,\alpha)O^2_{\alpha\alpha}, \tag{5.11}$$

which actually agrees with the ETH ansatz. However, this expression cannot provide us with a consistent description on off-diagonal matrix elements. To show this, consider the equality

$$\sum_{\nu} |O_{\mu\nu}|^2 = \langle\psi_\mu|O^2|\psi_\mu\rangle. \tag{5.12}$$

Now, analyzing the diagonal and off-diagonal terms of Eq. (5.12) separately, *i.e* $\sum_\nu |O_{\mu\nu}|^2 = |O_{\mu\mu}|^2 + \sum_{\nu\neq\mu} |O_{\mu\nu}|^2$, for the off-diagonal terms we have, given Eq. (5.11),

$$\sum_{\nu} |O_{\mu\nu}|^2_{\mu\neq\nu} \approx \sum_{\alpha} \Lambda(\mu,\alpha)O^2_{\alpha\alpha} \approx \overline{O^2_{\alpha\alpha}}, \tag{5.13}$$

where we have defined a microcanonical average around E_μ, $\overline{O^2_{\alpha\alpha}}$. Now, the sum of off-diagonal elements may also be obtained without use of the random wavefunction ansatz as

$$\begin{aligned}\sum_{\nu} |O_{\mu\nu}|^2_{\mu\neq\nu} &= (O^2)_{\mu\mu} - |O_{\mu\mu}|^2 \\ &\approx \sum_{\alpha} \Lambda(\mu,\alpha)O^2_{\alpha\alpha} - |\sum_{\alpha} \Lambda(\mu,\alpha)O_{\alpha\alpha}|^2 \\ &\approx \overline{O^2_{\alpha\alpha}} - \overline{O_{\alpha\alpha}}^2,\end{aligned} \tag{5.14}$$

where we have only assumed a self-averaging condition. Thus, comparing Eq. (5.14) and Eq. (5.13) we can observe that we obtain an inconsistency. We are thus led to conclude that there are indeed correlations between the coefficients, and that Eq. (5.11) is naïve. If instead we write

$$\sum_{\nu\neq\mu} |O_{\mu\nu}|^2 = \sum_{\nu\neq\mu}\sum_{\alpha} |c_\mu(\alpha)|^2|c_\nu(\alpha)|^2O^2_{\alpha\alpha} + \sum_{\nu\neq\mu}\sum_{\substack{\alpha\beta\\ \alpha\neq\beta}} c_\mu(\alpha)c_\nu(\alpha)c_\mu(\beta)c_\nu(\beta)O_{\alpha\alpha}O_{\beta\beta}, \tag{5.15}$$

we can then apply the self-averaging assumption once more, *i.e* the replacement $\sum_{\nu\neq\mu}\sum_{\substack{\alpha\beta\\ \alpha\neq\beta}} c_\mu(\alpha)c_\nu(\alpha)c_\mu(\beta)c_\nu(\beta)O_{\alpha\alpha}O_{\beta\beta} \to \overline{O_{\alpha\alpha}}^2 \sum_{\nu\neq\mu}\sum_{\substack{\alpha\beta\\ \alpha\neq\beta}} c_\mu(\alpha)c_\nu(\alpha)c_\mu(\beta)c_\nu(\beta)$

which we can see is consistent if this term is equal to $-\overline{O_{\alpha\alpha}}^2$. One can in-fact show simply from expanding the orthogonality condition $\sum_\nu \langle\psi_\mu|\psi_\nu\rangle = 0 \mid \mu \neq \nu$ the relation

$$\sum_{\nu\neq\mu}\sum_{\substack{\alpha\beta\\ \alpha\neq\beta}} c_\mu(\alpha)c_\nu(\alpha)c_\mu(\beta)c_\nu(\beta) = -1 + \mathrm{IPR}(|\phi_\alpha\rangle)). \tag{5.16}$$

where $\mathrm{IPR}(|\phi_\alpha\rangle) := \sum_\mu |c_\mu(\alpha)|^4$ is the inverse participation ratio (IPR)[2], which is small for systems in which our self-averaging procedure is correct. Thus we find that the self-averaging assumption is consistent when applied without use of the random wavefunction ansatz.

The above analysis indicates that correlations between probability amplitudes do in fact play a role, and that the common assumption that the coefficients may be treated as uncorrelated random numbers is naïve. The illustration above is valid for generic systems with no special symmetries or correlations caused by features of the interaction, and thus the only source of these correlations is the orthonormality requirement of eigenstates. Indeed, we will see below that by including these correlations the correct scaling is obtained.

5.4 Model for Generic Non-Integrable Quantum Systems

We now present the random matrix model from which we will base our analysis, consisting of a non-interacting diagonal part, and interactions modelled by a random matrix. Explicitly, the Hamiltonian in question is given by

$$H = H_0 + V, \quad H_{\alpha\beta} = f_\alpha\delta_{\alpha\beta} + h_{\alpha\beta}, \tag{5.17}$$

where the diagonal matrix elements, $f_\alpha = \alpha\omega_0$, are energies equally spaced by ω_0, and we choose energy units such that $\omega_0 = \frac{1}{\mathcal{N}}$, with $\mathcal{N}$ the total number of levels. The perturbation term is a real random Gaussian Hermitian matrix, h, which follows the probability distribution $P(h) \propto \exp\left[-\frac{1}{4}\mathcal{N}\,\mathrm{Tr}\,h^2/g^2\right]$, such that matrix elements $h_{\alpha\beta}$ have average $\overline{h_{\alpha\beta}} = 0$, and variance $\overline{(h_{\alpha\beta})^2} = g^2/\mathcal{N}$ for $\alpha \neq \beta$, and $\overline{(h_{\alpha\alpha})^2} = 2g^2/\mathcal{N}$ for diagonal elements. This is the same Hamiltonian used in the pioneering work by Deutsch [64, 65], which captures the behaviour of a generic non-integrable quantum system in the thermodynamic limit.

We no longer restrict ourselves to observables that are diagonal in the basis of H_0, and thus for a generic observable O we have,

$$|O_{\mu\nu}|^2_{\mu\neq\nu} = \sum_{\alpha\beta\alpha'\beta'} c_\mu(\alpha)c_\nu(\beta)c_\mu(\alpha')c_\nu(\beta')O_{\alpha\beta}O_{\alpha'\beta'}, \tag{5.18}$$

where, to reiterate, we have defined $O_{\mu\nu} := \langle\psi_\mu|O|\psi_\nu\rangle$, and $O_{\alpha\beta} := \langle\phi_\alpha|O|\phi_\beta\rangle$, such that α, β labels the non-interacting basis diagonalizing H_0, $\{|\phi_\alpha\rangle\}$, and μ, ν labels the

[2]Notice that our definition of IPR differs here from the one used in Ref. [12] and in other works in the field of quantum chaos (e.g. [70]) where the reciprocal quantity is defined as the IPR. Our definition in this work is more consistent with the original notion of Participation Ratio as the number of energy eigenstates or atomic orbitals involved in the initial state (see for example Ref. [165])

interacting basis diagonalizing H, $\{|\psi_\mu\rangle\}$. The coefficients $c_\mu(\alpha)$ are random variables representing the eigenstates of H, $|\psi_\mu\rangle = \sum_\alpha c_\mu(\alpha)|\phi_\alpha\rangle$.

In order to obtain a functional form for the off-diagonal observable elements $|O_{\mu\nu}|^2_{\mu\neq\nu}$ we are thus interested in finding the correlation function

$$\langle c_\mu(\alpha)c_\nu(\beta)c_\mu(\alpha')c_\nu(\beta')\rangle_V, \tag{5.19}$$

where the average $\langle\cdots\rangle_V$ is taken over realisations of the random Hamiltonian. We can see from the argument of the previous section that the $c_\mu(\alpha)$s are not true random variables, but have correlations due to orthogonality which must be accounted for. The probability distribution of the $c_\mu(\alpha)$ coefficients is given by

$$\begin{aligned} P(c) = A\delta(cc^T - I)\int \exp\left[-\sum_{\substack{\alpha\beta\\ \alpha>\beta}}\frac{h^2_{\alpha\beta}}{2g^2/\mathcal{N}} - \sum_\alpha \frac{h^2_{\alpha\alpha}}{4g^2/\mathcal{N}}\right] \\ \times\left(\prod_{\substack{\mu\nu\\ \mu>\nu}}\delta(\sum_{\alpha'\beta'} c_\mu(\alpha')H_{\alpha'\beta'}c_\nu(\beta'))\right)\prod_{\substack{\alpha\beta\\ \alpha\geq\beta}} dh_{\alpha\beta}. \end{aligned} \tag{5.20}$$

In Eq. (5.20) we use the shorthand notation, c, to represent the matrix of $c_\mu(\alpha)$s. A is a normalization constant, and we perform the integral over all independent entries of random Hamiltonian matrix elements, $h_{\alpha,\beta}$. Further, we have used $\exp[\sum_{\substack{\alpha\beta\\ \alpha\neq\beta}} h^2_{\alpha\beta}] = \exp[2\sum_{\substack{\alpha\beta\\ \alpha>\beta}} h^2_{\alpha\beta}]$, from which we can see that, for the random matrix selected from the Gaussian Orthogonal Ensemble (GOE), the width of the distribution diagonal elements is twice that of the off-diagonal elements. The first delta-function in $P(c)$ imposes an orthonormalization constraint whereas the last delta-function restricts the values of the $c_\mu(\alpha)$ to those of eigenstates of the Hamiltonian (5.17); the Hermiticity of H implies that the latter need only run over $\mu > \nu$. Working with the exact probability distribution $P(c)$ is obviously very difficult. Studies of quantum chaotic systems [68] indicate, however, that probability amplitudes behave as Gaussian distributed random variables, suggesting we may treat the $c_\mu(\alpha)$s as belonging to a Gaussian distribution with some width depending on μ, α. However, as we saw in Section 5.3 above, we must account for orthogonality in order to obtain a consistent result for off-diagonal matrix elements of observables. We thus look for an approximate probability distribution of the $c_\mu(\alpha)$'s of the form

$$p(c,\Lambda) = \frac{1}{Z_p}\exp\left[-\sum_{\mu\alpha}\frac{c^2_\mu(\alpha)}{2\Lambda(\mu,\alpha)}\right]\prod_{\substack{\mu\nu\\ \mu>\nu}}\delta(\sum_\alpha c_\mu(\alpha)c_\nu(\alpha)). \tag{5.21}$$

In Eq. (5.21) we assume an approximation in terms of independent Gaussian variables, however, we keep the orthonormality constraint to account for correlations. Wavefunctions fulfilling Eq. (5.21) are referred to as *chaotic wavefunctions*. To find the functions $\Lambda(\mu,\alpha)$

that lead to an optimal description of the problem we have to minimise the Free Energy,

$$F = -\int dc p(c,\Lambda) \ln \frac{P(c)}{p(c,\Lambda)}, \tag{5.22}$$

where we have written $\int dc$ as shorthand for an integral over all elements, $\int dc \to \prod_{\mu\alpha} \int dc_\mu(\alpha)$. The calculation of the distributions $\Lambda(\mu,\alpha)$ which fulfil this condition is performed (using a differing target probability distribution $p(c,\Lambda)$) in reference [65]. We repeat this calculation in Appendix A.1 for clarity. We obtain

$$\Lambda(\mu,\alpha) = \omega_0 \frac{\Gamma/\pi}{(\omega_0\mu - \omega_0\alpha)^2 + \Gamma^2}. \tag{5.23}$$

where $\Gamma = \frac{\pi g^2}{\mathcal{N}\omega_0}$, differing by a factor of 2 from reference [65] (this is corroborated below with a numerical calculation). Also required for the calculation of the correlation function (5.19) is the partition function of our approximate probability distribution, which is also obtained in Appendix A.1 (Eq. (A.24)):

$$Z_p = (2\pi)^{\mathcal{N}^2 - \mathcal{N}/2} \left(\prod_{\mu\alpha} (\Lambda(\mu,\alpha))^{\frac{1}{2}} \right) \left(\prod_{\substack{\mu\nu \\ \mu>\nu}} \left(\sum_\alpha \Lambda(\mu,\alpha)\Lambda(\nu,\alpha) \right)^{-\frac{1}{2}} \right). \tag{5.24}$$

In Eq. (5.24) the first product is the contribution from the free Gaussian term in $p(c,\Lambda)$, whereas the second product is a result of the orthonormality condition.

5.5 Calculation of Correlation Functions

We can see from Eq. (5.24) that the final form of the partition function describing the full system is a product of all eigenvector interactions occurring in pairs. We are interested now in the calculation of the correlation function (5.19) involving a pair of wavefunctions, $c_\mu(\alpha)$ and $c_\nu(\alpha)$. For that we define the generating function

$$\begin{aligned} G_{\mu,\nu}(\vec{\xi}_\mu, \vec{\xi}_\nu) = \int\int \exp\left[-\sum_\alpha \left(\frac{c_\mu^2(\alpha)}{2\Lambda(\mu,\alpha)} + \frac{c_\nu^2(\alpha)}{2\Lambda(\nu,\alpha)} + \xi_{\mu,\alpha} c_\mu(\alpha) + \xi_{\nu,\alpha} c_\nu(\alpha) \right) \right] \\ \times \delta\left(\sum_\alpha c_\mu(\alpha) c_\nu(\alpha)\right) \prod_\alpha dc_\mu(\alpha) dc_\nu(\alpha). \end{aligned} \tag{5.25}$$

We will calculate correlation functions by differentiation of $G_{\mu,\nu}$ with respect to the auxiliary fields $\xi_{\mu,\alpha}$, $\xi_{\nu,\alpha}$, described for all α by $\vec{\xi}_\mu, \vec{\xi}_\nu$. This approach involves an implicit approximation, namely, we are assuming that correlations involving two chaotic wavefunctions can be computed by singling out the contribution of those wavefunctions to the partition function and factoring out the rest. This approximation is well justified since it accounts for the effect of the orthonormality between μ and ν, which will determine the form of the correlation function.

Eq. (5.25) may be evaluated as a $2\mathcal{N}$-dimensional Gaussian integral after we express

the delta-function in its Fourier form,

$$\delta(\sum_{\alpha} c_{\mu}(\alpha)c_{\nu}(\alpha)) = \frac{1}{2\pi}\int \exp\left[i\lambda \sum_{\alpha} c_{\mu}(\alpha)c_{\nu}(\alpha)\right]d\lambda. \tag{5.26}$$

We write our generating function in the form

$$G_{\mu,\nu}(\vec{\xi}_{\mu},\vec{\xi}_{\nu}) = \frac{1}{2\pi}\int\int \exp\left[-\frac{1}{2}\vec{x}^{T}\mathbf{A}\vec{x} + \vec{J}^{T}\vec{x}\right]d^{2\mathcal{N}}x d\lambda, \tag{5.27}$$

where $\vec{x} = (c_{\mu}(1), c_{\nu}(1), ..., c_{\mu}(\mathcal{N}), c_{\nu}(\mathcal{N}))$ is a vector made up of coefficients of both relevant eigenvectors, $\mathbf{A}$ is a block diagonal matrix given by

$$\mathbf{A} = \begin{bmatrix} \frac{1}{\Lambda(\mu,1)} & i\lambda & & & & \\ i\lambda & \frac{1}{\Lambda(\nu,1)} & & & & 0 \\ & \ddots & \ddots & \ddots & & \\ & & & \frac{1}{\Lambda(\mu,\mathcal{N})} & i\lambda & \\ 0 & & & i\lambda & \frac{1}{\Lambda(\nu,\mathcal{N})} & \end{bmatrix},$$

and $\vec{J} = (\xi_{\mu,1}, \xi_{\nu,1}, ..., \xi_{\mu,\mathcal{N}}, \xi_{\nu,\mathcal{N}})$ is the generating function for the calculation of the correlation functions. Eq. (5.27) may then be calculated exactly, as the $2\mathcal{N}$-dimensional integral over x is now in Gaussian form, and is given by

$$\int \exp\left[-\frac{1}{2}\vec{x}^{T}\mathbf{A}\vec{x} + \vec{J}^{T}\vec{x}\right]d^{2\mathcal{N}}x = \frac{(2\pi)^{\mathcal{N}}}{|\mathbf{A}|^{\frac{1}{2}}}\exp\left[\frac{1}{2}\vec{J}^{T}\mathbf{A}^{-1}\vec{J}\right]. \tag{5.28}$$

where $|\mathbf{A}|$ is the determinant of the block diagonal matrix $\mathbf{A}$, given by the product of the determinants of each 2×2 block,

$$|\mathbf{A}| := \prod_{\alpha}|A_{\alpha}| := \prod_{\alpha}\left(\frac{1}{\Lambda(\mu,\alpha)\Lambda(\nu,\alpha)} + \lambda^{2}\right), \tag{5.29}$$

and

$$\frac{1}{2}\vec{J}^{T}\mathbf{A}^{-1}\vec{J} = -\frac{1}{2}\sum_{\alpha}\frac{1}{|A_{\alpha}|}\left[\frac{\xi^{2}_{\mu,\alpha}}{\Lambda(\nu,\alpha)} + \frac{\xi^{2}_{\nu,\alpha}}{\Lambda(\mu,\alpha)} - 2i\lambda\xi_{\mu,\alpha}\xi_{\nu,\alpha}\right]. \tag{5.30}$$

We then have,

$$G_{\mu,\nu}(\vec{\xi}_{\mu},\vec{\xi}_{\nu}) = \lim_{\vec{\xi}_{\mu,\nu}\to 0}(2\pi)^{\mathcal{N}-1}\int\frac{1}{|\mathbf{A}|^{\frac{1}{2}}}\exp\left[-\frac{1}{2}\sum_{\alpha}\frac{1}{|A_{\alpha}|}\left[\frac{\xi^{2}_{\mu,\alpha}}{\Lambda(\nu,\alpha)} + \frac{\xi^{2}_{\nu,\alpha}}{\Lambda(\mu,\alpha)} - 2i\lambda\xi_{\mu,\alpha}\xi_{\nu,\alpha}\right]\right]d\lambda, \tag{5.31}$$

which we write as

$$G_{\mu,\nu}(\vec{\xi}_{\mu},\vec{\xi}_{\nu}) = \lim_{\vec{\xi}_{\mu,\nu}\to 0}(2\pi)^{\mathcal{N}-1}\int\left(\prod_{\alpha}\left(\frac{1}{\Lambda(\mu,\alpha)\Lambda(\nu,\alpha)} + \lambda^{2}\right)^{-\frac{1}{2}}g(\xi_{\mu\alpha},\xi_{\nu\alpha})\right)d\lambda, \tag{5.32}$$

where

$$g(\xi_{\mu,\alpha},\xi_{\nu,\alpha}) = \exp\left[\frac{1}{2}\frac{\xi^2_{\mu,\alpha}\Lambda(\mu,\alpha)+\xi^2_{\nu,\alpha}\Lambda(\nu,\alpha)-2i\lambda\xi_{\mu,\alpha}\xi_{\nu,\alpha}\Lambda(\mu,\alpha)\Lambda(\nu,\alpha)}{1+\lambda^2\Lambda(\mu,\alpha)\Lambda(\nu,\alpha)}\right]. \tag{5.33}$$

Now, we can rewrite the integrand in Eq. (5.32) as

$$(2\pi)^{\mathcal{N}-1}\left(\prod_{\alpha}\left(\Lambda(\mu,\alpha)\Lambda(\nu,\alpha)\right)^{\frac{1}{2}}\right)\left(\prod_{\alpha'}\left(1+\lambda^2\Lambda(\mu,\alpha')\Lambda(\nu,\alpha')\right)^{-\frac{1}{2}}\right)\left(\prod_{\alpha''}g(\xi_{\mu\alpha''},\xi_{\nu\alpha''})\right). \tag{5.34}$$

Then, as $\ln(1+x)\approx x$ for small x, in the high $\mathcal{N}$ limit we have

$$\begin{aligned}\prod_{\alpha}\left(1+\lambda^2\Lambda(\mu,\alpha)\Lambda(\nu,\alpha)\right)^{-\frac{1}{2}} &= \exp\left[-\frac{1}{2}\sum_{\alpha}\ln\left(1+\lambda^2\Lambda(\mu,\alpha)\Lambda(\nu,\alpha)\right)\right]\\ &\approx \exp\left[-\frac{1}{2}\sum_{\alpha}\lambda^2\Lambda(\mu,\alpha)\Lambda(\nu,\alpha)\right].\end{aligned} \tag{5.35}$$

Thus, we obtain for the generating function

$$\begin{aligned}G_{\mu,\nu}(\vec{\xi}_\mu,\vec{\xi}_\nu) = \lim_{\vec{\xi}_{\mu,\nu}\to 0}(2\pi)^{\mathcal{N}-1}&\left(\prod_{\alpha}\Lambda(\mu,\alpha)\Lambda(\nu,\alpha)\right)^{\frac{1}{2}}\\ &\times\int\exp\left[-\frac{1}{2}\sum_{\alpha}\lambda^2\Lambda(\mu,\alpha)\Lambda(\nu,\alpha)\right]\left(\prod_{\alpha'}g(\xi_{\mu\alpha'},\xi_{\nu\alpha'})\right)d\lambda.\end{aligned} \tag{5.36}$$

The generating function can be checked to yield the correct $\vec{\xi}_\mu = 0$, $\vec{\xi}_\nu = 0$ limit,

$$G_{\mu\nu}(0,0) = (2\pi)^{\mathcal{N}-\frac{1}{2}}\left(\frac{\prod_\alpha\Lambda(\mu,\alpha)\Lambda(\nu,\alpha)}{\sum_\beta\Lambda(\mu,\beta)\Lambda(\nu,\beta)}\right)^{\frac{1}{2}}. \tag{5.37}$$

Taking the product over all pairs of eigenvectors μ,ν of the 2-eigenvector partition function of Eq. (5.37) we recover the interacting part of the partition function of the previous section, Eq. (5.24).

We can proceed now and simplify the generating function by simplifying Eq. (5.33) in the limit $\Gamma/\omega_0 \gg 1$. For this, we first notice that, due to the Gaussian term in Eq. (5.36), the integration variable λ is restricted to take values such that,

$$\lambda^2\sum_\alpha\Lambda(\mu,\alpha)\Lambda(\nu,\alpha)\lesssim 1. \tag{5.38}$$

Since the term $\sum_\alpha\Lambda(\mu,\alpha)\Lambda(\nu,\alpha)$ is of order $(\Gamma/\omega_0)^{-1}$, this implies that $\lambda\approx(\Gamma/\omega_0)^{1/2}$. On the other hand, in Eq. (5.33), we find in the denominator the term $\lambda^2\Lambda(\mu,\alpha)\Lambda(\nu,\alpha)$. Since the product $\Lambda(\mu,\alpha)\Lambda(\nu,\alpha)$ takes values of the order of $(\Gamma/\omega_0)^{-2}$, we find that

$$\lambda^2\Lambda(\mu,\alpha)\Lambda(\nu,\alpha) = \mathcal{O}\left(\frac{\Gamma}{\omega_0}\right)^{-1}\ll 1. \tag{5.39}$$

Using this approximation and carrying out the integration over λ we arrive at the following

form for the generating function,

$$G_{\mu,\nu}(\vec{\xi}_\mu,\vec{\xi}_\nu) \propto \exp\Bigg[\frac{1}{2}\sum_\alpha \xi^2_{\mu,\alpha}\Lambda(\mu,\alpha) + \frac{1}{2}\sum_\alpha \xi^2_{\nu,\alpha}\Lambda(\nu,\alpha) - \frac{1}{2}\sum_{\alpha,\beta}\xi_{\mu,\alpha}\xi_{\mu,\beta}\xi_{\nu,\alpha}\xi_{\nu,\beta}\frac{\Lambda(\mu,\alpha)\Lambda(\mu,\beta)\Lambda(\nu,\alpha)\Lambda(\nu,\beta)}{\sum_{\alpha'}\Lambda(\mu,\alpha')\Lambda(\nu,\alpha')}\Bigg], \tag{5.40}$$

where we have ignored the non-interacting factors, which are irrelevant for the calculation of the correlation functions. Eq. (5.40) is the basis of a self-consistent description of matrix elements in terms of chaotic wavefunctions.

We apply our result for the correlation function of interest (see Eq. (5.18)),

$$\langle c_\mu(\alpha)c_\nu(\beta)c_\mu(\alpha')c_\nu(\beta')\rangle_V = \frac{1}{G_{\mu\nu}}\partial_{\xi_{\mu,\alpha}}\partial_{\xi_{\nu,\beta}}\partial_{\xi_{\mu,\alpha'}}\partial_{\xi_{\nu,\beta'}}G_{\mu\nu}\Big|_{\xi_{\mu,\alpha}=0,\xi_{\nu,\alpha}=0}. \tag{5.41}$$

After calculating the derivatives of our simplified generating function (5.40) we obtain,

$$\langle c_\mu(\alpha)c_\nu(\beta)c_\mu(\alpha')c_\nu(\beta')\rangle_V = \Lambda(\mu,\alpha)\Lambda(\nu,\beta)\delta_{\alpha\alpha'}\delta_{\beta\beta'} - \frac{\Lambda(\mu,\alpha)\Lambda(\nu,\alpha)\Lambda(\mu,\beta)\Lambda(\nu,\beta)\delta_{\alpha\beta'}\delta_{\beta\alpha'}}{\sum_n\Lambda(\mu,n)\Lambda(\nu,n)} - \frac{\Lambda(\mu,\alpha)\Lambda(\nu,\alpha)\Lambda(\mu,\alpha')\Lambda(\nu,\alpha')\delta_{\alpha\beta}\delta_{\alpha'\beta'}}{\sum_n\Lambda(\mu,n)\Lambda(\nu,n)}. \tag{5.42}$$

In the last equation, the second and third terms in the right-hand side arise solely due to the interactions between chaotic wavefunctions that are induced by the orthonormality condition.

For an observable that is diagonal in the basis of H_0 we only need to consider the values $\alpha=\beta$ and $\alpha'=\beta'$. The relevant correlation function is then of the simpler form

$$\langle c_\mu(\alpha)c_\nu(\alpha)c_\mu(\beta)c_\nu(\beta)\rangle_V = \Lambda(\mu,\alpha)\Lambda(\nu,\beta)\delta_{\alpha\beta} - \frac{\Lambda(\mu,\beta)\Lambda(\nu,\alpha)\Lambda(\mu,\alpha)\Lambda(\nu,\beta)(1+\delta_{\alpha\beta})}{\sum_n\Lambda(\mu,n)\Lambda(\nu,n)}. \tag{5.43}$$

Eq. (5.43) is one of the most important results of this work. Note that the first term in the r.h.s. of this equation is the contribution one obtains by ignoring the interaction between chaotic wavefunctions, whereas the second term arises solely due to those interactions. It is thus necessary to understand whether the corrections induced by interactions are relevant or, on the contrary, can be neglected to leading order (as assumed in many previous works). For this we first notice that

$$\Lambda(\mu,\alpha)|_{E_\mu\approx E_\alpha} \approx \frac{\omega_0}{\Gamma}, \tag{5.44}$$

where the ratio $\omega_0/\Gamma \ll 1$, since it corresponds to the inverse number of states in the energy window defined by Γ. We find the following scaling

$$\Lambda(\mu,\alpha)\Lambda(\nu,\alpha) \quad \to \quad \mathcal{O}\left(\frac{\omega_0}{\Gamma}\right)^2, \tag{5.45}$$

$$\frac{\Lambda(\mu,\beta)\Lambda(\nu,\alpha)\Lambda(\mu,\alpha)\Lambda(\nu,\beta)}{\sum_n\Lambda(\mu,n)\Lambda(\nu,n)} \quad \to \quad \mathcal{O}\left(\frac{\omega_0}{\Gamma}\right)^3. \tag{5.46}$$

We could feel tempted to simply ignore the correlation term in Eq. (5.43), since it is of higher order in the small parameter ω_0/Γ. Neglecting the correlation term is a valid

approximation in the case $\alpha = \beta$, since we find that the leading term contribution is given by Eq. (5.45). On the contrary, for non-diagonal terms ($\alpha \neq \beta$), the lowest order contribution is given by Eq. (5.46) and it is of order $\mathcal{O}\left(\frac{\omega_0}{\Gamma}\right)^3$. However, there are of order Γ/ω_0 more non-diagonal than diagonal terms. Whenever we use the correlation function Eq. (5.43) to calculate the expectation value of an observable, we will need to sum over indices α, β. Thus we expect that the contribution of $\mathcal{O}\left(\frac{\Gamma}{\omega_0}\right)$ non-diagonal terms each contributing an amount of order $\mathcal{O}\left(\frac{\omega_0}{\Gamma}\right)^3$ will yield finally a contribution or order $\mathcal{O}\left(\frac{\omega_0}{\Gamma}\right)^2$, which is thus comparable to the contribution from the diagonal terms. We conclude that both terms in the r.h.s. of Eq. (5.43) are equally relevant.

The reasoning above also explains discrepancies that one may find when, for example, verifying the orthonormality sum rule with Eq. (5.43). Explicitly, orthonormality implies that,

$$\sum_{\nu} \langle c_\mu(\alpha) c_\nu(\alpha) c_\mu(\beta) c_\nu(\beta) \rangle = \Lambda(\mu, \alpha) \delta_{\alpha,\beta}. \tag{5.47}$$

However, Eq. (5.43) yields,

$$\sum_{\nu} \langle c_\mu(\alpha) c_\nu(\alpha) c_\mu(\beta) c_\nu(\beta) \rangle_V = \Lambda(\mu, \alpha) \delta_{\alpha,\beta} + \mathcal{O}\left(\frac{\omega_0}{\Gamma}\right)^2. \tag{5.48}$$

The correction of order $\mathcal{O}\left(\frac{\omega_0}{\Gamma}\right)^2$ can be ignored, since the leading contribution to the diagonal term is $\Gamma(\mu, \alpha)$, which is of order $\mathcal{O}\left(\frac{\omega_0}{\Gamma}\right)$. The attentive reader may find a contradiction in neglecting terms that are one order lower in ω_0/Γ in Eq. (5.48), while keeping the second term in the r.h.s. of Eq. (5.43). However, we recall that in the latter case, we have to sum over a large number of low-order non-diagonal corrections, and thus both Eqs. (5.45) and (5.46) may lead to contributions of the same order when calculating matrix elements of observables.

We also stress here that whilst the derivation of the Lorentzian form of $\Lambda(\mu, \alpha)$ is only accurate for small couplings, our result of Eq. (5.42) is more general and relies only on the condition that the wavefunction is spread over many non-interacting states. For example, a system with a Gaussian form for $\Lambda(\mu, \alpha)$ could be described by the approximate distribution (5.21), and yet lead to the same form for the chaotic wavefunction correlations.

5.6 Calculation of Off-Diagonal Matrix Elements

We can now use the functional form for $\langle c_\mu(\alpha) c_\nu(\beta) c_\mu(\alpha') c_\nu(\beta') \rangle_V$ developed in the previous section to calculate a generic form for $|O_{\mu\nu}|^2$. We have

$$|O_{\mu\nu}|^2_{\mu \neq \nu} = \sum_{\alpha\beta\alpha'\beta'} c_\mu(\alpha) c_\nu(\beta) c_\mu(\alpha') c_\nu(\beta') O_{\alpha\beta} O_{\alpha'\beta'}. \tag{5.49}$$

Now, exploiting self-averaging, we can make the replacement $c_\mu(\alpha) c_\nu(\beta) c_\mu(\alpha') c_\nu(\beta') \to \langle c_\mu(\alpha) c_\nu(\beta) c_\mu(\alpha') c_\nu(\beta') \rangle_V$. Then, using our expression for the correlation function, Eq.

(5.42) we can write

$$|O_{\mu\nu}|^2_{\mu\neq\nu} = \sum_{\alpha\beta\alpha'\beta'} \Bigg[\Lambda(\mu,\alpha)\Lambda(\nu,\beta)\delta_{\alpha\alpha'}\delta_{\beta\beta'} - \frac{\Lambda(\mu,\alpha)\Lambda(\nu,\alpha)\Lambda(\mu,\beta)\Lambda(\nu,\beta)\delta_{\alpha\beta'}\delta_{\beta\alpha'}}{\sum_n \Lambda(\mu,n)\Lambda(\nu,n)} - \frac{\Lambda(\mu,\alpha)\Lambda(\nu,\alpha)\Lambda(\mu,\alpha')\Lambda(\nu,\alpha')\delta_{\alpha\beta}\delta_{\alpha'\beta'}}{\sum_n \Lambda(\mu,n)\Lambda(\nu,n)}\Bigg] O_{\alpha\beta}O_{\alpha'\beta'}. \tag{5.50}$$

If we once more briefly focus on those observables that are diagonal in the H_0 eigenbasis, this becomes

$$|O_{\mu\nu}|^2_{\mu\neq\nu} = \sum_{\alpha} \Lambda(\mu,\alpha)\Lambda(\nu,\alpha)O^2_{\alpha\alpha} - \frac{\sum_\alpha \Lambda(\mu,\alpha)\Lambda(\nu,\alpha)O_{\alpha\alpha}\sum_\beta \Lambda(\mu,\beta)\Lambda(\nu,\beta)O_{\beta\beta}}{\sum_n \Lambda(\mu,n)\Lambda(\nu,n)} - \frac{\sum_\alpha \Lambda^2(\mu,\alpha)\Lambda^2(\nu,\alpha)O^2_{\alpha\alpha}}{\sum_n \Lambda(\mu,n)\Lambda(\nu,n)}. \tag{5.51}$$

Again, we find that a non-negligible contribution arises from the chaotic wavefunction correlations. To further approximate this expression we define the average

$$\overline{[O_{\alpha\alpha}]}_{\overline{\mu}} := \sum_\alpha \Lambda(\overline{\mu},\alpha)O_{\alpha\alpha}, \tag{5.52}$$

where $\overline{\mu} := (\mu+\nu)/2$, which one may observe is essentially a microcanonical average centered on the energy $E_{\overline{\mu}}$. A further approximation[3] allows this microcanonical average to be removed from the summation.

$$|O_{\mu\nu}|^2_{\mu\neq\nu} = \left(\overline{[O^2_{\alpha\alpha}]}_{\overline{\mu}} - \overline{[O_{\alpha\alpha}]}^2_{\overline{\mu}}\right)\sum_\alpha \Lambda(\mu,\alpha)\Lambda(\nu,\alpha) - \overline{[O^2_{\alpha\alpha}]}_{\overline{\mu}}\frac{\sum_\alpha \Lambda^2(\mu,\alpha)\Lambda^2(\nu,\alpha)}{\sum_n \Lambda(\mu,n)\Lambda(\nu,n)}. \tag{5.53}$$

Eq. (5.53) is one of the most important results of this work. Note that the result is now free from the pathology that we found when approximating many-body wavefunctions by independent random numbers in Eq. (5.11). Our final expression has a similar form, however correlations induce a second term that appears as a result of the orthonormality condition. Finally we note that the overall dependence of $|O_{\mu,\nu}|^2$ on the energies E_μ, E_ν agrees with the ETH ansatz for off-diagonal matrix elements in Eq. (5.9)[4].

We then take the continuum limit, substituting $\sum_\alpha \to \int \frac{dE_\alpha}{\omega_0}$, and thereby obtain

$$|O_{\mu\nu}|^2_{\mu\neq\nu} = \left(\overline{[O^2_{\alpha\alpha}]}_{\overline{\mu}} - \overline{[O_{\alpha\alpha}]}^2_{\overline{\mu}}\right)\int \frac{dE_\alpha}{\omega_0}\Lambda(\mu,\alpha)\Lambda(\nu,\alpha) - \overline{[O^2_{\alpha\alpha}]}_{\overline{\mu}}\int \frac{dE_\alpha}{\omega_0}\Lambda(\mu,\alpha)^2\Lambda(\nu,\alpha)^2\left(\int \frac{dE_n}{\omega_0}\Lambda(\mu,n)\Lambda(\nu,n)\right)^{-1}. \tag{5.54}$$

Whilst the second term in Eq. (5.54) is analytically obtainable, we may observe that this term is $\propto \omega_0^2$, and thus within our approximation is correctly ignored. We then see, as the convolution of two Lorentzian functions of widths Γ_1 and Γ_2 is simply a Lorentzian

[3] This is the smoothness assumption of Chapter 3

[4] See Appendix B for an extension to more general local observables.

of width $\Gamma_1 + \Gamma_2$, that the functional form for a diagonal observable is

$$|O_{\mu\nu}|^2_{\mu\neq\nu} = \overline{[\Delta O^2_{\alpha\alpha}]}_{\overline{\mu}} \frac{\omega_0 2\Gamma/\pi}{(E_\mu - E_\nu)^2 + (2\Gamma)^2}, \tag{5.55}$$

where $\overline{[\Delta O^2_{\alpha\alpha}]}_{\overline{\mu}} := \overline{[O^2_{\alpha\alpha}]}_{\overline{\mu}} - \overline{[O_{\alpha\alpha}]}^2_{\overline{\mu}}$. We see here that, to first order in ω_0, the off diagonal elements of a generic observable that is diagonal in H_0 are described by a Lorentzian of width 2Γ. For more general observables one simply uses the known structure in the non-interacting basis, as we will see below. This result corroborates the relation between the variances of diagonal and off-diagonal elements obtained in reference [66], and observed numerically in [113, 166], showing that they differ by a factor of two. One can see that the width of the distribution of diagonal elements is the same as that of the wavefunction, Γ, from Eq. (5.6).

Returning to our original argument indicating the failure of the random wavefunction ansatz, we may double check the consistency of the above RMT approach by repeating the calculation of $\sum_\nu |O_{\mu\nu}|^2_{\mu\neq\nu}$ using Eq. (5.55). This is obtained by replacing $\sum_{\nu\neq\mu} \to \int dE_\nu/\omega_0$ (the correction due to the $\mu = \nu$ term is $\propto \omega_0^2$ and thus ignored)

$$\begin{aligned} \int \frac{dE_\nu}{\omega_0} |O_{\mu\nu}|^2_{\mu\neq\nu} &= \int \frac{dE_\nu}{\omega_0} \overline{[\Delta O^2_{\alpha\alpha}]}_{\overline{\mu}} \frac{\omega_0 2\Gamma/\pi}{(E_\mu - E_\nu)^2 + (2\Gamma)^2} \\ &= \overline{[\Delta O^2_{\alpha\alpha}]}_{\overline{\mu}}, \end{aligned} \tag{5.56}$$

as expected. Thus the RMT approach, including correlations due to orthogonality, leads to a correct normalization of the matrix elements of observables.

We note here that the result from the RMT approach tells us more about the source of this scaling than we obtained from our previous discussion. Eq. (5.16) tells us that the sum over all off diagonal eigenstates contributes this scaling factor, but gives us no information about the contribution of any individual eigenstate. We can see from the RMT result of Eq. (5.55) that the scaling by $\overline{[\Delta O^2_{\alpha\alpha}]}_{\overline{\mu}}$ occurs on the level of each individual eigenstate, and not simply on average.

5.7 Comparison to Numerical Random Matrix Model

To check the results above we first compare them to a numerical random matrix model by diagonalizing Eq. (5.17) and calculating the off-diagonal distribution for the matrix elements of example observables. We choose our observables, O_{odd} and O_{sym}, to be defined such that in the non-interacting basis $\{|\phi_\alpha\rangle\}$ all off-diagonal elements are zero, and the diagonal elements are given by

$$(O_{\text{odd}})_{\alpha\alpha} = \begin{cases} 1, & \text{if } \alpha = \text{odd} \\ 0, & \text{if } \alpha = \text{even}, \end{cases} \tag{5.57}$$

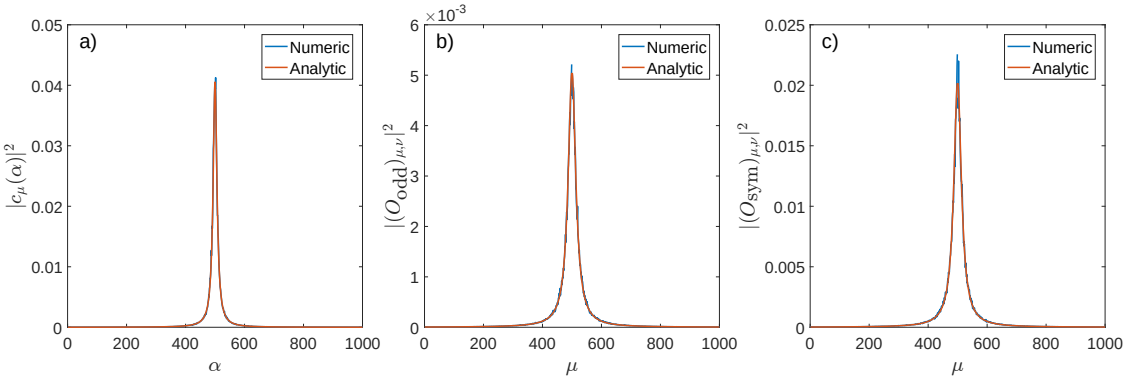

Figure 5.1: Numerical comparison to analytic results for $\mathcal{N} = 1000$, $g = 0.05$, average of 500 realisations of H. a) Shows the eigenstate $\mu = 500$, analytic result given by (5.23) b),c) Show the off-diagonal distributions ($\mu = \nu$ points are excluded) for $O_{\rm odd}$ and $O_{\rm sym}$ respectively analytic result given by Eq. (5.55).

and

$$(O_{\rm sym})_{\alpha\alpha} = \begin{cases} 1, & \text{if } \alpha = \text{odd} \\ -1, & \text{if } \alpha = \text{even.} \end{cases} \tag{5.58}$$

These observables are chosen as they have similar structure to realistic spin-observables, as well as having different $\overline{[\Delta O^2_{\alpha\alpha}]_{\overline{\mu}}}$ values such that the scaling may be adequately demonstrated. For simplicity we choose diagonal examples here, though the RMT method developed above can easily account for non-diagonal observables, as we will see below for a spin-chain system. To obtain the observable distributions we find the average distribution over many realisations of the Hamiltonian, Eq. (5.17), which is essentially the mathematical procedure to find the probability distribution in Eq. (5.20). Examples of the overlap of the RMT prediction are shown in Fig. 5.1. Here we see a very good agreement between the analytic predictions of Eq. (5.23) (Fig. 5.1a)) and Eq. (5.55) (Figs. 5.1b), 5.1c)) and the exact numerical results.

As shown in Fig. 5.1, the scaling of each observable $O_{\rm odd}$ and $O_{\rm sym}$ are different, and we can see here that the analytic prediction of an observable dependent rescaling is true to the numerics. We note that for couplings of $g \gtrapprox 0.2$ our analytic treatment is no longer a good approximation. This corresponds to the bulk eigenstates having significant value at the edges of the spectrum, and thus our assumptions made obtaining a functional form for $\Lambda(\mu, \alpha)$ (Appendix A.1) are not good for such coupling strengths.

Before making comparison to realistic systems, we comment here on an essential ingredient to the derivation of our analytic results: the self-averaging property. This property of random matrices is commonly assumed [66, 121], and has been an invaluable tool in the descriptive power of RMT, having seen much success in describing interacting spin systems [72], and atomic and nuclear physics [167, 168]. Further, the analysis of random matrices based on the above assumptions already makes up much of the basis of our understanding of the ETH [66], which has seen repeated numerical verifications in non-integrable models. One can write the essential assumption as it applies to the current

problem as,

$$|O_{\mu\nu}|^2 \approx \langle |O_{\mu\nu}|^2 \rangle_V = \sum_{\alpha\beta\alpha'\beta'} \langle c_\mu(\alpha) c_\nu(\beta) c_\mu(\alpha') c_\nu(\beta') \rangle_V O_{\alpha\beta} O_{\alpha'\beta'}, \tag{5.59}$$

such that the observable matrix elements are taken to be equal to their ensemble average. Note that $O_{\alpha\beta}$ are not averaged quantities, as they do not depend on the random perturbation. Appendix C is devoted to a more detailed discussion of the self-averaging property, and its proof from chaotic wavefunctions.

5.8 Comparison to Exact Diagonalization of Spin-Chain

We now perform a comparison of the theory from random matrices outlined above to a more physical system. We choose a 1D spin chain, with a Hamiltonian of the form

$$H = H_S + H_B + H_{SB}. \tag{5.60}$$

We reiterate here that the Lorentzian functional form for the wavefunction distribution $\Lambda(\mu, \alpha)$ is valid for small values of g (see Appendix A.1), and thus we only expect good agreement with our RMT result when the interaction Hamiltonian H_{SB} describes a weak interaction. However, the theory developed above for correlation functions, and thus the application to observable distributions, is more general. Previous numerical studies have shown that in the high coupling limit one observes a Gaussian wavefunction distribution [91, 97, 113, 115, 164], and thus for high coupling strengths we do not expect a good overlap with the developed RMT results, however the basic phenomenology should remain unchanged.

For our model, the system Hamiltonian H_S is simply given by a spin in perpendicular fields, B_x and B_z,

$$H_S = B_z^{(S)} \sigma_z^{(N_S)} + B_x^{(S)} \sigma_x^{(N_S)}, \tag{5.61}$$

where N_S labels the position of the system in the chain, between 1 and N. The bath Hamiltonian is a spin-chain with nearest-neighbour Ising interactions in both B_z and B_x fields,

$$H_B = \sum_{n \neq N_S} (B_z^{(B)} \sigma_z^{(n)} + B_x^{(B)} \sigma_x^{(n)}) + \sum_{n \neq N_S, N_S - 1} J_B (\sigma_z^{(n)} \sigma_z^{(n+1)} + \sigma_+^{(n)} \sigma_-^{(n+1)} + \sigma_-^{(n)} \sigma_+^{(n+1)}). \tag{5.62}$$

The interaction part of the Hamiltonian H_{SB} is given by

$$H_{SB} = J_I (\sigma_+^{(N_S)} \sigma_-^{(N_S \pm 1)} + \sigma_-^{(N_S)} \sigma_+^{(N_S \pm 1)}) + J_z \sigma_z^{(N_S)} \sigma_z^{(N_S \pm 1)}. \tag{5.63}$$

Thus we have $H_0 = H_S + H_B$, and $H_I = H_{SB}$. For the analysis below, we compare various limits of this system, to show where our assumptions made above do and do not hold. Each limit is non-integrable, and expected to thermalize.

We focus here on two cases: a homogeneous chain, and the case of a weakly coupled

impurity. It is the latter for which we expect the RMT description to work best, as it is here that the assumption that the density of states does not change over the coupling width is valid. It is this assumption that allows us to treat the interaction Hamiltonian as a full random matrix in Eq. (5.17). Should the density of states significantly change over the relevant coupling width, then a random matrix with some bandwidth would be required.

Initially, for the impurity case, we set $J_B = B_z^{(S)} = B_z^{(B)} = B_x^{(B)} = 1$, $J_z = B_x^{(S)} = 0$, and vary J_I. The second limit we study is when $B_x^{(S)} = 1$ and $J_z = J_I$, with the chain thus being truly homogeneous when $J_z = J_I = 1$. We calculate the off-diagonal matrix elements of system observables for varying system sizes from $N = 8$ to $N = 13$. We set the system position to be $N_S = 5$ throughout.

To test the RMT prediction for the observable and wavefunction distributions we calculate these distributions directly using exact diagonalization (ED) and perform a fit to the distribution to find the observed width Γ_{Fit}. This is then compared to the expected width from a random matrix framework, Γ_{RM}, which we discuss below. To perform the fit we first smooth the ED result by applying a Lorentzian mask over each point such that, for smoothed eigenstates we have

$$F_\mu(E_\alpha) = \sum_\alpha |c_\mu(\alpha)|^2 \delta_\epsilon(E_\alpha - E), \tag{5.64}$$

where $\delta_\epsilon(E_\alpha - E) = \epsilon\pi^{-1}/[(E_\nu - E) + \epsilon^2]$. This function is related to the strength function introduced in quantum chaos theory [72]. Similarly, for an observable O

$$S_O(E_\mu, E_\nu) = \sum_\nu |O_{\mu\nu}|^2 \delta_\epsilon(E_\nu - E). \tag{5.65}$$

We perform a three variable (central energy, peak width Γ, and peak height) fit to a Lorentzian to find the Γ_{Fit}. The values for Γ_{Fit} can then be compared to $\Gamma = \Gamma(W_0)$ found from the interaction Hamiltonian using the method outlined below.

5.8.1 Computation of RMT Width

For comparison of our RMT description to the ED calculation, we must be able to calculate an estimate for Γ from the random matrix perspective. This can be obtained from the Hamiltonian, as for the random matrix we have $\Gamma_{\text{RM}} = \frac{\pi g^2}{\mathcal{N}\omega_0}$, and $\frac{g}{\sqrt{\mathcal{N}}}$, which may be found by the average value of the random interaction Hamiltonian. Relating this to a physical system must be done with some care, however, as the average value should not be taken over the entire Hamiltonian, but over some energy width W, as discussed below. We can write Γ_{RM}, for a random matrix, as

$$\Gamma_{\text{RM}} = \pi \frac{\text{Tr}\{H_I^\dagger H_I\}}{\mathcal{N}^2} D(E), \tag{5.66}$$

where $D(E) = 1/\omega_0$ is the density of states. In this form we can see more easily the relation to a real Hamiltonian. However, we must treat the above expression carefully,

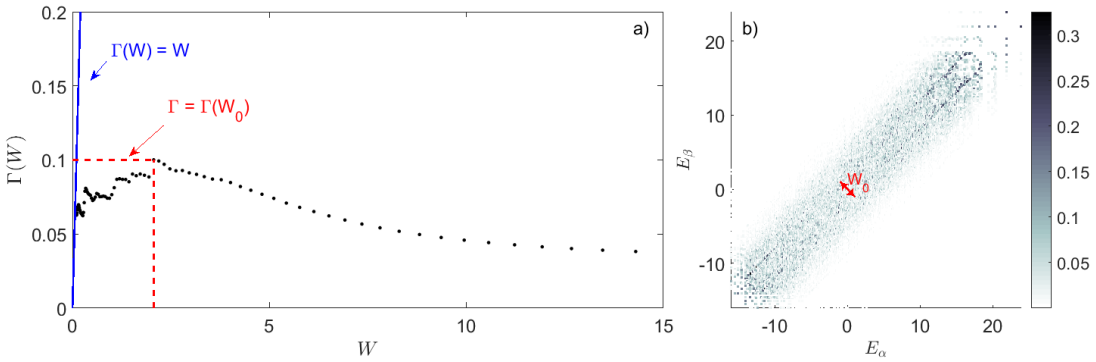

Figure 5.2: a) Plot of $\Gamma(W)$ (Eq. (5.67)) for varying values of W (black dots). Approximate $\Gamma = \Gamma(W_0)$ shown by red dashed line. We see that the plateau region indeed extends well past the $\Gamma(W) = W$ line (blue solid line). b) Shows all entries to the interaction Hamiltonian H_I above 10^{-6}. The width W_0, where $\Gamma = \Gamma(W_0)$ is shown in red. We can see that this does not extend past the coupling band. Shown for the impurity case, $J_z = B_x^{(S)} = 0$, with $N = 12$, $J_I = 0.4$.

as the association $g^2/\mathcal{N} \Leftrightarrow \mathrm{Tr}\{H_I^\dagger H_I\}/\mathcal{N}^2$ must be made with proper consideration of the physical relationship between the interaction Hamiltonian and a random matrix. To reiterate, the physical grounds for using a random interaction Hamiltonian here rely on the fact that for generic non-integrable systems the interaction Hamiltonian, when expressed in the basis of eigenstates of the non-interacting Hamiltonian, resembles a banded random matrix with some width W_{BW}. We can use a full random matrix for the low coupling limit as the density of states, which dictates the band width, does not change much over the width of the coupling energy Γ. Thus, there are two caveats to be considered in implementing Eq. (5.66): H_I must be expressed in the basis of H_0, and the trace must be taken over a finite width $W_0 < W_{BW}$. We thus define the trace over an energy width W, $\mathrm{Tr}_W\{\cdots\}$, as the trace over all states $\{|\phi_\alpha\rangle\}$ satisfying $W \geq |E_\alpha - E_\beta|$. This gives us Γ as a function of the energy width W

$$\Gamma(W) = \pi \frac{\mathrm{Tr}_W\{H_I^\dagger H_I\}}{N^{*2}} D(E), \tag{5.67}$$

where N^{*2} is the number of elements included in $\mathrm{Tr}_W\{\cdots\}$.

The question is, then, which is the physically relevant value, $\Gamma(W_0)$, of the possible values of $\Gamma(W)$? We know that Γ must satisfy $\Gamma(W_0) \ll W_{BW}$, as otherwise our assumption that the density of states does not change over the width Γ is invalid. Furthermore we must have $\Gamma(W_0) \ll W_0$ such that all states within the coupling energy $\Gamma := \Gamma(W_0)$ are counted. Thus we have the condition $\Gamma(W_0) \ll W_0 \ll W_{BW}$. We should expect to see a plateau in the function $\Gamma(W)$, giving the width over which the interaction Hamiltonian is effectively described by a random matrix. As W grows we should then expect to see $\Gamma(W)$ decay for $W > W_{BW}$, as the long range interaction terms vanish. It is the value of $\Gamma(W)$ on the plateau that is the physically relevant point, as assuming the interaction strength is weak enough, the structure of long-range interactions should not matter.

We can see from Fig. 5.2 that this description is a good approximation for the spin

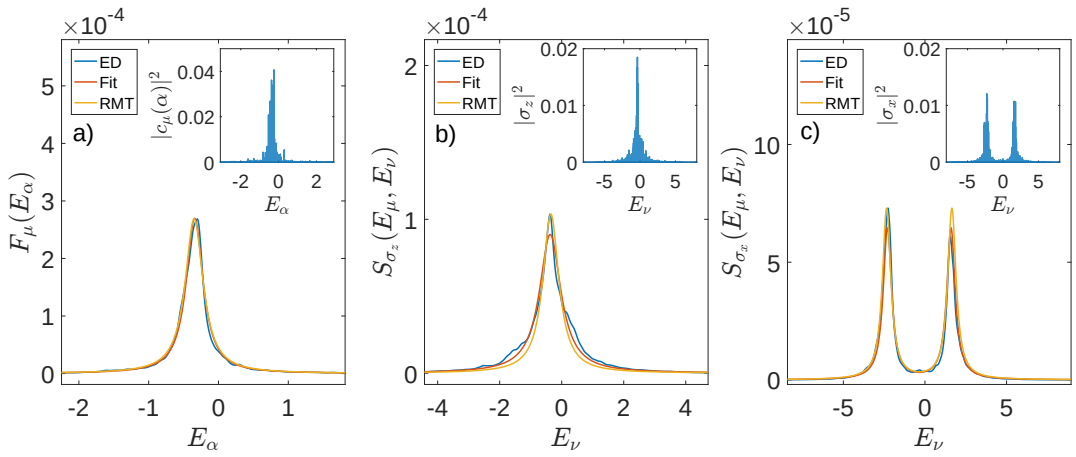

Figure 5.3: Smoothed ED calculation (blue) of the central eigenstate (a)), and off-diagonal elements of $|\sigma_z|^2$ (b)) and $|\sigma_x|^2$ (c)). Fit to a Eqs. (5.23), (5.68), and (5.70) respectively (red) and RMT prediction (yellow) using $\Gamma = \Gamma(W_0)$ (Eq. (5.67)) also shown for each. Raw data for each shown in insets. Each plot shown for $N = 13, N_S = 5, J_I = 0.5$, and for an energy E_μ in the centre of the spectrum.

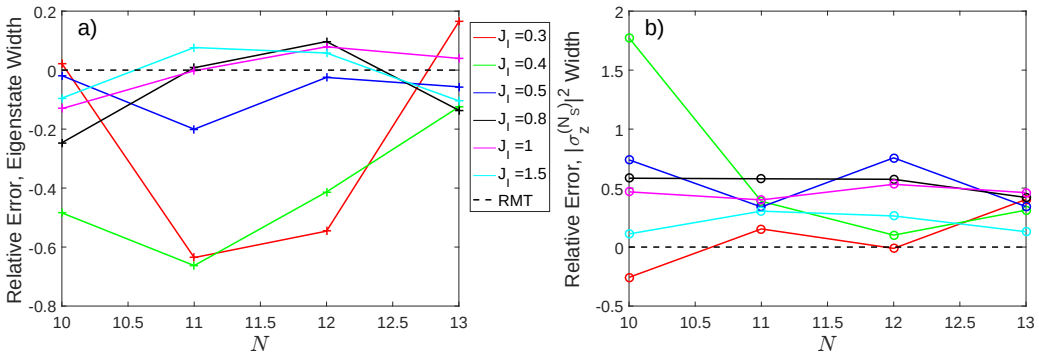

Figure 5.4: Comparison of fitted Γ_{Fit} values with $\Gamma = \Gamma(W_0)$ (Eq. (5.67)). Relative error of each distribution width given by $(\Gamma_{\text{Fit}} - \Gamma(W_0))/\Gamma(W_0)$. Comparisons shown for the central eigenstate ($\mu = 2^{N-1}$) for the fit to smoothed eigenstate distribution (a) and the $\sigma_z^{(N_S)}$ observable (b).

chain, however the estimation of Γ from this method is a likely source of error for the system sizes available, as the plateau region is not exactly flat as one would expect from a true random matrix. For larger sizes, one expects the initial structure of the Hamiltonian to be more 'washed out' by the change to the non-interacting basis. We can also see from Fig. 5.2 that as the interaction strength J_I increases the line $\Gamma(W) = W$ will extend further into the plateau region, as the average value of the interaction Hamiltonian elements in this region increases. The random matrix approximation becomes invalid in the limit where the line $\Gamma(W) = W$ extends past the plateau region, as it is in this case that the density of states begins to change significantly over the width Γ (hence the condition $\Gamma(W_0) \ll W_{BW}$).

5.8.2 Impurity

We begin by analyzing the simple case where $J_z = B_x^{(S)} = 0$. Here the system qubit behaves differently to the bath, and thus can be thought of as an impurity. The natural observables in this case are the Pauli operators the $\sigma_z^{(N_S)}$ and $\sigma_x^{(N_S)}$. It is straightforward to obtain the expected distribution for $\sigma_z^{(N_S)}$ from RMT by directly applying Eq. (5.55), obtaining

$$|(\sigma_z^{(N_S)})_{\mu\nu}|^2_{\mu\neq\nu} = \frac{\omega_0 2\Gamma/\pi}{(E_\mu - E_\nu) + (2\Gamma)^2}. \tag{5.68}$$

For the case of the $\sigma_x^{(N_S)}$ observable, we must instead use information we have about the structure of the observable in the non-interacting basis[5] to obtain a functional form for the observable distribution from the RMT formalism above. The useful observation here is that for $\sigma_x^{(N_S)}$

$$(\sigma_x^{(N_S)})_{\alpha\beta} = \begin{cases} 1, & \text{if } E_\beta = E_\alpha \pm 2B_z^{(S)} \\ 0, & \text{Otherwise.} \end{cases} \tag{5.69}$$

Thus, using Eq. (5.50), and writing $\Lambda(\mu,\alpha) \to \Lambda(E_\mu, E_\alpha)$ for clarity, we find

$$\begin{aligned} |(\sigma_x^{(N_S)})_{\mu\nu}|^2_{\mu\neq\nu} &= \frac{1}{2}\int \frac{dE_\alpha}{\omega_0}\Lambda(E_\mu,E_\alpha)[\Lambda(E_\nu, E_\alpha + 2B_z^{(S)}) + \Lambda(E_\nu, E_\alpha - 2B_z^{(S)})] + \mathcal{O}(\omega_0^2) \\ &= \frac{\omega_0\Gamma/\pi}{(E_\mu - E_\nu + 2B_z^{(S)}) + (2\Gamma)^2} + \frac{\omega_0\Gamma/\pi}{(E_\mu - E_\nu - 2B_z^{(S)}) + (2\Gamma)^2}, \end{aligned} \tag{5.70}$$

where the factor of $\frac{1}{2}$ is necessary for correct normalization. We can thus see that for the $\sigma_x^{(N_S)}$ observable we expect two peaks in the distribution of off-diagonal matrix elements, each of width Γ, separated by a width $4B_z^{(S)}$.

Shown in Fig. 5.3 is a comparison between the ED numerical calculation and the RMT prediction. We compare the value for Γ_{Fit} obtained from the fit to the smoothed distribution and the value found for $\Gamma(W_0)$ to obtain a relative error, shown in Fig. 5.4, which we observe to decrease on average with system size for varying interaction strengths J_I. Whilst the range in relative error here is high, this is largely due to the difficulty in estimating Γ for the available system sizes, and the fit to a Lorentzian distribution is very good.

5.8.3 Homogeneous Chain

The inclusion of a finite $B_x^{(S)}$ adds a level of complexity to the problem, as neither relevant observable $\sigma_z^{(N_S)}$ or $\sigma_x^{(N_S)}$ is diagonal in the non-interacting basis. A similar approach to that shown in above for $\sigma_x^{(N_S)}$ allows us to calculate a distribution for $|\sigma_z^{(N_S)}|^2$, which for $B_x^{(S)} = 1$ one would expect to be made up instead of three Lorentzian peaks at $E_\mu = E_\nu, E_\nu \pm 2\sqrt{2}$, with the central peak of twice the height.

We can see in Fig. 5.5a) that we obtain a good agreement for the weak coupling case.

[5] This is a particular explicit example of the non-diagonal components $n \neq 0$ in the sparsity condition in Chapter 3

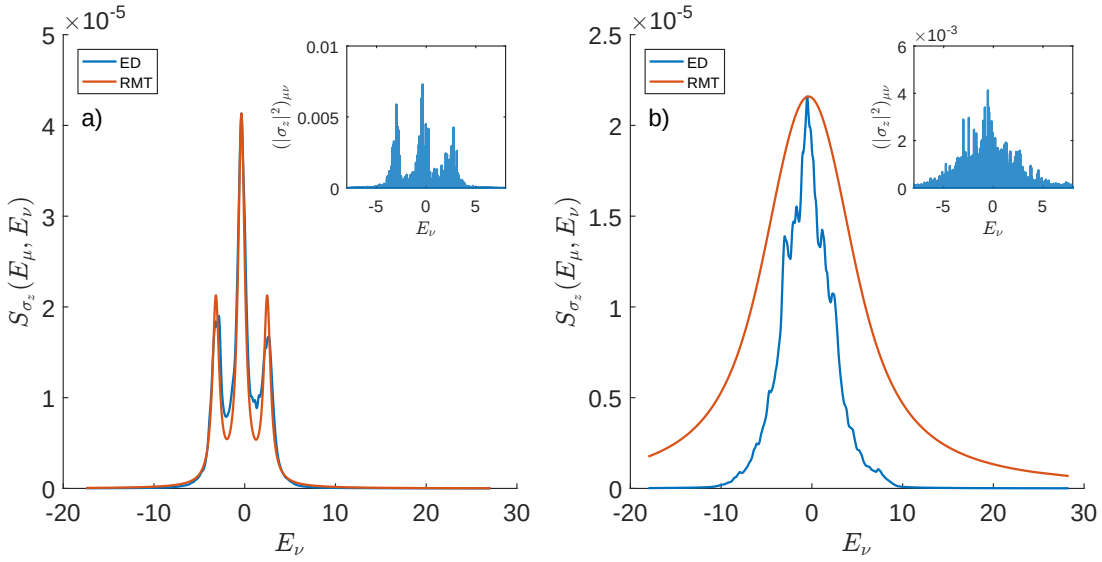

Figure 5.5: Smoothed ED calculation (blue) (raw data shown in insets) and RMT distribution (red) of smoothed $\sigma_z^{(N_S)}$ observable (analogous to Eq. (5.70)) for couplings $J_I = J_z = 0.3$ (a) and the fully homogeneous case (b) $J_I = J_z = 1$. Each has $N = 13$, $B_x^{(S)} = 1$, and E_μ in the centre of the spectrum.

As we approach the fully homogeneous case in Fig. 5.5b), however, we observe the RMT prediction no longer holds. We can see from Fig. 5.6 that the $\Gamma(W) = W$ line extends to the end of the plateau region, and thus the requirements for assuming a full random matrix perturbation are not fulfilled - the change in density of states also contributes to the distribution of the wavefunctions. Thus in this limit we no longer expect the wavefunction distribution to be a Lorentzian, nor do we expect the method outlined above to be a good indication of the distribution width.

Furthermore we note that the for high couplings there are also added technical challenges for the systems available to our study, as the interaction Hamiltonian structure is not sufficiently randomized by the transformation to the non-interacting basis. We note that most of this structure occurs at the edges of the spectrum, and thus one can simply take the trace over the central half of the energies, as indicated in Fig. 5.6b). This is justified for the bulk states we are analyzing.

5.9 Finite Size Scaling of Long Time Fluctuations

Off-diagonal elements of observables dominate the behaviour of their long-time fluctuations [69, 70, 112]. Indeed, the infinite time (diagonal ensemble) fluctuations of an observable are given by,

$$\delta_O^2(\infty) = \sum_{\substack{\mu\nu \\ \mu\neq\nu}} |c_\mu(\alpha)|^2 |c_\nu(\alpha)|^2 |O_{\mu\nu}|^2. \tag{5.71}$$

Using the RMT result above, we may evaluate Eq. (5.71) by the previous prescription of converting the sums to integrals, and integrating using the functional forms for $|c_\mu(\alpha)|^2$

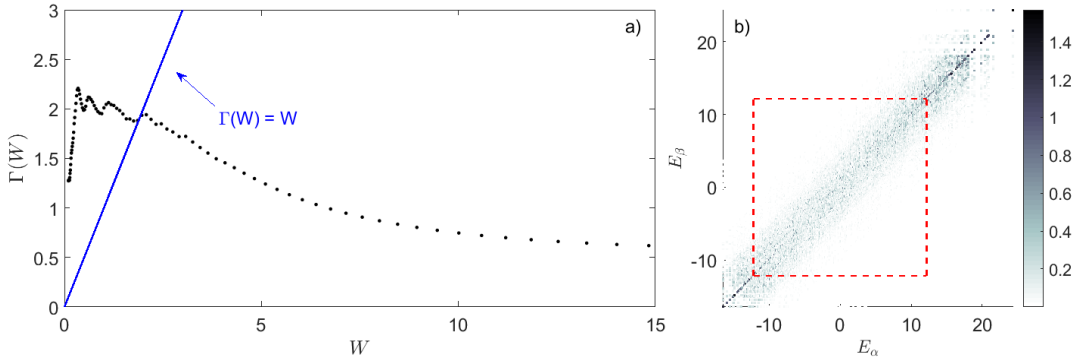

Figure 5.6: a) Plot of $\Gamma(W)$ (Eq. (5.67)) for varying values of W (black dots), found using central half of the Hamiltonian energies only. We see that the $\Gamma(W) = W$ line (blue solid line) now extends much further, and thus the change in $\Gamma(W)$ value over this width alters the wavefunction lineshape. b) Shows all entries to the interaction Hamiltonian H_I above 10^{-6}. Elements used in $\Gamma(W)$ calculation outlined by red dashed line, as elements outside this line retain structure due to finite size. Shown for $N = 12$, $B_x^{(S)} = 1$, $J_I = J_z = 1$.

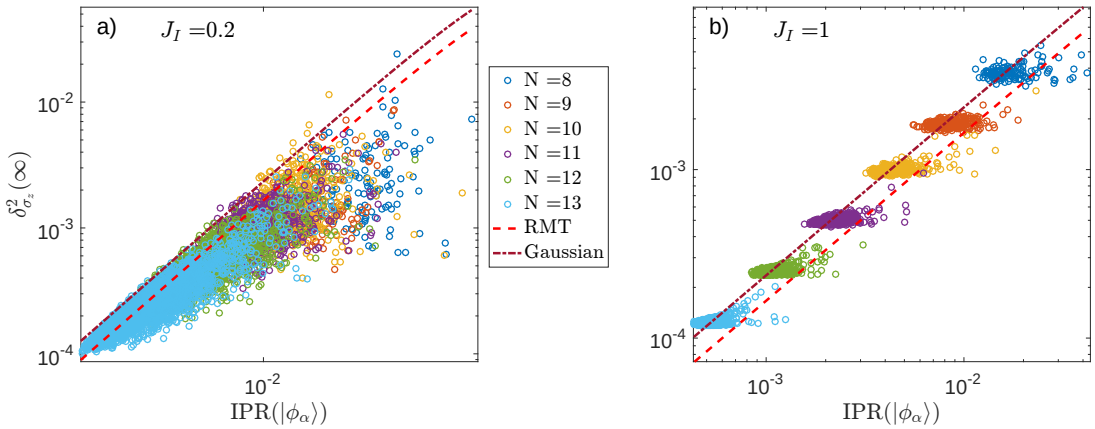

Figure 5.7: $\delta^2_{\sigma_z}(\infty)$ versus IPR($|\phi_\alpha\rangle$) for the central half of the spectrum of α values for the impurity case $B_x^{(S)} = J_z = 0$. a) Shows $J_I = 0.2$ b) Shows $J_I = 1$. Analytic result from RMT, Eq. (5.74) shown by red dashed line. Dash-dotted burgundy line shows prefactor obtained if $\Lambda(\mu, \alpha)$ is replaced by a Gaussian.

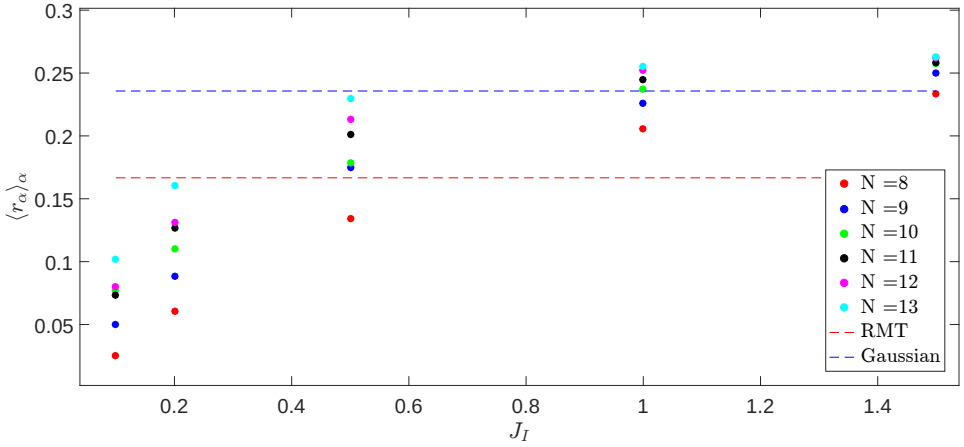

Figure 5.8: Plot of $\langle r_\alpha \rangle_\alpha$ (Eq. (5.75)) as coupling J_I is increased for impurity case $B_x^{(S)} = J_z = 0$. Average $\langle \cdots \rangle_\alpha$ taken over central 201 elements.

and $|O_{\mu\nu}|^2_{\mu\neq\nu}$ derived above. We obtain[6],

$$\delta_O^2(\infty) = \frac{\omega_0}{4\pi\Gamma}\overline{[\Delta O^2_{\alpha\alpha}]}_{\overline{\mu}} + \mathcal{O}(\omega_0^2) \tag{5.72}$$

where the $O(\omega_0^2)$ term is due to the subtraction of the $\mu = \nu$ part. A further parameter that is of interest [12] to the finite size scaling of closed quantum systems is the Inverse Participation Ratio (IPR), defined as $\text{IPR}(|\phi_\alpha\rangle) = \sum_\mu |c_\mu(\alpha)|^4$. This can also be obtained in a similar manner using the RMT result,

$$\text{IPR}(|\phi_\alpha\rangle) = \frac{3\omega_0}{2\pi\Gamma}, \tag{5.73}$$

where the factor of 3 comes from the ratio of the second and fourth order moments of Gaussian variables. From these we obtain

$$\delta_O^2(\infty) = \frac{1}{6}\overline{[\Delta O^2_{\alpha\alpha}]}_{\overline{\mu}}\text{IPR}(|\phi_\alpha\rangle). \tag{5.74}$$

We can see from Fig. (5.7) that the proportionality is indeed correct, which has previously been shown to be a consequence of the ETH in reference [12]. Similar results have also been previously observed in references [57, 128, 129], which obtain bounds on the late time fluctuations in terms if the IPR. Our work implies that in those systems that can be well described by a random matrix ansatz, the IPR determines not only an upper bound, but also the scale of the time-fluctuations. Similar dependencies have also been observed numerically in reference [169]. One also observes in Fig. 5.7 that the numerical prefactor, expected to be 1/6 for small couplings, as $\overline{[\Delta O^2_{\alpha\alpha}]}_{\overline{\mu}} = 1$ for the $\sigma_z^{(N_S)}$ observable here, seems to depend on the coupling strength. Motivated by previous numerical studies [91, 97, 113, 115, 164, 170], observing wavefunctions of non-integrable systems to be Gaussian for large coupling strengths, one may repeat a similar calculation to that leading to Eq. (5.74), however with $\Lambda(\mu, \alpha)$ replaced by a Gaussian. We then

[6] See Appendix D.3 for a full derivation

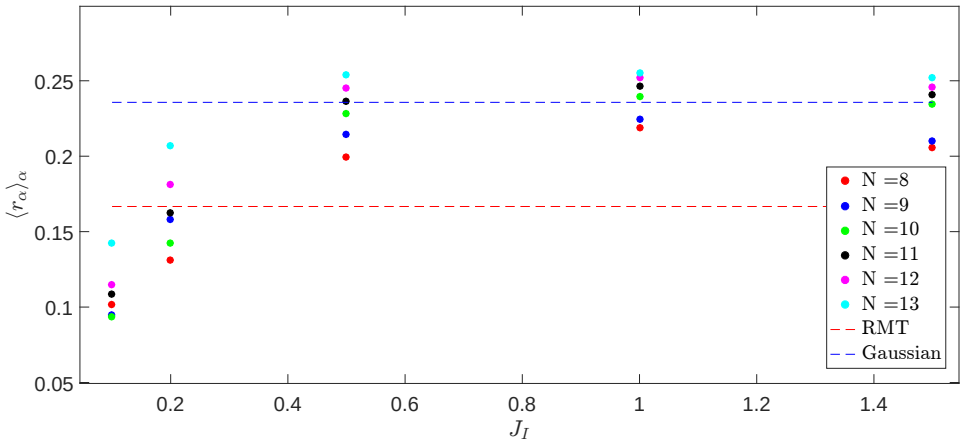

Figure 5.9: Plot of $\langle r_\alpha \rangle_\alpha$ (Eq. (5.75)) as coupling J_I is increased for homogeneous case $B_x^{(S)} = 1, J_z = J_I$. Average $\langle \cdots \rangle_\alpha$ taken over central 201 elements.

obtain a prefactor of $(3\sqrt{2})^{-1}$. We define

$$r_\alpha = \overline{[\Delta O^2_{\alpha\alpha}]}_{\overline{\mu}}^{-1} \delta_O^2(\infty) \mathrm{IPR}(|\phi_\alpha\rangle)^{-1} \tag{5.75}$$

in order to more closely analyse the dependence of the numerical prefactor as the coupling strengths are altered. For the case of Figs. 5.8 and 5.9 we show the change in $\langle r_\alpha \rangle_\alpha$, that is r_α averaged over many bulk α values, for the impurity and homogeneous cases respectively. Here we have $\overline{[\Delta O^2_{\alpha\alpha}]}_{\overline{\mu}} = 1$, and thus $\langle r_\alpha \rangle_\alpha$ gives the value of the prefactor directly. We indeed observe a growth of this prefactor to $\sim (3\sqrt{2})^{-1}$, the value expected by applying a Gaussian distributed wavefunction to the RMT approach above in both the impurity and homogeneous cases. We note that for low couplings the fact that $\langle r_\alpha \rangle_\alpha$ does not tend exactly to the expected value from RMT is not surprising, as this is where we are most limited by the Hilbert space sizes available to our study, and thus there is a high associated error in this limit. Similar phenomena are observed for a numerical random matrix model, where the high coupling limit is obtained by the replacement $\Lambda(\mu, \alpha) = \Lambda = \frac{1}{\mathcal{N}}$, the scaling of fluctuations for this case is analysed in Appendix A.2.

5.10 Discussion

We have analytically studied a random matrix Hamiltonian, Eq. (5.17), made up of a linear ensemble of states with random interactions, and expanded on previous work [64, 65] to find a functional form for generic observables, as well as clarifying many of the approximations made to obtain the wavefunction distribution (Appendix A.1). The form obtained for matrix elements of observables is in agreement with the ETH. We also predict that there is a linear relation between the time-fluctuations of an observable and the IPR. This relation may be relevant to detect quantum ergodicity by measuring the time-fluctuations in an experiment, if we understand quantum ergodicity as the participation of many Hamiltonian eigenstates in the initial state, which is implied by small IPR values.

Thus, measuring an exponential decrease of the time-fluctuations with system size would yield evidence that the IPR itself is exponentially decreasing with system size, which could be used as a smoking gun of quantum ergodicity.

We have assumed that an approximate description of the quantum dynamics of a subsystem in a many-body system can be achieved by an interaction term given by a structureless random Gaussian matrix. This approximation implies that the typical energy bandwidth of the coupling term, W_{BW}, is considered infinite compared to the coupling strength, $W_{BW} \gg \Gamma_\alpha$. Our results are thus immediately applicable to the situation of an impurity weakly coupled to a many-body bath, since in this case Γ_α depends on a different interaction strength (J_I in the spin chain example above) than the energy bandwidth, W_{BW}, and thus Γ_α can be made arbitrarily small. Our numerical calculations confirm that in this weak coupling limit many-body wavefunctions are well approximated by Lorentzian-shaped chaotic wavefunctions.

The weak coupling approximation may fail if, for example, we consider a subsystem in a homogeneous system where the coupling strength is not necessarily small compared to the bandwidth of the coupling term. Actually, in a homogeneous system we expect that $W_{BW} \approx \Gamma_\alpha$ since both energy scales are governed by the same interactions. For example, in the spin chain considered in the last section, both W_{BW} and Γ_α are determined by the spin-spin interactions in the bulk J_B. In this case, we have observed numerically that the chaotic wavefunction envelope is not necessarily a Lorentzian, but rather a Gaussian function. However, a valid chaotic wavefunction relying on the approximate distribution (5.21) is still possible by considering that $\Lambda(\mu, \alpha)$ are now normalized Gaussian functions. Most of the discussion in the subsequent sections remains intact, including expression (5.53) for the non-diagonal matrix elements of an observables. The only effect from the strong coupling condition is a different line-shape of envelope functions defined in Eqs. (5.64), (5.65), and a different prefactor in the scaling of the time-fluctuations as a function of the IPR, as shown in our numerical calculations (see Figs. 5.8 and 5.9).

Chapter 6

Quantum Chaotic Fluctuation-Dissipation Theorem: Effective Brownian Motion in Closed Quantum Systems

6.1 Abstract

We analytically describe the decay to equilibrium of generic observables of a non-integrable system after a perturbation in the form of a Random Matrix. We further obtain an analytic form for the time-averaged fluctuations of an observable in terms of the rate of decay to equilibrium. Our result shows the emergence of a Fluctuation-Dissipation theorem corresponding to a classical Brownian process, specifically, the Ornstein-Uhlenbeck process. Our predictions can be tested in quantum simulation experiments, thus helping to bridge the gap between theoretical and experimental research in quantum thermalization. We test our analytic results by exact numerical experiments in a spin-chain. We argue that our Fluctuation-Dissipation relation can be used to measure the density of states involved in the non-equilibrium dynamics of an isolated quantum system.

6.2 Introduction

Ubiquitous to nearly all fields of the natural sciences is the phenomenon of equilibration to a thermal state. However, in the context of quantum systems a full understanding of thermalization has remained enigmatic. This long-studied problem [3] has seen a resurgence of interest in recent years [58, 66, 67, 72, 73], largely driven by the modern experimental capability to study the unitary quantum dynamics of closed systems [12, 13, 45, 141, 162]. Of particular interest is the thermalization of initial pure-states, which cannot easily be expected to equilibrate to some statistical ensemble. This is the case treated in the present chapter.

On the theoretical side there have been advances in two key areas: Typicality, and

the Eigenstate Thermalization Hypothesis (ETH). The typicality approach has shown that most pure states of a large system correspond to a local canonical ensemble in some small (with respect to the total system size) subspace [57, 118, 122, 127], whilst the ETH has provided a mechanism for thermalization - the eigenstates themselves form an effective microcanonical ensemble [64, 70]. This has been supported by a large amount of numerical evidence [95, 109, 112, 156–159, 171].

Despite much recent progress on the understanding of thermalization, there has been less work describing the decay process [104, 133, 172] or the timescales of equilibration [134]. We address both of these using a Random Matrix Theory (RMT) model [64, 100], which we have seen in the previous chapter reproduces the ETH ansatz [16]. We describe the decay to equilibrium of generic non-integrable quantum systems, and obtain an expression for the time-averaged fluctuations of local observables in terms of their rate of decay to equilibrium; thus observing an emergent classical Fluctuation-Dissipation Theorem (FDT), analogous to those derived from a Langevin equation for Brownian motion.

FDTs describe a relationship between the linear response of a system to some perturbation and its fluctuations in thermal equilibrium [173]. An example that is particularly relevant for this work is the case of an Ornstein-Uhlenbeck process. This is a Brownian process with diffusion constant D where particle positions are additionally subjected to a deterministic drift of the form $\dot{x} = -\gamma x$. The particle position is a stochastic variable whose time-averaged fluctuations satisfy the relation [174],

$$\langle x^2 \rangle = \frac{D}{\gamma}. \tag{6.1}$$

In this chapter we show that the fluctuations of the expectation value of a local operator, $\langle O(t) \rangle$, of a quantum chaotic system follows a similar relation, with D replaced by the inverse of the density of states (DOS). Our result radically differs from previous theoretical results linking the *quantum* FDT for quantum fluctuations $\langle \Delta O^2 \rangle$ [110] to linear response theory and the ETH [70].

This chapter is arranged as follows. In section II we outline the physical scenario in question, our RMT approach [16], our key assumptions and their justifications, and how the the ETH may be derived, and exploited, from our methods. In section III we derive our main analytical result - an explicit expression for the equilibration in time of generic observables towards their microcanonical average. In section IV, we see that exploiting a result from [16], the results of section III provide a FDT for chaotic quantum systems. To confirm the applicability of our RMT description to realistic physical models, in section V we present exact diagonalization calculations of a quantum spin-chain, and apply this to a generalised FDT section VI. In section VII we propose and numerically simulate an approach to experimental verification of our findings. Finally, we conclude in Section VIII. Various details and derivations are provided in Appendices.

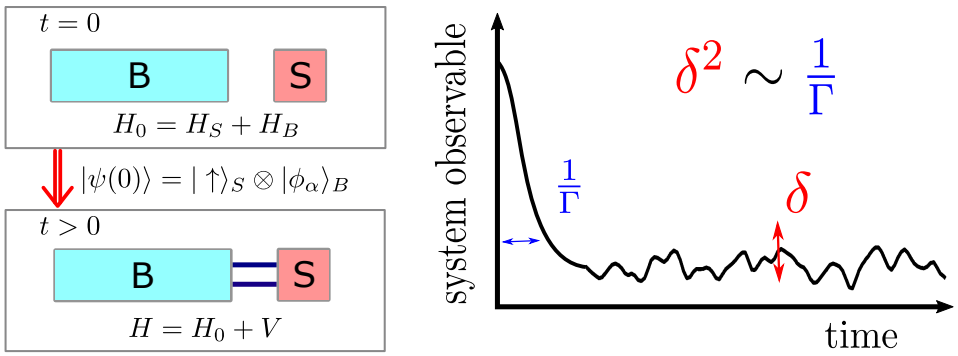

Figure 6.1: Diagram depicting quench at $t = 0$ from $H_0 = H_S + H_B$ to $H = H_0 + V$, where V couples system and bath. Initial state is an eigenstate $|\phi_\alpha\rangle$ of H_0 (this condition is relaxed below).

6.3 Random Matrix Theory approach to quantum thermalization

6.3.1 Physical Scenario

Our objective is to analyse the quantum dynamics of a many-body system whose total Hilbert space, $\mathcal{H}$, is divided in two subspaces, $\mathcal{H} = \mathcal{H}_S \otimes \mathcal{H}_B$. $\mathcal{H}_S$ is a local Hilbert space corresponding, for example, to one or a few sites in a quantum lattice system. $\mathcal{H}_B$ is a larger Hilbert space, which will play the role of a finite many-body quantum bath.

We investigate the case in which a non-interacting Hamiltonian of the form $H_0 = H_S + H_B$, is perturbed by a term V to form a fully interacting Hamiltonian,

$$H = H_0 + V. \tag{6.2}$$

H_S and H_B in H_0 act on Hilbert subspaces $\mathcal{H}_S$ and $\mathcal{H}_B$, respectively, and V is an interaction term between the system and the bath. The simplest situation that we will consider is a quantum quench scenario, in which the system is initially in an eigenstate of H_0 at $t = 0$, as illustrated in Fig. (6.1). We will see, however, that this assumption on the initial state can be relaxed under certain conditions. The goal of this work is to understand the general properties of the dynamics of an observable O acting on $\mathcal{H}_S$.

In a non-integrable system a qualitative description is obtained by replacing the coupling V by a random matrix. Typically, V is the sum of a few products of local operators which takes the form $V = \sum_n g_n O_{S,n} O_{B,n}$, where $O_{S,n}$ are local operators acting on $\mathcal{H}_S$, and $O_{B,n}$ are local operators acting on $\mathcal{H}_B$. If the bath Hamiltonian, H_B, is non-integrable, we expect that operators $O_{B,n}$ are well described by Gaussian random matrices (see for example [109, 112] for a recent numerical confirmation), and as such a random matrix ansatz should also be a good approximation for V.

Throughout this work we will consider a weak coupling limit, such that we can assume that the random matrix V is homogeneous. In general, one may expect that the coupling matrix V has some structure, for example, matrix elements $V_{\alpha\beta}$ typically decay as a function of the energy difference between states α and β. A reasonable assumption is to

consider that the matrix elements of V are constant within a typical energy band of width Γ_V. The approximation of V as a homogeneous Gaussian random matrix will be justified as long as $\Gamma \ll \Gamma_V$, where Γ is the energy scale associated to the system-bath coupling. The weak coupling limit can be satisfied in the case that H_S describes an impurity weakly coupled to a many-body bath described by H_B. However, this limit is not trivially fulfilled in the case that H represents a homogeneous system. In this case, Γ_V and Γ could be of similar magnitude, since Γ_V is associated to interactions in H_B, which in a homogeneous system would be similar in magnitude to the coupling term V. As explained in Appendix B.1, our theory and general results could be modified to account for this situation.

6.3.2 Random Matrix Model

The random matrix model under study is that used in the pioneering work of Deutsch [64]. The spirit of this approach is to model both H_0 and V, as well as operators describing local observables, by matrices that have the same properties as the equivalent operators in physical systems.

The non-interacting part in (6.2), H_0, is modelled by a diagonal matrix of size $\mathcal{N}$, with $\mathcal{N}$ the total dimension of the Hilbert space,

$$(H_0)_{\alpha\beta} = E_\alpha \delta_{\alpha\beta} \tag{6.3}$$

where $E_\alpha = \alpha\omega_0$, and $\omega_0 = 1/\mathcal{N}$ is the spacing between energy levels, which is assumed to be constant. This approximation will be relaxed later on by assuming an energy-dependent density of states. The perturbation term in Eq. (6.2) is modelled by a random matrix,

$$V_{\alpha\beta} = h_{\alpha\beta}, \tag{6.4}$$

where $h_{\alpha\beta}$ are independent random numbers selected from the Gaussian Orthogonal Ensemble (GOE), such that the matrix h has the probability distribution,

$$P(h) \propto \exp[-\frac{\mathcal{N}}{4g^2} \operatorname{Tr} h^2], \tag{6.5}$$

giving $\langle h_{\alpha\beta}\rangle = 0$, and $\langle h^2_{\alpha\beta}\rangle = g^2/\mathcal{N}$ for $\alpha \neq \beta$, and otherwise $\langle h^2_{\alpha\alpha}\rangle = 2g^2/\mathcal{N}$.

From here on, we denote the set of eigenstates of H (interacting basis) by $\{|\psi_\mu\rangle\}$,

$$H|\psi_\mu\rangle = E_\mu|\psi_\mu\rangle, \quad \mu = 1, 2, \ldots, \mathcal{N}, \tag{6.6}$$

and the eigenstates of H_0 (non-interacting basis) by $\{|\phi_\alpha\rangle\}$

$$H_0|\phi_\alpha\rangle = E_\alpha|\phi_\alpha\rangle, \quad \alpha = 1, 2, \ldots, \mathcal{N}. \tag{6.7}$$

We can approximate $E_\mu = \mu\omega_0$, since the perturbation is homogeneous, and thus will not change the average spacing between energy levels. To simplify the notation, we always refer to the non-interacting basis (interacting basis) by indexes with Greek letters α, β, (μ, ν). Sums over wavefunction indices in expressions below are always understood to run

over values $1, 2, \ldots, \mathcal{N}$.

We define the interacting wavefunctions, $c_\mu(\alpha)$,

$$|\psi_\mu\rangle = \sum_\alpha c_\mu(\alpha)|\phi_\alpha\rangle, \tag{6.8}$$

where $c_\mu(\alpha)$ are random variables whose statistical properties depend on the properties of the random matrix V. Deutsch [65] obtained an expression for the probability distribution of eigenstates,

$$\langle |c_\mu(\alpha)|^2\rangle_V := \Lambda(\mu,\alpha) = \frac{\omega_0\Gamma/\pi}{(E_\mu - E_\alpha)^2 + \Gamma^2}, \tag{6.9}$$

where $\Gamma = \frac{\pi g^2}{\mathcal{N}\omega_0}$, and $\langle\cdots\rangle_V$ denotes an average over realisations of the random perturbation V. We assume a feature of large random matrices known as self-averaging[1], and replace summations over coefficients by their ensemble average,

$$\sum_{\alpha\cdots\beta} c_\mu(\alpha)\cdots c_\nu(\beta) \to \sum_{\alpha\cdots\beta}\langle c_\mu(\alpha)\cdots c_\nu(\beta)\rangle_V. \tag{6.10}$$

This is a very common assumption in the treatment of random matrices [175], and is well justified numerically for this model in [16].

6.3.3 Correlation functions of quantum chaotic wavefunctions

The RMT approach will allow us to express the dynamics of local observables in a non-integrable system in terms of averages of products of random wavefunctions, $c_\mu(\alpha)$. At first sight, a reasonable approximation would be to consider that $c_\mu(\alpha)$ are independent Gaussian variables, such that any multi-point correlation function can be simply obtained as a product of two-point correlations for the form given by Eq. (6.9).

In the previous chapter we outlined a theoretical approach initially developed by J. Deutsch [64], and extended it to include the effect of the orthonormality between wavefunctions, which can be understood as an effective repulsive interaction in a statistical theory of the variables $c_\mu(\alpha)$. We showed that the inclusion of correlations between $c_\mu(\alpha)$ is essential to obtain the correct form of the ETH conjectured for off-diagonal elements of generic observables, in agreement with Srednicki's ansatz [70]. We review this proof in detail in Appendices B.1 and B.2, and discuss here the most relevant results.

We focus here on two sets of correlation functions of interest: $\langle c_\mu(\alpha)c_\nu(\beta)c_\mu(\alpha')c_\nu(\beta')\rangle_V$ for both $\mu = \nu$, and $\mu \neq \nu$:

(i) For $\mu = \nu$ we can show that the orthonormality constraint does not affect the calculation, such that the coefficients may be treated as independent Gaussian variables,

$$\begin{aligned}\langle c_\mu(\alpha)c_\mu(\beta)c_\mu(\alpha')c_\mu(\beta')\rangle_V &= \Lambda(\mu,\alpha)\Lambda(\nu,\beta)\delta_{\alpha\alpha'}\delta_{\beta\beta'} \\ &\quad + \Lambda(\mu,\alpha)\Lambda(\nu,\alpha')(\delta_{\alpha\beta}\delta_{\alpha'\beta'} + \delta_{\alpha\beta'}\delta_{\beta\alpha'}).\end{aligned} \tag{6.11}$$

We will see that this term plays a role in the prediction of time-averages of expect-

[1] which we discuss in more detail, and prove in Appendix C.2

ation values of observables $\langle O(t)\rangle$. We note that for this to reproduce the expected microcanonical average, the contributions of the latter two terms in Eq. (6.11) must be small, which is shown in Appendix B.2.

(ii) For $\mu \neq \nu$ we find

$$\langle c_\mu(\alpha)c_\nu(\beta)c_\mu(\alpha')c_\nu(\beta')\rangle_V = \Lambda(\mu,\alpha)\Lambda(\nu,\beta)\delta_{\alpha\alpha'}\delta_{\beta\beta'} - \frac{\Lambda(\mu,\alpha)\Lambda(\nu,\beta)\Lambda(\mu,\alpha')\Lambda(\nu,\beta')}{\Lambda^{(2)}(\mu,\nu)}(\delta_{\alpha\beta}\delta_{\alpha'\beta'} + \delta_{\alpha\beta'}\delta_{\beta\alpha'}). \tag{6.12}$$

This case is especially relevant for non-equilibrium dynamics, as it dictates both the equilibrium fluctuations, as well as the decay to equilibrium of a given observable O.

6.3.4 Assumptions on physical observables

A very non-trivial aspect of our theory is the introduction of matrices that model local observables in physical non-integrable systems. We impose two conditions on a Hermitian matrix, O, that are satisfied by local observables[2]:

Sparsity.- We assume that, O, expressed in the non-interacting basis, is represented by a diagonal matrix in the non-interacting basis or, at least, by a matrix with only a few non-diagonal entries. This implies that matrix elements in the non-interacting basis, $O_{\alpha\beta} := \langle\phi_\alpha|O|\phi_\beta\rangle$, can be written like

$$O_{\alpha\beta} = \sum_{n\in\mathcal{N}_O} O_{\alpha,\alpha+n}\delta_{\beta,\alpha+n} \tag{6.13}$$

where $\mathcal{N}_O$ is a set of N_O integer values which determine the non-diagonal finite matrix elements. The sparsity constraint is satisfied if $N_O \ll N$.

In a physical system, the sparsity condition is fulfilled as long as the observable O is defined on the local Hilbert space $\mathcal{H}_S$. To see this more clearly, let us express the non-interacting basis in the form of products of eigenstates of H_S and H_B. We define $|s\rangle_S$, with $s = 1,\ldots,\dim(\mathcal{H}_S)$ as the eigenstates of H_S with energy E_s^S, and $|\alpha_B\rangle_B$, with $\alpha_B = 1,\ldots,\dim(\mathcal{H}_B)$ the set of eigenstates of H_B, with energy $E_{\alpha_B}^B$. An eigenstate of the non-interacting Hamiltonian is given by

$$|\phi_\alpha\rangle = |s(\alpha)\rangle_S|\alpha_B(\alpha)\rangle_B, \tag{6.14}$$

where $s(\alpha)$ and $\alpha_B(\alpha)$ are the system and bath eigenstate number of the non-interacting state α, respectively. The energy of $|\phi_\alpha\rangle$ is

$$E_\alpha = E_{s(\alpha)}^S + E_{\alpha_B(\alpha)}^B. \tag{6.15}$$

A local operator will only couple states with different local quantum number s, and thus, $O_{\alpha\beta} \neq 0$ only if

$$E_\alpha - E_\beta = E_{s(\alpha)}^S - E_{s(\beta)}^S. \tag{6.16}$$

[2]Note that this section summarises the sparsity and smoothness conditions outlined in Chapter 3

In this case, O induces transitions between only a few states that are separated by one of the possible gaps of H_S. Consider for example that H_S is a local term in a spin chain. Then a local operator, $O = \sigma_z$ or σ_+, σ_- will only induce transitions between non-interacting states with a flipped local spin, such that $N_O = 3$.

Smoothness.- In the following calculations we will have to evaluate sums of observable matrix elements in the non-interacting basis weighted by probability distributions. For this we will define a smoothed version of the observable in the following way,

$$\overline{[O_{\alpha,\alpha+n}]}_\mu := \sum_\alpha \Lambda(\mu,\, \alpha) O_{\alpha,\alpha+n}. \tag{6.17}$$

The quantity $\overline{[O_{\alpha,\alpha+n}]}_\mu$ represents the average of non-interacting matrix elements along the n'th diagonal, weighted by the Lorentzian function (6.9). We will refer to the quantity $\overline{[O_{\alpha,\alpha+n}]}_\mu$ as the microcanonical average of the matrix elements $O_{\alpha,\alpha+n}$ around the energy E_μ. This average is well defined as long as (see below),

$$\begin{aligned} &\frac{\Gamma}{\omega_0} \gg 1 \\ &\Gamma^2 \frac{d^2}{dE_\mu^2} \overline{[O_{\alpha,\alpha+n}]}_\mu \ll 1. \end{aligned} \tag{6.18}$$

The first condition implies that a large number of matrix elements are averaged in the sum in Eq. (6.17). The second conditions implies that the average $\overline{[O_{\alpha,\alpha+n}]}_\mu$ varies smoothly as function of the energy E_μ.

The smoothness conditions (6.18) imply that, to a good approximation, we can substitute the matrix elements $O_{\alpha,\alpha+n}$ by their smoothed version, $\overline{[O_{\alpha,\alpha+n}]}_\mu$, whenever matrix elements appear within summations over a large number of states. Imagine for example that we have a function $F_{\alpha_0}(\alpha)$, which is centred around $\alpha = \alpha_0$ and has an energy width Γ_F, when expressed as a function of E_α. The smoothness condition implies that

$$\sum_\alpha O_{\alpha\alpha} F_{\alpha_0}(\alpha) \approx \overline{[O_{\alpha\alpha}]}_{\alpha_0} \sum_\alpha F_{\alpha_0}(\alpha), \tag{6.19}$$

provided that the variation of $\overline{[O_{\alpha\alpha}]}_{\alpha_0}$ as a function of E_{α_0} can be neglected within an energy interval of width Γ_F.

In practice, in the following calculations, matrix elements will always be evaluated in products with functions of typical width Γ. Hence, we observe that averages such as Eq. (6.17) can be seen as a microcanonical averaging of the matrix elements $O_{\alpha,\alpha+n}$ around the central energy $E_{\overline{\mu}}$. Our calculations going forward require that this average changes slowly over the width Γ of $\Lambda(\mu, \alpha)$.

Indeed, the conditions, (6.18), under which the smoothness assumption holds can be understood by considering the values $O_{\alpha\alpha}$ as random numbers with a mean value $\mathcal{O}(\alpha) = \overline{O_{\alpha\alpha}}$. This is obviously a rough approach to the study of the values of an observable in the non-interacting basis. However, this method will allow us to understand the conditions under which the smoothness assumption is satisfied.

Consider a certain probability function $p_{\alpha_0}(\alpha)$ centred around the value α_0, normalized with a width γ_p such that

$$\begin{aligned} \sum_\alpha p_{\alpha_0}(\alpha) &= 1, \\ \sum_\alpha p_{\alpha_0}(\alpha)(\alpha-\alpha_0) &= 0 \\ \sum_\alpha p_{\alpha_0}(\alpha)(\alpha-\alpha_0)^2 &= \gamma_p^2. \end{aligned} \tag{6.20}$$

We want to quantify to what extent the following approximation holds,

$$\sum_\alpha O_{\alpha\alpha} p_{\alpha_0}(\alpha) \approx \mathcal{O}(\alpha_0). \tag{6.21}$$

We thus calculate the variance

$$\Delta_O^2 = \overline{\left(\sum_\alpha O_{\alpha\alpha} p_{\alpha_0}(\alpha) - \mathcal{O}(\alpha_0)\right)^2}. \tag{6.22}$$

Now, by expanding Eq. (6.22),

$$\begin{aligned} \Delta_O^2 &= \sum_{\substack{\alpha\beta \\ \alpha\neq\beta}} \overline{O_{\alpha\alpha}O_{\beta\beta}} p_{\alpha_0}(\alpha)p_{\alpha_0}(\beta) + \mathcal{O}(\alpha_0)^2 + \sum_\alpha \overline{(O_{\alpha\alpha})^2} p_{\alpha_0}(\alpha)^2 \\ &\qquad - 2\mathcal{O}(\alpha_0)\sum_\alpha \overline{O_{\alpha\alpha}} p_{\alpha_0}(\alpha) \\ &= \sum_\alpha \left(\overline{(O_{\alpha\alpha})^2} - \mathcal{O}(\alpha)^2\right) p_{\alpha_0}(\alpha)^2 + \left(\sum_\alpha \mathcal{O}(\alpha) p_{\alpha_0}(\alpha) - \mathcal{O}(\alpha_0)\right)^2 \\ &:= \Delta_{O,1}^2 + \Delta_{O,2}^2 \end{aligned} \tag{6.23}$$

where to arrive at the second equality we add and subtract the term $\sum_\alpha \overline{O_{\alpha\alpha}}^2 p(\alpha)_{\alpha_0}^2$, and further use that that $\overline{O_{\alpha\alpha}O_{\beta\beta}} = \mathcal{O}(\alpha)\mathcal{O}(\beta)$ for $\alpha \neq \beta$.

Deviations from the approximation (6.21) therefore come from two terms: i) $\Delta_{O,1}$, which depends on both the variance of $O_{\alpha\alpha}$, and $p_{\alpha_0}^2$. The variance of $O_{\alpha\alpha}$ will be bounded for spin operators by 1, whereas $\sum_\alpha p_{\alpha_0}(\alpha)^2$ is of order $\frac{1}{\gamma_p D_{\alpha_0}}$, where D_{α_0} is the DOS at the peak of the distribution $p_{\alpha_0}(\alpha)$. ii) $\Delta_{O,2}$, which assuming that $\mathcal{O}(\alpha)$ is almost constant within an interval γ_p, can be approximated around α_0 in the form of a Taylor series, $\mathcal{O}(\alpha) \approx \mathcal{O}(\alpha_0) + \mathcal{O}'(\alpha_0)(\alpha-\alpha_0) + (1/2)\mathcal{O}''(\alpha_0)(\alpha-\alpha_0)^2$, such that

$$\begin{aligned} \Delta_{O,2}^2 &\approx (\mathcal{O}(\alpha_0)\sum_\alpha p_{\alpha_0}(\alpha) + \mathcal{O}'(\alpha_0)\sum_\alpha p_{\alpha_0}(\alpha)(\alpha_0-\alpha) \\ &\qquad + \frac{1}{2}\mathcal{O}''(\alpha_0)\sum_\alpha p_{\alpha_0}(\alpha)(\alpha_0-\alpha)^2 - \mathcal{O}(\alpha_0))^2 \\ &= \frac{1}{4}\mathcal{O}''(\alpha_0)^2\gamma_p^4. \end{aligned} \tag{6.24}$$

Therefore, we see that $\Delta_{O,2}$ is simply the variation in $\mathcal{O}$ over the width γ_p. Thus, we

recover the conditions of Eq. (6.18).

These considerations thus validate our intuition that, as long as the mean value of $O_{\alpha\alpha}$ varies slowly with respect to α, matrix elements $O_{\alpha\alpha}$ can be substituted by their average within summations over a large enough number of states in the non-interacting basis.

The smoothness condition is very reasonable when considered together with the sparsity condition above. Consider the product state basis defined in (6.14). A local observable can be written like $O = O_S \otimes \mathbf{1}_B$. Diagonal matrix elements, for example, are given by

$$O_{\alpha\alpha} = (O_S)_{s(\alpha),s(\alpha)}\delta_{\alpha_B(\alpha),\alpha_B(\alpha)}, \tag{6.25}$$

which implies that these matrix elements of the local operator O_S are distributed along the diagonal of O, in an order that will be determined by the energy ordering of states $|\phi_\alpha\rangle$.

6.3.5 Eigenstate Thermalization Hypothesis

The assumptions on observables detailed above may be exploited to derive both the diagonal, and off diagonal parts of the ETH, the form of which is given by Srednicki's ansatz [70]:

$$O_{\mu\nu} = \mathcal{O}(E) + \frac{1}{\sqrt{D(E)}} f(E,\omega)\mathcal{R}_{\mu\nu}, \tag{6.26}$$

where $\mathcal{O}(E)$ and $f(E,\omega)$ are smooth functions of their respective arguments, $E = \frac{E_\mu + E_\nu}{2}$ and $\omega = E_\mu - E_\nu$, $D(E)$ is the density of states, and $R_{\mu\nu}$ is a stochastic variable of mean zero and unit variance. Each term of the ETH is derived in Appendix B.2, for observables satisfying sparsity and smoothness conditions.

To describe the process of quantum thermalization consistently, both diagonal and off-diagonal elements of observables play important roles. We will see that the off-diagonal elements dictate both the route to equilibrium, as well as the time-averaged fluctuations, and are thus the main focus of our work. The diagonal elements, however, dictate the equilibrium value of a given observable, and are thus similarly indispensable for a consistent theory of thermalization. For the diagonal elements, our RMT predicts that

$$O_{\mu\mu} \approx \overline{[O_{\alpha\alpha}]}_\mu, \tag{6.27}$$

where $\overline{[O_{\alpha\alpha}]}_\mu$ is given in Eq. (6.17) with $n = 0$, and

$$|O_{\mu\nu}|^2_{\mu\neq\nu} \approx \sum_n a_n \Lambda^{(2)}(\mu, \nu - n), \tag{6.28}$$

where we define

$$\Lambda^{(n)}(\mu,\nu) := \frac{\omega_0 n\Gamma/\pi}{(E_\mu - E_\nu)^2 + (n\Gamma)^2}, \tag{6.29}$$

and

$$a_n = \begin{cases} \overline{[\Delta O^2_{\alpha\alpha}]}_{\bar{\mu}} := \overline{[O^2_{\alpha\alpha}]}_{\bar{\mu}} - \overline{[O_{\alpha\alpha}]}^2_{\bar{\mu}} & \text{if } n = 0 \\ \overline{[O^2_{\alpha,\alpha+n}]}_{\tilde{\mu}} & \text{otherwise.} \end{cases} \tag{6.30}$$

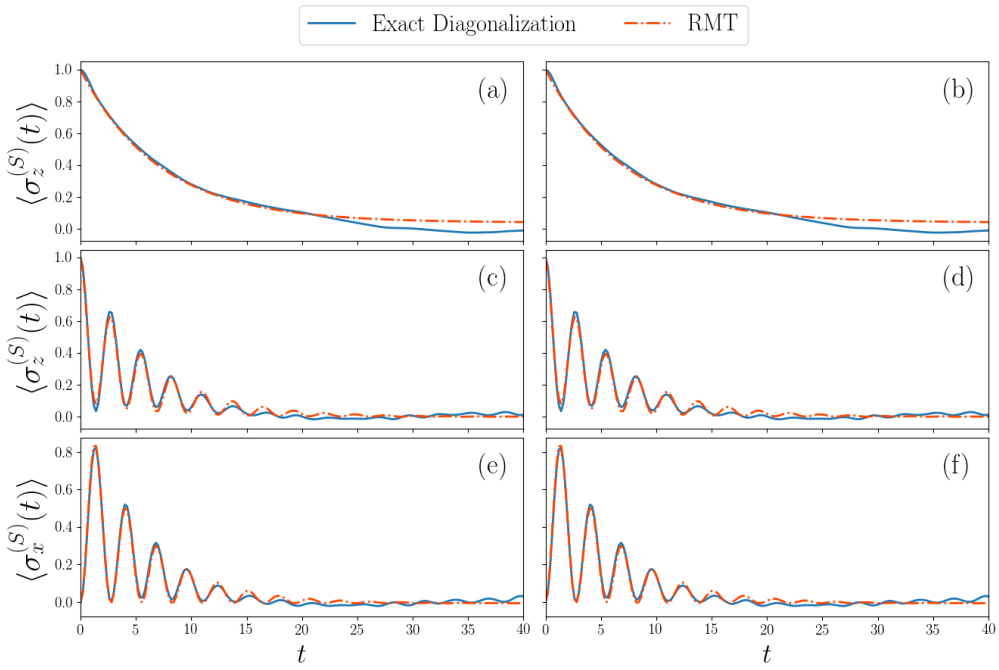

Figure 6.2: Time dependence of the Spin-Chain described be Eq. (6.47) using Exact Diagonalization (blue line) for initial eigenstates of H_0, $|\uparrow\rangle_S|\phi_\alpha\rangle_B$, (left column, (a), (c), (e)) and initial product states $|\uparrow\rangle_S|\uparrow,\downarrow,\cdots\rangle_B$ (right column, (b), (d), (f)). System fields are $B_z^{(S)} = 0.8$, and $B_x^{(S)} = 0$ (top row, (a), (b)) and $B_x^{(S)} = 0.8$ (middle and bottom rows (c)-(f)). RMT (red dot-dashed) lines thus show fit to Eq. (6.40) with $\langle O(t)\rangle_0 = 1$ in (a), (b), given by Eq. (D.11) in (c), (d), and by the analogous expression to that in (D.11) for $\sigma_x^{(S)}$ in (e), (f). Other parameters used are $N = 13, J_x^{(SB)} = 0.4, J_x = 1, B_z^{(B)} = 0, B_x^{(B)} = 0.3, J_z^{(SB)} = 0.2, J_z = 0$.

Here the microcanonical averages of matrix elements are centred around $\overline{\mu} = (\mu + \nu)/2$, and $\tilde{\mu} = (\mu+\nu-n)/2$ respectively. We thus see that off-diagonal matrix elements $|O_{\mu\nu}|^2_{\mu\neq\nu}$ are described by Lorentzians of width 2Γ [16], with peaks at energies $E_n = \omega_0 n$ separating those states coupled by O.

In Appendix B.2, we further show that the form obtained for the diagonal elements, Eq. (6.27), obtains the correct long-time average for observables. For the remainder of this chapter, we focus on the role of off-diagonal elements, which are the key aspect that determine both the route to equilibrium, and the fluctuations thereafter.

In Eqs. (6.27), (6.28), and in the rest of this chapter, we use "$\approx$" as an approximation that is valid to leading order in $\frac{\omega_0}{\Gamma}$.

6.4 Time-Dependence of Observables

From the details outlined above, we are now able to derive the full time dependence of observables satisfying our physical conditions. We will further see that important features of thermalization may be observed even without appeal to our conditions on observables, but are rather more generic. A full account of the dynamics of thermalization is revealed by application of the sparsity and smoothness assumptions of Section 6.3.4, as well as the

self-averaging property of random matrices, Eq. (6.10).

We consider the time evolution of an observable O, starting from an arbitrary initial pure state,

$$|\psi(0)\rangle = \sum_{\alpha_0} \psi_{\alpha_0} |\phi_{\alpha_0}\rangle, \tag{6.31}$$

where $\{|\phi_{\alpha_0}\rangle\}$ labels the basis of eigenstates of the non-interacting Hamiltonian H_0. We begin by defining the quantity

$$\Delta O(t) := \langle O(t)\rangle - \overline{\langle O(t)\rangle}, \tag{6.32}$$

where

$$\overline{\langle O(t)\rangle} := \lim_{T\to\infty} \frac{1}{T} \int_0^T dt \langle O(t)\rangle. \tag{6.33}$$

We may then write, assuming that the energies E_μ are non-degenerate,

$$\begin{aligned} \Delta O(t) = \sum_{\substack{\alpha_0,\beta_0,\\ \alpha,\beta}} \sum_{\substack{\mu,\nu\\ \mu\neq\nu}} & \psi_{\alpha_0}\psi^*_{\beta_0} c_\mu(\alpha_0) c_\nu(\beta_0) c_\mu(\alpha) c_\nu(\beta) \\ & \times O_{\alpha\beta} e^{-i(E_\mu - E_\nu)t}. \end{aligned} \tag{6.34}$$

Now, assuming self averaging, we treat the observable as equal to its ensemble average, such that $\Delta O(t) = \langle \Delta O(t)\rangle_V$. We then find

$$\begin{aligned} \Delta O(t) = \sum_{\substack{\alpha_0,\beta_0,\\ \alpha,\beta}} \sum_{\substack{\mu,\nu\\ \mu\neq\nu}} & \psi_{\alpha_0}\psi^*_{\beta_0} \langle c_\mu(\alpha_0) c_\nu(\beta_0) c_\mu(\alpha) c_\nu(\beta)\rangle_V \\ & \times O_{\alpha\beta} e^{-i(E_\mu - E_\nu)t}. \end{aligned} \tag{6.35}$$

We thus observe that the time evolution may be written in terms of the four-point correlation function $\langle c_\mu(\alpha_0) c_\nu(\beta_0) c_\mu(\alpha) c_\nu(\beta)\rangle_V$ of the off-diagonal ($\mu \neq \nu$) terms only. This correlation function was found in Ref. [16], and is given in Appendix B.1, Eq. (B.3). Substituting this into Eq. (6.35), we have,

$$\begin{aligned} \Delta O(t) = \sum_{\substack{\mu,\nu\\ \mu\neq\nu}} \Bigg[& \sum_{\alpha_0,\beta_0} \psi_{\alpha_0}\psi^*_{\beta_0} O_{\alpha_0\beta_0} \Lambda(\mu,\alpha_0)\Lambda(\nu,\beta_0) \\ & - \sum_{\alpha_0,\alpha} |\psi_{\alpha_0}|^2 O_{\alpha\alpha} \frac{\Lambda(\mu,\alpha_0)\Lambda(\nu,\alpha_0)\Lambda(\mu,\alpha)\Lambda(\nu,\alpha)}{\Lambda^{(2)}(\mu,\nu)} \\ & - \sum_{\alpha_0,\beta_0} \psi_{\alpha_0}\psi^*_{\beta_0} O_{\alpha_0\beta_0} \frac{\Lambda(\mu,\alpha_0)\Lambda(\nu,\alpha_0)\Lambda(\mu,\beta_0)\Lambda(\nu,\beta_0)}{\Lambda^{(2)}(\mu,\nu)} \Bigg] e^{-i(E_\mu - E_\nu)t}. \end{aligned} \tag{6.36}$$

Now, noting that for the bulk states we analyse we have $\Lambda(\mu,\alpha) = \Lambda(\mu-\alpha)$, we may evaluate the first term in (6.36) by defining $\tilde{\mu} = \mu - \alpha_0$, $\tilde{\nu} = \nu - \beta_0$, and thereby obtain

$$\begin{aligned} & \sum_{\alpha_0,\beta_0} \psi_{\alpha_0}\psi^*_{\beta_0} O_{\alpha_0\beta_0} e^{-i(E_{\alpha_0} - E_{\beta_0})t} \sum_{\tilde{\mu},\tilde{\nu}} \Lambda(\tilde{\mu})\Lambda(\tilde{\nu}) e^{-i(E_{\tilde{\mu}} - E_{\tilde{\nu}})t} \\ & \qquad = \langle O(t)\rangle_0 e^{-2\Gamma t}, \end{aligned} \tag{6.37}$$

where $\langle O(t)\rangle_0$ is the evolution of the observable O under the non-interacting Hamiltonian H_0, and we have taken the continuum limit of the summation $\sum_{\tilde{\mu}} \to \int \frac{dE_{\tilde{\mu}}}{\omega_0}$, such that we obtain Fourier transforms of each Λ, which result in the exponentially decaying factor.

We stress here that Eq. (6.37) did not require any assumption on the observable O, only the self-averaging property. We comment further on the implications of this at the end of this section.

Now, to evaluate the second term in (6.36) we require the smoothness condition (see Section 6.3.4). Explicitly, applied here, this can be seen as the removal of the microcanonical average of matrix elements from a summation of the form $\sum_\alpha O_{\alpha\alpha}\Lambda(\mu,\alpha)\Lambda(\nu,\alpha) \approx \overline{[O_{\alpha\alpha}]}_{\overline{\mu}}\Lambda^{(2)}(\mu,\nu)$, with $\overline{\mu} = \frac{\mu+\nu}{2}$. We thus see that the second term in (6.36) is given by

$$\begin{aligned}
&\sum_{\substack{\mu,\nu\\ \mu\neq\nu}} \frac{\sum_{\alpha_0}|\psi_{\alpha_0}|^2\Lambda(\mu,\alpha_0)\Lambda(\nu,\alpha_0)\sum_\alpha O_{\alpha\alpha}\Lambda(\mu,\alpha)\Lambda(\nu,\alpha)}{\Lambda^{(2)}(\mu,\nu)} e^{-i(E_\mu-E_\nu)t} \\
&\qquad = \sum_{\substack{\mu,\nu\\ \mu\neq\nu}}\sum_{\alpha_0} \overline{[O_{\alpha\alpha}]}_{\overline{\mu}}|\psi_{\alpha_0}|^2\Lambda(\mu-\alpha_0)\Lambda(\nu-\alpha_0)e^{-i(E_\mu-E_\nu)t} \\
&\qquad \approx \overline{[O_{\alpha\alpha}]}_{\overline{\alpha_0}} \sum_{\substack{\tilde{\mu},\tilde{\nu}\\ \tilde{\mu}\neq\tilde{\nu}}}\sum_{\alpha_0}|\psi_{\alpha_0}|^2\Lambda(\tilde{\mu})\Lambda(\tilde{\nu})e^{-i(E_{\tilde{\mu}}-E_{\tilde{\nu}})t} \\
&\qquad = \overline{[O_{\alpha\alpha}]}_{\overline{\alpha_0}} e^{-2\Gamma t},
\end{aligned} \tag{6.38}$$

where we have defined $\tilde{\mu} = \mu - \alpha$, $\tilde{\nu} = \nu - \alpha$, and $\overline{\alpha_0}$ is the central energy of the distribution $\{\psi_{\alpha_0}\}$. For the third step we have used $\sum_{\alpha_0}\overline{[O_{\alpha\alpha}]}_{\alpha_0}|\psi_{\alpha_0}|^2 = \overline{[O_{\alpha\alpha}]}_{\overline{\alpha_0}}\sum_{\alpha_0}|\psi_{\alpha_0}|^2 = \overline{[O_{\alpha\alpha}]}_{\overline{\alpha_0}}$, which can be seen to be a straightforward application of Eq. (6.19), and requires that the average $\overline{[O_{\alpha\alpha}]}_{\overline{\alpha_0}}$ is approximately constant over the width of the initial state distribution $\{\psi_{\alpha_0}\}$.

The third term in Eq. (6.36) is shown in Appendix D.1 to be bounded for all time by $\max_{\alpha_0\beta_0}(O_{\alpha_0\beta_0})N_O\frac{3\omega_0}{4\Gamma}$, which is small in comparison to other terms in the time evolution, and can thus be ignored. We note here that the sparsity condition is required in order to arrive at this bound.

For the time evolution of generic observables, we thus obtain

$$\langle O(t)\rangle = \left(\langle O(t)\rangle_0 - \overline{[O_{\alpha\alpha}]}_{\overline{\alpha_0}}\right)e^{-2\Gamma t} + \overline{\langle O(t)\rangle} + \mathcal{O}\left(\frac{\omega_0}{\Gamma}\right). \tag{6.39}$$

Interestingly, from the conditions $\langle O(t=0)\rangle = \langle O(t=0)\rangle_0$, Eq. (6.39) requires that the microcanonical average around the initial state energy $\overline{[O_{\alpha\alpha}]}_{\overline{\alpha_0}}$ is equal to the time average $\overline{\langle O(t)\rangle}$ up to an error on the order $\mathcal{O}(\frac{\omega_0}{\Gamma})$. We note that this long-time value can also be derived from the diagonal correlation function, Eq. (6.11), which is shown in Appendix B.2. Thus, the dominating contribution becomes

$$\langle O(t)\rangle \approx \langle O(t)\rangle_0 e^{-2\Gamma t} + \overline{\langle O(t)\rangle}(1-e^{-2\Gamma t}). \tag{6.40}$$

This is the main analytic result of this chapter. We note that the form is particularly useful, as for most systems of interest obtaining $\langle O(t)\rangle_0$ is a trivial calculation, as it

characterises the time evolution in the non-interacting Hamiltonian. We further note that a statistical theory for random wavefunctions $c_\mu(\alpha)$ that includes correlations induced by the orthonormality constraint is strictly required to arrive to Eq. (6.40).

For our applications below, Eq. (6.40) provides a method of obtaining Γ from the observable time dependence via a fit, which may account for non-trivial free evolution of the observable caused by *e.g*, a magnetic field. A specific application to such a case is shown in Appendix D.2, and its time-dependence shown in Fig. (6.2).

As Γ is the width of the random wavefunctions, and thus of the local density of states (LDOS), it may thus be obtained by a fit to the time-dependence of the survival probability, which is in general challenging for a many-body system. Eq. (6.40) may be seen as an extension of this methodology to generic observables. We will see below that combined with previous results on the time-averaged observable fluctuations [16] (see Appendix D.4 for details and extension of previous results), Eq. (6.40) provides an experimental protocol to test the applicability of the random matrix approach to realistic systems, as well as a method of measuring their DOS, in the form of an emergent classical FDT.

We further comment on some details of this derivation, and the form of Eq. (6.40), that provide some insight into the implications of our assumptions. As noted above, the first term in Eq. (6.40) is obtained without the need for any assumptions on the observable O, only requiring that the system is self-averaging. We can see that this term is, in essence, a 'decay of the initial observable value'. The second term in Eq. (6.40), which may be interpreted as a 'grow-in of the microcanonical average', requires the smoothness assumption - namely, that a consistent microcanonical average may be defined over the width Γ. In Appendix (D.1), we required the sparsity condition in order to show that the third term in Eq. (6.40) may be neglected.

Indeed, then, a consistent theory of thermalization may be developed on the basis of i) self-averaging, which dictates that information about the initial state decays in time, ii) the ability to define a microcanonical average via the smoothness condition, which, intuitively, allows the system to decay to the microcanonical value, and iii) the sparsity constraint, which reduces the contribution of off-diagonal elements $O_{\alpha\beta}$ in the decay process, which then simply contribute through their effect on the free evolution $\langle O(t)\rangle_O$.

Aside from the time-averaged observable expectation value being equal to the microcanonical average, a further requirement for thermalization is that the fluctuations around the equilibrium value are small. It is these fluctuations that are the focus of the remainder of this chapter, which we will see can be quantified analytically based on the same constrains.

6.5 Fluctuations from RMT

We now focus on the time-averaged fluctuations of an observable O, defined by

$$\delta_O^2(\infty) := \lim_{T\to\infty}\left[\frac{1}{T}\int_0^T dt\langle O(t)\rangle^2 - \left(\frac{1}{T}\int_0^T dt\langle O(t)\rangle\right)^2\right]. \tag{6.41}$$

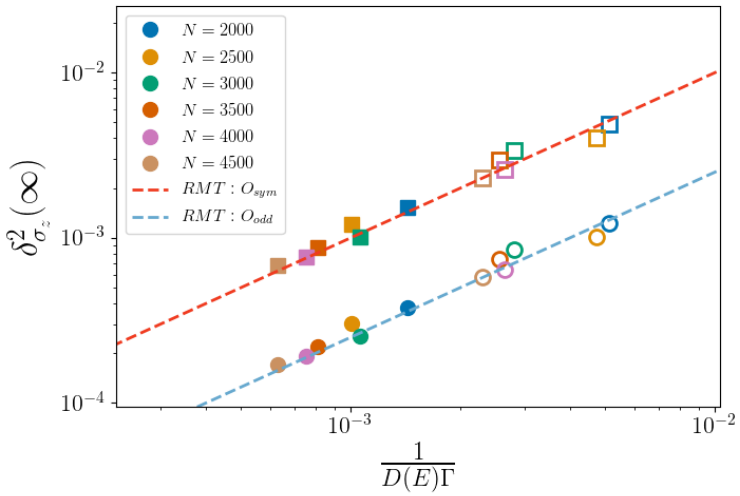

Figure 6.3: QC-FDT (Eq. (6.44)) for Random Matrix Hamiltonian. Squares show relation for O_{odd}, and diamonds for O_{sym}. Filled markers represent $g = 0.1$, unfilled represent $g = 0.05$. O_{odd} and O_{sym} differing as $\overline{[\Delta O^2_{\alpha\alpha}]}_{\alpha_0}$ is equal to $1/4, 1$ for O_{odd} and O_{sym} respectively. No averaging over realisations of the random matrix V is performed, and hence we observe the self-averaging property.

Let us assume for now that the system is initially in an eigenstate of H_0, $|\phi_{\alpha_0}\rangle$, with energy E_{α_0}. The off-diagonal elements $O_{\mu\nu}$ govern the infinite-time fluctuations of O [66], via,

$$\delta^2_O(\infty) = \sum_{\substack{\mu,\nu \\ \mu\neq\nu}} |c_\mu(\alpha_0)|^2 |c_\nu(\alpha_0)|^2 |O_{\mu\nu}|^2, \tag{6.42}$$

where we have assumed that the energies E_μ are non-degenerate. In order to evaluate Eq. (6.42), we may 'decouple' the coefficients $c_\mu(\alpha)$ describing the initial state part (with subscripted indices α_0), and observable, in the sense that, after performing the self-averaging assumption, we can write,

$$\langle |c_\mu(\alpha_0)|^2 |c_\nu(\alpha_0)|^2 |O_{\mu\nu}|^2 \rangle_V \to \langle |c_\mu(\alpha_0)|^2 |c_\nu(\alpha_0)|^2 \rangle_V \langle |O_{\mu\nu}|^2 \rangle_V. \tag{6.43}$$

This is shown in Appendix D.3. Then, following Ref. [16], using Eqs. (6.9), (6.28), and (6.42), we may convert the summations to integrals by the prescription $\sum_\mu \to \int dE_\mu D(E_\mu) = \int \frac{dE_\mu}{\omega_0}$, where $D(E)$ is the DOS.

For the simplest case where O is diagonal in the non-interacting basis, such that $n = 0$, we obtain

$$\delta^2_O(\infty) \approx \frac{\omega_0}{4\pi\Gamma} \overline{[\Delta O^2_{\alpha\alpha}]}_{\alpha_0}. \tag{6.44}$$

We note that the same relation holds up to a factor even if $\Lambda(\mu, \alpha)$ has another form, such as Gaussian [91, 113, 115], which we would expect outside of the low coupling regime. Eq. (6.44) shows an inverse relation between the observable time-fluctuations, $\delta^2_O(\infty)$, and the decay rate, Γ. We hereby refer to this result as the Quantum Chaotic Fluctuation-Dissipation Theorem (QC-FDT), since it establishes an effective description of $O(t)$ in terms of an effective Ornstein-Uhlenbeck process.

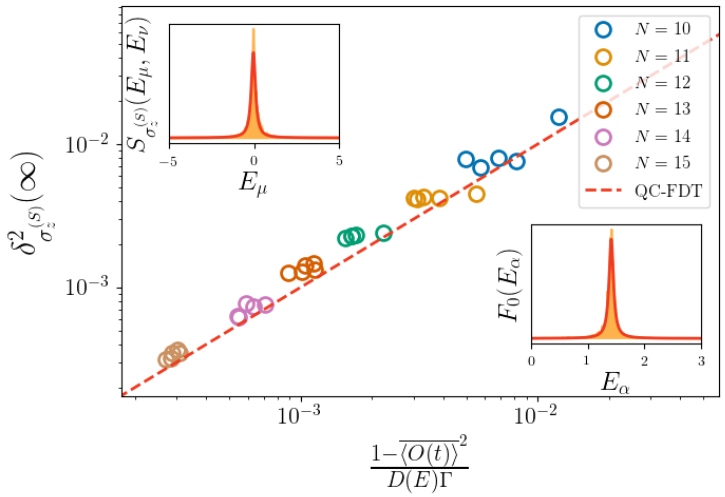

Figure 6.4: QC-FDT for Hamiltonian (6.47), observable $O = \sigma_z^{(S)}$. Initial state given by $|\uparrow\rangle_S|\phi_\alpha\rangle_B$, where $H_B|\phi_\alpha\rangle_B = E_\alpha^{(B)}|\phi_\alpha\rangle_B$. 5 different values of α are randomly selected from the central 1/2 of the energy spectrum $\{E_\alpha^{(B)}\}$. Parameters: $B_z^{(S)} = 0.8$, $B_z^{(B)} = 0$, $B_x^{(B)} = 0.3$, $J_z = 0.1$, $J_x = 1$, $J_x^{(SB)} = 0.4$, $J_z^{(SB)} = 0.2$.

It has been previously observed numerically [176] that the fluctuations of observable matrix elements $O_{\mu\mu}$ (where fluctuations are defined by taking the average eigenstates close in energy to $|\psi_\mu\rangle$) decay as $1/N_{pc}$, where N_{pc} is the number of principal components of a given eigenstate $|\psi_\mu\rangle$. We note that $N_{pc} \sim \Gamma D(E)$, and thus the QC-FDT shows this same relation.

In Fig. (6.3) we present numerical results that demonstrate the QC-FDT for the RMT Hamiltonian (6.4). We obtain Γ explicitly from a fit of the time dependence of the observables. The latter are given by O_{odd} and O_{sym}, which are chosen to be diagonal in the non-interacting basis (thereby trivially fulfilling the sparsity condition), with diagonal elements,

$$(O_{odd})_{\alpha\alpha} = \begin{cases} 1 & \text{if } \alpha = \text{odd} \\ 0 & \text{otherwise,} \end{cases} \tag{6.45}$$

for O_{odd}, and

$$(O_{sym})_{\alpha\alpha} = \begin{cases} 1 & \text{if } \alpha = \text{odd} \\ -1 & \text{otherwise,} \end{cases} \tag{6.46}$$

for O_{sym}. These 'observables' are chosen as they have a similar form to realistic observables made up of Pauli matrices: They are sparse, highly degenerate[177], and have a well defined structure in the non-interacting basis. These observables can further be seen to fulfil the smoothness conditions, as the average $\overline{[(O_{odd(sym)})_{\alpha\alpha}]}_{\alpha_0} = \frac{1}{2}(0)$ for all α_0.

In a non-integrable quantum many-body system that is well described by our RMT model, we expect the QC-FDT (6.44) to hold, with the modification $\omega_0 \to 1/D(E_{\alpha_0})$, that is, we need to introduce the average energy level spacing at the initial energy E_{α_0}.

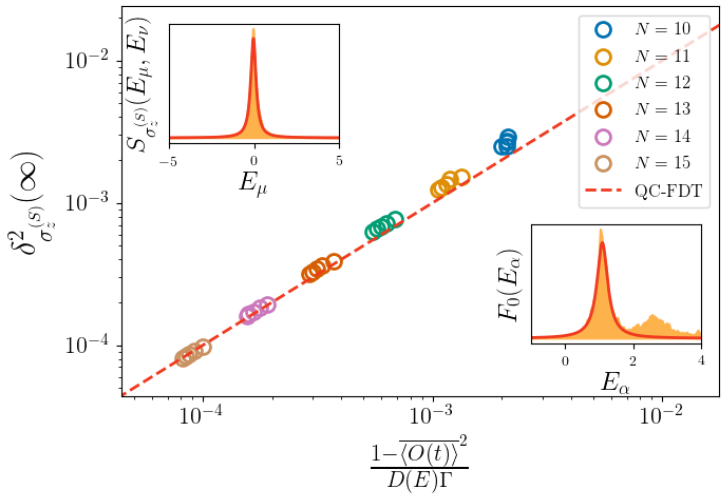

Figure 6.5: QC-FDT for Hamiltonian (6.47), observable $O = \sigma_z^{(S)}$. Initial state given by $|\psi(0)\rangle = |\uparrow\rangle_S|\downarrow,\downarrow,...,\downarrow\rangle_B$. Parameters: $B_z^{(S)} = [0.4, 0.5, 0.6, 0.7, 0.8]$, all others equal to Fig. (6.4).

6.6 Numerics - Spin Chain Model

We now investigate the applicability of the QC-FDT in quantum many-body Hamiltonians for the case described above, where $O_{\alpha\beta} \propto \delta_{\alpha\beta}$, and $|\psi(0)\rangle = |\phi_{\alpha_0}\rangle$, as described by Eq. (6.44). Our model is a spin chain, with a Hamiltonian of the form,

$$H = H_S + H_B + H_{SB}. \tag{6.47}$$

The system Hamiltonian H_S describes a single spin in a B_z field

$$H_S = B_z^{(S)}\sigma_z^{(1)}, \tag{6.48}$$

where $\{\sigma_i^{(j)}\}$ $i = x, y, z$ are the Pauli operators acting on site j. We take the system as site $j = 1$. The bath Hamiltonian is a spin-chain of length $N-1$, with nearest-neighbour Ising and XX interactions subjected to both B_z and B_x fields

$$H_B = \sum_{j>1}^{N}(B_z^{(B)}\sigma_z^{(j)} + B_x^{(B)}\sigma_x^{(j)}) + \sum_{j>1}^{N-1}(J_z\sigma_z^{(j)}\sigma_z^{(j+1)} + J_x(\sigma_+^{(j)}\sigma_-^{(j+1)} + \sigma_-^{(j)}\sigma_+^{(j+1)})). \tag{6.49}$$

The interaction part of the Hamiltonian describes a coupling of the system spin to a single bath ion of index N_m,

$$H_{SB} = J_z^{(SB)}\sigma_z^{(1)}\sigma_z^{(N_\mathrm{m})} + J_x^{(SB)}(\sigma_+^{(1)}\sigma_-^{(N_\mathrm{m})} + \sigma_-^{(1)}\sigma_+^{(N_\mathrm{m})}), \tag{6.50}$$

where $N_\mathrm{m} = 5$ throughout. Thus we have $H_0 = H_S + H_B$, and $V = H_{SB}$.

In Fig. (6.4) we present results for $N = 10, \ldots, 15$ and use as our observable $O = \sigma_z^{(1)}$. In order to obtain Γ we once again simulate the dynamics, and perform a fit to Eq.

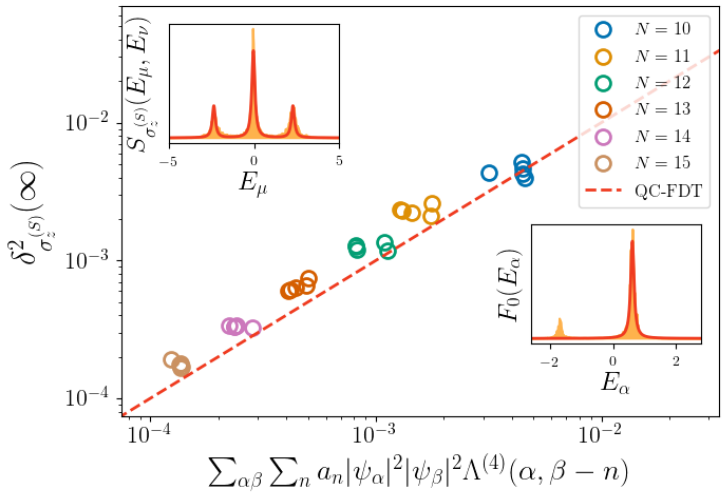

Figure 6.6: Generalised QC-FDT for Hamiltonian (6.47) with H_S given by (6.56). The QC-FDT is calculated explicitly for this case in Appendix D.5. Initial state given by $|\psi(0)\rangle = |\uparrow\rangle_S|\phi_\alpha\rangle_B$, where $\{|\phi_\alpha\rangle_B\}$ are the eigenstates of H_B. Parameters: $B_z^{(S)} = B_x^{(S)} = 0.8$, all others equal to Fig. (6.4).

(6.40). We show the QC-FDT for initial states randomly selected from the set of states $\{|\uparrow\rangle_S|\phi_\alpha\rangle_B\}$, with $|\phi_\alpha\rangle_B$ denoting an eigenstate of H_B with an energy in the central half of the spectrum $\{{}_B\langle\phi_\alpha|H_B|\phi_\alpha\rangle_B\}$. The insets of Figs. (6.4), (6.5), (6.6), and (6.7) show the smoothed initial state (bottom right) and observable (top left) distributions, obtained by the procedures

$$F_0(E_\alpha) = \sum_\mu |\langle\psi_\mu|\psi(0)\rangle|^2\delta_\epsilon(E_\mu - E_\alpha), \tag{6.51}$$

for the initial state, and

$$S_O(E_\mu, E_\nu) = \sum_{\mu\neq\nu} |O_{\mu\nu}|^2\delta_\epsilon(E_\mu - E_\nu), \tag{6.52}$$

for observables, where $\delta_\epsilon(E_\mu - E) = \epsilon\pi^{-1}/[(E_\mu - E)^2 + \epsilon^2]$. Fits to Eq. (6.9) and (6.28) are also shown (red line). We see that in each case we have a close agreement to a Lorentzian distribution, as expected from RMT.

6.7 Generalised QC-FDT

So far we have focussed on the simplest case of the QC-FDT, namely, for observables $O_{\alpha\beta} \propto \delta_{\alpha\beta}$, and initial states $|\psi(0)\rangle = |\phi_{\alpha_0}\rangle$. In Appendix D.4 we extend this to all observables fulfilling both the sparsity and smoothness conditions, and arbitrary initial states $|\psi(0)\rangle = \sum_\alpha \psi_\alpha|\phi_\alpha\rangle$, assuming only that the smoothness condition may be applied over the distribution $\{\psi_\alpha\}$, as well as $\{c_\mu(\alpha)\}$.

For this, more general case, the time-averaged fluctuations are now described by

$$\delta_O^2(\infty) = \sum_{\alpha\beta\alpha'\beta'} \sum_{\substack{\mu\nu \\ \mu\neq\nu}} \psi_\alpha \psi_\beta \psi_{\alpha'} \psi_{\beta'} c_\mu(\alpha) c_\nu(\beta) c_\mu(\alpha') c_\nu(\beta') |O_{\mu\nu}|^2. \tag{6.53}$$

As with the case above, see Eq. (6.42) and the following discussion, we observe that the correlations between coefficients of the initial state and observable decouple (see Appendix D.3), such that after taking the ensemble average $\langle \cdots \rangle_V$, we may substitute

$$\langle c_\mu(\alpha) c_\nu(\beta) c_\mu(\alpha') c_\nu(\alpha') |O_{\mu\nu}|^2 \rangle_V \to \langle c_\mu(\alpha) c_\nu(\beta) c_\mu(\alpha') c_\nu(\alpha') \rangle_V \langle |O_{\mu\nu}|^2 \rangle_V, \tag{6.54}$$

in Eq. (6.53). Applying this, we obtain the following form for the generalised QC-FDT,

$$\delta_O^2(\infty) \approx \sum_{\alpha\beta} \sum_n a_n |\psi_\alpha|^2 |\psi_\beta|^2 \Lambda^{(4)}(\alpha, \beta - n), \tag{6.55}$$

which is shown in Appendix D.4 in detail.

We start our numerical analysis by applying Eq. (6.55) to the case with an observable that is diagonal in the H_0 basis ($a_n = 0$ if $n \neq 0$). In this case we can see that, as long as the energy width of ψ_α is much smaller than the decay rate Γ, we recover Eq. (6.44). This is shown in Appendix D.4, along with various examples of why we expect the simple form of the QC-FDT, Eq. (6.44), to remain valid for many physical initial states.

We test the QC-FDT numerically in this case by choosing a product state as an initial state $|\psi(0)\rangle = |\uparrow\rangle_S |\downarrow, \downarrow, ..., \downarrow\rangle_B$. This is shown in Fig. (6.5), where we see the same scaling predicted by Eq. (6.44).

We have also numerically checked Eq. (6.55) in the case in which the system observable O is not diagonal in the basis of H_0, see Fig. (6.6). This case can be explored in our spin chain by adding an x-component to the system magnetic field, such that H_S now reads

$$H_S = B_z^{(S)} \sigma_z^{(1)} + B_x^{(S)} \sigma_x^{(1)}. \tag{6.56}$$

In this case, the initial state $|\uparrow\rangle_S$ is no longer an eigenstate of H_S, and is instead given by a superposition $|\uparrow\rangle_S = \psi_+ |\phi_+\rangle_S + \psi_- |\phi_-\rangle_S$. The observable distribution $(|\sigma_z|^2)_{\mu\nu}$ is split into three peaks, located at $E_n = 0, \pm 2E$, where $E = \sqrt{(B_x^{(S)})^2 + (B_z^{(S)})^2}$. We select the initial state of the bath to be a random mid energy eigenstate of H_B. We note in this case the approximation that the DOS does not change over relevant energy scales is a limiting factor, and may cause a deviation by a constant from the scaling seen in Eq. (6.55) for $E_n \gtrsim W$, where W is the width over which the significant change in the DOS occurs. We calculate explicitly the form of the QC-FDT for this case, which is shown as the dashed line in Fig. (6.6), in Appendix D.5.

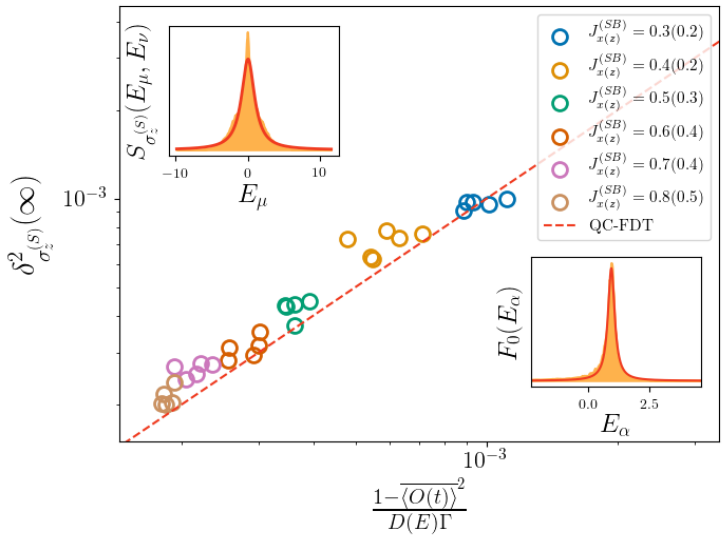

Figure 6.7: QC-FDT for Hamiltonian (6.47) demonstrated by varying coupling strengths only, for initial states randomly selected from mid-energy eigenstates of H_0. Parameters: $J_x^{(SB)}$ and $J_z^{(SB)}$ shown in legend, $N = 14$, all others equal to Fig. (6.4).

6.8 Experimental Application

Finally, we discuss the possibility of an experimental observation of the QC-FDT. Ideally, we would like to test our result without the need of an exact numerical diagonalization of the closed quantum system. Both Γ and $\delta^2_O(\infty)$ can be measured. However, the calculation of the DOS can be numerically challenging. One way around this problem is to calculate $D(E)$ for a non-interacting or integrable Hamiltonian that is sufficiently close to the real Hamiltonian. However, this approach relies on a detailed knowledge of the system and bath, and it may not always be possible.

A different approach is to explore the QC-FDT experimentally is to measure $\delta^2_O(\infty)$ and Γ for a constant system size N *but varying the coupling strength.* That is, assuming $V \propto g$, one could test the linear relation between $\delta^2_O(\infty)$ and $1/\Gamma$. We have numerically tested this approach as shown in Fig. (6.7). Our ideas could indeed be used to characterise the dimension of quantum system in terms of the quantity $\delta^2_O(\infty)\Gamma$, which on average is proportional to the DOS that are participating in the quantum thermalization process.

6.9 Conclusion and Outlook

In summary, we have obtained an analytic expression for the full time-dependence of the thermalization of physical observables to their microcanonical average. We further obtain an expression for the time-averaged fluctuations of observables in chaotic quantum systems in terms of the rate of decay to equilibrium after a perturbation. Our results show the emergence of a fluctuation-dissipation relation corresponding to an effective Ornstein-Uhlenbeck process. To the best of our knowledge this is the first time that such relation is derived for a closed quantum system. Our results rely on a RMT description of a

quantum thermalization process in which an interaction term coupling two parts of the quantum system is suddenly switched on triggering a quantum thermalization process. In our approach, the system-bath coupling is approximated by a Gaussian random matrix, an assumption that can be justified for a generic non-integrable system and weak system-bath couplings. We have successfully tested our result in a numerical experiment in a quantum spin chain.

Our result will help bridge the gap [178] between theoretical results on quantum thermalization and experiments with closed quantum systems. In those cases in which a good approximation for the DOS can be calculated, a check of the QC-FDT would involve measurable quantities like the decay rate and the time-fluctuations. Otherwise, the QC-FDT relation can still be checked experimentally as long as the coupling strength can be varied while keeping a constant system size. Our theory can thus be verified in quantum simulators working beyond the numerically tractable regime. Furthermore we argue that the product $\Gamma\delta_O^2(\infty)$ can be indeed considered as a measurement of the DOS of a non-integrable quantum system. As such, our work may prove useful in estimating the size of the Hilbert space in quantum devices.

Chapter 7

Ergodicity probes: using time-fluctuations to measure the Hilbert space dimension

7.1 Abstract

QUANTUM devices, such as quantum simulators, quantum annealers, and quantum computers, may be exploited to solve problems beyond what is tractable with classical computers. This may be achieved as the Hilbert space available to perform such 'calculations' is far larger than that which may be classically simulated. In practice, however, quantum devices have imperfections, which may limit the accessibility to the whole Hilbert space. We thus determine that the dimension of the space of quantum states that are available to a quantum device is a meaningful measure of its functionality, though unfortunately this quantity cannot be directly experimentally determined. Here we outline an experimentally realisable approach to obtaining the required Hilbert space dimension of such a device to compute its time evolution, by exploiting the thermalization dynamics of a probe qubit. This is achieved by obtaining a fluctuation-dissipation theorem for high-temperature chaotic quantum systems, which facilitates the extraction of information on the Hilbert space dimension via measurements of the decay rate, and time-fluctuations.

7.2 Introduction

The ability to control and manipulate microscopic systems at the single particle level is an essential requirement for many quantum technologies. Experimental setups where atoms or qubits can be arranged in ordered structures and studied in quantum non-equilibrium states include neutral atoms in optical lattices [56, 179, 180], trapped ions [12, 35, 160, 181], Rydberg atoms [15, 182], and superconducting circuits[13, 40]. These systems can be used for the quantum simulation of many-body models, or different forms of digital or adiabatic quantum computing. Most of these physical setups have limitations in the accessibility to certain observables. Thus, having extra tools to characterise quantum systems in a simple

and efficient way can be useful in the diagnosis and certification of quantum devices.

One of the most prominent properties of a quantum device is its size in terms of the dimension of the associated Hilbert space. The size of a quantum computer or simulator is often given in terms of number of qubits, such that the Hilbert space dimension is 2^N for N qubits. This is a measure that ignores the effect of disorder or the possible lack of connectivity between different zones in the device.

A more useful quantity would be the number of eigenstates of the Hamiltonian that take part in the quantum dynamics, which is bounded in this case by 2^N, but would exclude the degrees of freedom that do not contribute to the evolution of the initial state. A measurement of the number of eigenstates that contribute to the dynamics is thus a more useful measure of the true Hilbert space dimension of a quantum device. As such, in the following, we refer to this more useful measure as the Hilbert space of the quantum device. This Hilbert space dimension is, however, an elusive measure in realistic experimental situations.

In this chapter, we show that the equilibration dynamics [104, 132, 134, 172, 183–185] of a quantum system can be used to extract such information on the dimension of the Hilbert space of a quantum device, in terms of the effective number of states that contribute to the dynamics of a local observable. Indeed, advancements in quantum technologies described above have inspired a bounty of theoretical work in the field of quantum thermalization [57, 59, 63, 66, 67, 70, 71, 112, 158, 177, 186, 187]. In the following, we aim to help 'bridge the gap' between theoretical and experimental work in this field [178].

We assume a quantum quench scenario [15, 67, 187, 188] in which a quantum system is initialised in a fully-decohered, infinite temperature state, except for a subsystem that acts as a sensor and is prepared in a pure state. For simplicity, we assume that this subsystem is a single qubit, which we refer to as the 'probe' qubit. The relaxation dynamics of the probe qubit depends on the details of the underlying structure of the Hamiltonian, however, in the most generic case of non-integrable systems, an appropriate description can be given in terms of random matrix theory (RMT) [66, 71, 72, 89, 133, 189–191]. We show that the time-fluctuations of the probe in the long-time limit contain information about the Hilbert space dimension of the device.

This chapter is structured as follows. Firstly, in Section 7.3 we present the basic scheme and summarise our main result, which relies on an infinite-temperature fluctuation dissipation theorem (FDT) [173] for the dynamics of the probe qubit in order to extract information on the scaling of the effective Hilbert space of a quantum device. We continue, presenting numerical calculations that validate our predictions via exact diagonalization of a spin chain Hamiltonian in Section 7.4. We then outline in more detail our RMT model in Section 7.5. In Section 7.6 we derive an expression for the time dependence of generic observables in chaotic quantum systems, and discuss how this can be exploited for our measurements. We then derive the FDT, and extensions from the RMT model, and to finite temperatures, in Section 7.7. Finally, we summarise our findings in Section 7.8. Further details and proofs are included in Appendices. We note that this is arranged such that our key findings can be understood from sections 7.3 and 7.4, with the detailed

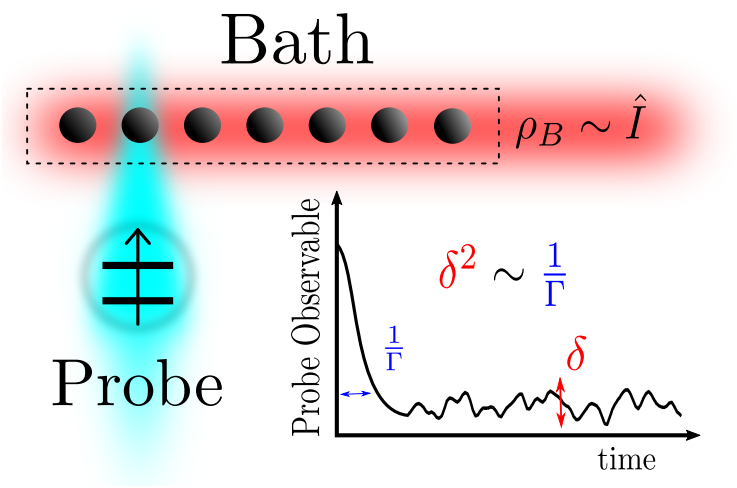

Figure 7.1: Illustration of our proposed setup (quantum device). A single qubit, labelled 'Probe', is coupled locally to a part of a larger non-integrable bath, initialised in an infinite temperature state $\rho_B \sim \hat{I}$ (this restriction is removed below). Experimentally, for our protocol, one needs access only to an observable of the Probe qubit.

calculations presented later in the text.

7.3 Setup and main results

7.3.1 Proposed setup

We assume that we have a quantum system (from here on, 'quantum device') made up of a single 'probe' qubit, initialised in a pure state, which at $t = 0$ is coupled to the rest of the quantum device (referred to as the 'bath'). We initialise the bath in an infinite temperature state. This is sketched in Figure 7.1. This can be routinely achieved, for example, in a quantum computer device that has not been properly initialised. Since quantum devices always suffer from some kind of decoherence, creating an infinite temperature (or fully decohered) state is typically a simple task. We then let this qubit evolve in time and reach an equilibrium state. The initial state is thus,

$$\rho(t = 0) = |\uparrow\rangle\langle\uparrow| \otimes \rho_B. \tag{7.1}$$

ρ_B is the density matrix of the bath in the fully decohered state,

$$\rho_B = \frac{1}{\mathcal{N}_B} \sum_{\beta}^{\mathcal{N}_B} |\phi_{B,\beta}\rangle\langle\phi_{B,\beta}|, \tag{7.2}$$

where $|\phi_{B,\alpha_B}\rangle$ is a set of orthonormal wave functions in the bath, which we take as the eigenstates of the bath Hamiltonian H_B. $\mathcal{N}_B$ is the Hilbert space dimension of the bath, and is the parameter on which we wish to infer information via measurements of the probe qubit. Later on the fully decohered state condition will be relaxed, allowing for finite temperatures.

The system evolves under the interacting Hamiltonian,

$$H = H_0 + V, \tag{7.3}$$

where $H_0 = \hat{1} \otimes H_B$ is the Hamiltonian of the uncoupled probe + bath device, and we assume that the probe qubit does not evolve at all in the absence of coupling to the bath, which is given by the operator V. A prominent role in the following discussions will be played by the eigensystems of the interacting Hamiltonian,

$$H|\psi_\mu\rangle = E_\mu|\psi_\mu\rangle, \tag{7.4}$$

and the eigensystem of the uncoupled probe-bath system

$$H_0|\phi_\alpha\rangle = E_\alpha^{(0)}|\phi_\alpha\rangle. \tag{7.5}$$

All throughout this work we will use the convention that indices μ, ν refer to summations over eigenstates of H, whereas α, β refer to eigenstates of H_0.

We focus on the quantum dynamics of the expectation value of a probe observable, which we take for concreteness to be $\langle\sigma_z(t)\rangle = \mathrm{Tr}(\rho(t)\sigma_z)$. Note that, however, the results should not depend on the particular choice for the probe observable, since H_0 has no probe energy term. The probe-bath coupling V, may introduce a dependence on the chosen observable, but the results below should hold in the general case of quantum chaotic or non-integrable systems.

The quantity under study, the time-averaged fluctuations of the probe observable, is defined by

$$\delta^2_{\sigma_z}(T) = \frac{1}{T}\int_0^T dt\left(\langle\sigma_z(t)\rangle - \mu_{\sigma_z}(T)\right)^2, \tag{7.6}$$

where $\mu_{\sigma_z}(T) = \frac{1}{T}\int_0^T dt\langle\sigma_z(t)\rangle$. Assuming only that the many-body eigenenergies are non-degenerate, and that also their energy gaps are non-degenerate, we may express the time fluctuations in terms of matrix elements between eigenstates of the coupled probe-bath system [66],

$$\delta^2_{\sigma_z}(\infty) = \sum_{\substack{\mu,\nu \\ \mu\neq\nu}} |\rho_{\mu\nu}|^2|(\sigma_z)_{\mu\nu}|^2, \tag{7.7}$$

where $\rho_{\mu\nu} = \langle\psi_\mu|\rho|\psi_\nu\rangle$, and $(\sigma_z)_{\mu\nu} = \langle\psi_\mu|\sigma_z|\psi_\nu\rangle$.

7.3.2 Summary of main results of this work

In many practical situations, the quantum device is a non-integrable, quantum chaotic system. We expect that in such cases a qualitative description can be obtained by assuming that V is a random matrix. This assumption leads to a statistical theory for the many body wave functions in Eqs. (7.4, 7.5) [16],

$$|\psi_\mu\rangle = \sum_\alpha c_\mu(\alpha)|\phi_\alpha\rangle, \tag{7.8}$$

where summations are understood to be taken from 1 to $2\mathcal{N}_B$, the dimension of the Hilbert space of the device. We will refer to $c_\mu(\alpha)$ as quantum chaotic or random wave functions. We assume that V belongs to the Gaussian Orthogonal Ensemble (GOE), appropriately scaled by a coupling strength g. In Ref. [16] we showed that this model can be solved and it allows us to calculate matrix elements in the interacting basis.

Special care must be taken to translate the probe initial state defined in Eq. (7.1) in the random matrix formalism. Without loss of generality we can assume that non-interacting eigenfunctions are ordered such that odd (even) values of α correspond to the probe qubit in state $|\uparrow\rangle$ ($|\downarrow\rangle$). This leads to the initial condition

$$\rho(t=0) = \frac{1}{\mathcal{N}_B} \sum_{\alpha \in \text{odd}}^{2\mathcal{N}_B} |\phi_\alpha\rangle\langle\phi_\alpha|. \tag{7.9}$$

In the following sections, we prove that random matrix theory leads to a relation between the time-fluctuations and the typical decay rate of the probe qubit. This relation is the main result of this chapter:

$$\delta^2_{\sigma_z}(\infty) = \chi(N)\overline{\Gamma^{-1}}, \tag{7.10}$$

where $\overline{\Gamma^{-1}} = \frac{1}{\Delta E}\int_0^{\Delta E} dE \Gamma(E)^{-1}$ is the average inverse decay rate of the qubit. This average is an unbiased average over all initially populated initial state energies, which spans the entire energy range ΔE of the device due to the initial infinite temperature bath state. We will see that this unbiased average originates from the decay to equilibrium of each state $|\phi_\alpha\rangle$ contributing to the initial state (7.9). In Sections 7.6 and 7.7 we will see that this can be related to the decay rate obtained from a fit to the decay to equilibrium of a local probe observable in our current set up. This quantity is thus simply an average of the decay rates experienced by the probe qubit.

The quantity $\chi(N)$, with N the total number of qubits, depends on the size of the system in the following way,

$$\chi(N) = C\frac{1}{\mathcal{N}_B \overline{D(E)}}. \tag{7.11}$$

$\overline{D(E)}$ is the average density of states (DOS) of the system, defined analogously to the average decay rate above (see also Eq. (7.61)). $\mathcal{N}_B$ is the bath Hilbert space dimension, and finally, C is a constant of order one that does not depend on the size of the system or coupling strength.

Eq. (7.10) can be understood as a fluctuation-dissipation relation, which relates the time-fluctuations in the steady-state with the decay rate after a quantum quench. The ratio between fluctuations and average decay time allows us to quantify the dimension of the Hilbert space over which the ergodic quantum dynamics takes place. In a physical system if V couples the probe qubit to the whole spectrum of the quantum device, we expect that the function $\chi \propto e^{cN_B}$ for some constant c, where N_B is the number of qubits in the part of the device that acts as a bath.

Our main result, Eq. (7.11), can be obtained by following these steps:

(i) We consider the random matrix model with an homogeneous coupling matrix V, and calculate $\delta_O^2(\infty)$ by extending the formalism developed in [16, 17] to mixed states (see Section 7.7.1). To carry out this calculation we assume a constant DOS, $D(E) = 1/\omega_0$, with ω_0 the mean energy separation.

This calculation allows us to predict an exponential decay for a probe observable of the form:

$$\langle O(t)\rangle = (\langle O(t)\rangle_0 - O_{\mathrm{DE}})e^{-2\Gamma t} + O_{\mathrm{DE}}, \tag{7.12}$$

where O_{DE} is the diagonal ensemble of the observable O, which we find to be equal to the long-time average of O as required, and $\langle O(t)\rangle_0$ refers to the free evolution of the observable O under the Hamiltonian H_0. This result is derived in Section 7.6. This is analogous to the result in Reference [17] for pure-states. We note that the same Equation has similarly been obtained in Ref. [189], which allows also for the perturbation matrix V to be inhomogeneous. In the specific case of interest here, Eq. (7.12) becomes,

$$\langle \sigma_z(t)\rangle = e^{-2\Gamma t}, \tag{7.13}$$

as $\langle \sigma_z(t)\rangle_0 = 1$ and $\langle \sigma_z\rangle_{\mathrm{DE}} = 0$.

Using this random matrix model we also obtain a preliminary version of the infinite temperature fluctuation-dissipation theorem, Eq. (7.11), with $\chi(N) = C\omega_0/\mathcal{N}_B$.

(ii) In a realistic system both the DOS and the coupling strength will depend on the energy. This leads to energy-dependent qubit decay rates, $\Gamma(E)$, and DOS, $D(E)$. Due to the infinite-temperature initial condition, it is not possible a priori to approximate those quantities to any single value, since the quantum dynamics of the probe qubit result from contributions from all possible initial states. It is thus necessary to extend the RMT formalism to allow for variations in both the DOS and the decay rate in energy over the width of the initial mixed state.

It is also important to note that when applied to a realistic system $\mathcal{N}_B$ should be thought of as the number of eigenstates that may contribute to the dynamics of a local observable - it is thus a measure of the effective Hilbert space dimension in the sense of the number of degrees of freedom that may be explored from a given initial state. This measure accounts for effects such as locality of interactions, and disorder, which will reduce the Hilbert space available for evolution of the system. As such, $\mathcal{N}_B$ will in general be bounded by the total Hilbert space dimension, but is a more realistic measure of the size of the explored Hilbert space in the thermalization dynamics of the device.

In Section 7.6 we show that the decay rate observed from such an initial state, defined with an energy dependent coupling strength, is the thermal average decay rate over the energy width defined by the initial state.

We formulate the generalisation of the FDT in Section 7.7.2, however a brief summary of the approach is as follows: To account for the energy variation of the DOS and decay rate we instead make the assumption that both change slowly in energy with respect to the energy width of a single eigenstate. In this case, one can reformulate the theory such that

the random wave functions have a smoothly varying width. In effect this is the statement that a given random wave function contributes as if it was the eigenstate of a random matrix model with a constant DOS and decay rate, as over the width of the wave function itself these parameters do not change appreciably.

In this case, we see that the average DOS and decay rate over the initially populated initial states contributes to the FDT, as in Eq. (7.10). This is extended to finite temperature systems, where instead a thermal average can be seen to contribute, in Section 7.7.3.

Finally, we may relate the two decay rate averages, as the thermal average observed from the decay differs slightly from that appearing in Eq. (7.10). These can be seen to be related by a constant factor that does not depend on the coupling strength, or bath size, and thus scaling information of the Hilbert space dimension may be recovered. This is shown in Section 7.7.3, and Appendix E.4, where the FDT is recast in terms of thermal averages.

In Section 7.6 we show that when an exponential decay of the form Eq. (7.12) is observed, this indicates that $\Gamma(E)$ is approximately constant over the bulk of the initially populated states. In this case we are able to extract the numerical value of the Hilbert space dimension directly, as the averages over $\Gamma(E)$ occurring in the FDT, and observed from the decay, are equal.

In summary, we observe the emergence of a classical fluctuation-dissipation theorem, relating the time-fluctuations and decay rate of our probe observable σ_z. The susceptibility $\chi(N)$ in Eq. (7.11) can be seen to be related to the Hilbert space dimension of the bath, $\mathcal{N}_B$, and thus measurements of the decay rate, Γ, and fluctuations $\delta^2_{\sigma_z}(\infty)$, which are both obtainable from the time evolution, can be exploited to obtain information on the device Hilbert space dimension, $\mathcal{N}_B$.

7.4 Numerical Experiments

Before going into the technical details of our derivation, we present numerical evidence that confirms the validity of the random matrix approach and our main results. In this section, we show the application to a spin-chain system using exact diagonalization [192, 193]. From this, we observe the FDT numerically using a realistic experimentally observable model.

In Fig. 7.2, we show the manifestation of Eq. (7.10) in a spin-chain system described by the Hamiltonian $H = H_S + H_B + H_{SB}$, where $H_S = 0$ is the system Hamiltonian (acting as our probe), H_B is our bath Hamiltonian, given by

$$\begin{aligned} H_B = &\sum_{j>1}^{N} (B_z^{(B)} \sigma_z^{(j)} + B_x^{(B)} \sigma_x^{(j)}) + \\ &\sum_{j>1}^{N-1} [J_z \sigma_z^{(j)} \sigma_z^{(j+1)} + J_x (\sigma_+^{(j)} \sigma_-^{(j+1)} + \sigma_-^{(j)} \sigma_+^{(j+1)})], \end{aligned} \tag{7.14}$$

which acts on sites with index > 1, which is the probe index. The probe and bath are

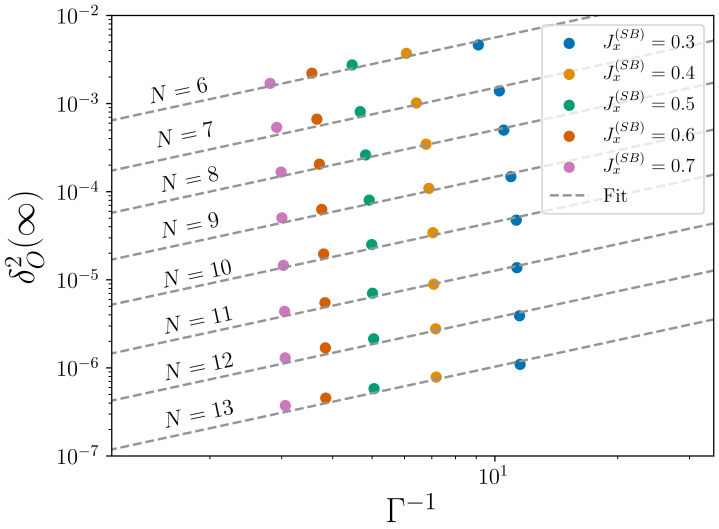

Figure 7.2: Observation of the FDT, Eq. (7.10), for varying coupling strength, for many bath sizes $N-1$ (labelled on plot). Fits (blue dashed lines) shown for each value of N, are linear fits to obtain $\chi(N)$ for each individual N value. We see in this case, then, that one does not require the ability to change the device length in order to observe our predictions experimentally. Parameters: $B_Z^{(B)} = 0.1, B_x^{(B)} = 0.3, J_z = 0.1, J_x = 1, J_z^{(SB)} = 0, \beta = 0$.

coupled by the interaction Hamiltonian,

$$\begin{aligned} H_{SB} = & J_z^{(SB)} \sigma_z^{(1)} \sigma_z^{(N_\mathrm{m})} \\ & + J_x^{(SB)} (\sigma_+^{(1)} \sigma_-^{(N_\mathrm{m})} + \sigma_-^{(1)} \sigma_+^{(N_\mathrm{m})}). \end{aligned} \tag{7.15}$$

Here N_m is the device site where the probe is coupled, which we set as 2 throughout. This spin-chain model may be related to the random matrix toy model, $H = H_0 + V$, via the prescription $H_0 \Leftrightarrow H_S + H_B$, and $V \Leftrightarrow H_{SB}$. In particular, we see that, as $\chi(N) = \frac{\delta_O^2(\infty)}{\overline{\Gamma^{-1}}} \propto \mathcal{N}_B^{-1}$, we expect that if all of the available Hilbert space is being utilised in the unitary dynamics we will observe the following scaling:

$$\chi(N) \propto e^{-cN_B}. \tag{7.16}$$

We test this relation in Fig. 7.3.

It is important to note that this exponential scaling of $\chi(N)$, Eq. (7.16), is expected from not only the contribution of $\mathcal{N}_B$, but also from the average DOS, $\overline{D(E)}$. This average is often trivially obtained, as for example, for an ensemble of N two-level systems $\overline{D(E)} = \frac{1}{\Delta E} \int_0^{\Delta E} dE D(E) = \frac{2^N}{\Delta E}$, where ΔE is the range of energies available $E_{max} - E_{min}$ (which may itself change with N), regardless of the microscopic properties of the DOS. We thus also study the quantity $\chi(N)\overline{D(E)}$, as this quantity has no dependence on the DOS, and an observation of the exponential scaling in system size is confirmation that, indeed, $\mathcal{N}_B \propto e^{cN}$. This is shown in Fig. 7.4, where we observe an exponential scaling of the Hilbert space dimension, with $c \approx 0.62$, compared to $\ln(2) \sim 0.69$ if the entire Hilbert space were explored in the dynamics.

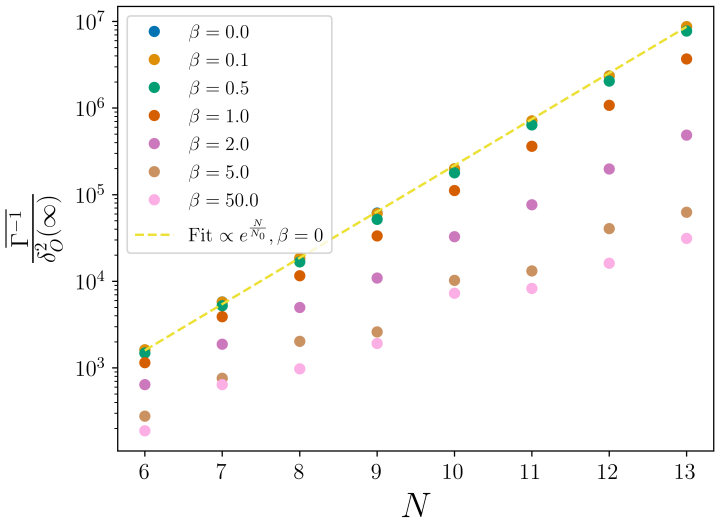

Figure 7.3: Observation of the FDT, Eq. (7.10), for varying bath size $N-1$, for temperatures β. Fit (yellow dashed line) is performed to the function $ae^{\frac{N}{N_0}}$ for the infinite temperature case, $\beta = 0$, and thus confirms the exponential scaling of $\chi(N)$. In this case, we observe an exponential scaling for all temperatures, as the average DOS also scales exponentially with N. Note that here we have $\Gamma \sim 0.2$ so the high temperature limit is defined by approximately $\beta \ll 5$. Parameters: as Fig. 7.2 with $J_x^{(SB)} = 0.5$.

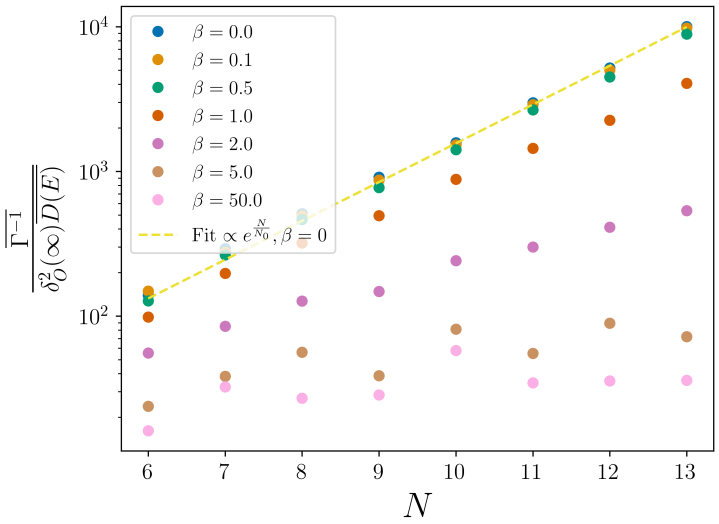

Figure 7.4: As in Fig. 7.3, however accounting for the exponential scaling of the average DOS with device size. Fit (yellow dashed line) is performed to the function $ae^{\frac{N}{N_0}}$ for the infinite temperature case, $\beta = 0$, and thus confirms the exponential scaling of $\chi(N)\overline{D(E)} \sim \frac{1}{\mathcal{N}_B}$. In this case, we observe an exponential scaling for only high temperatures, and confirm that for low temperatures $\chi(N)\overline{D(E)}$ is independent of N. Note that here we have $\Gamma \sim 0.2$ so the high temperature limit is defined by approximately $\beta \ll 5$. Parameters: as Fig. 7.2 with $J_x^{(SB)} = 0.5$.

We further observe in Figs. 7.3 and 7.4, that the FDT similarly applies at finite temperatures $\beta = \frac{1}{k_B T} > 0$. The extension of our theoretical approach to this case is discussed below, with additional details given in Appendix E.4. Indeed, we can show that for high temperatures, such that $\beta^{-1} \gg \Gamma$, we obtain an FDT of the same form as Eq. (7.10), by employing a high energy cut-off $(\rho_B)_{\alpha\alpha} \sim e^{-\beta E_\alpha}$ to the bath state occupation.

For finite temperatures we show below that the FDT depends on the partition function Z_β itself, rather than the Hilbert space dimension. Indeed, one can see that in the infinite temperature limit $Z_0 = \lim_{\beta\to 0} \sum_\alpha e^{-\beta E_\alpha} \delta_{\alpha,\text{odd}} = \mathcal{N}_B$.

Finally, we see that when the observable is found to decay exponentially to its equilibrium value, this indicates that the decay rate is approximately constant over the bulk of the initially occupied states. This is shown in Section 7.6. Exploiting this observation, we are able to directly obtain the Hilbert space dimension, as for an infinite temperature initial bath state the average $\overline{\Gamma^{-1}}$ is equal to the measured decay rate. The bath Hilbert space dimension $\mathcal{N}_B$, as calculated from Eq. (7.10), is plotted for varying device sizes in Fig. 7.5. Here we observe that $\mathcal{N}_B$ indeed increases exponentially with systems size, yet is somewhat smaller than its maximum possible value 2^{N-1}, which is expected to the locality of interactions within the chain.

We again note that in Fig. 7.5 the measurement of $\mathcal{N}_B$ is a measurement of the explored Hilbert space, or the total number of eigenstates that contribute to the evolution of the initial state. Thus, for a maximally connected device this would be 2^{N-1}, whereas locality of interactions in this case restricts some areas of the Hilbert space.

We note that for models where $\Gamma(E)$ is not approximately constant in energy, which would be marked by a deviation from the exponential decay in Eq. (7.12), one would still have access to Figs. 7.2-7.4, and thus scaling information of the Hilbert space dimension, yet the numerical value $\mathcal{N}_B$ would be obscured. This is explained in more detail in Section 7.6, where we see how information on $\Gamma(E)$ is extracted from the decay, and in Section 7.7 and Appendix E.4, where we see how this relates to the observed FDT. The key detail is that when the FDT is expressed in terms of the same value measured from the decay it differs by a constant, thereby leaving the scaling of $\mathcal{N}_B$ with system size or decay rate accessible, yet obscuring the numerical value.

We note that in the previous chapter we described a FDT for pure states, which can be seen to be recovered in the low temperature limit, $\beta^{-1} \ll \Gamma$, for which $\chi(N)$ does not depend explicitly on the Hilbert space dimension $\mathcal{N}_B$. This can also be analytically seen to be the same as the low temperature limit of our treatment below, which indicates that there is a smooth transition between these two cases. This is indeed observed in the numerics of Figs 7.3 and 7.4.

7.5 Model

7.5.1 RMT Approach

Our approach relies on the calculation of correlation functions from a statistical theory of random wave functions $c_\mu(\alpha)$. Here we summarise the essential ingredients to our model,

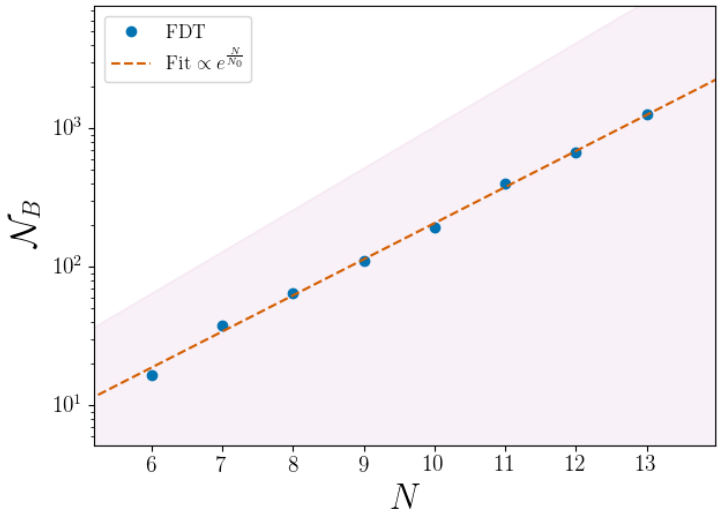

Figure 7.5: Hilbert space dimension of the bath $\mathcal{N}_B$ for varying device size N inferred from the FDT, Eq. (7.10) (blue dots), $C = \frac{3}{8\pi}$, which can be easily obtained from the observable (see Section 7.7). For a fully connected device the maximum possible $\mathcal{N}_B$ is $\mathcal{N}_B = 2^{N-1}$, the region below this limit is shaded. We observe that the measured Hilbert space dimension indeed scales exponentially with system size (dashed line is exponential fit), though is somewhat smaller than the maximum dimension of a fully connected device. Parameters as in Fig. 7.2, with $J_x^{(SB)} = 0.5$ and $\beta = 0$.

and give details on the calculations in the sections below[1].

Our theory, developed in Ref. [16] by extending Deutch's RMT model [64, 65, 100], can be used to obtain arbitrary correlation functions $\langle c_\mu(\alpha)c_\nu(\alpha)\cdots\rangle_V$, where $\langle\cdots\rangle_V$ denotes the ensemble average over an ensemble of random matrix perturbations, V, for a $\mathcal{N}\times\mathcal{N}$ Hamiltonian of the form (7.3), with $(H_0)_{\alpha\beta} = \alpha\omega_0\delta_{\alpha\beta}$, with $\omega_0 = \frac{1}{\mathcal{N}}$ and V a random matrix selected from the GOE, with $\langle V_{\alpha\beta}^2\rangle_V = \frac{(1+\delta_{\alpha\beta})g^2}{\mathcal{N}}$. In practice, those correlations allow us to calculate any dynamical quantity of interest within the RMT formalism.

To illustrate the use of such correlation functions we briefly consider the simple example of the diagonal observable matrix elements $O_{\mu\mu}$. These can be written as

$$O_{\mu\mu} = \sum_{\alpha\beta} c_\mu(\alpha)c_\mu(\beta)O_{\alpha\beta}. \tag{7.17}$$

Now, using the self-averaging property of random matrices, which we prove for this model in Appendix C.2, we see that

$$O_{\mu\mu} = \sum_{\alpha\beta}\langle c_\mu(\alpha)c_\mu(\beta)\rangle_V O_{\alpha\beta}. \tag{7.18}$$

Note that only the random wave functions $c_\mu(\alpha)$ remain inside the ensemble average, as all other factors are in the non-interacting basis and thus do not depend on V. We thus observe that the diagonal observable matrix elements depend on the correlation function

[1]Note that this section begins by summarising the formalism outlined Chapter 5, and the observable assumptions of Chapter 3.

$\langle c_\mu(\alpha)c_\mu(\beta)\rangle_V$ (note that we will see how to deal with the summation and non-interacting observable elements in Section 7.5.3 below).

More generally, when calculating more complicated quantities, we have that there is also a non-trivial contribution of a four-point correlation function of the form $\langle c_\mu(\alpha)c_\nu(\beta)c_\mu(\alpha')c_\nu(\beta')\rangle$ which is given by (for $\mu \neq \nu$),

$$\begin{aligned}\langle c_\mu(\alpha)c_\nu(\beta)c_\mu(\alpha')c_\nu(\beta')\rangle_V = &\Lambda(\mu,\alpha)\Lambda(\nu,\beta)\delta_{\alpha\alpha'}\delta_{\beta\beta'} \\ &- \frac{\Lambda(\mu,\alpha)\Lambda(\nu,\beta)\Lambda(\mu,\alpha')\Lambda(\nu,\beta')}{\Lambda^{(2)}(\mu,\nu)}(\delta_{\alpha\beta}\delta_{\alpha'\beta'}+\delta_{\alpha\beta'}\delta_{\beta\alpha'}),\end{aligned} \tag{7.19}$$

where $\Lambda(\mu,\alpha)$ is defined as

$$\langle c_\mu(\alpha)c_\nu(\beta)\rangle_V = \Lambda(\mu,\alpha)\delta_{\alpha\beta}\delta_{\mu\nu} \tag{7.20a}$$

$$\Lambda(\mu,\alpha) := \frac{\omega_0\Gamma/\pi}{(E_\alpha-E_\mu)^2+\Gamma^2} \tag{7.20b}$$

with $\Gamma = \frac{\pi g^2}{\mathcal{N}\omega_0}$. $\Lambda^{(2)}(\mu,\nu)$ is defined similarly to Eq. (7.20b), with $\Gamma \to 2\Gamma$. The Lorentzian form of Eq. (7.20) is found for a homogeneous perturbation V [16, 65], selected from the GOE. We obtain that the four-point correlation function, Eq. (7.19), can be described in terms of product of two-point correlators $\Lambda(\mu,\alpha)$, as if the random wave function distribution was purely Gaussian, plus a correction term originating from the effective interaction due to the mutual orthogonality of random wave functions. We will see below that an approach in terms of Gaussian and non-Gaussian contractions can be formulated to describe more general correlation functions.

We note that our theory can be extended to account for different forms of the quantum chaotic wave function $\Lambda(\mu,\alpha)$. This may appear, for example, for non-homogeneous V. In this case, the form of the function Λ would change, however the algebraic structure of our theory would remain.

In order to evaluate Eq. (7.7), we thus use Eq. (7.8) to write $\delta_O^2(\infty)$ in terms of the random wave functions $c_\mu(\alpha)$, and non-interacting matrix elements $\rho_{\alpha\beta}$ and $(\sigma_z^2)_{\alpha\beta}$. We then use the self-averaging property of random matrices (which we discuss in more detail and prove in Appendix C), and obtain the relevant correlation functions $\langle c_\mu(\alpha)c_\nu(\beta)\cdots\rangle_V$.

7.5.2 Computing Correlation Functions

As we have seen, it is important to have a systematic approach to obtaining correlation functions for this model. This is a non-trivial task as the random wave functions of our theory are not Gaussian independent variables, but include an effective interaction due to the orthogonality condition $\langle\psi_\mu|\psi_\nu\rangle = \delta_{\mu\nu}$ [16].

Below, we present such a systematic approach to obtaining arbitrary correlation functions in terms of contractions representing the Gaussian and non-Gaussian terms in the four-point correlator (which is the largest non-factorizable correlation function of our theory).

The four-point correlation function of Eq. (7.19) may be understood in terms of the contractions of non-interacting indices, indeed it can be seen to be the sum of a Gaussian

contraction $\langle c_\mu(\overbrace{\alpha)c_\nu(\beta)c_\mu(\alpha'}^{}\underbrace{)c_\nu(\beta')}_{}\rangle_V \Rightarrow \langle c_\mu^2(\alpha)\rangle_V\langle c_\nu^2(\beta)\rangle_V\delta_{\alpha\alpha'}\delta_{\beta\beta'} = \Lambda(\mu,\alpha)\Lambda(\nu,\beta)\delta_{\alpha\alpha'}\delta_{\beta\beta'}$ and non-Gaussian contractions, given by

$$\begin{aligned}\langle c_\mu(\overbrace{\alpha)c_\nu(\beta}^{}\underline{\underline{)c_\mu(\alpha'}}\underline{\underline{)c_\nu(\beta')}}\rangle_V &\Rightarrow L_{\mu\nu}^{\alpha\beta\alpha'\beta'}\delta_{\alpha\beta}\delta_{\alpha'\beta'}\\ \langle c_\mu(\underline{\underline{\alpha)c_\nu(\beta}}\overbrace{c_\mu(\alpha'}^{}\underline{\underline{)c_\nu(\beta')}}\rangle_V &\Rightarrow L_{\mu\nu}^{\alpha\beta\alpha'\beta'}\delta_{\alpha\beta'}\delta_{\alpha'\beta},\end{aligned} \tag{7.21}$$

where

$$L_{\mu\nu}^{\alpha\beta\alpha'\beta'} := \frac{\Lambda(\mu,\alpha)\Lambda(\nu,\beta)\Lambda(\mu,\alpha')\Lambda(\nu,\beta')}{\Lambda^{(2)}(\mu,\nu)}. \tag{7.22}$$

We reserve the double line contraction notation of Eq. (7.21) for the non-Gaussian case. Note that these must occur in pairs of contractions between different interacting indices $\mu \neq \nu$.

Now, we can see from Eq. (7.21) that each contracted pair of indices contributes a Kronecker-δ symbol, and thus, when the correlation function is summed over its non-interacting indices, the number of summations is reduced. We see that as each Λ contributes a factor on the order $\mathcal{O}(\frac{\omega_0}{\Gamma})$, and a summation on the order $\mathcal{O}(\frac{\Gamma}{\omega_0})$, a reduced summation will act to render a term negligible in comparison to a term with no such reduction. Further, we see that the contribution of the non-Gaussian term Eq. (7.22) is of order $\mathcal{O}(\frac{\omega_0^3}{\Gamma^3})$, whereas that of the Gaussian term is $\sim \Lambda^2$, and thus $\mathcal{O}(\frac{\omega_0^2}{\Gamma^2})$, and as such, one can see that for the non-Gaussian contractions to contribute, they must be acted on by an extra summation. Indeed, one can see that this occurs for one of the two non-Gaussian terms when one has repeated summations, i.e. $\alpha', \beta' \to \alpha, \beta$ in Eq. (7.21).

For further details we refer the reader to Ref. [17], and the calculations in Appendices E.2 and C.2. Here we have seen the key intuition, however: that repeated indices in correlation functions leads to the dominant contribution of contractions that would otherwise have contracted the pair of equal indices.

7.5.3 Assumptions on Observables

After obtaining the relevant correlation function, one needs to perform the summations over remaining indices. See, for example, the simple case of Eq. (7.18) above. To perform the summations, certain assumptions on the form of observable matrix elements in the non-interacting basis must be made. We note that in this basis, local system observables are usually of a known form.

Our theory relies on assumptions that we expect to be satisfied for such local observables. The key assumption is related to the behaviour of matrix elements, which must have a well-defined average that does not vary pathologically with energy. A more formal definition of our assumption can be written in terms of the function Λ, as,

$$\sum_\alpha \Lambda(\mu,\alpha)\Lambda(\nu,\alpha)O_{\alpha\alpha} = \overline{[O_{\alpha\alpha}]}_{\overline{\mu}}\Lambda^{(2)}(\mu,\nu), \tag{7.23}$$

with $E_{\overline{\mu}} := \frac{E_\mu + E_\nu}{2}$, and

$$\overline{[O_{\alpha\alpha}]}_{\overline{\mu}} = \sum_\alpha \Lambda(\overline{\mu}, \alpha) O_{\alpha\alpha}. \tag{7.24}$$

We will see that this assumption will be necessary in order to compute summations over the non-interacting indices. In this section, we explain in more detail the requirements on the form of $O_{\alpha\alpha}$ for Eq. (7.23) to be valid, as well as the physical interpretation of the assumption.

The essential assumption here, which we label *smoothness* of $O_{\alpha\alpha}$, as in Ref. [17], is that the microcanonical average $\overline{[O_{\alpha\alpha}]}_{\overline{\mu}}$ changes slowly over the width Γ of the function $\Lambda(\mu, \alpha)\Lambda(\nu, \alpha)$. We showed in Ref. [17] that this is the case under the assumptions,

$$\begin{aligned} &\frac{\Gamma}{\omega_0} \gg 1, \\ &\Gamma^2 \frac{d^2}{dE_\mu^2} \overline{[O_{\alpha,\alpha}]}_\mu \ll 1, \end{aligned} \tag{7.25}$$

which thus leads us to two reasonable conditions,

1. There are many states in the energy width Γ

2. The microcanonical average changes slowly over the width Γ.

We note that the latter condition, combined with the fact that the microcanonical average and time average are equal (which is shown below), is equivalent to the statement that the time-average of the observable is not sensitive to the particular initial state (microstate), rather, its macroscopic energy. In fact, one can see that the conditions (7.25) are precisely those required in order to define a microcanonical average that does not vary pathologically with small changes in the energy window. In this sense, this assumption is the minimal assumption one would expect to require for thermalization to a microcanonical average that changes smoothly with initial state energy to occur.

We further note that in the consideration of time evolution below, we will consider more general observables that are not necessarily diagonal in the non-interacting basis, but fulfil a *sparsity* condition. This can be written as $\sum_{\alpha\beta} O_{\alpha\beta} = \sum_\alpha \sum_n^{N_O} O_{\alpha,\alpha+n}\delta_{\beta,\alpha+n}$, where for a given observable there is a non-extensive number N_O of groups of non-zero matrix elements at given energy widths, such that after the coarse graining procedure the observable matrix elements are non-zero for energy gaps $E_\alpha - E_\beta$ that are the possible energy gaps of H_S. This form can be seen [17] to be reasonable for local observables. We note that it is of course possible to find observables that do not fulfil this assumption, although it is easily seen to be true for e.g. local Pauli operator observables. We will see below that our treatment of time evolution could potentially also capture a wider range of observables as well, if the form in the non-interacting basis is known. In the following, we refer to observables fulfilling the above assumptions as 'generic' observables.

7.6 Equilibration Dynamics

In this section, we present a description of the time dependence of 'generic' observables as defined above, from an arbitrary initial condition

$$\rho(0) = \sum_{\alpha\beta} w_{\alpha\beta} |\phi_\alpha\rangle\langle\phi_\beta|. \tag{7.26}$$

This calculation may be performed by exploiting the methods outlined in Section 7.5. The general approach may be summarised in three steps: i) Writing the observable time dependence in terms of parameters in the non-interacting basis, ii) computing the relevant correlation functions (see Section 7.5.2), and iii) performing summations using the assumptions on observables (see Section 7.5.3).

Proceeding as such, we write the time dependent density operator in the form,

$$\rho(t) = \sum_{\alpha\beta}\sum_{\mu\nu} w_{\alpha\beta} c_\mu(\alpha) c_\nu(\beta) e^{-i(E_\mu - E_\nu)t} |\psi_\mu\rangle\langle\psi_\nu|, \tag{7.27}$$

which may be used to obtain the time evolved observable expectation value by $\langle O(t)\rangle = \mathrm{Tr}(\rho(t)O)$. By taking the trace over the interacting basis $\{|\psi_\mu\rangle\}$, we thus obtain

$$\langle O(t)\rangle = \sum_{\mu'} \langle\psi_{\mu'}| \sum_{\alpha\beta\mu\nu} w_{\alpha\beta} c_\mu(\alpha) c_\nu(\beta) e^{-i(E_\mu - E_\nu)t} |\psi_\mu\rangle\langle\psi_\nu|O|\psi_{\mu'}\rangle. \tag{7.28}$$

Noting the so-called diagonal ensemble contribution is defined by,

$$O_{\mathrm{DE}} = \sum_{\alpha\mu} w_{\alpha\alpha} c_\mu^2(\alpha) O_{\mu\mu}, \tag{7.29}$$

which can be seen to be equal to the long-time average value of the observable

$$\langle\langle O(t)\rangle\rangle_\tau := \lim_{\tau\to\infty} \frac{1}{\tau}\int_0^\tau dt \langle O(t)\rangle = O_{\mathrm{DE}}, \tag{7.30}$$

assuming no degenerate energy levels, we thus define

$$\begin{aligned}\Delta O(t) &:= \langle O(t)\rangle - O_{\mathrm{DE}} \\ &= \sum_{\alpha\beta}\sum_{\substack{\mu\nu \\ \mu\neq\nu}} w_{\alpha\beta} e^{-i(E_\mu - E_\nu)t} O_{\mu\nu} c_\mu(\alpha) c_\nu(\beta).\end{aligned} \tag{7.31}$$

Using that $O_{\mu\nu} = \sum_{\alpha\beta} c_\mu(\alpha) c_\nu(\beta) O_{\alpha\beta}$, we have

$$\Delta O(t) = \sum_{\alpha\beta\alpha'\beta'}\sum_{\substack{\mu\nu \\ \mu\neq\nu}} w_{\alpha\beta} e^{-i(E_\mu - E_\nu)t} O_{\alpha'\beta'} c_\mu(\alpha) c_\nu(\beta) c_\mu(\alpha') c_\nu(\beta'). \tag{7.32}$$

We see that, using the self-averaging property, this depends on the four-point correlation

function given by Eq. (7.19), such that

$$\Delta O(t) = \sum_{\substack{\mu\nu \\ \mu\neq\nu}} e^{-i(E_\mu - E_\nu)t} \Bigg[\sum_{\alpha\beta} w_{\alpha\beta} O_{\alpha\beta} \Lambda(\mu,\alpha)\Lambda(\nu,\beta) - \sum_{\alpha\beta} w_{\alpha\alpha} O_{\beta\beta} \frac{\Lambda(\mu,\alpha)\Lambda(\mu,\beta)\Lambda(\nu,\alpha)\Lambda(\nu,\beta)}{\Lambda^{(2)}(\mu,\nu)} - \sum_{\alpha\beta} w_{\alpha\beta} O_{\alpha\beta} \frac{\Lambda(\mu,\alpha)\Lambda(\mu,\beta)\Lambda(\nu,\alpha)\Lambda(\nu,\beta)}{\Lambda^{(2)}(\mu,\nu)} \Bigg]. \tag{7.33}$$

The third term can be shown to be negligible, proof of which is given in Appendix E.3. We note that it is this bound that requires the sparsity assumption above. We now use the smoothness assumption, exploiting Eqs. (7.23) and (7.24), we obtain,

$$\Delta O(t) = \langle O(t)\rangle_0 e^{-2\Gamma t} - \sum_{\substack{\mu\nu \\ \mu\neq\nu}} \sum_{\alpha} \overline{[O_{\alpha\alpha}]}_{\overline{\mu}} w_{\alpha\alpha} e^{-i(E_\mu - E_\nu)t} \Lambda(\mu,\alpha)\Lambda(\nu,\alpha), \tag{7.34}$$

where to obtain the first term one may note that $\Lambda(\mu,\alpha) = \Lambda(\mu-\alpha) = \Lambda(\alpha-\mu)$, and make the change of variables $\mu(\nu) \to \mu(\nu) - \alpha(\beta)$ to perform the integrals over the new variables. Here $\langle O(t)\rangle_0 := \sum_{\alpha\beta} w_{\alpha\beta} O_{\alpha\beta} e^{-i(E_\alpha - E_\beta)t}$ is the free evolution of the observable under the Hamiltonian H_0. The second term may be re-expressed by defining $\tilde{\mu} = \mu - \alpha$, to obtain,

$$\Delta O(t) = \langle O(t)\rangle_0 e^{-2\Gamma t} - \sum_{\substack{\tilde{\mu}\tilde{\nu} \\ \tilde{\mu}\neq\tilde{\nu}}} \sum_{\alpha} \overline{[O_{\alpha\alpha}]}_m w_{\alpha\alpha} e^{-i(E_{\tilde{\mu}} - E_{\tilde{\nu}})t} \Lambda(\tilde{\mu})\Lambda(\tilde{\nu}), \tag{7.35}$$

where $E_m := \frac{E_{\tilde{\mu}} + E_{\tilde{\nu}}}{2} + E_\alpha$. Noting, then, that as $\Lambda(\tilde{\mu})$ is peaked around $E_{\tilde{\mu}} = 0$, and that $\overline{[O_{\alpha\alpha}]}_\alpha$ changes slowly over the width Γ of the function Λ, we can make the replacement $\overline{[O_{\alpha\alpha}]}_m \to \overline{[O_{\alpha\alpha}]}_\alpha$. This allows the summations over $\tilde{\mu}, \tilde{\nu}$ to be performed, which become Fourier transforms of the Lorentzian functions Λ in the continuum limit $\sum_\mu \to \int \frac{dE_\mu}{\omega_0}$. We thus find,

$$\Delta O(t) = \langle O(t)\rangle_0 e^{-2\Gamma t} - \sum_{\alpha} \overline{[O_{\alpha\alpha}]}_\alpha w_{\alpha\alpha} e^{-2\Gamma t}. \tag{7.36}$$

Noting that at $t = 0$ we by definition have $\Delta O(0) := \langle O(0)\rangle - O_{\rm DE} = \langle O(0)\rangle_0 - \sum_\alpha \overline{[O_{\alpha\alpha}]}_\alpha w_{\alpha\alpha}$, we obtain that $\sum_\alpha \overline{[O_{\alpha\alpha}]}_\alpha w_{\alpha\alpha} = O_{\rm DE}$. Noting Eq. (7.30), we see that the equality of the time and microcanonical averages is derived from our RMT approach. Thus, using the definition in Eq. (7.31), we obtain

$$O(t) = (\langle O(t)\rangle_0 - O_{\rm DE}) e^{-2\Gamma t} + O_{\rm DE}. \tag{7.37}$$

This is the same as that obtained in Reference [17] for pure-states.

The approach outlined above is valid assuming that the decay rate Γ is constant in energy. In fact, for the system under consideration, we have to allow Γ to change with the

initial state energy, such that $\Gamma \to \Gamma_\alpha$ (note that here the change in DOS does not affect the calculation). Accounting for this, rather than Eq. (7.34), we obtain

$$\Delta O(t) = \sum_{\alpha\beta} w_{\alpha\beta} O_{\alpha\beta} e^{-i(E_\alpha - E_\beta)t} e^{-(\Gamma_\alpha + \Gamma_\beta)t} - \sum_\alpha \overline{[O_{\alpha\alpha}]}_\alpha w_{\alpha\alpha} e^{-2\Gamma_\alpha t}. \tag{7.38}$$

Now, for our system we have that, as $H_S = 0$, the microcanonical average $\overline{[O_{\alpha\alpha}]}_\mu = 0$ for all μ in the bulk of the spectrum. Also, using that for our proposed experimental protocol, both the initial state and observable are diagonal in the non-interacting basis, we have

$$\Delta O(t) = \sum_\alpha w_\alpha O_{\alpha\alpha} e^{-2\Gamma_\alpha t}. \tag{7.39}$$

We have that, as the initial state $\langle O(0)\rangle = \sum_\alpha w_\alpha O_{\alpha\alpha} = 1$ for all initial device states, $O_{\alpha\alpha} = 1$ for all non-zero w_α, and thus

$$\Delta O(t) = \sum_\alpha w_\alpha e^{-2\Gamma_\alpha t}. \tag{7.40}$$

We thus wish to obtain the value Γ that will be obtained when measuring the decay of an observable. To find this, one may simply consider the time integration of the evolution obtained above from the initial state,

$$\rho_\alpha = \frac{1}{Z_\beta} e^{-\beta E_\alpha} \delta_{\alpha,\text{odd}}, \tag{7.41}$$

describing our probe-bath model, with an initial finite temperature bath state at inverse temperature β. The time integration is then,

$$\begin{aligned} \lim_{\tau\to\infty} \int_0^\tau dt \Delta O(t) &= \lim_{\tau\to\infty} \int_0^\tau dt \sum_\alpha w_\alpha e^{-2\Gamma_\alpha t} \\ &= -\frac{1}{2} \sum_\alpha \Gamma_\alpha^{-1} w_\alpha \\ &= -\frac{1}{2Z_\beta} \sum_\alpha \Gamma_\alpha^{-1} e^{-\beta E_\alpha} \delta_{\alpha,\text{odd}} \\ &:= -\frac{1}{2} \langle\langle \Gamma(E)^{-1} \rangle\rangle_\beta, \end{aligned} \tag{7.42}$$

where we have used in the second line that $O_{\text{DE}} = 0$, and defined the thermal average $\langle\langle \cdots \rangle\rangle_\beta$ at inverse temperature β, and we have defined Γ_α as the decay rate of the initial state $|\phi_\alpha\rangle$. We thus see that it is the thermal average of the inverse decay rate that is measured by a fit to the time dependence of an observable.

The integral form of the thermal average of a function $A(E)$, is given by,

$$\langle\langle A(E) \rangle\rangle_\beta := \frac{1}{Z'_\beta} \int_0^{\Delta E} dE D(E) e^{-\beta(E-E_0)} A(E), \tag{7.43}$$

with $Z'_\beta := \int_0^{\Delta E} dE D(E) e^{-\beta(E-E_0)}$. We will see below that the FDT will be initially

expressed in terms of a different average over the values $\Gamma(E)$. This difference is resolved in Appendix E.4, where we re-express our FDT in terms of the thermal average above. We show that the form differs only by a constant that is independent of N and the coupling strength, and thus the scaling with Hilbert space dimension remains the same. This difference is thus not important for our application.

Finally, we note that when $\Gamma_\alpha \approx \Gamma$ is approximately constant across the bulk of the initially populated initial states; the thermal average above is approximately equal to the unbiased average appearing in (7.10). We also see that in this case, from Eq. (7.40), one expects to observe an exponential decay at the rate Γ, as in Eq. (7.13). Indeed, this is what we observe in our numerical example in Section 7.4 above, and thus we are able to recover the Hilbert space dimension directly in Fig. 7.5. If a non-exponential decay is observed, then the average $\langle\langle\Gamma(E)^{-1}\rangle\rangle_\beta$ is obtainable via integration as above, and the scaling of the Hilbert space dimension is still obtainable as in Fig. 7.4.

7.7 Fluctuation-Dissipation Theorem

7.7.1 Derivation from RMT

Here we perform the full derivation of the FDT for the random matrix model described above. We initially focus on the case of a diagonal initial bath state $\rho_{\alpha\beta} = w_\alpha \delta_{\alpha\beta}$. We then restrict the treatment to the specific protocol outlined in Section 7.3, where the initial state is the product of a single probe qubit in a pure state, and a bath in an infinite temperature state, see Eq. (7.9). We will follow very similar steps as those outlined in the previous section; however, we will see here that the correlation function calculation is somewhat more complicated.

The RMT model here is limited to the case of constant decay rate and DOS; we will thus extend the treatment to more realistic cases in the next section.

We are interested in the calculation of the long-time fluctuations, defined by the diagonal ensemble result,

$$\delta^2_{\sigma_z}(\infty) = \sum_{\substack{\mu,\nu \\ \mu\neq\nu}} |\rho_{\mu\nu}|^2 |(\sigma_z)_{\mu\nu}|^2. \tag{7.44}$$

We begin by writing the initial density operator matrix elements as,

$$\rho_{\mu\nu} = \sum_\alpha w_\alpha c_\mu(\alpha) c_\nu(\alpha), \tag{7.45}$$

then using Eqs. (7.44), and that $|\psi_\mu\rangle = \sum_\alpha c_\mu(\alpha)|\phi_\alpha\rangle$, we may write the time fluctuations as,

$$\delta^2_O(\infty) = \sum_{\substack{\mu\nu \\ \mu\neq\nu}} \sum_{\alpha\beta} w_\alpha w_\beta c_\mu(\alpha) c_\nu(\alpha) c_\mu(\beta) c_\nu(\beta) \sum_{\alpha'\beta'} O_{\alpha'\alpha'} O_{\beta'\beta'} c_\mu(\alpha') c_\nu(\alpha') c_\mu(\beta') c_\nu(\beta'), \tag{7.46}$$

where coefficients of the initial state are labelled as unprimed indices α, β, and coefficients of the observable are labelled by primed indices.

Using the self-averaging property of random matrices (see Appendix C), we may replace the product of coefficients $c_\mu(\alpha)c_\nu(\alpha)\cdots$ by their ensemble average $\langle c_\mu(\alpha)c_\nu(\alpha)\cdots\rangle_V$; the above expression may then be written in terms of a sum over 8-point correlation functions, weighted by the initial state and observable coefficients w_α and $O_{\alpha\alpha}$:

$$\delta_O^2(\infty) = \sum_{\substack{\mu\nu \\ \mu\neq\nu}} \sum_{\alpha\beta\alpha'\beta'} w_\alpha w_\beta O_{\alpha'\alpha'} O_{\beta'\beta'} \langle c_\mu(\alpha)c_\nu(\alpha)c_\mu(\beta)c_\nu(\beta)c_\mu(\alpha')c_\nu(\alpha')c_\mu(\beta')c_\nu(\beta')\rangle_V. \tag{7.47}$$

Now, using the method of contractions outlined in Section 7.5.2, we see that this 8-point correlation function may be split up into to four-point correlation functions, each consisting of both Gaussian and non-Gaussian contractions. These are computed explicitly in Appendix E.2, in which we see that there are three dominating contributions to the fluctuations, given by,

$$\delta_G^2(\infty) = \sum_{\substack{\mu\nu \\ \mu\neq\nu}} \left[\overline{[w_\alpha^2]}_{\overline{\mu}} \overline{[O_{\alpha\alpha}^2]}_{\overline{\mu}} + 2\overline{[w_\alpha O_{\alpha\alpha}]}_{\overline{\mu}}^2 \right] \Lambda^{(2)}(\mu,\nu)^2, \tag{7.48}$$

$$\delta_{NG}^2(\infty) = 3 \sum_{\substack{\mu\nu \\ \mu\neq\nu}} \overline{[w_\alpha]}_{\overline{\mu}}^2 \overline{[O_{\alpha\alpha}]}_{\overline{\mu}}^2 \Lambda^{(2)}(\mu,\nu)^2, \tag{7.49}$$

and,

$$\delta_M^2(\infty) = -\sum_{\substack{\mu\nu \\ \mu\neq\nu}} \Lambda^{(2)}(\mu,\nu)^2 \left[\overline{[w_\alpha^2]}_{\overline{\mu}} \overline{[O_{\alpha\alpha}]}_{\overline{\mu}}^2 4\overline{[w_\alpha]}_{\overline{\mu}} \overline{[O_{\alpha\alpha}]}_{\overline{\mu}} \overline{[w_\alpha O_{\alpha\alpha}]}_{\overline{\mu}} + \overline{[w_\alpha]}_{\overline{\mu}}^2 \overline{[O_{\alpha\alpha}^2]}_{\overline{\mu}} \right]. \tag{7.50}$$

These three terms can be seen as the contributions to the 8-point correlation function arising due to products of Gaussian, non-Gaussian, and mixed Gaussian and non-Gaussian 4-point correlation functions respectively. In the above, in order to perform the summations over non-interacting indices in Eq. (7.47) we define coarse grained averages of observable elements $O_{\alpha\alpha}$ as in Eq. (7.23), as well as the mixed averages,

$$\begin{aligned} \sum_\alpha \Lambda(\mu,\alpha)\Lambda(\nu,\alpha) w_\alpha &= \overline{[w_\alpha]}_{\overline{\mu}} \Lambda^{(2)}(\mu,\nu) \\ \sum_\alpha \Lambda(\mu,\alpha)\Lambda(\nu,\alpha) w_\alpha O_{\alpha\alpha} &= \overline{[w_\alpha O_{\alpha\alpha}]}_{\overline{\mu}} \Lambda^{(2)}(\mu,\nu). \end{aligned} \tag{7.51}$$

We thus define $W_{\overline{\mu}}$ by

$$\begin{aligned} \delta_O^2(\infty) &= \delta_G^2(\infty) + \delta_{NG}^2(\infty) + \delta_M^2(\infty) \\ &= \sum_{\substack{\mu\nu \\ \mu\neq\nu}} W_{\overline{\mu}} \Lambda^{(2)}(\mu,\nu)^2, \end{aligned} \tag{7.52}$$

with,

$$W_\mu = \overline{[w_\alpha^2]}_\mu \overline{[O_{\alpha\alpha}^2]}_\mu + 2\overline{[w_\alpha O_{\alpha\alpha}]}_\mu^2 + 3\overline{[w_\alpha]}_\mu^2 \overline{[O_{\alpha\alpha}]}_\mu^2 - \overline{[w_\alpha^2]}_\mu \overline{[O_{\alpha\alpha}]}_\mu^2 - 4\overline{[w_\alpha]}_\mu \overline{[O_{\alpha\alpha}]}_\mu \overline{[w_\alpha O_{\alpha\alpha}]}_\mu - \overline{[w_\alpha]}_\mu^2 \overline{[O_{\alpha\alpha}^2]}_\mu. \tag{7.53}$$

We now take our bath to be in an initial infinite temperature state, such that $\overline{[w_\alpha]}_\mu = \overline{[w_\alpha]} = \frac{1}{2\mathcal{N}_B}$, and $\overline{[w_\alpha^2]}_\mu = \overline{[w_\alpha^2]} = \frac{1}{2\mathcal{N}_B^2}$. As such, $W_{\overline{\mu}} = W$ is in fact energy independent, as the probe Hamiltonian $H_S = 0$, so microcanonical averages of probe observables are also energy independent. Now, as $\overline{[w_\alpha^2]} = 2\overline{[w_\alpha]}^2$, all terms in W are $\propto \overline{[w_\alpha^2]}$, we define,

$$\begin{aligned} W_O &= \frac{W}{\overline{[w_\alpha^2]}} \\ &= \overline{[O_{\alpha\alpha}^2]} + O_\uparrow^2 + \frac{3}{2}\overline{[O_{\alpha\alpha}]}^2 - \overline{[O_{\alpha\alpha}]}^2 - 2\overline{[O_{\alpha\alpha}]}O_\uparrow - \frac{1}{2}\overline{[O_{\alpha\alpha}^2]}, \end{aligned} \tag{7.54}$$

where $O_\uparrow = \langle\uparrow|O|\uparrow\rangle$, and we have used that $\overline{[w_\alpha O_{\alpha\alpha}]} = O_\uparrow \overline{[w_\alpha]}$. We see that W_O is a constant of the order of unity that depends only on the observable (e.g. $W_O = 3/2$ for $O = \sigma_z$). Finally, taking the thermodynamic limit, such that $\sum_{\mu\nu} \to \int_0^{\Delta E}\int_0^{\Delta E} \frac{dE_\mu dE_\nu}{\omega_0^2}$ (not that the diagonal terms in the summation can be seen to be negligible, as they contribute to a higher order in $\frac{\omega_0}{\Gamma}$), we have

$$\delta_O^2(\infty) = \frac{W_O}{2\mathcal{N}_B^2}\int_0^{\Delta E}\int_0^{\Delta E} \frac{dE_\mu dE_\nu}{\omega_0^2}\Lambda^{(2)}(\mu,\nu)^2, \tag{7.55}$$

which may be evaluated using,

$$\begin{aligned} \int_0^{\Delta E}\int_0^{\Delta E} \frac{dE_\mu dE_\nu}{\omega_0^2}\Lambda^{(2)}(\mu,\nu)^2 &= \int_0^{\Delta E} dE_\mu \frac{\operatorname{arccot}\left(\frac{2\Gamma}{\Delta E}\right)}{2\pi\Gamma} \\ &\approx \frac{\Delta E}{4\pi\Gamma}, \end{aligned} \tag{7.56}$$

where in the last line we have used that $\Delta E \gg \Gamma$, such that $\operatorname{arccot}\left(\frac{2\Gamma}{\Delta E}\right) \approx \frac{\pi}{2}$. We then obtain,

$$\delta_O^2(\infty) = \frac{W_O\omega_0}{4\pi\mathcal{N}_B\Gamma}, \tag{7.57}$$

where we have used that $\Delta E := 2\mathcal{N}_B\omega_0$.

We can see, then, that Eq. (7.57) is of the form of our main result, Eq. (3) of the main text, where $C = \frac{W_O}{4\pi}$. What follows is to generalise this relation, allowing the DOS and Γ to vary in energy, and for finite temperatures.

7.7.2 Extension to Realistic Systems

The key issue with directly applying the RMT results to realistic models is that in general the DOS, and decay rate, are energy dependent, and thus change over the width of the initial state distribution (this is especially important for the high/infinite temperatures considered here). In order to account for this, we must then go back to the evaluation of

the integrals over energy, in Eq. (7.55), and substitute $\Gamma \to \Gamma(E)$, and $\omega_0^{-1} \to D(E)$. This is justified under the assumption that neither $\Gamma(E)$, nor $D(E)$, vary appreciably over the width Γ. i.e. $\frac{\Gamma(E)-\Gamma(E+\Gamma(E))}{\Gamma(E)} \ll 1$, and $\frac{D(E)-D(E+\Gamma(E))}{D(E)} \ll 1$.

We see then, that the integral in Eq. (7.55) is now

$$\delta_O^2(\infty) = \frac{W_O}{2\mathcal{N}_B^2} \int_0^{\Delta E} \int_0^{\Delta E} dE_\mu dE_\nu \frac{D(E_\mu)D(E_\nu)}{D(E)^2} \left(\frac{2\Gamma(E)/\pi}{(E_\mu - E_\nu)^2 + 4\Gamma(E)^2} \right)^2, \tag{7.58}$$

where we have used that,

$$\Lambda^{(2)}(\mu,\nu) = \frac{1}{D(E)} \frac{2\Gamma(E)/\pi}{(E_\mu - E_\nu)^2 + 4\Gamma(E)^2}, \tag{7.59}$$

with $E = \frac{E_\mu + E_\nu}{2}$. This can be seen to be valid as long as the above conditions on $D(E)$ and $\Gamma(E)$ hold, that is, as long as they change sufficiently slowly over the energy width Γ. The contribution of each eigenstate $\Lambda(\mu,\alpha)$ to the fluctuations at a given energy is then that of a local (in energy) random matrix model, with a constant DOS and decay rate. $D(E)$ and $\Gamma(E)$ can then be allowed to change over an energy much wider than a the width of $\Lambda(\mu,\alpha)$, as over such energy widths the contributions of relevant eigenstates are independent.

Now, we further define $\omega = E_\mu - E_\nu$, and make the change of variables $E_\mu, E_\nu \to \omega, E$, and thus obtain

$$\begin{aligned} \delta_O^2(\infty) &= \frac{W_O}{2\mathcal{N}_B^2} \int_0^{\Delta E} \int_{-\Delta E}^{\Delta E} dE d\omega \\ &\times \frac{D(E+\frac{\omega}{2})D(E-\frac{\omega}{2})}{D(E)^2} \left(\frac{2\Gamma(E)/\pi}{\omega^2 + 4\Gamma(E)^2} \right)^2 \\ &\approx \frac{W_O}{2\mathcal{N}_B^2} \int_0^{\Delta E} dE \frac{1}{4\pi\Gamma(E)}, \end{aligned} \tag{7.60}$$

where in the second line we have assumed that $D(E)$ and $\Gamma(E)$ is approximately constant over the width Γ. Now, we define the unbiased average of a function $A(E)$ as,

$$\overline{A(E)} = \frac{1}{\Delta E} \int_0^{\Delta E} dE A(E), \tag{7.61}$$

(not to be confused with the average $\overline{[\cdots]}_\mu$ above) and see that, noting $\Delta E = \frac{2\mathcal{N}_B}{D(E)}$,

$$\begin{aligned} \delta_O^2(\infty) &= \frac{W_O}{4\pi\mathcal{N}_B \overline{D(E)}} \overline{\Gamma(E)^{-1}} \\ &= C \frac{1}{\mathcal{N}_B \overline{D(E)}} \overline{\Gamma(E)^{-1}}, \end{aligned} \tag{7.62}$$

where $C = \frac{W_O}{4\pi}$ depends only on the choice of observable. We note that for the random matrix model, as the DOS and $\Gamma(E)$ are both constant in energy, the average $\overline{\Gamma(E)^{-1}}$ is equal to the thermal average $\langle\langle \Gamma(E)^{-1} \rangle\rangle_{\beta=0}$ obtained from a fit to the decay of an observable (see Section 7.6 above). In the case above, however, where the DOS and $\Gamma(E)$

change in energy, the unbiased average decay rate is not necessarily the same as that obtained from a fit to the decay. We may fix this problem directly, as we do in the last section, where we see that the unbiased thermal averages may be replaced by regular thermal averages weighted by the DOS at the expense of a constant that depends on the functional form of $D(E)$ and $\Gamma(E)$ (but importantly, not on N, or the coupling strength). We can also see, that if $\Gamma(E)$ is approximately constant over the width of the DOS, which is often the case in such systems (in fact from Eq. (7.40) this can be seen to be the case if an exponential decay of the observable is observed), then the biased and unbiased thermal averages of $\Gamma(E)^{-1}$ are approximately equal for $\beta \to 0$, and Eq. (7.62) may be directly experimentally confirmed as in Fig. 7.5.

7.7.3 Finite Temperature FDT

In this section, we extend the above approach to finite temperature initial bath states, where the initial state is described by

$$\rho(t=0) = \sum_{\alpha}^{2\mathcal{N}_B} w_\alpha |\phi_\alpha\rangle\langle\phi_\alpha|, \tag{7.63}$$

where the joint probe-bath Hamiltonian eigenbasis is built by ordering product states such that $|\phi_\alpha\rangle = |\uparrow\rangle|\phi_{B,\frac{\alpha+1}{2}}\rangle$ (α odd) , $|\phi_\alpha\rangle = |\downarrow\rangle|\phi_{B,\frac{\alpha}{2}}\rangle$ (α even). In this case, we have

$$w_\alpha = \begin{cases} \frac{1}{Z_\beta} e^{-\beta E_\alpha} & \text{if } \alpha \in \text{odd} \\ 0 & \text{otherwise} \end{cases}, \tag{7.64}$$

where $Z_\beta = \sum_\alpha e^{-\beta E_\alpha}\delta_{\alpha,\text{odd}}$, when the bath is initially a finite temperature state at inverse temperature $\beta = \frac{1}{k_B T}$, and the probe qubit is initially in state $|\uparrow\rangle$. We thus obtain for the microcanonical averages of w_α, assuming that $\beta^{-1} \gg \Gamma$,

$$\overline{[w_\alpha]}_\mu = \frac{1}{2Z_\beta} e^{-\beta E_\mu} \tag{7.65}$$

and

$$\overline{[w_\alpha^2]}_\mu = \frac{1}{2Z_\beta^2} e^{-2\beta E_\mu}, \tag{7.66}$$

such that $\overline{[w_\alpha^2]}_\mu = 2\overline{[w_\alpha^2]}_\mu$. Now, our most general form for the long-time fluctuations (which assumes only the ability to define the required microcanonical averages that vary smoothly over a width Γ) is

$$\delta_O^2(\infty) = \sum_{\substack{\mu\nu \\ \mu\neq\nu}} W_{\overline{\mu}} \Lambda^{(2)}(\mu,\nu)^2, \tag{7.67}$$

where $E_{\overline{\mu}} := \frac{E_\mu + E_\nu}{2}$, and W_μ is written in Eq. (7.53). Indeed, noting that the mixed average $\overline{[w_\alpha O_{\alpha\alpha}]}_\mu = 2\overline{[w_\alpha]}_\mu O_\uparrow$, where $O_\uparrow := \langle\uparrow|O|\uparrow\rangle$, and that as each term in W_μ is

$\propto \overline{[w_\alpha]}^2_\mu$ (see Eq. (7.53)), we may define

$$W_\mu = W_O \overline{[w_\alpha^2]}_\mu = \frac{W_O}{2Z_\beta^2} e^{-2\beta E_\mu}, \tag{7.68}$$

so

$$\delta_O^2(\infty) = \frac{W_O}{2Z_\beta^2} \sum_{\substack{\mu\nu \\ \mu\neq\nu}} e^{-2\beta E_{\overline{\mu}}} \Lambda^{(2)}(\mu,\nu)^2. \tag{7.69}$$

This may be evaluated, including a variable DOS $D(E)$, as in the main text for the infinite temperature case, via

$$\begin{aligned} \delta_O^2(\infty) &= \frac{W_0}{2Z_\beta^2} \int_0^{\Delta E} \int_{-\Delta E}^{\Delta E} dE d\omega e^{-2E\beta} \frac{D(E+\frac{\omega}{2})D(E-\frac{\omega}{2})}{D(E)^2} \left(\frac{2\Gamma(E)/\pi}{\omega^2 + 4\Gamma(E)^2} \right)^2 \\ &\approx \frac{W_O}{4Z_\beta^2} \int_0^{\Delta E} dE e^{-2\beta E} \frac{1}{4\pi\Gamma(E)}, \end{aligned} \tag{7.70}$$

where in the second line we have made the change of variables $E_\mu, E_\nu \to E, \omega$ with $E = \frac{E_\mu + E_\nu}{2}$ and $\omega = E_\mu - E_\nu$, and used that $\Delta E \gg \Gamma$ as in the main text. We now define the unbiased thermal average of the function $A(E)$ as,

$$\langle A(E) \rangle_\beta := \frac{1}{\Delta E'(\beta)} \int_0^{\Delta E} dE A(E) e^{-\beta E}, \tag{7.71}$$

where $\Delta E'(\beta) = \int_0^{\Delta E} dE e^{-\beta E}$. Now, we have

$$\delta_O^2(\infty) = \frac{W_O \Delta E'(\beta)}{8\pi Z_\beta^2} \langle \Gamma(E)^{-1} \rangle_{2\beta}. \tag{7.72}$$

Noting, then, that $\lim_{\beta\to 0} Z_\beta = \mathcal{N}_B$, and $\lim_{\beta\to 0} \Delta E'(E) = \Delta E = \frac{2\mathcal{N}_B}{\overline{D(E)}}$, we recover the infinite temperature case as required,

$$\delta_O^2(\infty) = \frac{W_O}{4\pi \mathcal{N}_B \overline{D(E)}} \overline{\Gamma(E)^{-1}}. \tag{7.73}$$

We note that, unlike in the RMT case above, the average $\langle \Gamma(E)^{-1} \rangle_\beta$ is not equal to the thermal average $\langle\langle \Gamma(E)^{-1} \rangle\rangle_\beta$, which is that obtained from a fit to the decay. In Appendix E.4 we show how the FDT may be defined in terms of this thermal average. Importantly for our proposed application, we obtain that the FDT in this form is related simply by a constant C'_β, defined in Appendix E.4, that does not depend on the the size of the device or coupling strength (within the weak coupling regime). For infinite temperatures we thus have

$$\delta_O^2(\infty) = C'_0 \frac{W_O}{4\pi \mathcal{N}_B \langle\langle D(E) \rangle\rangle_0} \langle\langle \Gamma(E)^{-1} \rangle\rangle_0. \tag{7.74}$$

Therefore, we can directly relate the measured inverse decay rate $\langle\langle\Gamma(E)^{-1}\rangle\rangle_0$ to the time-averaged fluctuations, and from measurement of each for changing device size or coupling strength, as shown in the numerical experiments of Section 7.4, yields information on the scaling of the Hilbert space dimension. We finally note that it is simply the lack of direct knowledge of the constant C'_β which prevents measurements where there is a non-negligible change in the decay rate with energy (a non-exponential decay to equilibrium) from constituting a direct measurement of the value of the Hilbert space dimension. This constant depends on the functional form $D(E)$ and $\Gamma(E)$, and thus, if these are known, inference of the Hilbert space dimension itself is thus obtainable.

Finally, we note that the finite temperature approach above can be extended to the low temperature regime, as shown in Appendix E.4, from which we can recover the pure state FDT found in Ref. [17] in the low temperature limit.

7.8 Discussion

The results shown above demonstrate how the chaotic dynamics of thermalization may be exploited in order to gain information on the complexity of the unitary quantum dynamics of a system. We have proposed an experimentally viable protocol, by which measurements of a local observable of a probe qubit may be exploited to measure the Hilbert space dimension of an ergodic quantum device, initialised in an infinite temperature state. We note that this measures the dimension of the states directly involved in dynamics only, and thus provides a more accurate measure of the complexity of the dynamics than a simple estimate of the Hilbert space dimension from the number of qubits. In this sense, such a measurement of a large enough quantum device, if shown to be ergodic in the sense outlined above, would be a convincing indicator of the so called 'quantum supremacy' of the quantum device.

On a practical level, for a generic non-integrable Hamiltonian, our results may be observed in two ways: measurement of a probe observable for (i) changing the number of qubits/ions/... in the quantum device (as in Figs. 7.3 and 7.4) , or (ii) changing the probe-bath coupling (as in Fig. 7.2). The latter is perhaps the simplest experimental methodology, which we show can confirm the ergodic behaviour of a system, that is, that the unitary dynamics requires an extensive proportion of the Hilbert space, by showing a linear relationship between the long-time fluctuations and decay rate. For a model where the device size may be altered, our FDT provides even deeper insight, allowing also for the experimental observation of the scaling of the Hilbert space dimension with system size.

For cases where an exponential decay to equilibrium is observed, which we show implies that the decay rate is constant over a large range of energies, our method allows the experimenter to access the numerical value of the Hilbert space dimension itself, not simply its scaling with size or coupling strength. This can be obtained from a single time trace of the decay to equilibrium of the observable, from the measurement of the decay rate, and fluctuations around equilibrium.

Chapter 8

Emergent classicality in quantum experiments

In the above chapters we have seen how thermalization dynamics can be described in terms of chaotic wavefunctions. The decay to equilibrium of local observables of non-integrable quantum systems can be accurately described in terms of random matrix theory (RMT), yielding an equilibrium state that varies smoothly with initial state energy, and fluctuations that decrease exponentially with systems size. This therefore constitutes a foundation for quantum statistical physics, based on physical properties of individual eigenstates of chaotic quantum systems.

The world around us, whilst quantum in fundamental description, is classical in its behaviour at the level of observation, except for in extremely idealised scenarios. At some point, then, quantum statistical physics should give rise to the classical theory, the equilibrium properties of which we discussed in Chapter 1. The non-equilibrium properties of classical statistical physics are still a topic of much active research. Of particular interest is the description of classical trajectories of Brownian particles. Indeed, Brownian motion has formed the backbone of non-equilibrium classical statistical physics [173, 194, 195].

More recently, the methods of stochastic thermodynamics [149] have revolutionised the field, enabling the description of individual trajectories in classical stochastic models. The 'paradigm in the field' [148], is once more the description of the Brownian motion of an overdamped colloidal particle. It is this which I will describe in terms of quantum chaotic wavefunctions in this chapter, thus establishing an approach to classical statistical physics rooted in the unitary quantum dynamics of non-integrable systems. Specifically, I will show that the thermalization dynamics $\langle O(t)\rangle$ of a local observable may be shown to evolve under the *effective* description of an Ornstein-Uhlenbeck (OU) process - a model for describing the Brownian motion of an overdamped particle in a harmonic potential.

For a consistent physical interpretation of the emergence of classical statistical physics, however, the dynamics of the observable expectation value $\langle O(t)\rangle$ is not sufficient. An experimentalist in general has no access to this quantity outside of exceedingly idealised conditions, and she certainly cannot obtain $\langle O(t)\rangle$ from a single experiment, as a quantum measurement interrupts the thermalization dynamics. In a more realistic experimental scenario she instead has access to the time-dependence of an observable O in the form of

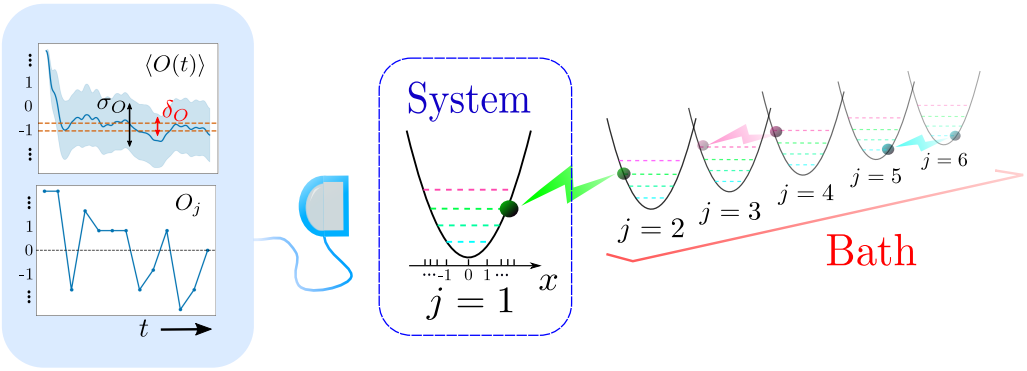

Figure 8.1: Diagram of general scheme. We consider systems with many energy levels, and thus many possible observable outcomes (diagram of Hamiltonian (8.30)). Local system observables may be measured via expectation value $\langle O(t)\rangle$ or via sequence of projective measurements O_j.

a sequence of measurement outcomes O_j at times $t_j = j\Delta t$. Such an experimental scheme is illustrated in Fig. 8.1. Such protocols are often described as *quantum jump trajectories* [196], and the description of sequential quantum measurements in terms of quantum chaos and RMT constitutes a more physical understanding of typical experimental scenarios under which thermalization dynamics are observed. Furthermore, we will see that a link may be made between these approaches and modern work in stochastic thermodynamics, as it allows for the description of a single experimental trajectory in a quantum experiment.

This link will be exemplified by the description of the time dependence of the non-equilibrium Gibbs entropy[1] [197]. From this, we study a further important feature of statistical physics: entropy growth [197–201], and bound the derivative of the Gibbs entropy, such that it can be seen to be non-decreasing in time.

In this chapter, I will begin by introducing classical Brownian motion in the form of an OU process. We will then see that in the corresponding limit the description of closed quantum systems in terms of RMT and quantum chaos indeed heralds an effective description in terms of an OU process. That is, we will observe that non-integrable quantum systems not only evolve into a thermal state, but actually, expectation values of macroscopic observables effectively evolve in time like stochastic variables whose variance satisfies the celebrated Einstein relation (see below), and the equipartition theorem. These relations manifest at the level of individual eigenstates.

We will then see that these results apply naturally to a quantum jump trajectory of a system undergoing chaotic dynamics. Applying the results from RMT to such a case we observe emergent classical trajectories of repeated quantum measurements. Finally, we will discuss a fluctuation theorem that arises naturally from the results of these discussions. Continuing the theme of attempting to apply quantum chaos to characterise quantum devices, we will observe that this fluctuation theorem may be exploited to measure the density of states of a quantum system. As in previous chapters, numerical results confirming our results will be presented alongside analytical calculations.

[1] Note that this should not be confused with the Gibbs entropy in Chapter 1, which is strictly constant.

8.1 Classical Brownian Motion

Before discussing the emergence of classical statistical physics from quantum chaos, we briefly summarise an important paradigmatic example in non-equilibrium classical statistical physics, the Ornstein-Uhlenbeck (OU) process. This will be the model to which we look to compare the results from quantum chaos in an appropriate regime.

The OU process describes the Brownian motion [194] of the position $x(t)$ of a particle in a medium subjected to random collisions with its environment. This is described by the Langevin equation,

$$\frac{dx(t)}{dt} = -\frac{k}{\gamma}(x(t) - \overline{x}) + \xi(t), \tag{8.1}$$

where γ and $\overline{x}$ are constants, and $\xi(t)$ is a stochastic random variable fulfilling $\langle \xi(t) \rangle_\xi = 0$, $\langle \xi(t)\xi(t') \rangle_\xi = 2D\delta(t-t')$, where $\langle \cdots \rangle_\xi$ indicates an average over stochastic trajectories, and D is known as the diffusion constant. The OU process thus describes the motion of an overdamped harmonic oscillator driven by white noise, with an oscillator potential $V(x) = \frac{k}{2}x^2$. This is easily solved [150, 202] to find (setting $\overline{x} = 0$),

$$x(t) = x(0)e^{-\frac{k}{\gamma}t}, \tag{8.2}$$

and $\langle x^2(t) \rangle_\xi = \langle x(t) \rangle_\xi^2 + \frac{D\gamma}{k}(1 - e^{-2\frac{k}{\gamma}t})$. The long-time observable variance may be written as $\sigma_x^2(\infty) = \frac{D\gamma}{k}$.

We then use that, for a system in thermal equilibrium, the time-average energy is $\overline{\langle E \rangle} = \frac{1}{2}k_B T$ by the equipartition theorem. We then see that the long-time average energy gives $\overline{\langle V \rangle} = \frac{1}{2}D\gamma$, such that

$$D = \frac{k_B T}{\gamma}. \tag{8.3}$$

This is the celebrated Einstein relation of Brownian motion, a manifestation of the fluctuation-dissipation theorem (FDT) [173]. Note that this is a different form of the FDT that discussed in Chapter 6, which is a FDT for time-fluctuations, rather than the variance, of an observable.

We thus obtain,

$$\sigma_x^2(\infty) = \frac{k_B T}{k}. \tag{8.4}$$

Similarly, $\delta_x^2(\infty) := \lim_{T\to\infty}[\frac{1}{T}\int_0^T dt \langle x(t) \rangle_\xi^2 - (\frac{1}{T}\int_0^T dt \langle x(t) \rangle_\xi)^2]$ can be seen to be trivially equal zero from Eq. (8.2). Notice that in the notation used for the time-fluctuations we have implied the equivalence $\langle \cdots \rangle \leftrightarrow \langle \cdots \rangle_\xi$. Indeed, a key finding of the description in terms of RMT is precisely this equivalence.

8.2 Quantum Thermalization as an OU Process

8.2.1 Random Matrix Theory

From the description of the OU process above the key features can be seen immediately to resemble the results of the previous sections. In particular, the main result of Chapter

6 [17], describing the thermalization dynamics of an observable O, which is repeated here for convenience:

$$\langle O(t)\rangle = (\langle O(t)\rangle_0 - \overline{[O_{\alpha\alpha}]}_{\alpha_0})e^{-2\Gamma t} + \overline{[O_{\alpha\alpha}]}_{\alpha_0}. \tag{8.5}$$

Comparing to the OU process, where we chose the long-time average value $\overline{x} = 0$, we can we can see that we have equivalent dynamics when similarly setting the time average $\overline{[O_{\alpha\alpha}]}_{\alpha_0} = 0$, and assuming that the observable dynamics under H_0, $\langle O(t)\rangle_0$, is constant. The latter occurs for observables that are diagonal in the non-interacting basis, $O_{\alpha\beta} \propto \delta_{\alpha\beta}$.

To continue the comparison of RMT results to the OU process we wish to study the time-averaged variance of the local observable O. From Eq. (8.5), we arrive at

$$\sigma_O^2(\infty) = \overline{[\Delta O^2_{\alpha\alpha}]}_{\alpha_0}, \tag{8.6}$$

where $\overline{[\Delta O^2_{\alpha\alpha}]}_{\alpha_0} := \overline{[O^2_{\alpha\alpha}]}_{\alpha_0} - \overline{[O_{\alpha\alpha}]}^2_{\alpha_0}$. Finally, we further recall that the time-fluctuations of O may be written as,

$$\delta_O^2(\infty) = \frac{\overline{[\Delta O^2]}_{\alpha_0}}{4\pi D(E)\Gamma}, \tag{8.7}$$

as obtained in Chapter 5, and discussed in more detail in Chapter 6. Importantly for the comparison to the OU process, Eq. (8.7) decays exponentially with system size, and in the classical limit one expects $\delta_O^2(\infty) \to 0$.

Making the analogy to the OU process, then, we have a straightforward equivalence of the position x of the colloidal particle and the quantum observable O for both the dynamics: $\langle O(t)\rangle \leftrightarrow \langle x(t)\rangle_\xi$, and the time-fluctuations $\delta_x^2(\infty)$. This indicates that we may expect a similar relation for the variance $\sigma_x^2(\infty)$ and the quantum fluctuations $\sigma_O^2(\infty)$. This would imply an Einstein relation for the quantum fluctuations.

8.2.2 Einstein Relation

We now come to the main analytical result of this chapter: the quantity $\overline{[\Delta O^2_{\alpha\alpha}]}_{\alpha_0}$, can be shown to be the source of the microcanonical temperature $T(E)$ for a macroscopic observable ($d_B \gg d_S \gg 1$). To observe this, we re-express $\overline{[O_{\alpha\alpha}]}_{\alpha_0}$ via,

$$\overline{[O_{\alpha\alpha}]}_{\alpha_0} = \sum_s^{d_S} (O_S)_{ss} p(s), \tag{8.8}$$

where $p(s)$ may be written in terms of the DOS of the bath,

$$p(s) = \frac{D_B(E_{\alpha_0} - \epsilon_s)}{\sum_s^{d_S} D_B(E_{\alpha_0} - \epsilon_s)}, \tag{8.9}$$

which was derived in Chapter 3 (Eq. (3.25)).

Standard quantum statistical physics assumes that the DOS of the bath depends exponentially on the energy. This is not true in a finite system, however we can write,

$$D_B(E) = D_0 \exp(\beta(E)E)), \tag{8.10}$$

where $\beta(E)$ is the inverse microcanonical temperature, which we assume changes slowly over the width Γ in the sense of the conditions (3.34). In this case, we have,

$$p(s) = \frac{e^{-\beta(E_{\alpha_0})\epsilon_s}}{\sum_s^{d_S} e^{-\beta(E_{\alpha_0})\epsilon_s}}. \tag{8.11}$$

It is now clear that there has to be some dependence on $\overline{[\Delta O_{\alpha\alpha}]}_{\alpha_0}$ with (microcanonical) temperature, however, the actual relation is going to depend on the microscopic details of the model.

We may expect to observe the Einstein relation when considering a particle trapped in an harmonic potential [150]. We therefore consider, $(O_S)_{ss} = s$ and $\epsilon_s = \frac{1}{2}ms^2$, and assume that the temperature is small compared to the system bandwidth but large compared to the system energy spacing, $1 \ll m\beta \ll d_S$. In this case, we have the partition function

$$\mathcal{Z}(\beta) = \sum_s^{d_s} e^{-\beta\epsilon_s} = \sum_{s=-d_S/2}^{d_s/2} e^{-\frac{1}{2}\beta m s^2}, \tag{8.12}$$

where s takes $2S+1$ possible values from $[-S, S]$, and $\beta = \beta(E_\alpha)$. This can itself be evaluated as a Gaussian integral assuming that we have many system energy levels, $\sum_{s=-d_S/2}^{d_s/2} \to \int_{-\infty}^{\infty} ds$, such that

$$\begin{aligned} \mathcal{Z}(\beta') &= \int_{-\infty}^{\infty} ds e^{-\frac{1}{2}\beta' s^2} \\ &= \sqrt{\frac{2\pi}{\beta'}}, \end{aligned} \tag{8.13}$$

where we have defined $\beta' := m\beta$. Now, we can see that

$$\begin{aligned} \overline{[O^2_{\alpha\alpha}]}_{\alpha_0} &= \sum_s p(s) o_{ss}^2 \\ &= \frac{1}{Z(\beta')} \sum_{s=-d_S/2}^{d_s/2} s^2 e^{-\frac{1}{2}\beta' s^2} \\ &= \frac{1}{Z(\beta')} \int_{-\infty}^{\infty} ds s^2 e^{-\frac{1}{2}\beta' s^2} \\ &= \frac{1}{\beta'}. \end{aligned} \tag{8.14}$$

Similarly, we can see from the same approach that $\overline{[O_{\alpha\alpha}]}_{\alpha_0}$ vanishes as $\int_{-\infty}^{\infty} ds s e^{-\frac{1}{2}\beta' s^2} = 0$. We thus have,

$$\overline{[O^2_{\alpha\alpha}]}_{\alpha_0} = \frac{1}{m\beta(E_{\alpha_0})}. \tag{8.15}$$

Then, using (8.5), we see,

$$\overline{\langle E(t)\rangle} = \frac{1}{2} m \overline{\langle O^2(t)\rangle} = \frac{1}{2\beta(E_{\alpha_0})}, \tag{8.16}$$

which is precisely the equipartition theorem.

The remarkable feature of this formulation of the equipartition theorem is that it is a property of a single eigenstate; $\overline{[O^2_{\alpha\alpha}]}_{\alpha_0}$ averages diagonal observable elements over a single chaotic wavefunction $\Lambda(\mu, \alpha)$. This motivates the description of (8.15) as an 'eigenstate equipartition theorem' (EET).

The EET extends the intuition of the ETH all the way to the classical regime - thermalization occurs *at the level of individual eigenstates*. The ETH asserts that these eigenstates each define their own microcanonical energy shell - the EET is a much stronger statement, where we have that they each have their own associated temperature. Previous studies have observed results on similar lines numerically [176].

To obtain the Einstein relation from here is straightforward, as making the analogy to the Ornstein-Uhlenbeck (OU) process we observe that the dynamics of a closed quantum chaotic system is described by an effective OU process with an effective diffusion constant

$$D = \frac{k_B T \Gamma}{m}, \tag{8.17}$$

via the substitutions $\frac{k}{\gamma} \to 2\Gamma$, and $k_B T \to m\overline{[O^2_{\alpha\alpha}]}_{\alpha_0}$.

We note that in the OU process the equipartition theorem is asserted in order to obtain the Einstein relation, Eq. (8.4). We can see that in the derivation from chaotic wavefunctions, both expressions emerge simultaneously, and are ultimately equivalent statements in this formulation.

We may now make the relation between the formalism of quantum chaos and the OU process explicit by the following relations:

$$\begin{aligned} \langle O(t) \rangle &\Rightarrow \langle x(t) \rangle_\xi \\ \delta^2_O(\infty) &\Rightarrow \delta^2_x(\infty) \\ \sigma^2_O(\infty) &\Rightarrow \sigma^2_x(\infty) \\ \langle \cdots \rangle &\Rightarrow \langle \cdots \rangle_\xi, \end{aligned} \tag{8.18}$$

where on the left hand side we have our quantity for a chaotic quantum system, and on the right hand side we have the corresponding quantity for the OU process. The arrow $\Rightarrow$ can thus be understood as pointing towards the higher-level effective theory, emergent from a description in terms of quantum chaotic wavefunctions. In this case, the fundamental description is Schrödinger dynamics of a quantum chaotic system, which we see to have an emergent description in terms of Langevin dynamics.

We may additionally note that a fluctuation theorem may be formulated out of the above analysis. In fact, from Eq. (8.6) and (8.7) we may observe a remarkable feature of fluctuations of chaotic systems, that is, their ratio after equilibration,

$$\frac{\sigma^2_O(\infty)}{\delta^2_O(\infty)} = 4\pi D(E_{\alpha_0})\Gamma, \tag{8.19}$$

which may be understood as a signature of quantum ergodicity in many-body systems, and further reveals the DOS in terms of only measurable quantities. This latter statement is analysed numerically in Fig. 8.3 below.

Eq. (8.19) may be thought of as a ubiquitous feature of finite chaotic quantum systems that further to revealing the DOS of a system, is an important extension of the QC-FDT from Chapter 6. Indeed it is interesting to note that one may edit the OU process in order to display this same feature.

As noted above, the RMT model reproduces the classical OU process in the limit of infinite size $D(E) \to \infty$, as the time fluctuations of the OU process are equal to zero. However, if one modifies the stochastic noise $\xi(t)$ such that $\langle \xi(t) \rangle_\xi = v(s)$, with v a random variable itself, with $\overline{v(s)} = 0$, and $\overline{v(s)v(s')} = v^2\delta(s-s')$, we obtain,

$$\delta_x^2(\infty) = \frac{v^2\gamma^2}{k^2}. \tag{8.20}$$

In this case, we can make the association

$$\frac{\overline{[\Delta O^2]}_{\alpha_0}\Gamma}{4\pi D(E)} = \frac{k_B T\Gamma}{4\pi D(E)m} \Rightarrow v^2, \tag{8.21}$$

to recover the form of time-fluctuations expected by RMT for finite size systems. The modified time-fluctuation can be thought of as an equivalent of the Einstein relation for time-fluctuations of finite classical systems.

The final comparison, $\langle \cdots \rangle \Rightarrow \langle \cdots \rangle_\xi$, drawn in (8.18) above is crucial for our physical interpretation of the relationship between quantum chaos and classical Markov processes. We relate the average over noise realisations ξ to the expectation value at any given time. We thus observe an equivalence between the average over realisations of a classical system and the average over *measurements* of a quantum system.

Concretely, we picture a quantum system initialised in some state $|\psi(0)\rangle$, with an initial known expectation value $\langle O(0) \rangle$. To experimentally obtain the value $\langle O(t_1) \rangle$ at time t_1 one must prepare the initial state, let time evolve until $t = t_1$, and perform a measurement. This ends this experiment, and must then be repeated many times. The average over measurements gives an estimate for the expectation value $\langle O(t_1) \rangle$. This must be repeated for all t to build the dynamics of the expectation value.

Not only is the above experimental scenario exceedingly idealistic, and not realistic for typical experimental protocols, but relating this experimental procedure to classical physics has a major issue: the measurement process ends the experiment. For a classical system, one may observe the thermalization occur in time, and average over experimental trajectories. The OU process is a description of this average. This motivates a description of repeated measurements of closed quantum systems.

8.3 Quantum Jump Trajectories

A more realistic experimental scenario is that where a set of quantum measurements are made at times t_1, t_2, ..., generating a set of outcomes O_1, O_2, ... In this case, we may describe the experiment as a series of thermalization experiments of the above form. The total system is initialised in some state, and each measurement projects the system state to an eigenstate of the local observable. In between successive measurements, unitary

thermalization dynamics occurs as above. Note that in the following, we no longer limit ourselves to harmonic system potentials and the considered observable used to obtain the OU process, which can be seen as a particular case of a more general treatment.

From the realisation that between measurements a thermalization scenario takes place, with each measurement performing an effective 'measurement quench' [203], we may directly apply the results of the previous sections. In detail, we have the sequence of measurement quenches

$$|\epsilon_{s_0}\rangle|E^{(B)}_{\beta_0 g}\rangle \to |\epsilon_{s_1}\rangle|\psi^{(B)}_1\rangle \to |\epsilon_{s_2}\rangle|\psi^{(B)}_2\rangle \to \dots, \tag{8.22}$$

where $|\psi^{(B)}_j\rangle$ is the state of the bath at step j. Assuming that the total energy is not significantly perturbed by the measurement process, we have that the quantum dynamics is restricted to many-body states with energies close to the initial energy, $E_{\alpha_0} = \epsilon_{s_0} + E^{(B)}_\beta$. This assumption is valid assuming the range of system energies is negligible in comparison to the bath. This assumption is checked numerically below for model systems (see Fig. 8.2), however can be seen easily to be valid for cases where the total energy range of the system is negligible compared to that of the bath.

In describing a quantum jump trajectory we will make use of the projection operator $P_s = |\epsilon_s\rangle_S\langle\epsilon_s| \otimes \mathbb{1}_B$. This itself is a local observable, sharing similar properties to O. Thus, between each successive measurement one may imagine a quantum thermalization scenario, where we define $p(s_f, s_i; t_f, t_i)$ as the probability of measuring the value s_f at time t_f, assuming that a previous observation yielded a value s_i at time t_i. We may thus apply Eq. (8.5) to the operator P, obtaining

$$p(s_f, s_i; t_f, t_i) = \left(\delta_{s_f,s_i} - p_\infty(s_f)\right) e^{-2\Gamma\Delta t} + p_\infty(s_f), \tag{8.23}$$

where $p_\infty(s_f) = \overline{[(P_{s_f})_{\alpha\alpha}]}_{\alpha_0}$, and $\Delta t = t_f - t_i$. $p_\infty(s_f)$ is the steady-state probability for the system to be in state s_f, which is written in terms of a microcanonical ensemble around the initial energy E_{α_0}.

We observe that the dynamical record $R_{\Delta t} = \{O_0, O_1, \cdots, O_n\}$, of measurement outcomes O_i at time $i\Delta t$ depends crucially on the time interval Δt. For finite systems the decay cannot be exactly exponential at early times, and hence for $\Delta t \ll \Gamma^{-1}$ there is minimal change in $\langle P_s(t)\rangle$, leading to the Zeno effect [204] for $\Delta t \to 0$. For $\Delta t \gg \Gamma^{-1}$ we obtain that time-fluctuations of the quantum jump trajectory are equal to the observable variance $\delta^2_{R_{\Delta t}}(\infty) = \sigma^2_O(\infty)$.

More importantly, however, in the case $\Delta t < 1/\Gamma$, the measurement process will be able to resolve the decay of the observable X in time. In-fact, Eq. (8.23) predicts that the measurement outcomes form a Markov chain. Furthermore, we can show that the average over all the resulting stochastic trajectories of a measurement outcome, s_j at time t_j, is the same as the expectation value $\langle X(t_j)\rangle$ at time t_j. In other words, if we measure the expectation value $\langle X(t_j)\rangle$, the value is independent of whether we have subjected the systems to a quantum measurement at times $t < t_j$ or not. This can be seen by assuming that a measurement yields a value s_i at time t_i and a future observation yields the value

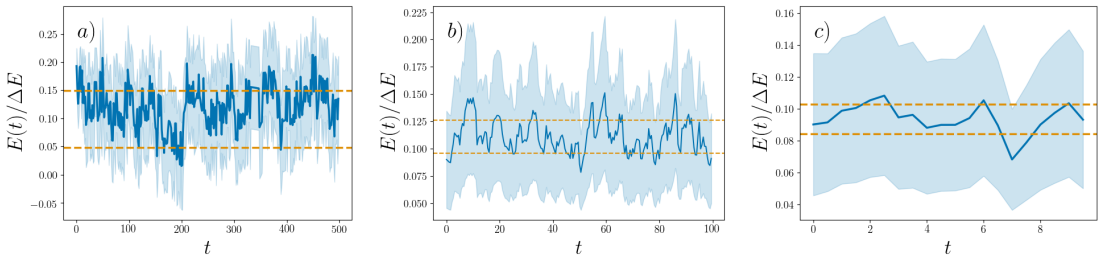

Figure 8.2: Change of total energy $E(t) = \langle H(t) \rangle$ in time due to action of repeated projective measurements (blue solid line). Variance of energy $\sigma_E(t)$ shown in shaded area. Dashed lines show time-fluctuations of energy $\delta_E(\infty)$. $\Delta E = E_{max} - E_{min}$. a) Quantum harmonic oscillator chain of main text, Parameters: $J = 0.8, h_x = 0.7, S = 3, N = 4$. Time averages variance $\overline{\sigma_E(t)}$ of order $\frac{\overline{\sigma_E(t)}}{\Delta E} \approx 0.05$ b) and c) Spin chain of Eq. (8.31) under action of local observable S_z^1 and global observable $\sum_i S_z^i$ respectively. $\frac{\overline{\sigma_E(t)}}{\Delta E} \approx 0.015, 0.009$ for local and global observables respectively. Parameters: $N = 4, S = 3, h_z = 1, h_x = 0.2, J = 0.8, \Delta = 0.3, q = 1.5$

s_f at time t_f. At some intermediate time, an observation is performed a time $t_i < t' < t_f$, with outcome s'. It then follows that the conditioned probability distribution in (8.23) satisfies that,

$$\begin{aligned}
&\sum_{s_m} p(s_f, s_m; t_f, t_m) p(s_m, s_i; t_m, t_i) \\
&\quad = \sum_{s_m} \left((\delta_{s_f, s_m} - p_\infty(s_f)) e^{-2\Gamma(t_f - t_m)} + p_\infty(s_f) \right) \left((\delta_{s_m, s_i} - p_\infty(s_m)) e^{-2\Gamma(t_m - t_i)} + p_\infty(s_m) \right) \\
&\quad = (\delta_{s_f, s_i} - p_\infty(s_f)) e^{-2\Gamma(t_f - t_i)} + p_\infty(s_f) \\
&\quad = p(s_f, s_i; t_f, t_i).
\end{aligned} \tag{8.24}$$

By induction, Eq. (8.24) can be extended to the case where an average is taken over a set of intermediate measurement outcomes, yielding the result that the average distribution probability at some time is independent of whether the system measured. This result is of course not valid in the Zeno regime, where the exponential decay assumption of the expectation value of an observable is not valid.

We further analyse the time-dependence of the non-equilibrium Gibbs entropy,

$$S_G(t) = - \sum_{s - d_S/2}^{d_S/2} p(s, s_i; t, t_0) \ln p(s, s_i; t, t_0), \tag{8.25}$$

In fact, from Eq. (8.5) we may show that $\frac{dS_G(t)}{dt} \geq 0$, and thus the emergence of the second law for this entropy measure as follows. For simplicity of notation we remove the initial state variables, defining $p(s_f, t_f) := p(s_f, s_i; t_f, t_i)$. Then, using that

$$p(s, t) = p(s, 0) e^{-2\Gamma t} + (1 - e^{-2\Gamma t}) p_\infty(s), \tag{8.26}$$

where $p_\infty(s)$ is the equilibrium probability of obtaining the outcome s from a measurement of O. We have, then, that

$$\frac{dS_G(t)}{dt} = -\sum_s [2\Gamma e^{-2\Gamma t}(p_\infty(s) - p(s,0))(\ln p(s,t) + 1)] \tag{8.27}$$

which, using that $1 - \frac{1}{x} \leq \ln x \leq x - 1$, we obtain

$$\begin{aligned} \frac{dS_G(t)}{dt} &\geq 2\Gamma e^{-2\Gamma t} \sum_s [p(s,0)p(s,t) - p_\infty(s)(2 - \frac{1}{p(s,t)})] \\ &\geq 2\Gamma e^{-2\Gamma t}[p(s_0,t) - 2 + \sum_s \frac{1}{p(s,t)}] \end{aligned} \tag{8.28}$$

where in the second line we have used that $p(s,0) = \delta_{s,s_0}$, where s_0 is the initial value of O_S. Now, we can thus see that at $t \to 0$, the factor $\sum_s \frac{1}{p(s,t)} \to \infty$. This indicates that at early times the rate of entropy growth is increased. For $t > 0$, we can note that $\frac{1}{p(s,t)} \geq 1$ and $p(s_0,t) \geq 0$, so

$$\frac{dS_G(t)}{dt} \geq 2\Gamma e^{-2\Gamma t}[d_s - 2] > 0, \tag{8.29}$$

for observables with more than one possible outcome $d_s \geq 2$.

We thus see that the Gibbs entropy is non-decreasing in time. This is observed in Fig 8.4 for two model systems described below. We see that for small Δt this growth is significantly slower due to proximity to the Zeno regime.

The definition of a non-equilibrium Gibbs entropy for quantum jump trajectories makes an important connection to results in stochastic thermodynamics [148, 149, 197]. In particular, we have seen that $p(s, s_i; t, t_0)$ may be described by effective Langevin dynamics, and thus Eq. (8.25) may be seen to parallel the classical non-equilibrium Gibbs entropy defined in e.g. [197].

We finally note that an entropy may be defined for an *individual* trajectory, by taking the probability distribution of measurement outcomes over all times. In equilibrium we have an equivalence between the quantum fluctuations $\sigma_O^2(\infty)$, and time-fluctuations of a single trajectory with $\Delta t \gg \Gamma^{-1}$, as each projective measurement occurs with a variance $\sigma_O^2(\infty)$. Thus, by taking a single quantum trajectory for many time steps, and building a probability distribution $p_{traj}(s)$ over the observable outcomes of the experiment, one expects the single trajectory entropy $S_{traj} = -\sum_s p_{traj}(s) \ln p_{traj}(s)$ to be equal to the equilibrium (maximal) value of $S_G(t)$. This is confirmed numerically below.

8.4 Numerical Experiments

In this section, we perform numerical experiments via exact diagonalization to obtain the thermalization dynamics, and quantum jump trajectory dynamics, of two distinct quantum models.

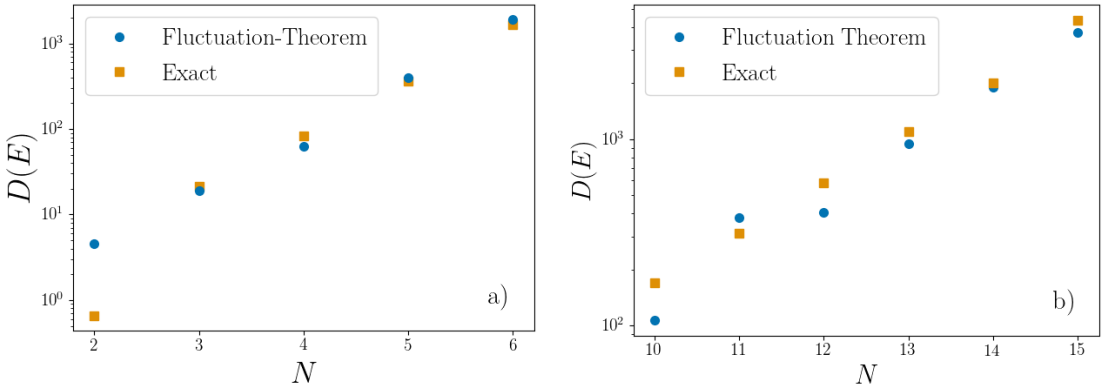

Figure 8.3: Comparison of density of states as inferred from the fluctuation theorem of Eq. (8.19) (yellow squares) with exact value (blue circles). a) For system of coupled quantum harmonic oscillators described in main text. Parameters: $J = 1.2$, $h_x = 0.8$, $S = 2$ b) For chain of spin-$\frac{1}{2}$ particles with Hamiltonian (6.47). Parameters: $B_x^{(S)} = 0, B_z^{(B)} = 0, B_x^{(B)} = 0.3, J_x^{(S)} = 0.4, J_z^{(S)} = 0.2, J_z^{(B)} = 0.1, J_x^{(B)} = 1, B_z^{(S)} = 0.8$.

- *Coupled quantum harmonic oscillators.* We consider a set of particles confined to move in a grid of discretized positions in one-dimensional harmonic potentials. The Hilbert space is formed by states $|s, i\rangle$, where $s = -S, \cdots, S$ is the position in the i^{th} potential,

$$H_0 = \sum_{i=1}^{N} \sum_{s=-S}^{S} \epsilon_s |s, i\rangle\langle s, i| \tag{8.30}$$

with $\epsilon_s = s^2$. To this, we add the coupling term

$$\begin{aligned} V = h_x \sum_{i=1}^{N} \sum_{s=-S}^{S-1} (|s, i\rangle\langle s+1, i| + H.c.) \\ + J \sum_{i=1}^{N-1} \sum_{s=-S}^{S-1} (|s, i\rangle\langle s+1, i+1| + |s+1, i\rangle\langle s, i+1| + H.c.), \end{aligned}$$

which includes both a kinetic energy term proportional to h_x, and a hopping J between adjacent sites and energy levels in each oscillator. The observable is taken to be the oscillator position at $i = 1$, $O = X_1 = \sum_s s|s, 1\rangle\langle s, 1|$.

Numerical results are shown in Fig. 8.4a)-c). In particular, in Fig. 8.4b) we see that the decay rate of averaged quantum jump trajectories indeed converges to that of $\langle O(t)\rangle$ outside of the Zeno regime. Corresponding thermalization dynamics and quantum jump trajectories for each value of Δt are shown in Fig. 8.5. Further, we observe in Fig. 8.4c) the growth of non-equilibrium Gibbs entropy in time to the value of the single trajectory entropy.

- *Quantum Spin-Chains.* The second system we consider is a Bilinear-Biquadtratic spin-

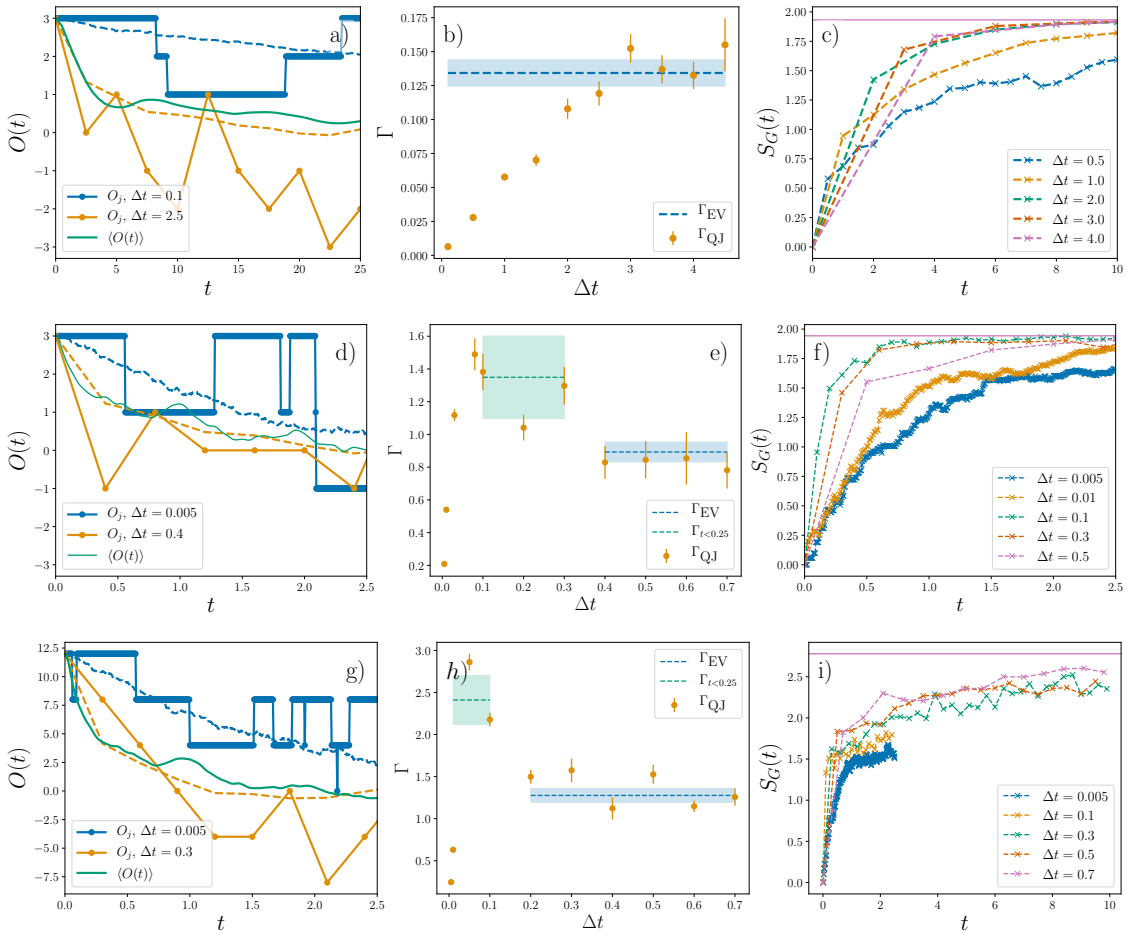

Figure 8.4: Exact diagonalization calculations of QHO Hamiltonian (8.30), (8.31) a)-c), and the spin-chain Hamiltonian (8.31) for local observable $O = S_z^1$ d)-f) and global observable $\sum_i^N S_z^i$ g)-i). a), d), g) Examples of observable dynamics as obtained from $\langle O(t) \rangle$, quantum jump trajectories O_j, and their averages over 500 realisations (dashed lines). b), e), h) Convergence of the decay rate as measured by quantum jump trajectories to that of thermalization dynamics. Trajectories shown in Figs. 8.5, 8.6 and 8.7 for the QHO model, and local and global observables of the spin-chain system, respectively. c), f), i) Growth of the non-equilibrium Gibbs entropy. Solid line shows single trajectory entropy for maximal Δt value of each plot. Parameters: $J = 0.8, h_x = 0.7, S = 3, N = 4$.

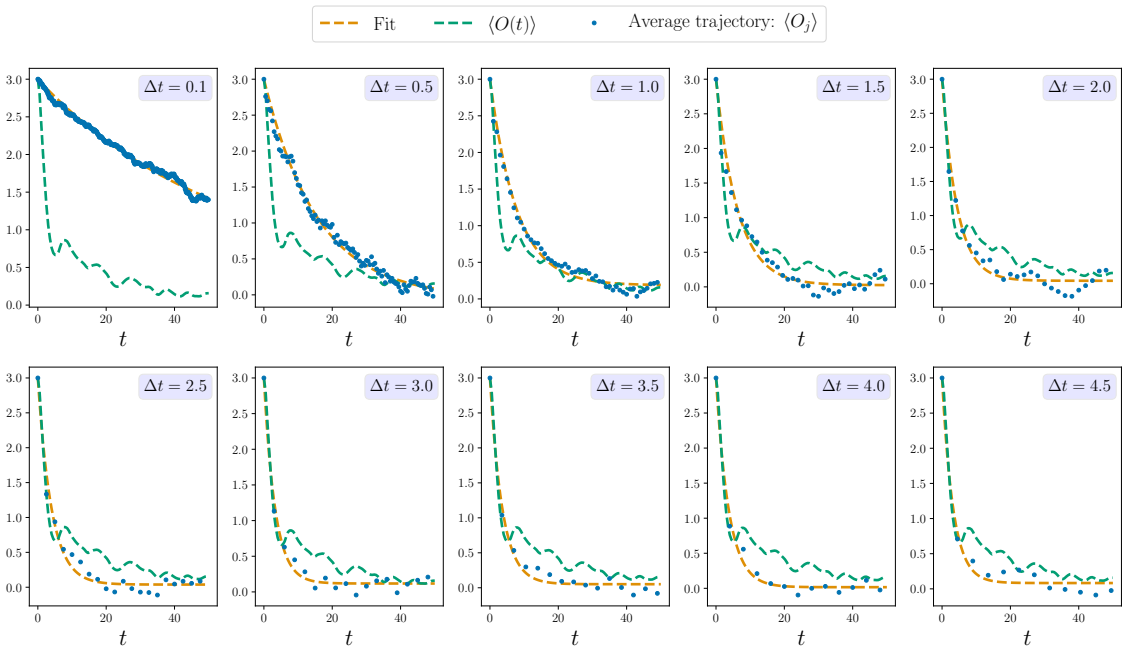

Figure 8.5: Average quantum jump trajectories of $O = X_1$ quantum harmonic oscillator Hamiltonian of the main text for varying Δt. Here we see that as Δt is increased the decay rate of the average jump trajectory decays at the same rate as the expectation value (green dashed line). Orange dashed line shows fit to exponential decay used to obtain Γ_{QJ} in Fig. 8.4b). For small Δt, the decay is slowed due to proximity to the Zeno regime of completely frozen dynamics at $\Delta t \to 0$. Averages over 500 realisations of quantum trajectories (100 realisations for $\Delta t = 0.1, 0.5$). Parameters: $J = 0.8, h_x = 0.7, S = 3, N = 4$.

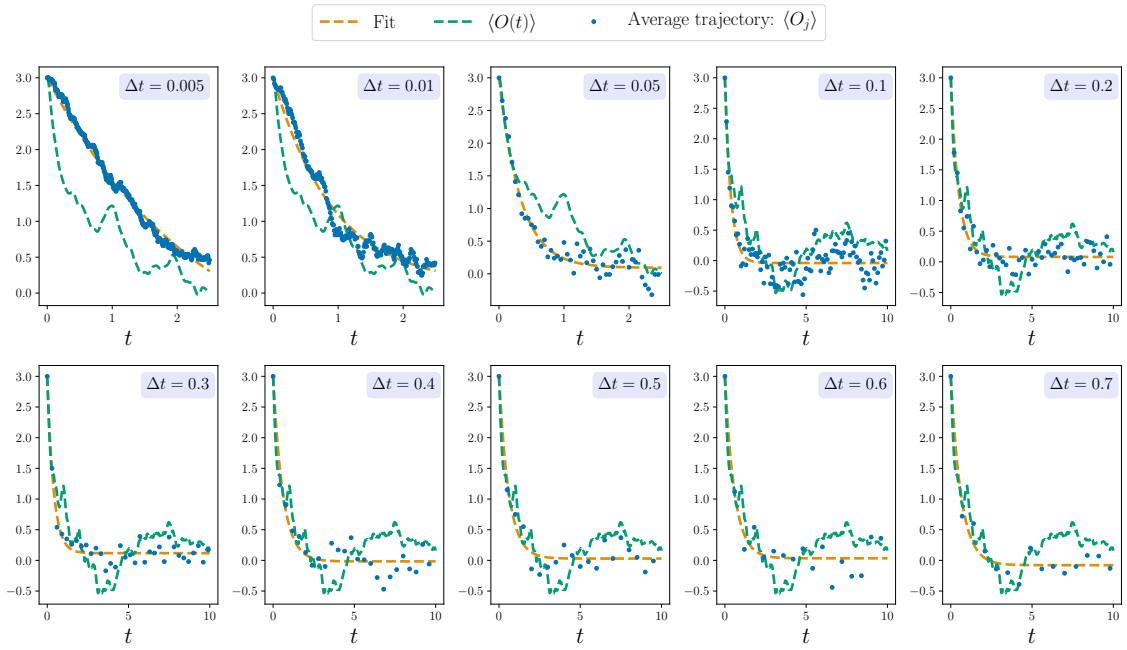

Figure 8.6: Average quantum jump trajectories of $O = S_z^1$ of spin-chain Hamiltonian of Eq. (8.31) for varying Δt. Here we see that as Δt is increased the decay rate of the average jump trajectory decays at the same rate as the expectation value (green dashed line). Orange dashed line shows fit to exponential decay used to obtain Γ_{QJ} in Fig. 8.4e). For small Δt, the decay is slowed due to proximity to the Zeno regime of completely frozen dynamics at $\Delta t \to 0$. Averages over 100 realisations of quantum trajectories. Parameters: $N = 4, S = 3, h_z = 1, h_x = 0.2, J = 0.8, \Delta = 0.3, q = 1.5$.

chain [205–207]. given by the Hamiltonian

$$H_0 = \sum_j^N \Big[h_z S_z^j + h_x S_x^j \Big], \tag{8.31}$$

where $j = 1$ is the system spin. The coupling Hamiltonian is

$$\begin{aligned} V = \frac{1}{2} J \sum_i^{N-1} \Big[& S_x^i S_x^{i+1} + S_y^i S_y^{i+1} + \Delta S_z^i S_z^{i+1} \\ & + q\big((S_x^i S_x^{i+1})^2 + (S_y^i S_y^{i+1})^2 + \Delta (S_z^i S_z^{i+1})^2\big) + H.c \Big], \end{aligned} \tag{8.32}$$

where $S_{x,y,z}^i$ are spin operators on site i. Notice that this Hamiltonian does not have a quadratic energy dispersion of the system at $i = 1$, which is required only to obtain the Einstein relation in the form of the OU process. Further, we consider both a local and global observable of this model, finding that our analysis is valid in each case - our assumptions simply require the observable has a sufficiently sparse structure in the free basis [17]. Indeed, the sparsity condition obtained in Chapter 3 for local observables extends to 'k-local' observables, $O^{(k)} = \sum_i^k O_i$, where O_i is a local observable on site i. For such k-local observables, the sparsity condition still holds - even for global observables, with $k = N$.

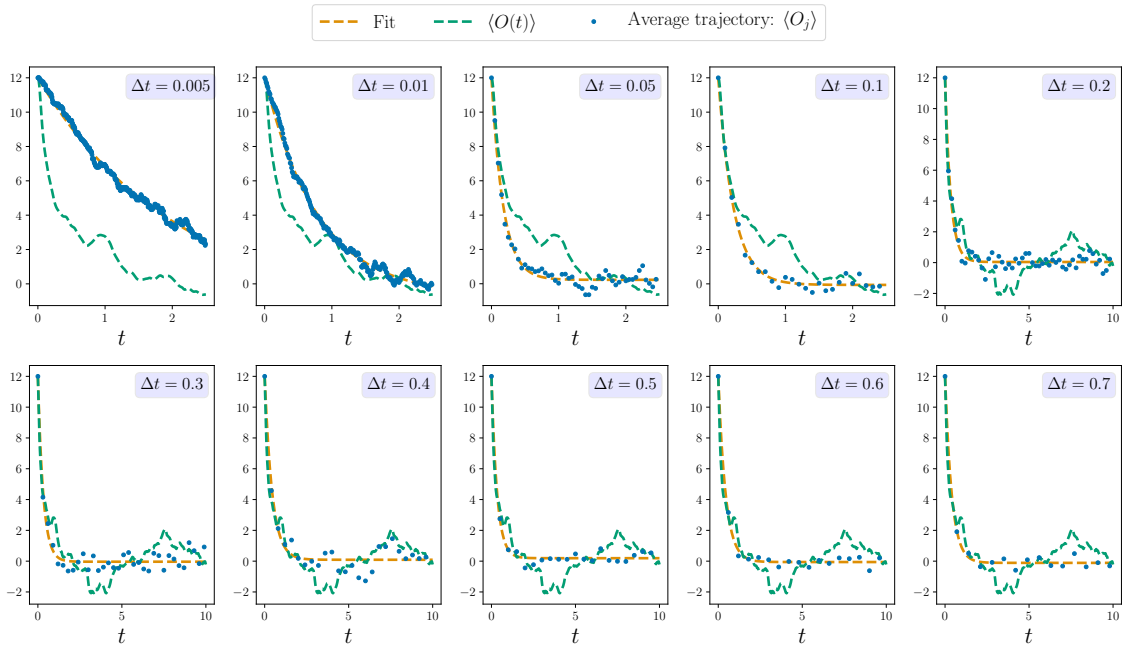

Figure 8.7: As in Fig. 8.6, with observable $O = \sum_i S_z^i$. Trajectories used for Fig. 8.4h).

Here we have used the local observable $O = S_z^1$, as well as the global observable $O = \sum_i^N S_z^i$. Numerical results are shown in Fig. 8.4d)-f) for the local observable, and Fig. 8.4g)-i) for the global observable. Corresponding dynamics of both the expectation value and quantum jump trajectories for Figs. 8.4e) and 8.4h) are shown in Figs. 8.6 and 8.7 respectively.

Interestingly, we observe that in both cases the expectation value dynamics consists of two separate timescales. At very short times, the decay is fast, however after some time, a slower decay dominates. Notice that this more complicated dynamics is mirrored in the quantum jump trajectories. In Fig. 8.4e), h), unlike the harmonic oscillator chain, the quantum jump trajectory decay rate is actually faster than the expectation value decay for a range of Δt. For this intermediate range of Δt values, the quantum jump trajectories decay at the same rate as the short time dynamics of the expectation value. As Δt is increased, the decay rate slows to that of a fit to the whole dynamics of the trajectory.

We thus see that more complex dynamics may also be resolved in the quantum jumps framework. Indeed, as previously noted, the approach from quantum chaos is more general than the specific RMT model applied in the main text, and may describe systems where Λ is of a different form to a Lorentzian. In such cases, the decay deviates from a purely exponential form. This may allow quantum jump trajectories to resolve such phenomena as prethermalization [73].

In each case, we initialise the system a mid-energy eigenstate of the non-interacting Hamiltonian, H_0, choosing such that $\langle O(0)\rangle = \max(O)$, and obtain Γ from a fit to Eq. (8.5).

8.5 Conclusions

In this chapter, we have shown how a closed quantum system initialised in a pure state may reproduce a *classical* temperature dependent fluctuation-dissipation theorem of Brownian motion. Specifically, we have reproduced the Einstein relation for the Ornstein-Uhlenbeck process. This result is a direct analytical observation of the emergence of classical statistical physics from unitary quantum dynamics - indeed, we similarly observe an 'eigenstate equipartition theorem', and thus see that microcanonical temperature relations can be seen on the level of individual eigenstates, thus extending the intuition afforded by the ETH.

Our results apply directly to quantum jump trajectories induced by repeated quantum measurements, finding that the variance of the trajectory is similarly described by a classical OU process. Indeed, establishing the quantum chaotic dynamics of probability distributions of observable outcomes to classical Markov processes may further provide an important link to more recent work in classical statistical physics, that of stochastic thermodynamics, which entails the description of classical Brownian processes in terms of individual trajectories. Here we observe quantum jump trajectories, and define a non-equilibrium Gibbs entropy that may be described by effective Langevin dynamics, thus opening a relation to the stochastic thermodynamics models in e.g. [148, 197].

Further, we have shown that the fluctuations of chaotic quantum systems may be exploited to accurately measure its density of states. This can be done using measurements of a local observable of a quantum spin-chain systems of modest sizes, realisable, for example, on trapped-ion quantum simulator devices.

Our calculations are based on a random matrix theoretic approach, building on the theoretical model of earlier chapters, where we obtained an analytic description of the full time-dependent decay to equilibrium [17]. The current work formalises an important consequence of this approach, the emergence of a description of the fluctuations of local observables in terms of a microcanonical temperature. This hints at a more fundamental foundation of classical statistical physics, as we see the important properties of this theory directly from the quantum dynamics of pure states. We have confirmed our results by a numerical ED of a chain of interacting QHOs, and a quantum spin chain.

Chapter 9

Conclusions and Outlook

9.1 Conclusions

9.1.1 Methods and Analysis

In this thesis I have outlined an approach to the description of thermalization of closed quantum systems from the assumption of quantum chaos. The fundamental assumption underlying this approach is that chaotic systems are well described by a statistical theory of chaotic wavefunctions. The key assumption of this statistical theory is that eigenstates of a non-integrable Hamiltonian, when expressed in the non-interacting (mean-field) basis, may be described by a Gaussian probability distribution, up to a correction due to the necessary mutual orthogonality of eigenstates. Under this assumption the chaotic wavefunction may be represented via a smooth function $\Lambda(\mu, \alpha)$.

Within this statistical theory a generic form for correlation functions is derived, for which the correction due to orthogonality is seen to be vital for the consistent description of observables. It is this description of correlation functions that forms the basis of calculations with this model under the condition of self-averaging. The latter condition, which is proven in Chapter 7, allows eigenstate coefficients in summations to be replaced with their respective correlation function. In fact, it is precisely this property that justifies the use of a probability distribution on the eigenstates of a single Hamiltonian, as averages over a relevant ensemble yield equivalent results.

The chaotic wavefunctions for the random matrix ensemble of Deutsch [64] have played a central role in this work. This model has been solved in Chapter 5, to find $\Lambda(\mu, \alpha)$ in a Lorentzian form[1]. This is observed to well describe realistic quantum systems, using a spin-chain as an example, in the limit where the system is weakly coupled to the bath. The description of Λ by this model is seen to break down in the limit of strong coupling, where Λ is observed to have a Gaussian form. Indeed, a Gaussian ansatz in this limit can be seen to well describe features of realistic strongly coupled models.

[1] This had been seen previously in unpublished notes in Ref. [65] in a rather hand-waving manner. The derivation is formalised in Appendix A.1 in the limit of large $\mathcal{N}$ and small coupling.

9.2 Results

Using this model of chaotic wavefunctions, I have developed a theory of statistical physics describing the thermalization of local observables of a closed quantum system. The key results can be split into two themes. The first, relating to thermalization and the foundations of statistical physics, are showing that from the developed theory of chaotic wavefunctions key results of statistical physics are reproduced. This is extended in an important and novel direction by obtaining analytical results on the properties of quantum jump trajectories. The second theme is focussed on the application of this model, which I have shown can be exploited to obtain methods for characterisation of quantum devices, such as quantum computers and quantum simulators.

Key results of the former, regarding foundations of statistical physics, are summarised as follows:

- A Gaussian ansatz on the wavefunction distribution of closed quantum systems is shown to be insufficient in the description of off-diagonal matrix elements of observables, giving contradictory results if assumed. This contradiction can be avoided by including interactions due to orthogonality.

- A generic form for local observables is obtained, which allows for the calculation of properties of such physical observables in a random matrix theoretic format. This overcomes common criticisms of random matrix models, which are typically restricted to unphysical non-local observables.

- The key assumptions involved in performing calculations are phrased in terms of physical quantities of the system in question. These conditions may be written in terms of the density of states or microcanonical temperature of a system, and are congruent with (but more general than) standard approaches to statistical physics.

- From these assumptions, the eigenstate thermalization hypothesis may be derived in full for local observables.

- The long-time fluctuations of observables are shown to be sufficiently small, that is, they are shown to decay exponentially with system size. Interestingly, the derived equality for the random matrix model is found to scale with the saturation of generic bounds from typicality approaches[2].

- Long-time fluctuations are further shown to behave according to a 'quantum chaotic fluctuation-dissipation theorem'. This links the non-equilibrium property of the decay rate to the fluctuations from equilibrium in time of a closed quantum system.

- The full time dependence of thermalization of local observables is derived. This shows the decay to an equilibrium state described by the microcanonical ensemble. This is shown for both pure and mixed initial states under reasonable conditions.

[2]Compare e.g. Eq. (2.20) to Eq. (5.74).

- The equipartition theorem is derived, and shown to emerge at the level of individual eigenstates. This extends the intuition afforded by the ETH: that thermal behaviour originates as a property of eigenstates of chaotic quantum systems.
- The Einstein relation of Brownian motion is obtained for the quantum fluctuations of thermalization dynamics, establishing thermalization in closed quantum systems for certain local observables as an emergent Ornstein-Uhlenbeck process, described by an effective Langevin equation.
- Quantum jump trajectories of local observables in closed quantum systems are described in terms of repeated thermalization procedures. This allows application of many of the prior results to an important new regime. From here, it is shown that from repeated quantum projective measurements, a classical Brownian process is observed in chaotic quantum systems.
- The non-equilibrium Gibbs entropy may be defined in terms of averages over measurement outcomes such quantum jump trajectories. This entropy is shown analytically to be non-decreasing.

Each of these results has been tested via numerical exact diagonalization calculations of a realistic quantum spin-chain systems, and additionally, for a system of coupled quantum harmonic oscillators for the quantum jump trajectory calculations. Together these results formalize a foundation for quantum statistical physics based on quantum chaos, that may even be shown to reproduce paradigmatic results of classical statistical physics such as the Einstein relation, and the equipartition theorem.

Further, results regarding the characterisation of quantum devices are:

- A meaningful measure of the 'complexity' of calculated observable dynamics of a quantum device is developed in terms of the effective Hilbert space dimension. This can be understood as the minimum required Hilbert space dimension required to reproduce the calculated dynamics with a fully connected device, and thus factors in limiting qualities of a realistic device, such as locality of interactions. Importantly, this effective Hilbert space dimension is shown to be obtainable via measurable quantities - the decay rate, and time-fluctuations, of thermalization dynamics for a system initialised in an infinite temperature state, with a probe qubit in an initial pure state.
- The density of states is shown to be measurable via initialisation of a system in a pure state, and measurement of the decay rate, time-fluctuations, and equilibrium quantum fluctuations, of thermalization dynamics.

Similarly, the above results are confirmed via exact diagonalization calculations.

9.3 Outlook

The results listed above are important steps forward in the effort to establish a concrete foundation for statistical physics based on physical principles. Starting with a chaotic

wavefunction ansatz (which can be physically motivated, and has been numerically confirmed at the onset of non-integrability in a quantum spin-chain), a statistical theory has been developed that not only reproduces core features of statistical physics, but makes concrete predictions that have been verified by numerical calculations on experimentally accessible systems.

Importantly, this approach confirms and extends the 'eigenstate thermalization' picture of quantum thermalization, which claims that thermalization occurs at the level of individual eigenstates. This can be seen as the distribution of eigenstate probability amplitudes of chaotic quantum systems (when expressed in an appropriate non-interacting or mean-field basis) form an effective microcanonical ensemble. The intuition afforded by this picture has been extended even as far as to observe features of classical thermodynamics for individual eigenstates - relations such as the equipartition theorem, and the Einstein relation for Brownian motion, can themselves be shown to emerge as properties of chaotic wavefunctions.

Beyond eigenstate thermalization, a fully dynamical picture of thermalization is developed from quantum chaos. The decay to equilibrium is obtained with two important features. The decay itself is attributed to the Fourier transform of the observable off-diagonal element distribution. For the RMT model, this is of a Lorentzian form, and thus the decay is exponential. Secondly, the decay process is modulated by the non-interacting observable dynamics. For observables that have some non-diagonal structure in the non-interacting basis, this may occur as e.g. Rabi oscillations on the decay to equilibrium. These non-interacting dynamics have been calculated explicitly for the case of a quantum spin-chain, and the resulting modulation of the decay process is shown to match numerical exact-diagonalization calculations.

In physical realisations of thermalization processes an experimentalist rarely has access to the time-evolution of expectation values of observables. In more typical scenarios, an experimentalist may be able to perform repeated measurements of a system as it evolves in time. Indeed, in classical situations, thermalization should occur under continuous measurement (which in the classical limit is assumed to have no effect on dynamics). The case of repeated quantum projective measurements can be described from the perspective of thermalization - where thermalization of the expectation value as above occurs between successive measurements. This enables a treatment of quantum jump trajectories in terms of chaotic wavefunctions and random matrix theory, and thus links important recent work on quantum and stochastic thermodynamics, to random matrix theory and eigenstate thermalization. Indeed, outside of the Zeno regime, thermalization is observed in a statistical treatment of quantum jump trajectories, and further, their dynamics are shown to be equivalent to classical Brownian motion.

The developed statistical theory of chaotic wavefunctions may be further extended. The ability to calculate arbitrary correlation functions of wavefunction distributions is a powerful calculational tool, and leaves open the ability to study more complicated properties of chaotic systems. These include observable correlation functions, which are a key feature in the understanding of ergodicity and chaos in classical and quantum systems.

A further important extension would be application to a generalised RMT model, which accounted for the banded nature of the interaction Hamiltonian. This would allow the model to well describe high coupling regimes, such as homogeneous spin-chains. The theoretical model of chaotic wavefunctions is valid in this limit; however, a rigorous derivation of the form of the wavefunction envelope Λ would be an important extension.

It can thus be seen that the approach outlined in this thesis provides a satisfying picture for the mechanism of thermalization in closed quantum systems, which occurs for interaction Hamiltonians independently mixing a sufficient number of non-interacting basis states such that their coarse grained distribution takes a Gaussian form. From this picture, a mechanism for thermalization - the eigenstate thermalization hypothesis - can be derived in full. Further, in relevant limits important results of classical statistical physics are obtained. This suggests, and provides a significant contribution towards, a foundational theory of statistical mechanics based on chaotic wavefunctions.

Appendices

Appendix A

Solution To RMT Model

A.1 Variational Calculation of RMT Wavefunction Distribution

To find the distribution of eigenstates for the random matrix system we must obtain a functional form of $\Lambda(\mu,\alpha)$ by minimising Eq. (5.22). Note that the integral in Eq. (5.22) is taken over all elements of $\{c_\mu(\alpha)\}$, *i.e* $\int dc \rightarrow \prod_{\mu\alpha}\int dc_\mu(\alpha)$. The original probability distribution for the random wave-functions is given by Eq. (5.20), which may be re expressed by writing the second delta-function in Fourier form

$$\begin{aligned} P(c) = A\delta(cc^T - I)\int\int \exp\Big[&- \sum_{\substack{\alpha'\beta' \\ \alpha'>\beta'}} \frac{\mathcal{N}h^2_{\alpha'\beta'}}{2g_1^2} - \sum_{\alpha'}\frac{\mathcal{N}h^2_{\alpha'\alpha'}}{2g_2^2} \\ &- i\sum_{\substack{\mu'\nu' \\ \mu'>\nu'}} \lambda_{\mu'\nu'}\Big(\sum_{\substack{\alpha'\beta' \\ \alpha'>\beta'}} c_{\mu'}(\alpha')h_{\alpha'\beta'}c_{\nu'}(\beta') + \sum_{\substack{\alpha'\beta' \\ \beta'>\alpha'}} c_{\mu'}(\alpha')h_{\alpha'\beta'}c_{\nu'}(\beta') \\ &+ \sum_{\alpha'} c_{\mu'}(\alpha)h_{\alpha'\alpha'}c_{\nu'}(\alpha) + \sum_{\alpha'} c_{\mu'}(\alpha')f_{\alpha'}c_{\nu'}(\alpha')\Big)\Big]\Big(\prod_{\substack{\alpha\beta \\ \alpha\geq\beta}} dh_{\alpha\beta}\Big)\Big(\prod_{\substack{\mu\nu \\ \mu>\nu}} d\lambda_{\mu\nu}\Big), \end{aligned} \tag{A.1}$$

where we have expressed the independent widths of the off-diagonal and diagonal element distributions as g_1 and g_2 respectively. This further differs from that used in [65] by appropriate symmetrization of the random interaction Hamiltonian. This may be rewritten

as

$$P(c) = A\delta(cc^T - I)\int\int \exp\Bigg[- \sum_{\substack{\alpha'\beta' \\ \alpha'\geq\beta'}} \Bigg(\frac{\mathcal{N}h^2_{\alpha'\beta'}}{2g_1^2}(1-\delta_{\alpha'\beta'}) - \frac{\mathcal{N}h^2_{\alpha'\alpha'}}{2g_2^2}\delta_{\alpha'\beta'}$$
$$- i \sum_{\substack{\mu'\nu' \\ \mu'>\nu'}} \lambda_{\mu'\nu'} \Bigg(\Big(c_{\mu'}(\alpha')h_{\alpha'\beta'}c_{\nu'}(\beta') + c_{\mu'}(\beta')h_{\alpha'\beta'}c_{\nu'}(\alpha') \Big)(1-\delta_{\alpha'\beta'}) + c_{\mu'}(\alpha)h_{\alpha'\alpha'}c_{\nu'}(\alpha)\delta_{\alpha'\beta'} \Bigg) \Bigg)$$
$$- i \sum_{\substack{\mu'\nu' \\ \mu'>\nu'}} \lambda_{\mu'\nu'} \sum_{\alpha'} c_{\mu'}(\alpha')f_{\alpha'}c_{\nu'}(\alpha') \Bigg] \Bigg(\prod_{\substack{\alpha\beta \\ \alpha\geq\beta}} dh_{\alpha\beta} \Bigg) \Bigg(\prod_{\substack{\mu\nu \\ \mu>\nu}} d\lambda_{\mu\nu} \Bigg). \tag{A.2}$$

The Gaussian integrals over $h_{\alpha\beta}$ may then be performed, giving

$$P(c) = A'\delta(cc^T - I)\int \exp\Bigg[- \sum_{\substack{\alpha'\beta' \\ \alpha'\geq\beta'}} \Bigg(\frac{g_1^2}{2\mathcal{N}} \Bigg(\sum_{\substack{\mu'\nu' \\ \mu'>\nu'}} \lambda_{\mu'\nu'} \Big(c_{\mu'}(\alpha')c_{\nu'}(\beta') + c_{\mu'}(\beta')c_{\nu'}(\alpha') \Big) \Bigg)^2 (1-\delta_{\alpha'\beta'})$$
$$- \frac{g_2^2}{2\mathcal{N}} \Bigg(\sum_{\substack{\mu'\nu' \\ \mu'>\nu'}} \lambda_{\mu'\nu'}c_{\mu'}(\alpha')c_{\nu'}(\beta') \Bigg)^2 \delta_{\alpha'\beta'} \Bigg) - i \sum_{\substack{\mu'\nu' \\ \mu'>\nu'}} \lambda_{\mu'\nu'} \sum_{\alpha} c_{\mu'}(\alpha)f_{\alpha}c_{\nu'}(\alpha) \Bigg] \prod_{\substack{\mu\nu \\ \mu>\nu}} d\lambda_{\mu\nu}, \tag{A.3}$$

where we have absorbed any constant prefactors into the new constant A'. Now, the above equation may be transformed into a Gaussian integral by noting the following expansion of the first term in the exponent,

$$\sum_{\substack{\alpha'\beta' \\ \alpha'\geq\beta'}} \sum_{\substack{\mu'\nu' \\ \mu'>\nu'}} \sum_{\substack{\mu\nu \\ \mu>\nu}} \lambda_{\mu\nu}\lambda_{\mu'\nu'} \Big(c_\mu(\alpha')c_\nu(\beta') + c_\mu(\beta')c_\nu(\alpha') \Big) \Big(c_{\mu'}(\alpha')c_{\nu'}(\beta') + c_{\mu'}(\beta')c_{\nu'}(\alpha') \Big)(1-\delta_{\alpha'\beta'})$$
$$= \frac{1}{2} \sum_{\substack{\mu'\nu' \\ \mu'>\nu'}} \sum_{\substack{\mu\nu \\ \mu>\nu}} \lambda_{\mu\nu}\lambda_{\mu'\nu'} \sum_{\alpha'\beta'} \Big(c_\mu(\alpha')c_\nu(\beta')c_{\mu'}(\alpha')c_{\nu'}(\beta') + c_\mu(\beta')c_\nu(\alpha')c_{\mu'}(\alpha')c_{\nu'}(\beta') +$$
$$c_\mu(\alpha')c_\nu(\beta')c_{\mu'}(\beta')c_{\nu'}(\alpha') + c_\mu(\beta')c_\nu(\alpha')c_{\mu'}(\beta')c_{\nu'}(\alpha') \Big)$$
$$- 2 \sum_{\substack{\mu'\nu' \\ \mu'>\nu'}} \sum_{\substack{\mu\nu \\ \mu>\nu}} \lambda_{\mu\nu}\lambda_{\mu'\nu'} \sum_{\alpha'} c_\mu(\alpha')c_\nu(\alpha')c_{\mu'}(\alpha')c_{\nu'}(\alpha')$$
$$= \sum_{\substack{\mu'\nu' \\ \mu'>\nu'}} \sum_{\substack{\mu\nu \\ \mu>\nu}} \lambda_{\mu\nu}\lambda_{\mu'\nu'} \Big(\delta_{\mu\mu'}\delta_{\nu\nu'} + \delta_{\nu\mu'}\delta_{\mu\nu'} \Big)$$
$$- 2 \sum_{\substack{\mu'\nu' \\ \mu'>\nu'}} \sum_{\substack{\mu\nu \\ \mu>\nu}} \lambda_{\mu\nu}\lambda_{\mu'\nu'} \sum_{\alpha'} c_\mu(\alpha')c_\nu(\alpha')c_{\mu'}(\alpha')c_{\nu'}(\alpha')$$
$$= \sum_{\substack{\mu\nu \\ \mu>\nu}} \lambda_{\mu\nu}^2 - 2 \sum_{\substack{\mu'\nu' \\ \mu'>\nu'}} \sum_{\substack{\mu\nu \\ \mu>\nu}} \lambda_{\mu\nu}\lambda_{\mu'\nu'} \sum_{\alpha'} c_\mu(\alpha')c_\nu(\alpha')c_{\mu'}(\alpha')c_{\nu'}(\alpha'). \tag{A.4}$$

Where in the last step we have used that $\lambda_{\mu\nu} = \lambda_{\nu\mu}$. Now, we have, assuming $g_2 = \sqrt{2}g_1 = \sqrt{2}g$, such that the random matrix perturbation is selected from the GOE,

$$\begin{aligned} P(c) = A'\delta(cc^T - I) \int \exp\Bigg[& -\frac{g_1^2}{2\mathcal{N}} \sum_{\substack{\mu'\nu' \\ \mu'>\nu'}} \lambda_{\mu'\nu'}^2 \\ & + 2\frac{g_1^2}{2\mathcal{N}} \sum_{\substack{\mu'\nu' \\ \mu'>\nu'}} \sum_{\substack{\mu\nu \\ \mu>\nu}} \lambda_{\mu\nu}\lambda_{\mu'\nu'} \sum_{\alpha'} c_\mu(\alpha')c_\nu(\alpha')c_{\mu'}(\alpha')c_{\nu'}(\alpha') \\ & - \frac{g_2^2}{2\mathcal{N}} \sum_{\substack{\mu'\nu' \\ \mu'>\nu'}} \sum_{\substack{\mu\nu \\ \mu>\nu}} \lambda_{\mu\nu}\lambda_{\mu'\nu'} \sum_{\alpha'} c_\mu(\alpha')c_\nu(\alpha')c_{\mu'}(\alpha')c_{\nu'}(\alpha') \\ & - i \sum_{\substack{\mu'\nu' \\ \mu'>\nu'}} \lambda_{\mu'\nu'} \sum_{\alpha} c_{\mu'}(\alpha) f_\alpha c_{\nu'}(\alpha) \Bigg] \prod_{\substack{\mu\nu \\ \mu>\nu}} d\lambda_{\mu\nu} \\ = A'\delta(cc^T - I) \prod_{\substack{\mu\nu \\ \mu>\nu}} \int \exp\Bigg[& -\frac{g^2}{2\mathcal{N}}\lambda_{\mu\nu}^2 - i\lambda_{\mu\nu} \sum_\alpha c_\mu(\alpha) f_\alpha c_\nu(\alpha) \Bigg] d\lambda_{\mu\nu}. \end{aligned} \tag{A.5}$$

Carrying out the second Gaussian integral over $\lambda_{\mu\nu}$ we have,

$$P(c) = A''\delta(cc^T - I) \exp\Bigg[- \sum_{\substack{\mu\nu \\ \mu>\nu}} \frac{\mathcal{N}\big(\sum_\alpha c_\mu(\alpha) f_\alpha c_\nu(\alpha)\big)^2}{2g^2} \Bigg]. \tag{A.6}$$

We note here that this leaves us with the same integral as would be obtained if we had enforced orthogonality of only two eigenvectors at a time, as in reference [65], up to a factor of two. Now, we observe

$$\begin{aligned} -\sum_{\substack{\mu\nu \\ \mu>\nu}} (\sum_\alpha c_\mu(\alpha) f_\alpha c_\nu(\alpha))^2 &= -\frac{1}{2} \sum_{\substack{\mu\nu \\ \mu\neq\nu}} (\sum_\alpha c_\mu(\alpha) f_\alpha c_\nu(\alpha))^2 \\ &= -\frac{1}{2} \sum_{\mu\nu} (\sum_\alpha c_\mu(\alpha) f_\alpha c_\nu(\alpha))^2 + \frac{1}{2} \sum_\mu (\sum_\alpha f_\alpha c_\mu^2(\alpha))^2 \\ &= -\frac{1}{2} \sum_\alpha f_\alpha^2 + \frac{1}{2} \sum_\mu (\sum_\alpha f_\alpha c_\mu^2(\alpha))^2, \end{aligned} \tag{A.7}$$

as $\sum_\alpha c_\mu(\alpha)c_\nu(\alpha) = \delta_{\mu\nu}$. We then have,

$$P(c) = A''\delta(cc^T - I) \exp\Bigg[- \frac{\mathcal{N}\sum_\alpha f_\alpha^2}{4g^2} + \sum_\mu \frac{\mathcal{N}\big(\sum_\alpha f_\alpha c_\mu^2(\alpha)\big)^2}{4g^2} \Bigg]. \tag{A.8}$$

Thus, we finally obtain

$$P(c) = \frac{1}{Z_P} \Bigg(\prod_{\mu\nu} \delta(\sum_\alpha c_\mu(\alpha)c_\nu(\alpha)) \Bigg) \Bigg(\prod_\mu \delta(\sum_\alpha c_\mu^2(\alpha) - 1) \Bigg) \exp\Bigg[\frac{\mathcal{N}}{4g^2} \sum_\mu (\sum_\alpha f_\alpha c_\mu^2(\alpha))^2 \Bigg], \tag{A.9}$$

where we have absorbed the constant terms into a new constant $1/Z_P$, and written explicitly the full form of the delta-function $\delta(cc^T - I)$. One can see by Gibbs' inequality, $p(c,\Lambda)\ln\frac{P(c)}{p(c,\Lambda)} \leq 0$, that we can obtain the best possible approximation $p(c,\Lambda)$ by obtaining the functional form of Λ that fulfils

$$\frac{\partial F}{\partial \Lambda} = 0, \tag{A.10}$$

as well as any constraints on Λ we may require. This is the problem solved in reference [65], though using a different target distribution $p(c,\Lambda)$. The Free energy integral of Eq. (5.22) can be split into two parts, which we heuristically label the 'energy', E, and 'entropy', S, with $F = E - S$, we have

$$E = -\int p(c,\Lambda)\ln\frac{\left(\prod_\mu \delta(\sum_\alpha c_\mu^2(\alpha)-1)\right)\exp\left[\frac{\mathcal{N}}{4g^2}\sum_\mu(\sum_\alpha f_\alpha c_\mu^2(\alpha))^2\right]}{Z_P}dc \tag{A.11}$$

and

$$S = -\int p(c,\Lambda)\ln\frac{\exp\left[-\sum_{\mu\alpha}\frac{c_\mu^2(\alpha)}{2\Lambda(\mu,\alpha)}\right]}{Z_p}dc. \tag{A.12}$$

Note that the orthogonality condition delta-functions in $P(c)$ and $p(c,\Lambda)$ cancel in Eq. (5.22) to obtain the above expressions for S and E. To calculate the Free Energy we need to evaluate the partition function Z_p, which is given by

$$Z_p = \int\int \exp\left[-\sum_{\mu\alpha}\frac{c_\mu^2(\alpha)}{2\Lambda(\mu,\alpha)} - i\sum_{\substack{\mu\nu\\ \mu>\nu}}\lambda_{\mu\nu}\sum_\alpha c_\mu(\alpha)c_\nu(\alpha)\right]\left(\prod_{\mu,\alpha}dc_\mu(\alpha)\right)\left(\prod_{\substack{\mu\nu\\ \mu>\nu}}d\lambda_{\mu\nu}\right), \tag{A.13}$$

where we have written the delta-function as a Fourier integral. The condition $\mu > \nu$ is required such that pairwise interactions are not doubly counted. From the second equality, one may recognise that this integral may be seen as an average over a Gaussian distribution of $c_\mu(\alpha)$s, thus we write

$$Z_p = \int Z_G\left\langle \exp\left[-i\sum_{\substack{\mu\nu\\ \mu>\nu}}\lambda_{\mu\nu}\sum_\alpha c_\mu(\alpha)c_\nu(\alpha)\right]\right\rangle_G \prod_{\substack{\mu\nu\\ \mu>\nu}}d\lambda_{\mu\nu}, \tag{A.14}$$

where we have defined

$$\langle A\rangle_G := \frac{1}{Z_G}\int A\exp\left[-\sum_{\mu\alpha}\frac{c_\mu^2(\alpha)}{2\Lambda(\mu,\alpha)}\right]\prod_{\mu\alpha}dc_\mu(\alpha), \tag{A.15}$$

with

$$Z_G := \int \exp\left[-\sum_{\mu\alpha}\frac{c_\mu^2(\alpha)}{2\Lambda(\mu,\alpha)}\right]\prod_{\mu\alpha}dc_\mu(\alpha) = \prod_{\mu\alpha}(2\pi\Lambda(\mu,\alpha))^{\frac{1}{2}}. \tag{A.16}$$

Expanding the exponent, we may write

$$Z_p = \int Z_G \left\langle \sum_{n=0}^{\infty} \frac{(-i)^n}{n!} \Big(\sum_{\substack{\mu\nu \\ \mu>\nu}} \lambda_{\mu\nu} O_{\mu\nu} \Big)^n \right\rangle_G \prod_{\substack{\mu\nu \\ \mu>\nu}} d\lambda_{\mu\nu}, \tag{A.17}$$

where $O_{\mu\nu} := \sum_\alpha c_\mu(\alpha) c_\nu(\alpha)$. From this, we can see each term in the power series of Eq. (A.17) scales as the average of increasing powers of the operator O, summed over the eigenstates. As odd moments of O are identically zero we are immediately left with only even terms. Furthermore, as the average is taken with a Gaussian distribution of $c_\mu(\alpha)$s, the only non-zero terms in the average occur when labels are equal in pairs. For example, for the first non-zero term ($n = 2$) we have

$$\langle O_{\mu\nu} O_{\mu'\nu'} \rangle_G = \langle \sum_{\alpha\alpha'} c_\mu(\alpha) c_\nu(\alpha) c_{\mu'}(\alpha') c_{\nu'}(\alpha') \rangle_G \approx \langle \sum_\alpha c_\mu(\alpha)^2 c_\nu(\alpha)^2 \rangle_G, \tag{A.18}$$

so

$$\begin{aligned} \sum_{\substack{\mu'\nu' \\ \mu'>\nu'}} \sum_{\substack{\mu\nu \\ \mu>\nu}} \lambda_{\mu\nu} \lambda_{\mu\prime\nu\prime} \langle O_{\mu\nu} O_{\mu\prime\nu\prime} \rangle_G &= \sum_{\substack{\mu'\nu' \\ \mu'>\nu'}} \sum_{\substack{\mu\nu \\ \mu>\nu}} \lambda_{\mu\nu} \lambda_{\mu'\nu'} \langle \sum_{\alpha\alpha'} c_\mu(\alpha) c_\nu(\alpha) c_{\mu'}(\alpha') c_{\nu'}(\alpha') \rangle_G \\ &= \sum_{\substack{\mu\nu \\ \mu>\nu}} \lambda_{\mu\nu}^2 \langle \sum_\alpha c_\mu(\alpha)^2 c_\nu(\alpha)^2 \rangle_G. \end{aligned} \tag{A.19}$$

We then obtain

$$\begin{aligned} \langle \sum_\alpha c_\mu^2(\alpha) c_\nu^2(\alpha) \rangle_G &= \frac{1}{Z_G} \int \sum_\alpha c_\mu^2(\alpha) c_\nu^2(\alpha) \exp\Big[- \sum_{\mu\alpha} \frac{c_\mu^2(\alpha)}{2\Lambda(\mu,\alpha)} \Big] \prod_{\mu\alpha} dc_\mu(\alpha) \\ &= \sum_\alpha \Lambda(\mu,\alpha) \Lambda(\nu,\alpha). \end{aligned} \tag{A.20}$$

To calculate the full average in Eq. (A.17), we need to calculate the average of all the even powers,

$$\langle (\sum_{\substack{\mu\nu \\ \mu>\nu}} O_{\mu,\nu})^{2n} \rangle_G = \sum_{\substack{\mu_1\nu_1 \\ \mu_1>\nu_1}} \sum_{\substack{\mu_2\nu_2 \\ \mu_2>\nu_2}} \cdots \sum_{\substack{\mu_{2n}\nu_{2n} \\ \mu_{2n}>\nu 2n}} \langle O_{\mu_1\nu_1} O_{\mu_2\nu_2} \ldots O_{\mu_{2n}\nu_{2n}} \rangle. \tag{A.21}$$

In the limit of large participation ratios, $\Gamma/\omega_0 \gg 1$, the dominant contribution comes from contractions between pairs, O_{μ_i,ν_i} and O_{μ_j,ν_j}, such that,

$$\sum_{\substack{\mu_1\nu_1 \\ \mu_1>\nu_1}} \sum_{\substack{\mu_2\nu_2 \\ \mu_2>\nu_2}} \cdots \sum_{\substack{\mu_{2n}\nu_{2n} \\ \mu_{2n}>\nu_{2n}}} \langle O_{\mu_1\nu_1} O_{\mu_2\nu_2} \ldots O_{\mu_{2n}\nu_{2n}} \rangle \approx (2n-1)!! \Big(\sum_{\substack{\mu\nu \\ \mu>\nu}} \lambda_{\mu\nu}^2 \sum_\alpha \Lambda(\mu,\alpha) \Lambda(\nu,\alpha) \Big)^n, \tag{A.22}$$

where the factor $(2n-1)!! := 1 \cdot 3 \cdot 5 \cdots (2n-1)$, arises after the counting of all possible combinations of pairs. In this approximation we are neglecting those terms where indices are not contracted by pairs, however, those terms have at least one less summation over one of the indices α_j, and thus they are supressed by a factor $(\Gamma/\omega_0)^{-1}$. We may thus

re-express the average in (A.14) as

$$\left\langle \sum_{n=0}^{\infty} \frac{(-i)^n}{n!} (\sum_{\substack{\mu\nu \\ \mu>\nu}} \lambda_{\mu\nu} O_{\mu\nu})^n \right\rangle_G \approx \sum_{n=0}^{\infty} \frac{(-i)^{2n}}{(2n)!} (2n-1)!! \Big(\sum_{\substack{\mu\nu \\ \mu>\nu}} \lambda_{\mu\nu}^2 \sum_{\alpha} \Lambda(\mu,\alpha)\Lambda(\nu,\alpha) \Big)^n. \tag{A.23}$$

Now, as $(2n-1)!! = \frac{(2n)!}{2^n n!}$ and $(-i)^{2n} = (-1)^n$, we can finally write

$$\begin{aligned} Z_p &= Z_G \int \exp\left[-\frac{1}{2} \sum_{\substack{\mu\nu \\ \mu>\nu}} \lambda_{\mu\nu}^2 \sum_{\alpha} \Lambda(\mu,\alpha)\Lambda(\nu,\alpha) \right] \prod_{\substack{\mu\nu \\ \mu>\nu}} d\lambda_{\mu\nu} \\ &= (2\pi)^{\mathcal{N}^2 - \mathcal{N}/2} \left(\prod_{\mu\alpha} (\Lambda(\mu,\alpha))^{\frac{1}{2}} \right) \left(\prod_{\substack{\mu\nu \\ \mu>\nu}} \Big(\sum_{\alpha} \Lambda(\mu,\alpha)\Lambda(\nu,\alpha) \Big)^{-\frac{1}{2}} \right). \end{aligned} \tag{A.24}$$

Now, the entropy, Eq. (A.12) may be easily evaluated to obtain (noting once more that the integral is understood by $\int dc \to \prod_{\mu\alpha} \int dc_\mu(\alpha)$)

$$S = \sum_{\mu\alpha} \Lambda(\mu,\alpha) \frac{\partial Z_p}{\partial \Lambda(\mu,\alpha)} + \ln Z_p. \tag{A.25}$$

Using the partition function found in Eq. (A.24), and ignoring any constant terms, which do not contribute to the final form of $\Lambda(\mu,\alpha)$, we write,

$$\ln(Z_p) = \frac{1}{2} \sum_{\mu\alpha} \ln(\Lambda(\mu,\alpha)) - \frac{1}{4} \sum_{\mu\nu} \ln(\sum_{\alpha} \Lambda(\mu,\alpha)\Lambda(\nu,\alpha)) \tag{A.26}$$

so

$$\begin{aligned} S = -\sum_{\mu\alpha} \frac{\Lambda(\mu,\alpha)}{2} \sum_{\mu' \neq \mu} \frac{\Lambda(\mu',\alpha)}{\sum_{\alpha'} \Lambda(\mu,\alpha')\Lambda(\mu',\alpha')} \\ + \frac{1}{2} \sum_{\mu\alpha} \ln(\Lambda(\mu,\alpha)) - \frac{1}{4} \sum_{\mu\nu} \ln(\sum_{\alpha} \Lambda(\mu,\alpha)\Lambda(\nu,\alpha)). \end{aligned} \tag{A.27}$$

Now, we can see that the first term is also constant, as the sum over α cancels that over α', thus this term does not contribute, and we obtain

$$S = \frac{1}{2} \sum_{\mu\alpha} \ln \Lambda(\mu,\alpha) - \frac{1}{4} \sum_{\mu\nu} \ln \sum_{\alpha} \Lambda(\mu,\alpha)\Lambda(\nu,\alpha). \tag{A.28}$$

We note that in ref [65] the first term is here labelled entropy, and the second term is labelled a repulsion energy. The final calculation required for evaluation of the free energy is the energy part, Eq. (A.11). As Z_P does not depend on $\Lambda(\mu,\alpha)$, we can ignore this part (as we require F only for it's derivative with respect to $\Lambda(\mu,\alpha)$). We can also re-write the delta-function factor as $\prod_\mu \delta(\sum_\alpha c_\mu^2(\alpha) - 1) \to \lim_{\mathcal{U}\to\infty} \exp\left[\mathcal{U} \sum_\mu (\sum_\alpha c_\mu^2(\alpha) - 1)^2\right]$, and

thus we are left with

$$E = -\frac{1}{Z_p}\int\int \exp\Big[-\sum_{\mu\alpha}\frac{c_\mu^2(\alpha)}{2\Lambda(\mu,\alpha)} - i\sum_{\substack{\mu\nu\\ \mu>\nu}}\lambda_{\mu\nu}\sum_{\alpha}c_\mu(\alpha)c_\nu(\alpha)\Big]$$
$$\times\Big[\lim_{\mathcal{U}\to\infty}\mathcal{U}\sum_{\mu}(\sum_{\alpha}c_\mu^2(\alpha)-1)^2 + \frac{\mathcal{N}}{4g^2}\sum_{\mu}(\sum_{\alpha}f_\alpha c_\mu^2(\alpha))^2\Big]\left(\prod_{\mu\alpha}dc_\mu(\alpha)\right)\left(\prod_{\substack{\mu\nu\\ \mu>\nu}}d\lambda_{\mu\nu}\right) \tag{A.29}$$

We can see that the first term here ensures normalization of the $c_\mu(\alpha)$s, and is zero provided this condition is met. The second term, similarly to the partition function, may be re-expressed as the Gaussian average

$$E = -\frac{1}{Z_p}\int Z_G\Big\langle\frac{\mathcal{N}}{4g^2}\sum_{\mu'}(\sum_{\alpha'}f_{\alpha'}c_{\mu'}^2(\alpha'))^2\sum_{n=0}^{\infty}\frac{(-i)^n}{n!}(\sum_{\substack{\mu\nu\\ \mu>\nu}}\lambda_{\mu\nu}O_{\mu\nu})^n\Big\rangle_G\prod_{\substack{\mu\nu\\ \mu>\nu}}d\lambda_{\mu\nu}. \tag{A.30}$$

Now, as with the partition function this cannot be calculated exactly, but we can use the fact that the average is taken over a Gaussian distribution of $c_\mu(\alpha)$s to find the dominant part. This is most clearly seen by writing the average in the form

$$\Big\langle\frac{\mathcal{N}}{4g^2}\sum_{\mu'}(\sum_{\alpha'\alpha''}f_{\alpha'}f_{\alpha''}c_{\mu'}^2(\alpha')c_{\mu'}^2(\alpha''))\sum_{n=0}^{\infty}\frac{(-i)^n}{n!}(\sum_{\substack{\mu\nu\\ \mu>\nu}}\lambda_{\mu\nu}\sum_{\alpha}c_\mu(\alpha)c_\nu(\alpha))^n\Big\rangle_G. \tag{A.31}$$

The key observation here is that as the only non-zero terms in Eq. (A.31) are those with even powers of $c_\mu(\alpha)$ any terms that have correlations between the 'bias' factor $H_b = \frac{\mathcal{N}}{4g^2}\sum_\mu(\sum_\alpha f_\alpha c_\mu^2(\alpha))^2$ from the Hamiltonian and the orthogonality factor are either excluded by the fact that $\mu\neq\nu$ or reduced by the need for $\alpha=\alpha',\alpha''$. Thus the dominant cause of correlations, leading to non-zero terms in the average, are from correlations *within* each factor, and not between. This leads to the approximation, which is equivalent to that made in the partition function evaluation above,

$$\begin{aligned}E &\approx \frac{1}{Z_p}\int Z_G\Big\langle\frac{\mathcal{N}}{4g^2}\sum_{\mu'}(\sum_{\alpha'}f_{\alpha'}c_{\mu'}^2(\alpha'))^2\exp\Big[-\frac{1}{2}\sum_{\substack{\mu\nu\\ \mu>\nu}}\lambda_{\mu\nu}^2\sum_{\alpha}\Lambda(\mu,\alpha)\Lambda(\nu,\alpha)\Big]\Big\rangle_G\prod_{\substack{\mu\nu\\ \mu>\nu}}d\lambda_{\mu\nu}\\ &= -\Big\langle\frac{\mathcal{N}}{4g^2}\sum_{\mu}(\sum_{\alpha}f_\alpha c_\mu^2(\alpha))^2\Big\rangle_G\\ &:= -\langle H_b\rangle_G.\end{aligned} \tag{A.32}$$

Explicitly, we have

$$\begin{aligned} E &= -\frac{1}{Z_G}\int \frac{\mathcal{N}}{4g^2}\sum_\mu (\sum_\alpha f_\alpha c_\mu^2(\alpha))^2 \exp\Big[-\sum_{\mu\alpha}\frac{c_\mu^2(\alpha)}{2\Lambda(\mu,\alpha)}\Big]\prod_{\mu\alpha} dc_\mu(\alpha) \\ &= -\left\langle \frac{\mathcal{N}}{4g^2}\sum_\mu (\sum_\alpha f_\alpha c_\mu^2(\alpha))^2 \right\rangle_G \\ &= -\frac{\mathcal{N}}{4g^2}\sum_\mu (\sum_\alpha f_\alpha \Lambda(\mu,\alpha))^2, \end{aligned} \tag{A.33}$$

as $\langle c_\mu^2(\alpha)\rangle_G = \Lambda(\mu,\alpha)$ and $\langle c_\mu^4(\alpha)\rangle_G = \Lambda(\mu,\alpha)^2$. We are now able to write the full functional form of the Free Energy from $F = E - S$,

$$F = -\frac{\mathcal{N}}{4g^2}\sum_\mu (\sum_\alpha f_\alpha \Lambda(\mu,\alpha))^2 + \frac{1}{4}\sum_{\mu\nu}\ln\sum_\alpha \Lambda(\mu,\alpha)\Lambda(\nu,\alpha) - \frac{1}{2}\sum_{\mu\alpha}\ln\Lambda(\mu,\alpha). \tag{A.34}$$

Now, we wish to find the function $\Lambda(\mu,\alpha)$ that minimises Eq. (A.34) under the conditions $\sum_\alpha \Lambda(\mu,\alpha) = \sum_\mu \Lambda(\mu,\alpha) = 1$. We thus introduce the corresponding Lagrange multipliers into Eq. (A.34), and find the derivative with respect to $\Lambda(\mu',\alpha')$. We thus wish to find the functional form for $\Lambda(\mu,\alpha)$ satisfying

$$\frac{\partial F}{\partial \Lambda(\mu',\alpha')} + \eta_{\mu'} + \eta_{\alpha'} = 0, \tag{A.35}$$

where we have introduced the Lagrange coefficients $\eta_{\mu(\alpha)}$ of their respective multipliers $\eta_{\mu(\alpha)}(\sum_{\mu(\alpha)}\Lambda(\mu,\alpha) - 1)$. Now, we have

$$\frac{\partial F}{\partial \Lambda(\mu',\alpha')} = -\frac{\mathcal{N}}{2g^2}f'_\alpha \sum_\alpha f_\alpha \Lambda(\mu',\alpha) + \frac{1}{2}\sum_\nu \frac{\Lambda(\nu,\alpha')}{\sum_\alpha \Lambda(\mu',\alpha)\Lambda(\nu,\alpha)} - \frac{1}{2}\frac{1}{\Lambda(\mu',\alpha')}, \tag{A.36}$$

which we may simplify given that due to the normalization condition we have 'incompressibility'[65] of bulk eigenstates, and thus

$$\Lambda(\mu,\alpha) = \Lambda(\mu-\alpha), \tag{A.37}$$

and

$$\sum_\alpha \alpha\Lambda(\mu,\alpha) = \sum_\alpha \alpha\Lambda(\mu-\alpha) = \mu, \tag{A.38}$$

after a suitable change of variables. Thus we have

$$\frac{\partial F}{\partial \Lambda(\mu',\alpha')} = -\frac{\mathcal{N}\omega_0^2\alpha'\mu'}{2g^2} + \frac{1}{2}\sum_\nu \frac{\Lambda(\nu,\alpha')}{\sum_\alpha \Lambda(\mu',\alpha)\Lambda(\nu,\alpha)} - \frac{1}{2}\frac{1}{\Lambda(\mu',\alpha')}. \tag{A.39}$$

Now, we make the ansatz

$$\Lambda(\mu,\alpha) = \frac{\omega_0\Gamma/\pi}{(E_\mu - E_\alpha)^2 + \Gamma^2}. \tag{A.40}$$

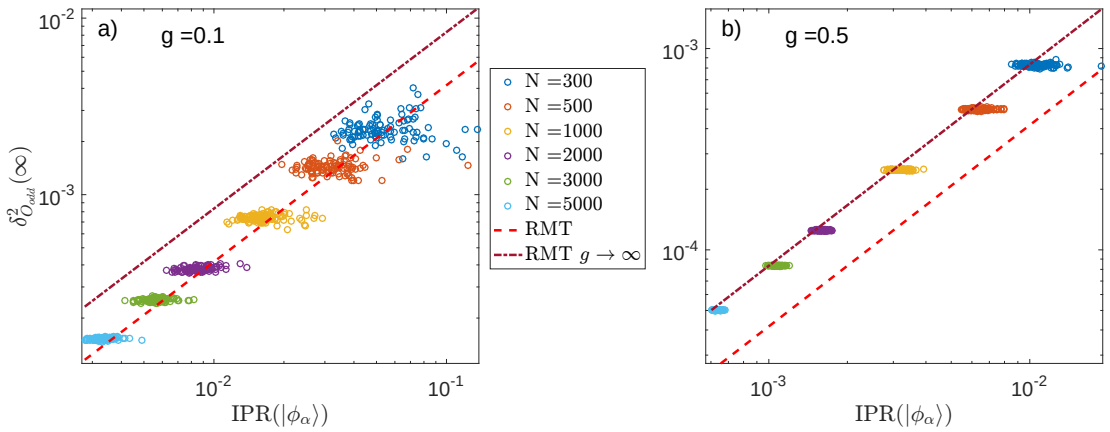

Figure A.1: $\delta^2_{O_{\text{odd}}}$ versus IPR($|\phi_\alpha\rangle$) for the central 100 values of α in the spectrum for a single realisation (no averaging) of the random matrix system. a) Shows $g = 0.1$ b) Shows $g = 0.5$. Analytic result from RMT, Eq. (5.74) shown by red dashed line, $g \to \infty$ limit of RMT result, Eq. (A.46), shown by dash-dotted burgundy line.

Taking the continuum limit and noting that

$$\int \frac{dE_\alpha}{\omega_0} \Lambda(\mu,\alpha)\Lambda(\nu,\alpha) = \frac{2\omega_0\Gamma/\pi}{(E_\mu - E_\nu)^2 + 4\Gamma^2} \tag{A.41}$$

we thus obtain

$$-\frac{\mathcal{N}\omega_0^2\alpha'\mu'}{2g^2} + \frac{\omega_0\pi}{4\Gamma}\mu'^2 + \frac{\omega_0\pi}{2\Gamma}\mu'\alpha' + \frac{\omega_0\pi}{2\Gamma}(\mu'^2 + \alpha'^2) + \eta_{\mu'} + \eta_{\alpha'} = 0, \tag{A.42}$$

where we have absorbed all constant terms into the Lagrange multipliers $\eta_{\mu'}$ and $\eta_{\alpha'}$. We now note that terms in α' may be absorbed into the Lagrange multiplier $\eta_{\mu'}$ and vice versa, thus we can readily observe that the condition Eq (A.42) is fulfilled for $\Gamma = \frac{\pi g^2}{\mathcal{N}\omega_0}$.

A.2 Scaling of Fluctuations for Random Matrix Hamiltonian

If we analyze the $g \to \infty$ limit of our random matrix system, where we have simply a real Hermitian random matrix as our Hamiltonian. In this limit we thus expect to see $\Lambda(\mu,\alpha) = 1/\mathcal{N}$. This can be easily seen to minimise our free energy, Eq. (A.34), in the $g \to \infty$ limit. Repeating, then, the analysis above, we find in this limit

$$\langle c_\mu(\alpha)c_\nu(\alpha)c_\mu(\beta)c_\nu(\beta)\rangle_V = \frac{1}{\mathcal{N}^2}\delta_{\alpha\beta} - \frac{1}{\mathcal{N}^3}(1+\delta_{\alpha\beta}), \tag{A.43}$$

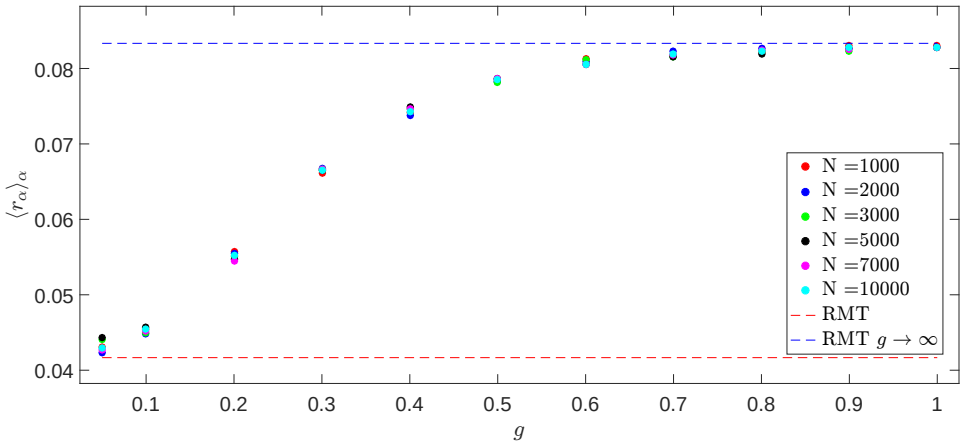

Figure A.2: Plot of $\langle r_\alpha \rangle_\alpha$ (see Eq. (5.75)) as coupling g is increased for random matrix Hamiltonian of Eq. (5.17). Average $\langle \cdots \rangle_\alpha$ taken over central 201 elements.

from which we obtain

$$\begin{aligned} |O_{\mu\nu}|^2_{\mu\neq\nu} &= \sum_{\alpha\beta} \left(\frac{1}{\mathcal{N}^2}\delta_{\alpha\beta} - \frac{1}{\mathcal{N}^3}(1+\delta_{\alpha\beta}) \right) O_{\alpha\alpha}O_{\beta\beta} \\ &\approx \overline{[O^2_{\alpha\alpha}]_{\overline{\mu}}} \sum_{\alpha} \left(\frac{1}{\mathcal{N}^2} - \frac{1}{\mathcal{N}^3} \right) - \overline{[O_{\alpha\alpha}]_{\overline{\mu}}}^2 \sum_{\alpha\beta} \frac{1}{\mathcal{N}^3} \\ &\approx \frac{\overline{[\Delta O^2_{\alpha\alpha}]_{\overline{\mu}}}}{\mathcal{N}}. \end{aligned} \tag{A.44}$$

Now, the infinite time fluctuations may now be obtained via Eq. (5.71), from which we find

$$\delta^2_O(\infty) = \sum_{\mu\nu} \frac{1}{\mathcal{N}^2} \frac{\overline{[\Delta O^2_{\alpha\alpha}]_{\overline{\mu}}}}{\mathcal{N}} \approx \frac{\overline{[\Delta O^2_{\alpha\alpha}]_{\overline{\mu}}}}{\mathcal{N}}. \tag{A.45}$$

The IPR may be easily seen to be equal to $3/\mathcal{N}$, where once again the factor of three originates in the relationship between the second and fourth moments of Gaussian distributed variables. From this we obtain

$$\delta^2_O(\infty) = \frac{1}{3}\overline{[\Delta O^2_{\alpha\alpha}]_{\overline{\mu}}} \mathrm{IPR}(|\phi_\alpha\rangle), \tag{A.46}$$

as the expected scaling of infinite time fluctuations for the $g \to \infty$ limit. Thus we can see from Fig. (A.2) that the factor of two emerges from our RMT model when the coupling is large.

Appendix B

Methods of Quantum Chaos

B.1 Diagonal and Off-Diagonal Partition Functions

In the main text a consistent theoretical model of chaotic wavefunctions has been developed in order to describe the thermalization of closed non-integrable quantum systems. These results have been based on correlation functions calculated from the generating function,

$$\begin{aligned} G^{(\mathrm{od})}_{\mu\nu}(\vec{\xi}_\mu,\vec{\xi}_\nu) &= \int\int \exp\Big[-\sum_\alpha\Big(\frac{c^2_\mu(\alpha)}{2\Lambda(\mu,\alpha)}+\frac{c^2_\nu(\alpha)}{2\Lambda(\nu,\alpha)}+\xi_{\mu,\alpha}c_\mu(\alpha)+\xi_{\nu,\alpha}c_\nu(\alpha)\Big)\Big] \\ &\qquad \times\delta(\sum_\alpha c_\mu(\alpha)c_\nu(\alpha))\prod_\alpha dc_\mu(\alpha)dc_\nu(\alpha) \\ &\propto \exp\Big[\frac{1}{2}\sum_\alpha \xi^2_{\mu,\alpha}\Lambda(\mu,\alpha)+\frac{1}{2}\sum_\alpha\xi^2_{\nu,\alpha}\Lambda(\nu,\alpha) \\ &\qquad -\frac{1}{2}\sum_{\alpha,\beta}\xi_{\mu,\alpha}\xi_{\mu,\beta}\xi_{\nu,\alpha}\xi_{\nu,\beta}\frac{\Lambda(\mu,\alpha)\Lambda(\mu,\beta)\Lambda(\nu,\alpha)\Lambda(\nu,\beta)}{\Lambda^{(2)}(\mu,\nu)}\Big], \end{aligned} \tag{B.1}$$

where in the second line we have re-expressed the δ-functions in their Fourier form. The superscript (od) indicates that this is the 'off-diagonal' generating function, requiring $\mu\neq\nu$. The diagonal case is discussed below. The correlation functions may then be calculated by performing successive derivatives with respect to the force terms ξ via

$$\langle c_\mu(\alpha)c_\nu(\beta)\cdots c_\mu(\alpha'_1)c_\nu(\beta'_1)\rangle_V = \frac{1}{G_{\mu\nu}}\partial_{\xi_{\mu,\alpha}}\partial_{\xi_{\nu,\beta}}\cdots\partial_{\xi_{\mu,\alpha'_1}}\partial_{\xi_{\nu,\beta'_1}}G_{\mu\nu}\Big|_{\xi_{\mu,\alpha}=0,\xi_{\nu,\alpha}=0}. \tag{B.2}$$

In particular, the correlation function $\langle c_\mu(\alpha_0)c_\nu(\beta_0)c_\mu(\alpha)c_\nu(\beta)\rangle_V$ was found in Chapter 5 [16] for $\mu\neq\nu$ to be equal to

$$\begin{aligned} \langle c_\mu(\alpha_0)c_\nu(\beta_0)c_\mu(\alpha)c_\nu(\beta)\rangle_V &= \Lambda(\mu,\alpha_0)\Lambda(\nu,\beta_0)\delta_{\alpha_0\alpha}\delta_{\beta_0\beta} \\ &\quad -\frac{\Lambda(\mu,\alpha_0)\Lambda(\nu,\alpha_0)\Lambda(\mu,\alpha)\Lambda(\nu,\alpha)\delta_{\alpha_0\beta_0}\delta_{\alpha\beta}}{\Lambda^{(2)}(\mu,\nu)} \\ &\quad -\frac{\Lambda(\mu,\alpha_0)\Lambda(\nu,\alpha_0)\Lambda(\mu,\beta_0)\Lambda(\nu,\beta_0)\delta_{\alpha_0\beta}\delta_{\beta_0\alpha}}{\Lambda^{(2)}(\mu,\nu)}, \end{aligned} \tag{B.3}$$

for $\mu \neq \nu$, with

$$\Lambda^{(2)}(\mu,\nu) := \sum_{\alpha} \Lambda(\mu,\alpha)\Lambda(\nu,\alpha). \tag{B.4}$$

The latter two terms in Eq. (B.3) arise as an explicit result of the orthogonality factor in Eq. (B.1). We comment further on the form of the correlation function (B.3) at the beginning of Appendix D.3.

We stress here that the generating function Eq. (B.1) explicitly requires $\mu \neq \nu$, as it models the interactions due to mutual orthogonality of two random wavefunctions. For the diagonal part, we have the much simpler generating function,

$$G^{(d)}_{\mu\mu} = \int \exp\left[-\sum_{\alpha} \frac{c^2_\mu(\alpha)}{2\Lambda(\mu,\alpha)}\right] \prod_{\alpha} dc_\mu(\alpha). \tag{B.5}$$

Thus, we have,

$$\begin{aligned} \langle c_\mu(\alpha)c_\mu(\beta)c_\mu(\alpha')c_\mu(\beta')\rangle_V &= \Lambda(\mu,\alpha)\Lambda(\mu,\alpha')\delta_{\alpha\beta}\delta_{\alpha'\beta'} \\ &\quad + \Lambda(\mu,\alpha)\Lambda(\mu,\beta)(\delta_{\alpha\alpha'}\delta_{\beta\beta'} + \delta_{\alpha\beta'}\delta_{\alpha'\beta}), \end{aligned} \tag{B.6}$$

for the diagonal case.

We note here that the generating functions above are general in the sense that they do not rely on any particular form of the distribution $\Lambda(\mu,\alpha)$. Indeed, for our model, with a homogeneous perturbation V, one can derive a Lorentzian form for the chaotic-wavefunctions Λ shown in Appendix A.1. More generally, however, the theory of chaotic wavefunctions may apply for various smooth functions Λ, which for example, is expected to be Gaussian for strongly coupled or homogeneous systems.

B.2 Full ETH from RMT

Here we calculate the diagonal, and off-diagonal matrix elements of observables from the above approach, using the sparsity and smoothness conditions outlined Section 6.3.4.

B.2.1 Diagonal ETH

We can see that the diagonal matrix elements are given by

$$\begin{aligned} \langle O_{\mu\mu}\rangle_V &= \sum_{\alpha\beta} \langle c_\mu(\alpha)c_\mu(\beta)\rangle_V O_{\alpha\beta} \\ &= \sum_{\alpha} \Lambda(\mu,\alpha) O_{\alpha\alpha} \\ &= \overline{[O_{\alpha\alpha}]}_\mu. \end{aligned} \tag{B.7}$$

One can observe that the fluctuations of the diagonal elements can also be analysed, considering the quantity

$$\begin{aligned}\langle O_{\mu\mu}^2\rangle_V &= \sum_{\alpha\beta\alpha'\beta'} \langle c_\mu(\alpha)c_\mu(\beta)c_\mu(\alpha')c_\mu(\beta')\rangle_V O_{\alpha\beta}O_{\alpha'\beta'} \\ &= \sum_{\alpha\beta\alpha'\beta'} \Big[\Lambda(\mu,\alpha)\Lambda(\mu,\alpha')\delta_{\alpha\beta}\delta_{\alpha'\beta'} + \Lambda(\mu,\alpha)\Lambda(\mu,\beta)(\delta_{\alpha\alpha'}\delta_{\beta\beta'} + \delta_{\alpha\beta'}\delta_{\alpha'\beta})\Big] O_{\alpha\beta}O_{\alpha'\beta'} \\ &= \sum_{\alpha\beta} \Lambda(\mu,\alpha)\Lambda(\mu,\beta)\left(O_{\alpha\alpha}O_{\beta\beta} + O_{\alpha\beta}^2 + O_{\alpha\beta}O_{\beta\alpha}\right).\end{aligned} \tag{B.8}$$

Now, we see that the first term in Eq. (B.8) is equal to $\langle O_{\mu\mu}\rangle_V^2$. For the second term, assuming the sparsity and smoothness conditions (see Section 6.3.4), we have

$$\begin{aligned}\sum_{\alpha n} \Lambda(\mu,\alpha)\Lambda(\mu,\alpha+n)O_{\alpha\alpha+n}^2 &\approx \sum_n \overline{[O_{\alpha\alpha+n}^2]}_\mu \Lambda^{(2)}(\mu,n) \\ &\leq \sum_n \overline{[O_{\alpha\alpha+n}^2]}_\mu \frac{\omega_0}{2\pi\Gamma},\end{aligned} \tag{B.9}$$

and similarly, following the same approach we observe that the third term in Eq. (B.8) is bounded by $\sum_n \overline{[O_{\alpha+n\alpha}O_{\alpha\alpha+n}]}_\mu \frac{\omega_0}{2\pi\Gamma}$. We thus observe that the fluctuations of the diagonal terms are small, in the sense that $\langle O_{\mu\mu}^2\rangle_V - \langle O_{\mu\mu}\rangle_V^2 \sim \mathcal{O}\left(\frac{\omega_0}{\Gamma}\right)$. Indeed, we can see that the smallness of the contributions of these terms is also necessary for the correct long-time average of observables Eq. (6.33), which itself can be written as, for an arbitrary initial state $|\psi(0)\rangle = \sum_{\alpha_0} \psi_{\alpha_0}|\phi_{\alpha_0}\rangle$,

$$\overline{\langle O(t)\rangle} = \sum_\mu \sum_{\alpha_0\beta_0\alpha\beta} \psi_{\alpha_0}\psi_{\beta_0}^* c_\mu(\alpha_0)c_\mu(\beta_0)c_\mu(\alpha)c_\mu(\beta)O_{\alpha\beta}. \tag{B.10}$$

Using Eq. (B.6), we have

$$\begin{aligned}\overline{\langle O(t)\rangle} = \sum_\mu \sum_{\alpha_0\beta_0\alpha\beta} \psi_{\alpha_0}\psi_{\beta_0}^* \Big[&\Lambda(\mu,\alpha_0)\Lambda(\mu,\alpha)\delta_{\alpha_0\beta_0}\delta_{\alpha_0\beta_0} \\ &+ \Lambda(\mu,\alpha_0)\Lambda(\mu,\beta_0)(\delta_{\alpha_0\alpha}\delta_{\beta_0\beta} + \delta_{\alpha_0\beta}\delta_{\alpha\beta_0})\Big] O_{\alpha\beta}.\end{aligned} \tag{B.11}$$

Now, we see that the latter two terms may be bounded by

$$\sum_{\alpha_0\beta_0} \psi_{\alpha_0}\psi_{\beta_0}\Lambda^{(2)}(\alpha_0,\beta_0)O_{\alpha_0\beta_0} \leq \langle O(0)\rangle \frac{\omega_0}{2\pi\Gamma}, \tag{B.12}$$

which may be seen using that $\sum_\mu \Lambda(\mu,\alpha_0)\Lambda(\mu,\beta_0) = \Lambda^{(2)}(\alpha_0,\beta_0) \leq \frac{\omega_0}{2\pi\Gamma}$, and $\langle O(0)\rangle = \sum_{\alpha_0\beta_0} \psi_{\alpha_0}\psi_{\beta_0}O_{\alpha_0\beta_0}$. We thus see that these contributions are negligible in comparison to

that of the first term:

$$\begin{aligned}\overline{\langle O(t)\rangle} &= \sum_{\mu}\sum_{\alpha\beta}\Lambda(\mu,\alpha)\Lambda(\mu,\beta)|\psi_\alpha|^2 O_{\beta\beta} \\ &= \sum_{\mu}\overline{[\psi_\alpha]}_\mu\overline{[O_{\alpha\alpha}]}_\mu \\ &\approx O_{mc},\end{aligned} \tag{B.13}$$

which we can see returns the microcanonical average as required. We thus see that a consistent description of the long-time observable expectation value may be obtained in terms of our RMT approach. Moreover, we observe here that the microcanonical average of matrix elements described by the smoothness assumption emerges naturally as this equilibrium value.

B.2.2 Off-diagonal ETH

In order to calculate the distribution of the off-diagonal observable elements, we use the squared value (as they average to zero), and thus we write

$$|O_{\mu\nu}|^2 = \sum_{\alpha\beta\alpha'\beta'} c_\mu(\alpha)c_\nu(\beta)c_\mu(\alpha')c_\nu(\beta')O_{\alpha\beta}O_{\alpha'\beta'}, \tag{B.14}$$

which, assuming self-averaging, and using Eq. (B.3), we have

$$\begin{aligned}|O_{\mu\nu}|^2_{\mu\neq\nu} = &\sum_{\alpha\beta}\Lambda(\mu,\alpha)\Lambda(\nu,\beta)O^2_{\alpha\beta} \\ &- \sum_{\alpha\alpha'}\frac{\Lambda(\mu,\alpha)\Lambda(\nu,\alpha)\Lambda(\mu,\alpha')\Lambda(\nu,\alpha')}{\Lambda^{(2)}(\mu,\nu)}O_{\alpha\alpha}O_{\alpha'\alpha'} \\ &- \sum_{\alpha\beta}\frac{\Lambda(\mu,\alpha)\Lambda(\nu,\alpha)\Lambda(\mu,\beta)\Lambda(\nu,\beta)}{\Lambda^{(2)}(\mu,\nu)}O_{\alpha\beta}O_{\beta\alpha}.\end{aligned} \tag{B.15}$$

We separate this into terms describing diagonal, $O_{\alpha\alpha}$, and non-diagonal, $O_{\alpha\beta}\,|\,\alpha\neq\beta$, contributions,

$$\begin{aligned}|O_{\mu\nu}|^2_{\mu\neq\nu} = &\sum_{\alpha}\Lambda(\mu,\alpha)\Lambda(\nu,\alpha)O^2_{\alpha\alpha} - \sum_{\alpha\alpha'}\frac{\Lambda(\mu,\alpha)\Lambda(\nu,\alpha)\Lambda(\mu,\alpha')\Lambda(\nu,\alpha')}{\Lambda^{(2)}(\mu,\nu)}O_{\alpha\alpha}O_{\alpha'\alpha'}(1+\delta_{\alpha\alpha'}) \\ &+ \sum_{\substack{\alpha\beta\\ \alpha\neq\beta}}\Lambda(\mu,\alpha)\Lambda(\nu,\beta)O^2_{\alpha\beta} - \sum_{\substack{\alpha\beta\\ \alpha\neq\beta}}\frac{\Lambda(\mu,\alpha)\Lambda(\nu,\alpha)\Lambda(\mu,\beta)\Lambda(\nu,\beta)}{\Lambda^{(2)}(\mu,\nu)}O_{\alpha\beta}O_{\beta\alpha},\end{aligned} \tag{B.16}$$

and, as above, using the microcanonical averaging of matrix elements afforded by the smoothness assumption, $\sum_\alpha\Lambda(\mu,\alpha)\Lambda(\nu,\alpha)O_{\alpha\alpha}\approx\overline{[O_{\alpha\alpha}]}_{\overline{\mu}}\Lambda^{(2)}(\mu,\nu)$, on the diagonal con-

tributions. We thereby obtain,

$$|O_{\mu\nu}|^2_{\mu\neq\nu} = \overline{[O^2_{\alpha\alpha}]}_{\overline{\mu}}\Lambda^{(2)}(\mu,\nu) - \overline{[O_{\alpha\alpha}]}^2_{\overline{\mu}}\Lambda^{(2)}(\mu,\nu) + \sum_{\substack{\alpha\beta\\ \alpha\neq\beta}} \Lambda(\mu,\alpha)\Lambda(\nu,\beta)O^2_{\alpha\beta} - \sum_{\substack{\alpha\beta\\ \alpha\neq\beta}} \frac{\Lambda(\mu,\alpha)\Lambda(\nu,\alpha)\Lambda(\mu,\beta)\Lambda(\nu,\beta)}{\Lambda^{(2)}(\mu,\nu)} O_{\alpha\beta}O_{\beta\alpha}, \tag{B.17}$$

where the term in $\delta_{\alpha\alpha'}$ is does not contribute, due to the reduced number of summations (see Appendix D.3). Now, to obtain the contribution of the latter two terms in Eq. (B.17), we employ the sparsity assumption $O_{\alpha\beta} = \sum_{n\in N_O} O_{\alpha,\alpha+n}\delta_{\beta,\alpha+n}$, to obtain,

$$|O_{\mu\nu}|^2_{\mu\neq\nu} = \overline{[\Delta O^2_{\alpha\alpha}]}_{\overline{\mu}}\Lambda^{(2)}(\mu,\nu) + \sum_{\alpha,n\neq 0} \Lambda(\mu,\alpha)\Lambda(\nu,\alpha+n)O_{\alpha,\alpha+n}O_{\alpha,\alpha+n} - \sum_{\alpha,n\neq 0} \frac{\Lambda(\mu,\alpha)\Lambda(\nu,\alpha)\Lambda(\mu,\alpha+n)\Lambda(\nu,\alpha+n)}{\Lambda^{(2)}(\mu,\nu)} O_{\alpha,\alpha+n}O_{\alpha+n,\alpha}, \tag{B.18}$$

where the summations over $n \neq 0$ are understood to be on the set $\mathcal{N}_O$, as defined in Section 6.3.4 as the off-diagonal finite matrix elements. Here we may see that the final term may be ignored, as the restricted summation relegates the order to $\sim \mathcal{O}\left(\left(\frac{\omega_0}{\Gamma}\right)^2\right)$. Finally, we may define an equivalent microcanonical averaging of matrix elements to that above for finite n, such that $\sum_\alpha \Lambda(\mu,\alpha)\Lambda(\nu,\alpha+n)O^2_{\alpha,\alpha+n} \approx \overline{[O^2_{\alpha,\alpha+n}]}_{\tilde{\mu}} \sum_\alpha \Lambda(\mu,\alpha)\Lambda(\nu,\alpha+n)$, where $\tilde{\mu} = \frac{\mu+\nu-n}{2}$, and $\overline{[O^2_{\alpha,\alpha+n}]}_{\tilde{\mu}} = \sum_\alpha \Lambda(\tilde{\mu},\alpha)O^2_{\alpha,\alpha+n}$. We thus obtain

$$|O_{\mu\nu}|^2_{\mu\neq\nu} = \overline{[\Delta O^2_{\alpha\alpha}]}_{\overline{\mu}}\Lambda^{(2)}(\mu,\nu) + \sum_{n\neq 0} \overline{[O^2_{\alpha,\alpha+n}]}_{\tilde{\mu}}\Lambda^{(2)}(\mu,\nu-n), \tag{B.19}$$

which may be written as

$$|O_{\mu\nu}|^2_{\mu\neq\nu} = \sum_n a_n \Lambda^{(2)}(\mu,\nu-n), \tag{B.20}$$

where we have defined $a_n = a_n(E_{\overline{\mu}}) = \overline{[\Delta O^2_{\alpha\alpha}]}_{\overline{\mu}}$ for $n = 0$, and $\overline{[O^2_{\alpha,\alpha+n}]}_{\tilde{\mu}}$ otherwise.

We thus observe that the square of the off-diagonal elements are given by a smooth function, proportional to $\omega_0 = \frac{1}{D(E)}$, which agrees with Srednicki's ansatz [70]. We thus have that the full ETH is recovered from our RMT description.

B.3 Method of Contractions

Here we will see that a useful approach to the calculation of correlation functions can be formulated in terms of 'contractions' between wavefunction indices. We begin by discussing the form of correlation functions within the theory developed in Chapter 5 (Ref. [16]), and note that below we explicitly discus the off-diagonal, $\mu \neq \nu$, case, relevant for the time-averaged fluctuations. Using the method described here, we can in principle calculate any arbitrary correlation function from successive derivatives of the generating function,

Eq. (B.1), as shown in Eq. (B.2). We can see from the generating function (B.1), arbitrary correlation functions can be expressed in terms of products of two- and four-point correlation functions. Two point correlation functions are given by $\langle c_\mu(\alpha)c_\nu(\beta)\rangle = \Lambda(\mu,\alpha)\delta_{\mu\nu}\delta_{\alpha\beta}$, which is the same as one would expect for coefficients behaving as Gaussian distributed random variables of width $\Lambda(\mu,\alpha)$. Now, the four-point correlation function, Eq. (B.3), may be seen as the sum of a Gaussian contraction,

$$\begin{aligned}\langle c_\mu(\overline{\alpha)c_\nu(\beta)c_\mu(\alpha'}\underline{)c_\nu(\beta')}\rangle_V &\Rightarrow \langle c_\mu^2(\alpha)\rangle_V\langle c_\nu^2(\beta)\rangle_V\delta_{\alpha\alpha'}\delta_{\beta\beta'}\\ &= \Lambda(\mu,\alpha)\Lambda(\nu,\beta)\delta_{\alpha\alpha'}\delta_{\beta\beta'},\end{aligned} \tag{B.21}$$

and non-Gaussian, or 'four-leg', contractions, of which there are two:

$$\langle c_\mu(\overline{\overline{\alpha)c_\nu(\beta}})c_\mu(\underline{\alpha')c_\nu(\beta')}\rangle_V \Rightarrow \frac{\Lambda(\mu,\alpha)\Lambda(\nu,\alpha)\Lambda(\mu,\alpha')\Lambda(\nu,\alpha')\delta_{\alpha\beta}\delta_{\alpha'\beta'}}{\Lambda^{(2)}(\mu,\nu)} \tag{B.22a}$$

$$\langle c_\mu(\underline{\underline{\alpha)c_\nu(\beta}}\overline{\overline{c_\mu(\alpha')c_\nu(\beta')}}\rangle_V \Rightarrow \frac{\Lambda(\mu,\alpha)\Lambda(\nu,\alpha)\Lambda(\mu,\alpha')\Lambda(\nu,\alpha')\delta_{\alpha\beta'}\delta_{\alpha'\beta}}{\Lambda^{(2)}(\mu,\nu)}. \tag{B.22b}$$

We reserve the double line contractions for the four-leg case. We note that the four-leg contractions arise as a consequence of enforcing the orthogonality of eigenstates of the random matrix Hamiltonian, such that if the $c_\mu(\alpha)$ coefficients were Gaussian distributed random numbers, as is commonly assumed, one would simply be left with the Gaussian contraction term. We further note that two point correlation functions are only explicitly required for correlation functions of $4n+2\,|\,n\in\mathbb{N}_0$ coefficients, as they are included here in the Gaussian contractions of the four-point correlation function.

Appendix C

Self-Averaging

C.1 Discussion of Self-Averaging

A property fundamental to the approach in this thesis is that of the self-averaging of random matrices. Specifically, in summations we use that the observable time dependence and fluctuations are equal to the ensemble average over perturbations V, such that $\langle O(t)\rangle \approx \langle\langle O(t)\rangle\rangle_V$. This has been previously checked for this model numerically in Refs. [16, 17], and can also be seen to be valid numerically in this case from Figs. E.1 and E.2, which compare our analytical calculations to single realisations of the random matrix Hamiltonian. Self-averaging is a common tool in RMT [121], and whilst examples of behaviour that violates a self-averaging assumption indeed exist [102, 208], these are generally due to additional constraints preventing such statistical behaviour, for global observables such as the survival probability, or in more exotic regimes e.g. close to critical points [209, 210].

A recent and timely study [102] has looked in detail at the self-averaging behaviour of multiple quantities for both a full GOE, and a realistic spin chain, finding that in general one should be wary of simply applying self-averaging. It is shown, for example, that the survival probability is not self-averaging at any timescale. Indeed, it has recently been shown that this quantity cannot be expected to behave ergodically, and thus RMT should not apply to the survival probability [208]. In the light of such studies, as well as such counterexamples to self-averaging outlined above, it is important to further justify the use of this property in more detail.

The definition for self-averaging used in [102] is that the vanishing of the quantity

$$\mathcal{R}_O(t) = \frac{\langle\langle O(t)\rangle^2\rangle_V - \langle\langle O(t)\rangle\rangle_V^2}{\langle\langle O(t)\rangle\rangle_V^2}, \tag{C.1}$$

as the system size increases. Indeed, a very similar quantity was bounded for this RMT model in Ref. [189]. In Appendix C.2, we will show that self-averaging in the sense of the vanishing of Eq. (C.1) indeed occurs for local observables of chaotic systems.

We further note that as the realistic Hamiltonians of interest are not necessarily disordered, in the sense that they themselves may have no random component, we do not require that they be self-averaging themselves (indeed this has no real meaning in this

case). Rather, the assumption in our case is that when expressed in that non-interacting basis, a chaotic interaction Hamiltonian is suitably 'random', such that it resembles a single realisation of the ensemble we describe above, which itself is self-averaging. In fact, it is not important that the *entire* interaction Hamiltonian resembles an element of this ensemble, we require instead that locally, for any energy E within the bulk, the interaction Hamiltonian resembles an element of the random matrix ensemble within a width $\sim \Gamma$ from E.

C.2 Proof of Self-Averaging

In addition to the numerical demonstration in Figs. E.1 and E.2, we are now able to analytically demonstrate that self-averaging, in the sense of Eq. (C.1), occurs for this model. We have already obtained $\langle\langle O(t)\rangle\rangle_V$ in Section 7.6 (note that here we assumed self-averaging, and thus simply used the notation $\langle O(t)\rangle$, in the current section we require the self-averaging step to be explicit, so use the angle brackets $\langle\cdots\rangle_V$ whenever self-averaging is performed), and thus, what remains is a calculation of $\langle\langle O(t)\rangle^2\rangle_V$. We can do this by writing,

$$\begin{aligned}\Delta O(t)^2 &= \sum_{\substack{\mu\nu\\ \mu\neq\nu}}\sum_{\substack{\mu'\nu'\\ \mu'\neq\nu'}}\sum_{\alpha\beta\alpha'\beta'}\sum_{\alpha_1\beta_1\alpha_1'\beta_1'} w_{\alpha\beta}w_{\alpha'\beta'}O_{\alpha'\beta'}O_{\alpha_1'\beta_1'}\\ &\qquad\times c_\mu(\alpha)c_\nu(\beta)c_\mu(\alpha')c_\nu(\beta')c_{\mu'}(\alpha_1)c_{\nu'}(\beta_1)c_{\mu'}(\alpha_1')c_{\nu'}(\beta_1')\\ &= \sum_{\substack{\mu\nu\\ \mu\neq\nu}}\sum_{\substack{\mu'\nu'\\ \mu'\neq\nu'}}\sum_{\alpha\beta\alpha'}\sum_{\alpha_1\beta_1\alpha_1'}\sum_{n,n_1}^{N_O} w_{\alpha\beta}w_{\alpha'\beta'}O_{\alpha',\alpha'+n}O_{\alpha_1',\alpha_1'+n_1}\\ &\qquad\times c_\mu(\alpha)c_\nu(\beta)c_\mu(\alpha')c_\nu(\alpha'+n)c_{\mu'}(\alpha_1)c_{\nu'}(\beta_1)c_{\mu'}(\alpha_1')c_{\nu'}(\alpha_1'+n_1)\end{aligned} \tag{C.2}$$

from which, we see that the relevant correlation function after self-averaging is $\langle c_\mu(\alpha)c_\nu(\beta)c_\mu(\alpha')c_\nu(\alpha'+n)c_{\mu'}(\alpha_1)c_{\nu'}(\beta_1)c_{\mu'}(\alpha_1')c_{\nu'}(\alpha_1'+n_1)\rangle_V$. Indeed, the contribution from Gaussian contractions (see Appendix B.3) can easily be seen to be identical to that of $\langle\Delta O(t)\rangle_V^2$, as these correlators only contract identical interacting indices μ,ν. Furthermore, we see that when non-Gaussian contractions are defined between primed and unprimed interacting indices, μ,ν, there is a reduction in the number of summations. For example, we compare the contribution

$$\sum_{\mu\nu\mu'\nu'}\sum_{\alpha\beta\alpha'}\sum_{\alpha_1\beta_1\alpha_1'}\langle c_\mu(\underline{\alpha})c_\nu(\beta)c_\mu(\underline{\alpha'})c_\nu(\underline{\alpha'})\rangle_V\langle c_{\mu'}(\underline{\alpha_1})c_{\nu'}(\beta_1)c_{\mu'}(\underline{\alpha_1'})c_{\nu'}(\underline{\alpha_1'})\rangle_V, \tag{C.3}$$

to that with mixed interacting indices,

$$\sum_{\mu\nu\mu'\nu'}\sum_{\alpha\beta\alpha'}\sum_{\alpha_1\beta_1\alpha_1'}\langle c_\mu(\underline{\alpha})c_{\nu'}(\beta_1)c_\mu(\underline{\alpha'})c_{\nu'}(\underline{\alpha_1'})\rangle_V\langle c_{\mu'}(\underline{\alpha_1})c_\nu(\beta)c_{\mu'}(\underline{\alpha_1'})c_\nu(\underline{\alpha'})\rangle_V, \tag{C.4}$$

and observe that the latter contribution is negligible, due to the extra reduced summation, as there are no repeated non-interacting indices within the non-Gaussian contraction. We

note that the dominating contribution from non-Gaussian contractions is inevitably from the $n, n_1 = 0$ term shown above (as this reduced summation does not change the order of the contribution as $N_O \ll \mathcal{N}$). Thus we have a single dominating contribution given by the 4-point correlation functions defined with primed, or unprimed, interaction indices only:

$$\begin{aligned}
\langle \Delta O(t)^2 \rangle_V &= \sum_{\substack{\mu\nu \\ \mu\neq\nu}} \sum_{\substack{\mu'\nu' \\ \mu'\neq\nu'}} \sum_{\alpha\beta\alpha'} \sum_{\alpha_1\beta_1\alpha_1'} \sum_{n,n_1}^{N_O} w_{\alpha\beta} w_{\alpha'\beta'} O_{\alpha',\alpha'+n} O_{\alpha_1',\alpha_1'+n_1} e^{-i(E_\mu - E_\nu + E_{\mu'} - E_{\nu'})t} \\
&\qquad \times \langle c_\mu(\alpha) c_\nu(\beta) c_\mu(\alpha') c_\nu(\alpha'+n) c_{\mu'}(\alpha_1) c_{\nu'}(\beta_1) c_{\mu'}(\alpha_1') c_{\nu'}(\alpha_1'+n_1) \rangle_V \\
&= \left(\sum_{\substack{\mu\nu \\ \mu\neq\nu}} \sum_{\alpha\beta\alpha'} \sum_{n}^{N_O} w_{\alpha\beta} O_{\alpha',\alpha'+n} e^{-i(E_\mu - E_\nu)t} \langle c_\mu(\alpha) c_\nu(\beta) c_\mu(\alpha') c_\nu(\alpha'+n) \rangle_V \right) \\
&\times \left(\sum_{\substack{\mu'\nu' \\ \mu'\neq\nu'}} \sum_{\alpha_1\beta_1\alpha_1'} \sum_{n_1}^{N_O} w_{\alpha'\beta'} O_{\alpha_1',\alpha_1'+n_1} e^{-i(E_{\mu'} - E_{\nu'})t} \langle c_{\mu'}(\alpha_1) c_{\nu'}(\beta_1) c_{\mu'}(\alpha_1') c_{\nu'}(\alpha_1'+n_1) \rangle_V \right) \\
&= \langle \Delta O(t) \rangle_V^2 .
\end{aligned} \tag{C.5}$$

Therefore, we can see that the transient component $\Delta O(t)$ of the time evolution is indeed self-averaging. Now, we can similarly see that the long-time average is self-averaging via,

$$\begin{aligned}
O_{\mathrm{MC}} &= \sum_{\mu} \sum_{\alpha\beta} w_{\alpha\beta} O_{\mu\mu} c_\mu(\alpha) c_\mu(\beta) \\
&= \sum_{\mu} \sum_{\alpha\beta\alpha'\beta'} w_{\alpha\beta} O_{\alpha'\beta'} c_\mu(\alpha) c_\mu(\beta) c_\mu(\alpha') c_\mu(\beta') \\
&= \sum_{\mu} \sum_{\alpha\beta\alpha'} \sum_{n}^{N_O} w_{\alpha\beta} O_{\alpha',\alpha'+n} c_\mu(\alpha) c_\mu(\beta) c_\mu(\alpha') c_\mu(\alpha'+n).
\end{aligned} \tag{C.6}$$

The ensemble average of this is then,

$$\begin{aligned}
\langle O_{\mathrm{MC}} \rangle_V &= \sum_{\mu} \sum_{\alpha\beta\alpha'} \sum_{n}^{N_O} w_{\alpha\beta} O_{\alpha',\alpha'+n} \langle c_\mu(\alpha) c_\mu(\beta) c_\mu(\alpha') c_\mu(\alpha'+n) \rangle_V \\
&= \sum_{\mu} \sum_{\alpha\alpha'} w_{\alpha\alpha} O_{\alpha'\alpha'} \Lambda(\mu,\alpha) \Lambda(\mu,\alpha'),
\end{aligned} \tag{C.7}$$

where one can easily see that the terms with $n \neq 0$ require an additional contraction, and thus the contribution is on a lower order, with fewer summations over the non-interacting

indices. We then see that,

$$\begin{aligned} O_{\mathrm{MC}}^2 &= \sum_{\mu\nu}\sum_{\alpha\beta\alpha_1\beta_1} w_{\alpha\beta}w_{\alpha_1\beta_1}O_{\mu\mu}O_{\nu\nu}c_\mu(\alpha)c_\mu(\beta)c_\nu(\alpha_1)c_\nu(\beta_1) \\ &= \sum_{\mu\nu}\sum_{\alpha\beta\alpha_1\beta_1}\sum_{\alpha'\beta'\alpha_1'\beta_1'} w_{\alpha\beta}w_{\alpha_1\beta_1}O_{\alpha'\beta'}O_{\alpha_1'\beta_1'}c_\mu(\alpha) \\ &\qquad\qquad \times c_\mu(\beta)c_\nu(\alpha_1)c_\nu(\beta_1)c_\mu(\alpha')c_\mu(\beta')c_\nu(\alpha_1')c_\nu(\beta_1') \\ &= \sum_{\mu\nu}\sum_{\alpha\beta\alpha_1\beta_1}\sum_{\alpha'\alpha_1'}\sum_{nn'}^{N_O} w_{\alpha\beta}w_{\alpha_1\beta_1}O_{\alpha',\alpha'+n}O_{\alpha_1',\alpha_1'+n'} \\ &\qquad\qquad \times c_\mu(\alpha)c_\mu(\beta)c_\nu(\alpha_1)c_\nu(\beta_1)c_\mu(\alpha')c_\mu(\alpha'+n)c_\nu(\alpha_1')c_\nu(\alpha_1'+n'), \end{aligned} \tag{C.8}$$

which, after self-averaging becomes,

$$\begin{aligned} \langle O_{\mathrm{MC}}^2\rangle_V &= \sum_{\mu\nu}\sum_{\alpha\beta\alpha_1\beta_1}\sum_{\alpha'\alpha_1'}\sum_{nn'}^{N_O} w_{\alpha\beta}w_{\alpha_1\beta_1}O_{\alpha',\alpha'+n}O_{\alpha_1',\alpha_1'+n'} \\ &\qquad\qquad \times \langle c_\mu(\alpha)c_\mu(\beta)c_\nu(\alpha_1)c_\nu(\beta_1)c_\mu(\alpha')c_\mu(\alpha'+n)c_\nu(\alpha_1')c_\nu(\alpha_1'+n')\rangle_V \\ &= \sum_{\mu\nu}\sum_{\alpha\alpha_1}\sum_{\alpha'\alpha_1'} w_{\alpha\alpha}w_{\alpha_1\alpha_1}O_{\alpha'\alpha'}O_{\alpha_1'\alpha_1'}\Lambda(\mu,\alpha)\Lambda(\nu,\alpha_1)\Lambda(\mu,\alpha')\Lambda(\nu,\alpha_1') \\ &= \langle O_{\mathrm{MC}}\rangle_V^2 \end{aligned} \tag{C.9}$$

where we see once more that the $n, n' = 0$ terms dominate, and that contractions between the primed and unprimed indices induce additional kronecker-delta factors, and thus are negligible.

Thus, we have that $\mathcal{R} = 0$ (see Eq. (C.1)), and we analytically observe self-averaging in this model. We note here that in the derivation of the 4-point correlator, we assume that the only 'interactions' between the eigenstates themselves are those enforced due to the mutual orthogonality of eigenstates via the condition $\sum_\alpha c_\mu(\alpha)c_\nu(\alpha) = \delta_{\mu\nu}$ [16]. As these interactions occur pairwise between eigenstates, correlation functions with more than two interacting indices μ, ν contribute an additional $\delta_{\mu\nu}$.

Appendix D

Proofs for Chapter 6

D.1 A Bound

In this section we obtain a bound on the third term in Eq. (6.36), and thus show that it is negligible in comparison to the others, which are obtained in the main text. The term we wish to bound is given by, $|A(t)|$, where

$$A(t) = \sum_{\substack{\mu,\nu \\ \mu\neq\nu}} \sum_{\alpha_0,\beta_0} \psi_{\alpha_0}\psi^*_{\beta_0} O_{\alpha_0\beta_0} \frac{\Lambda(\mu,\alpha_0)\Lambda(\nu,\alpha_0)\Lambda(\mu,\beta_0)\Lambda(\nu,\beta_0)}{\Lambda^{(2)}(\mu,\nu)} e^{-i(E_\mu - E_\nu)t}. \tag{D.1}$$

We first note that no similar microcanonical averaging procedure to those used in the evaluation of the other terms in Eq. (6.36) can be performed, as the average would be required over the coefficients ψ_α. This means that a sum over α_0 or β_0 cannot be expected to cancel, even approximately, with the denominator. As such, the smoothness condition is not useful for this bound, which will be seen instead to be a feature of the sparsity local of observables in the non-interacting basis.

Now, we proceed using $|\sum_i a_i| \leq \sum_i |a_i|$ (which can be seen for any sequence $\{a_i\}$ by noting that the bound is saturated for when $a_i > 0 \; \forall \; i$, and that swapping the sign of any a_i decreases the LHS, and the RHS remains the same), we can write

$$\begin{aligned}
|A(t)| &\leq \sum_{\substack{\mu,\nu \\ \mu\neq\nu}} \left| \sum_{\alpha_0,\beta_0} \psi_{\alpha_0}\psi^*_{\beta_0} O_{\alpha_0\beta_0} \frac{\Lambda(\mu,\alpha_0)\Lambda(\nu,\alpha_0)\Lambda(\mu,\beta_0)\Lambda(\nu,\beta_0)}{\Lambda^{(2)}(\mu,\nu)} \right| \left| e^{-i(E_\mu - E_\nu)t} \right| \\
&\leq \sum_{\substack{\mu,\nu \\ \mu\neq\nu}} \sum_{\alpha_0,\beta_0} \left| \psi_{\alpha_0}\psi^*_{\beta_0} O_{\alpha_0\beta_0} \frac{\Lambda(\mu,\alpha_0)\Lambda(\nu,\alpha_0)\Lambda(\mu,\beta_0)\Lambda(\nu,\beta_0)}{\Lambda^{(2)}(\mu,\nu)} \right| \\
&= \sum_{\alpha_0,\beta_0} \left| \psi_{\alpha_0}\psi^*_{\beta_0} O_{\alpha_0\beta_0} \right| \sum_{\substack{\mu,\nu \\ \mu\neq\nu}} \frac{\Lambda(\mu,\alpha_0)\Lambda(\nu,\alpha_0)\Lambda(\mu,\beta_0)\Lambda(\nu,\beta_0)}{\Lambda^{(2)}(\mu,\nu)} \\
&\leq \frac{3\omega_0}{4\Gamma} \sum_{\alpha_0,\beta_0} \left| \psi_{\alpha_0}\psi^*_{\beta_0} O_{\alpha_0\beta_0} \right|,
\end{aligned} \tag{D.2}$$

where we have used that

$$\sum_{\substack{\mu,\nu \\ \mu\neq\nu}} \frac{\Lambda(\mu,\alpha_0)\Lambda(\nu,\alpha_0)\Lambda(\mu,\beta_0)\Lambda(\nu,\beta_0)}{\Lambda^{(2)}(\mu,\nu)} = \omega_0 \frac{(E_{\alpha_0}-E_{\beta_0})^2\Gamma + 12\Gamma^3}{\pi((E_{\alpha_0}-E_{\beta_0})^2+4\Gamma^2)^2} \leq \frac{3\omega_0}{4\Gamma}. \tag{D.3}$$

Now, applying the sparsity condition, such that $\sum_{\alpha\beta} O_{\alpha\beta} \approx \sum_{\alpha}\sum_{n\in N_O} O_{\alpha,\alpha+n}$, we thus have,

$$\begin{aligned}
\sum_{\alpha_0,\beta_0} |\psi_{\alpha_0}\psi^*_{\beta_0}O_{\alpha_0\beta_0}| &\approx \sum_{\alpha_0,n} |\psi_{\alpha_0}\psi^*_{\alpha_0+n}O_{\alpha_0\alpha_0+n}| \\
&\leq \max_{\alpha_0\beta_0}(O_{\alpha_0\beta_0}) \sum_{\alpha_0,n} |\psi_{\alpha_0}\psi^*_{\alpha_0+n}| \\
&\leq \max_{\alpha_0\beta_0}(O_{\alpha_0\beta_0}) \sum_{n} \left(\left(\sum_{\alpha_0} |\psi_{\alpha_0}|^2\right)\left(\sum_{\alpha_0} |\psi^*_{\alpha_0+n}|^2\right)\right)^{\frac{1}{2}} \\
&= \max_{\alpha_0\beta_0}(O_{\alpha_0\beta_0}) N_O,
\end{aligned} \tag{D.4}$$

where we have used the Cauchy-Schwarz inequality in the penultimate step. Thus, finally, we see that $|A(t)|$ is bounded for all time by

$$|A(t)| \leq \max_{\alpha_0\beta_0}(O_{\alpha_0\beta_0}) N_O \frac{3\omega_0}{4\Gamma}, \tag{D.5}$$

which is small in comparison to other terms in the time evolution, and can thus be ignored.

D.2 Time Dependence in Longditudinal and Transverse Fields

In the final case analysed in Chapter 6 (see Fig. (6.6)), we have an initial state $|\uparrow\rangle_S$, in the Hamiltonian $H_S = B_z^{(S)}\sigma_z^{(1)} + B_x^{(S)}\sigma_x^{(1)}$, we thus have

$$|\uparrow\rangle_S = \psi_+|\phi_+\rangle_S + \psi_-|\phi_-\rangle_S, \tag{D.6}$$

with

$$\begin{aligned}
\psi_+ &= \frac{B_z^{(S)} + E}{\sqrt{(B_z^{(S)}+E)^2 + (B_x^{(S)})^2}} \\
\psi_- &= \frac{B_x^{(S)}}{\sqrt{(B_z^{(S)}+E)^2 + (B_x^{(S)})^2}},
\end{aligned} \tag{D.7}$$

and $E := \sqrt{(B_z^{(S)})^2 + (B_x^{(S)})^2}$. To obtain the full time dependence of the state in the Hamiltonian $H = H_S + H_B + H_{SB}$, from Eq. (6.40), we require the time evolution in the non-interacting part $\langle O(t)\rangle_0$. This is easily obtained, and is equal to

$$\langle O(t)\rangle_0 = \sum_{\alpha_0,\beta_0} \psi_{\alpha_0}\psi^*_{\beta_0}O_{\alpha_0\beta_0}e^{-i(E_{\alpha_0}-E_{\beta_0})t}, \tag{D.8}$$

with $\{\alpha_0\} = \{+, -\}$, and thus

$$\begin{aligned}\langle\phi_+|\sigma_z|\phi_+\rangle &= -\langle\phi_-|\sigma_z|\phi_-\rangle \\ &= \frac{(B_z^{(S)}+E)^2 - (B_x^{(S)})^2}{(B_z^{(S)}+E)^2 + (B_x^{(S)})^2},\end{aligned} \tag{D.9}$$

and

$$\begin{aligned}\langle\phi_+|\sigma_z|\phi_-\rangle &= \langle\phi_-|\sigma_z|\phi_+\rangle \\ &= -2\frac{(B_z^{(S)}+E)B_x^{(S)}}{(B_z^{(S)}+E)^2 + (B_x^{(S)})^2}.\end{aligned} \tag{D.10}$$

Then, from Eq. (D.8), we see that

$$\langle O(t)\rangle_0 = \left(\frac{(B_z^{(S)}+E)^2 - (B_x^{(S)})^2}{(B_z^{(S)}+E)^2 + (B_x^{(S)})^2}\right)^2 + 4\left(\frac{(B_z^{(S)}+E)(B_x^{(S)})}{(B_z^{(S)}+E)^2 + (B_x^{(S)})^2}\right)^2 \cos(2Et). \tag{D.11}$$

An example of this case is shown in Fig. (6.2).

D.3 Proof of Decoupling of Initial State and Observable Coefficients

Here we prove the 'decoupling' process required in Eqs. (6.42) and (6.53), which may essentially be summarised by the statement that in the calculation of time-averaged fluctuations the coefficients $c_\mu(\alpha)$ contributed by the initial state may be considered independently of those in the observable elements $|O_{\mu\nu}|^2_{\mu\neq\nu}$, such that in the most general form we may replace

$$\langle c_\mu(\alpha)c_\nu(\beta)c_\mu(\alpha')c_\nu(\alpha')|O_{\mu\nu}|^2\rangle_V \to \langle c_\mu(\alpha)c_\nu(\beta)c_\mu(\alpha')c_\nu(\alpha')\rangle_V\langle|O_{\mu\nu}|^2\rangle_V \tag{D.12}$$

in Eq. (6.53). This will be shown using the method of contractions outlined in Appendix B.3.

Now, we wish to analyze the long-time fluctuations of a given observable O, defined in Eq. (6.41). In general, the initial state may be expressed as a superposition in the non-interacting basis,

$$|\psi(0)\rangle = \sum_\alpha \psi_\alpha|\phi_\alpha\rangle. \tag{D.13}$$

We thus have, assuming non degenerate energy levels, E_μ, and energy gaps, $E_\mu - E_\nu$,

$$\delta_O^2(\infty) = \sum_{\alpha\beta\alpha'\beta'}\sum_{\substack{\mu\nu\\ \mu\neq\nu}} \psi_\alpha\psi_\beta\psi_{\alpha'}\psi_{\beta'}c_\mu(\alpha)c_\nu(\beta)c_\mu(\alpha')c_\nu(\beta')|O_{\mu\nu}|^2. \tag{D.14}$$

Now, assuming self averaging, we write

$$\begin{aligned}\delta_O^2(\infty) &= \sum_{\alpha\beta\alpha'\beta'}\sum_{\substack{\mu\nu\\ \mu\neq\nu}}\psi_\alpha\psi_\beta\psi_{\alpha'}\psi_{\beta'}\langle c_\mu(\alpha)c_\nu(\beta)c_\mu(\alpha')c_\nu(\beta')|O_{\mu\nu}|^2\rangle_V \\ &= \sum_{\alpha\beta\alpha'\beta'}\sum_{\alpha_1\beta_1\alpha_1'\beta_1'}\sum_{\substack{\mu\nu\\ \mu\neq\nu}}\psi_\alpha\psi_\beta\psi_{\alpha'}\psi_{\beta'}O_{\alpha_1\beta_1}O_{\alpha_1'\beta_1'} \\ &\qquad \times\langle c_\mu(\alpha)c_\nu(\beta)c_\mu(\alpha')c_\nu(\beta')c_\mu(\alpha_1)c_\nu(\beta_1)c_\mu(\alpha_1')c_\nu(\beta_1')\rangle_V,\end{aligned} \tag{D.15}$$

which, if the initial state $|\psi(0)\rangle$ is a single eigenstate of H_0, $|\phi_\alpha\rangle$, we obtain simply

$$\delta_O^2(\infty) = \sum_{\substack{\mu\nu\\ \mu\neq\nu}}\langle|c_\mu(\alpha)|^2|c_\nu(\alpha)|^2|O_{\mu\nu}|^2\rangle_V. \tag{D.16}$$

In principle, for a generic initial state, we thus require the calculation of an arbitrary 8-point correlation function, as seen in Eq. (D.15). We can see this requires four-leg contractions of all possible indices. We will observe, however, that the sections of the correlation function arising from the initial state coefficients (no subscript) and observable coefficients (subscript 1), decouple, and we obtain

$$\delta_O^2(\infty) = \sum_{\substack{\mu\nu\\ \mu\neq\nu}}\langle|c_\mu(\alpha)|^2|c_\nu(\alpha)|^2\rangle_V\langle|O_{\mu\nu}|^2\rangle_V, \tag{D.17}$$

such that only correlation functions within the respective coefficient types are required. We note that for generic initial states and observables this occurs as a consequence of the sparsity assumption. The remainder of this section we introduce a method of contractions for four-point correlation functions in order to show this decoupling.

Suppose one wishes to evaluate the sum of correlation functions of initial state and observable coefficients

$$\sum_{\alpha\beta\alpha_1\beta_1\alpha_1\alpha_1'}\langle c_\mu(\alpha)c_\nu(\alpha)c_\mu(\beta)c_\nu(\beta)c_\mu(\alpha_1)c_\nu(\alpha_1')c_\mu(\beta_1)c_\nu(\beta_1')\rangle_V, \tag{D.18}$$

which, as discussed above, is made up of four point correlation functions of Gaussian, and four-leg contractions. One can see that an arbitrary four-point correlation function is of the order $\mathcal{O}\left(\left(\frac{\omega 0}{\Gamma}\right)^\lambda\right)$, where $\lambda = N_\Lambda - N_\Sigma$, with N_Λ the number of Λ factors in the numerator minus the number of factors in the denominator, and N_Σ is the number of summations. In this sense we have each Λ contributing a factor on the order $\mathcal{O}\left(\frac{\omega_0}{\Gamma}\right)$, and each summation contributing on the order $\mathcal{O}\left(\frac{\Gamma}{\omega_0}\right)$.

One can easily see in Eq. (D.18), that particular contractions, Gaussian or non-Gaussian, in general reduce the number of summations over the non-interacting indices $\alpha, \beta, \cdots$. However, due to the repeated coefficient on the initial state side, contractions may be defined that require fewer summation restrictions, and thus these contractions

dominate to lowest order in $\frac{\omega_0}{\Gamma}$. For example

$$\sum_{\alpha\beta\alpha_1\beta_1\cancel{\alpha_1'\beta_1'}} \langle c_\mu(\overline{\alpha)c_\nu(\alpha)}c_\mu(\overline{\beta)c_\nu(\beta)}\rangle_V \langle c_\mu(\overline{\alpha_1)c_\nu(\alpha_1'})c_\mu(\overline{\beta_1)c_\nu(\beta_1'})\rangle_V, \tag{D.19}$$

shows a single four-leg contraction for correlation functions within coefficient types, and

$$\sum_{\alpha\cancel{\beta}\alpha_1\beta_1\cancel{\alpha_1'\beta_1'}} \langle c_\mu(\overline{\alpha)c_\nu(\alpha)}c_\mu(\overline{\beta)c_\nu(\beta_1'})\rangle_V \langle c_\mu(\overline{\alpha_1)c_\nu(\alpha_1'})c_\mu(\overline{\beta_1)c_\nu(\beta)}\rangle_V, \tag{D.20}$$

similarly shows an example with a single coefficient swapped between types. The strikethroughs show the summations that are restricted due to the contractions. Note that due to the repeated coefficients in Eq. (D.19) a four-leg contraction may be defined with no required restriction on summations.

Now, for the simple case of Eq. (D.16), we can see that the required correlation functions have repeated indices in the initial state coefficients, and thus only contractions within coefficient types contribute.

In the general case of Eq. (D.15) we have no such repeated indices. We thus employ the sparsity condition, that $O_{\alpha\beta}$ is in general sparse, and has a well defined form in the non-interacting basis, which is generally either diagonal, or has non-zero values at some energy E_n from the diagonal. This can be easily seen for local observables made up of Pauli matrices. We thus replace $\sum_{\alpha\beta} O_{\alpha\beta} \to \sum_\alpha \sum_{n\in N_O} O_{\alpha,\alpha+n}$. We thus have

$$\begin{aligned}\delta_O^2(\infty) = &\sum_{\alpha\beta\alpha'\beta'}\sum_{\alpha_1\alpha_1'}\sum_{\substack{\mu\nu\\ \mu\neq\nu}}\sum_n \psi_\alpha\psi_\beta\psi_{\alpha'}\psi_{\beta'}O_{\alpha_1,\alpha_1+n}O_{\alpha_1',\alpha_1'+n}\\ &\times\langle c_\mu(\alpha)c_\nu(\beta)c_\mu(\alpha')c_\nu(\beta')c_\mu(\alpha_1)c_\nu(\alpha_1+n)c_\mu(\alpha_1')c_\nu(\alpha_1'+n)\rangle_V,\end{aligned} \tag{D.21}$$

and therefore observe that we now have repeated indices in the observable type. We then see that, once again, contractions between coefficient types may be ignored to leading order. Thus, we obtain

$$\delta_O^2(\infty) = \sum_{\alpha\beta\alpha'\beta'}\sum_{\substack{\mu\nu\\ \mu\neq\nu}} \psi_\alpha\psi_\beta\psi_{\alpha'}\psi_{\beta'}\langle c_\mu(\alpha)c_\nu(\beta)c_\mu(\alpha')c_\nu(\beta')\rangle_V\langle|O_{\mu\nu}|^2\rangle_V. \tag{D.22}$$

D.4 QC-FDT for Arbitrary Initial States and Non-Diagonal Observables

After the simplification obtained by the method of contractions above, we see that correlations between initial state and observable factors of the time averaged fluctuations only contribute up to $\mathcal{O}\left(\left(\frac{\omega_0}{\Gamma}\right)^2\right)$, and may thus be ignored. As such, in the calculation of time-averaged fluctuations, Eq. (D.15), we may make the replacement Eq. (D.12), leading to a general form given by Eq. (D.22).

Considering initially the simplest generalisation, the case of arbitrary initial states,

where observables are diagonal in the non-interacting basis, $O_{\alpha\beta} \propto \delta_{\alpha\beta}$, we have

$$\begin{aligned}\delta_O^2(\infty) = \sum_{\alpha\beta}\sum_{\substack{\mu\nu\\ \mu\neq\nu}} |\psi_\alpha|^2|\psi_\beta|^2 \Big[\Lambda(\mu,\alpha)\Lambda(\nu,\beta) \\ - 2\frac{\Lambda(\mu,\alpha)\Lambda(\nu,\alpha)\Lambda(\mu,\beta)\Lambda(\nu,\beta)}{\Lambda^{(2)}(\mu,\nu)}\Big]\overline{[\Delta O^2_{\alpha\alpha}]}_{\overline{\mu}}\Lambda^{(2)}(\mu,\nu) \\ \approx \sum_{\alpha\beta}|\psi_\alpha|^2|\psi_\beta|^2\Lambda^{(4)}(\alpha,\beta)\overline{[\Delta O^2_{\alpha\alpha}]}_{\overline{\alpha}} - 2\sum_{\alpha\beta}\overline{[\Delta O^2_{\alpha\alpha}]}_{\overline{\alpha}}|\psi_\alpha|^2|\psi_\beta|^2\left(\Lambda^{(2)}(\alpha,\beta)\right)^2\end{aligned} \tag{D.23}$$

where $\overline{\alpha} = (\alpha+\beta)/2$, and we have used for the off-diagonal elements of O[16],

$$|O_{\mu,\nu}|^2_{\mu\neq\nu} = \overline{[\Delta O^2_{\alpha\alpha}]}_{\overline{\mu}}\Lambda^{(2)}(\mu,\nu). \tag{D.24}$$

The summations over μ,ν have been performed in Eq. (D.23) by the prescription $\sum_\mu \to \int dE_\mu/\omega_0$, and the effective microcanonical average $\overline{[\Delta O^2_{\alpha\alpha}]}_{\overline{\alpha}}$ is taken at the energy $(E_\alpha + E_\beta)/2$ via the smoothness property. Now, we may bound the second term by (using $\max(\Lambda^{(2)}(\alpha,\beta)) = \frac{\omega}{2\pi\Gamma}$), obtaining,

$$\begin{aligned}2\sum_{\alpha\beta}\overline{[\Delta O^2_{\alpha\alpha}]}_{\overline{\alpha}}|\psi_\alpha|^2|\psi_\beta|^2\left(\Lambda^{(2)}(\alpha,\beta)\right)^2 &\leq 2\sum_{\alpha\beta}\overline{[\Delta O^2_{\alpha\alpha}]}_{\overline{\alpha}}|\psi_\alpha|^2|\psi_\beta|^2\frac{\omega_0^2}{4\pi^2\Gamma^2} \\ &\leq \max_{\alpha_0}\left(\overline{[\Delta O^2_{\alpha\alpha}]}_{\alpha_0}\right)\frac{\omega_0^2}{4\pi^2\Gamma^2},\end{aligned} \tag{D.25}$$

which is on the order of ω_0^2, and thus negligible. Now, we have for arbitrary initial states,

$$\delta_O^2(\infty) \approx \overline{[\Delta O^2_{\alpha\alpha}]}_{\overline{\alpha_0}}\sum_{\alpha\beta}|\psi_\alpha|^2|\psi_\beta|^2\Lambda^{(4)}(\alpha,\beta). \tag{D.26}$$

Now, we note here that whilst this form of the QC-FDT looks rather different, one expects many typical initial states to show a very similar relation to the simpler form of $\delta^2 \sim \frac{1}{D(E)\Gamma}$. To illustrate this, we evaluate the relation (D.26) for some example initial state distributions $\{\psi_\alpha\}$.

The first example we analyze is the case where H_0 itself may be split into interacting and non-interacting parts $H_0 = H_0^{(0)} + H_0^{(I)}$, where $H_0^{(I)}$ may be treated as a random matrix. In which case, the distribution of $|\psi_\alpha|^2$ is given by a Lorentzian of width Γ_0, $\Lambda_0(\overline{\mu},\alpha)$, and thus

$$\begin{aligned}\delta_O^2(\infty) &= \overline{[\Delta O^2_{\alpha\alpha}]}_{\overline{\alpha_0}}\frac{\omega_0(4\Gamma+2\Gamma_0)/\pi}{(4\Gamma+2\Gamma_0)^2} \\ &= \overline{[\Delta O^2_{\alpha\alpha}]}_{\overline{\alpha_0}}\frac{\omega_0}{\pi(4\Gamma+2\Gamma_0)},\end{aligned} \tag{D.27}$$

and we thus recover the CQ-FDT in the same form as for an initial state $|\phi_\alpha\rangle$, however with an altered effective width.

Next, we consider a bimodal distribution $|\psi(0)\rangle = \psi_\alpha|\phi_{\alpha_1}\rangle + \psi_\beta|\phi_{\alpha_2}\rangle$. Here we have

$$\delta_O^2(\infty) = \overline{[\Delta O_{\alpha\alpha}^2]}_{\overline{\alpha_0}} \frac{1}{2}\left(\frac{\omega_0}{4\pi\Gamma} + \Lambda^{(4)}(\alpha_1,\alpha_2)\right), \tag{D.28}$$

which we can see resembles the simple case in the first term, and follows a Lorentzian distribution in the second. This reduces to the simple case for $E_{\alpha_1} - E_{\alpha_2} \ll \Gamma$. Continuing in the same manner, we see that we can rewrite the QC-FDT for an arbitrary distribution, $|\psi(0)\rangle = \sum_\alpha \psi_\alpha|\phi_\alpha\rangle$, as

$$\delta_O^2(\infty) = \overline{[\Delta O_{\alpha\alpha}^2]}_{\overline{\alpha_0}}\left(\sum_\alpha |\psi_\alpha|^4 \frac{\omega_0}{4\pi\Gamma} + 2\sum_{\substack{\alpha\beta \\ \alpha>\beta}} |\psi_\alpha|^2|\psi_\beta|^2\Lambda^{(4)}(\alpha,\beta)\right), \tag{D.29}$$

and thus we see that the contribution of the first term reduces substantially. Finally, for a microcanonical distribution $\psi_\alpha = 1/\sqrt{N^*}\,\forall\,\alpha \in [E_0 - \delta/2, E_0 + \delta/2]$, we have

$$\delta_O^2(\infty) = \overline{[\Delta O_{\alpha\alpha}^2]}_{\overline{\alpha_0}} \frac{1}{N^*} \tag{D.30}$$

as $N^* \approx D(E_0)\delta$, assuming that $D(E)$ does not change much over the width δ, we once again recover the QC-FDT in its original form.

We may also analyse Eq. (D.26) using another example of the smoothness relation Eq. (6.19). We see that the summation

$$\sum_\alpha |\psi_\alpha|^2\Lambda^{(4)}(\alpha,\beta), \tag{D.31}$$

may be obtained when the width of the distribution $\{|\psi_\alpha|^2\}$ is $\ll \Gamma$, we have that $\Lambda^{(4)}(\alpha,\beta)$ is essentially constant in this summation, such that $\sum_\alpha |\psi_\alpha|^2\Lambda^{(4)}(\alpha,\beta) \approx \Lambda^{(4)}(\alpha_0,\beta)\sum_\alpha |\psi_\alpha|^2 = \Lambda^{(4)}(\alpha_0,\beta)$. Repeating the same step with the sum over β, we obtain

$$\begin{aligned}\delta_O^2(\infty) &\approx \overline{[\Delta O_{\alpha\alpha}^2]}_{\overline{\alpha_0}}\Lambda^{(4)}(\alpha_0,\alpha_0) \\ &= \overline{[\Delta O_{\alpha\alpha}^2]}_{\overline{\alpha_0}}\frac{\omega_0}{4\pi\Gamma},\end{aligned} \tag{D.32}$$

and thus the original QC-FDT is recovered.

We have thus observed that for many physical initial states we expect that Eq. (D.26) reduces to the simpler form of $\delta \sim \frac{1}{D(E)\Gamma}$.

We now turn our attention to observables that are not necessarily diagonal in the non-interacting basis, but fulfil instead the sparsity condition. Such observables were shown above to fulfil the ETH, and may be described by Eq. (B.20). Using this, as well as Eqs.

(D.22) and (B.3), we have

$$\delta_O^2(\infty) = \sum_{\alpha\beta} |\psi_\alpha|^2 |\psi_\beta|^2 \sum_{\substack{\mu\nu \\ \mu\neq\nu}} \Lambda(\mu,\alpha)\Lambda(\nu,\beta) \sum_n a_n \Lambda^{(2)}(\mu,\nu-n) \\ - 2\sum_{\alpha\beta} |\psi_\alpha|^2 |\psi_\beta|^2 \sum_{\substack{\mu\nu \\ \mu\neq\nu}} \frac{\Lambda(\mu,\alpha)\Lambda(\nu,\alpha)\Lambda(\mu,\beta)\Lambda(\nu,\beta)}{\Lambda^{(2)}(\mu,\nu)} \sum_n a_n \Lambda^{(2)}(\mu,\nu-n), \tag{D.33}$$

where the sum over n is understood to be over the set $\mathcal{N}$. The second term can be seen to be bounded by

$$2\sum_{\alpha\beta} |\psi_\alpha|^2 |\psi_\beta|^2 \sum_{\substack{\mu\nu \\ \mu\neq\nu}} \frac{\Lambda(\mu,\alpha)\Lambda(\nu,\alpha)\Lambda(\mu,\beta)\Lambda(\nu,\beta)}{\Lambda^{(2)}(\mu,\nu)} \sum_n a_n \frac{\omega_0}{2\pi\Gamma} \tag{D.34}$$

which in turn, using Eq. (D.3), and assuming $a_n(E_{\overline{\mu}})$ is essentially independent of $E_{\overline{\mu}}$ over a width Γ, is bounded by

$$\sum_n a_n \frac{3\omega_0^2}{4\pi\Gamma^2}, \tag{D.35}$$

and may thus be ignored. Now, as $\sum_\mu \Lambda(\mu,\alpha)\Lambda^{(2)}(\mu,\nu-n) = \Lambda^{(3)}(\nu-n,\alpha) = \Lambda^{(3)}(\nu,\alpha+n)$, and, similarly, $\sum_\mu \Lambda(\mu,\alpha+n)\Lambda^{(3)}(\mu,\beta) = \Lambda^{(4)}(\alpha,\beta-n)$, we have

$$\delta_O^2(\infty) = \sum_{\alpha\beta,n} a_n |\psi_\alpha|^2 |\psi_\beta|^2 \Lambda^{(4)}(\alpha,\beta-n), \tag{D.36}$$

where a_n is taken at the initial state energy. We now have the most general form of the QC-FDT. We note here that in order that the factor a_n may be treated as both independent of μ,ν, and evaluated finally at the initial state energy $E_{\overline{\alpha_0}}$, requires that both $a_n(E_{\overline{\mu}})$ is a smooth function, approximately invariant over the width Γ around this energy.

D.5 QC-FDT For σ_z in B_x and B_z Fields

For an observable that is diagonal in the basis of eigenstates of the non-interacting Hamiltonian we have observed that the QC-FDT takes a remarkably simple form, which generalises (see Appendix D.4) to a similar relationship when these conditions are relaxed. In this section, we explicitly calculate the generalised case for the spin-chain system analyzed in the main text, given by

$$H_S = B_z^{(S)}\sigma_z^{(1)} + B_x^{(S)}\sigma_x^{(1)}, \tag{D.37}$$

such that we have for an initial state $|\uparrow\rangle_S$, we have

$$|\uparrow\rangle_S = \psi_+|\phi_+\rangle_S + \psi_-|\phi_-\rangle_S, \tag{D.38}$$

with

$$\begin{aligned}\psi_+ &= \frac{B_z^{(S)} + E}{\sqrt{(B_z^{(S)} + E)^2 + (B_x^{(S)})^2}} \\ \psi_- &= \frac{B_x^{(S)}}{\sqrt{(B_z^{(S)} + E)^2 + (B_x^{(S)})^2}},\end{aligned} \tag{D.39}$$

and $E := \sqrt{(B_z^{(S)})^2 + (B_x^{(S)})^2}$. The eigenenergies are $\pm E$. Now, we find for the matrix elements of the observable σ_z,

$$\begin{aligned}{}_S\langle\phi_+|\sigma_z|\phi_+\rangle_S &= -{}_S\langle\phi_-|\sigma_z|\phi_-\rangle_S \\ &= \frac{(B_z^{(S)} + E)^2 - (B_x^{(S)})^2}{(B_z^{(S)} + E)^2 + (B_x^{(S)})^2},\end{aligned} \tag{D.40}$$

and

$$\begin{aligned}{}_S\langle\phi_+|\sigma_z|\phi_-\rangle_S &= {}_S\langle\phi_-|\sigma_z|\phi_+\rangle_S \\ &= -2\frac{(B_z^{(S)} + E)B_x^{(S)}}{(B_z^{(S)} + E)^2 + (B_x^{(S)})^2}.\end{aligned} \tag{D.41}$$

The relative value of the observable matrix elements dictates the relative height of the broadened peaks of the observable in the interacting basis $(|\sigma_z|^2)_{\mu\nu}$. The observable in the interacting basis is then, from Eq. (B.20), is given by

$$|O_{\mu\nu}|^2_{\mu\neq\nu} = a_0\Lambda^{(2)}(\mu,\nu) + a_1\Lambda^{(2)}(\mu,\nu+2E) + a_2\Lambda^{(2)}(\mu,\nu-2E), \tag{D.42}$$

where $\{a_i\}_{i=0,1,2}$ are the respective height of the three peaks at energies $0, \pm 2E$. Thus, we have

$$\begin{aligned}a_0 &= \overline{[\Delta O_{\alpha\alpha}]_{\overline{\alpha_0}}} \\ &= \sum_\alpha \Lambda(\overline{\alpha_0},\alpha)O_{\alpha\alpha}^2 - \left(\sum_\alpha \Lambda(\overline{\alpha_0},\alpha)O_{\alpha\alpha}\right)^2,\end{aligned} \tag{D.43}$$

where $\overline{[\Delta O_{\alpha\alpha}]_{\overline{\alpha_0}}}$ is evaluated at $\overline{\alpha_0}$ as it is the elements $O_{\mu\nu}$ around this energy that contribute to $\delta_O^2(\infty)$ in Eq. (6.55). Further, we note that the second term in Eq. (D.43) can be identified with the square of the long-time average value of the observable, see Eq. (6.40). To evaluate the first term, we must understand the sum over α to also run over the bath states, in the sense that we may write

$$\sum_\alpha O_{\alpha\alpha} = \sum_{\alpha_+} O_{\alpha_+\alpha_+} + \sum_{\alpha_-} O_{\alpha_-\alpha_-}, \tag{D.44}$$

where $O_{\alpha_\pm\alpha_\pm} = {}_B\langle\phi_\alpha|{}_S\langle\phi_\pm|O|\phi_\pm\rangle_S|\phi_\alpha\rangle_B$. Using that $O = \sigma_z^{(S)} \otimes \mathbb{1}^{(B)}$, we have that $O_{\alpha\alpha} = {}_S\langle\phi_\pm|O|\phi_\pm\rangle_S$ does not explicitly depend on the bath state, and thus

$$a_0 = \sum_{\alpha_+} \Lambda(\overline{\alpha_0}, \alpha_+)|{}_S\langle\phi_+|\sigma_z|\phi_+\rangle_S|^2 + \sum_{\alpha_-} \Lambda(\overline{\alpha_0}, \alpha_-)|{}_S\langle\phi_-|\sigma_z|\phi_-\rangle_S|^2 - \left(\overline{\langle O(t)\rangle}\right)^2. \tag{D.45}$$

Now, noting that the bath degrees of freedom have an associated density of states that is half that of the whole system + bath. Thus, we have $\sum_{\alpha_\pm} \Lambda(\overline{\alpha_0}, \alpha_\pm) \to \int \frac{dE}{\omega_0} \frac{\omega_0 2\Gamma/\pi}{(E_{\alpha_0}-E)^2+(\Gamma)^2} = \frac{1}{2}$. Using Eq. (D.40), we thus have,

$$\begin{aligned} a_0 =& \frac{1}{2}\left(|{}_S\langle\phi_+|\sigma_z|\phi_+\rangle_S|^2 + |{}_S\langle\phi_-|\sigma_z|\phi_-\rangle_S|^2\right) - \left(\overline{\langle O(t)\rangle}\right)^2 \\ =& \frac{(B_z^{(S)})^2}{(B_z^{(S)})^2 + (B_x^{(S)})^2} - \left(\overline{\langle O(t)\rangle}\right)^2. \end{aligned} \tag{D.46}$$

A similar argument reveals,

$$a_1 = a_2 = \frac{1}{2}|{}_S\langle\phi_+|\sigma_z|\phi_-\rangle_S|^2 = \frac{1}{2}\frac{(B_x^{(S)})^2}{(B_z^{(S)})^2 + (B_x^{(S)})^2}. \tag{D.47}$$

We note that this satisfies the sum rule $\sum_\nu |O_{\mu\nu}|^2 = (O^2)_{\mu\mu} = 1$, as $\sum_n a_n = \sum_{\nu\neq\mu} |O_{\mu\nu}|^2 = 1 - O_{\mu\mu}^2$, noting $O_{\mu\mu} = \sum_{\alpha\beta} c_\mu(\alpha)c_\mu(\beta)O_{\alpha\beta} = \sum_\alpha \Lambda(\mu,\alpha)O_{\alpha\alpha}$. Now, using Eqs. (6.55), (D.38), and (D.42), we obtain

$$\begin{aligned} \delta_{\sigma_z}^2(\infty) = \frac{1}{D(E_{\overline{\alpha_0}})}\Bigg(&\left(|\psi_+|^4 + |\psi_-|^4\right)\left(\frac{a_0}{4\pi\Gamma} + 2a_1\frac{4\Gamma/\pi}{(2E)^2+(4\Gamma)^2}\right) \\ &+ 2|\psi_+|^2|\psi_-|^2\left(a_0\frac{4\Gamma/\pi}{(2E)^2+(4\Gamma)^2} + \frac{a_1}{4\pi\Gamma} + a_1\frac{4\Gamma/\pi}{(4E)^2+(4\Gamma)^2}\right)\Bigg). \end{aligned} \tag{D.48}$$

Here we note that in Eq. (6.55) $\Lambda(\alpha, \beta+n)$ is a function of $E_\alpha - E_\beta + E_n$, with $E_\alpha - E_\beta$ giving the possible values $0, \pm 2E$. E_n has the same possible values, as it labels the peak energies of the observable. Observe that in various physical limits we also recover the QC-FDT of the simpler form $\delta \sim \frac{1}{\Gamma}$, for example, when $E \gg \Gamma$, the Lorentzian terms are small, and the original scaling is obtained. In fact, as with the case for diagonal observables and general initial states, we expect this simpler form to hold up to a factor for most cases.

We further comment that in the generalised case the assumption that the density of states does not change over the relevant widths is not always valid, and may cause deviations from the result above by the effective rescaling of the a_n factors for large E_n. This occurs as the implicit assumption is now $\Gamma < E_n < W$, where W is the characteristic width of the density of states.

Appendix E

Proofs for Chapter 7

E.1 RMT Numerics

Here we confirm our analytical results with numerical calculations with the random matrix Hamiltonian. In particular, we show in Fig. E.1a, that the infinite temperature fluctuation-dissipation theorem (FDT),

$$\delta_O^2(\infty) = \frac{W_O \omega_0}{4\pi \mathcal{N}_B \Gamma}, \tag{E.1}$$

is satisfied in this model. This is shown for two 'observables' of the RMT model, O_{odd} and O_{sym}, which are chosen to be diagonal in the non-interacting basis, with diagonal elements given by,

$$(O_{odd})_{\alpha\alpha} = \begin{cases} 1 & \text{if } \alpha = \text{odd} \\ 0 & \text{otherwise,} \end{cases} \tag{E.2}$$

for O_{odd}, and

$$(O_{sym})_{\alpha\alpha} = \begin{cases} 1 & \text{if } \alpha = \text{odd} \\ -1 & \text{otherwise,} \end{cases} \tag{E.3}$$

for O_{sym}. These observables are chosen, as in Refs. [16, 17], as they resemble realistic observables, such as local Pauli operators, in the sense that they are well defined, sparse, and highly degenerate [177] in the non-interacting basis. For our RMT numerical calculations, we define the initial state as

$$\rho_{\alpha\beta} = e^{-\beta(E_\alpha - E_0)} \delta_{\alpha\beta} \delta_{\alpha,\text{odd}}, \tag{E.4}$$

such that $\langle O(0) \rangle = 1$. The energy shift E_0 is simply to avoid edge effects at lower temperatures, where a large fraction of the initial state population would otherwise be in the ground state.

In Fig. E.2 we plot the time dependence of the above observables for an infinite temperature initial state, and compare these to the observable time dependence of Eq. (7.37), derived below.

The high temperature limit, in which our FDT is derived, is defined by $\beta^{-1} \gg \Gamma$. In the numerics, we use $g = 0.05$, and thus $\Gamma \sim 0.007$, so the high temperature limit requires

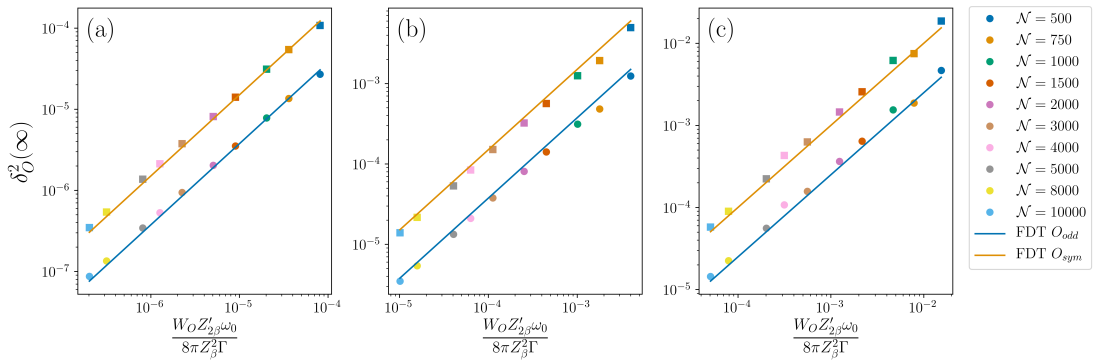

Figure E.1: (a) Numerical confirmation of the random matrix FDT for an infinite temperature initial state, Eq. (E.25) for observables O_{odd} and O_{sym}. (b) Shows the random matrix FDT for a high temperature initial state $\beta = 100$, and (c) for a low temperature ($\beta = 500$). Here $g = 0.04$, so $\Gamma \sim 0.007$, and thus the high temperature limit $\beta \ll \Gamma^{-1}$ is approximately $\beta \ll 125$. We thus observe that the finite temperature result Eqs. (7.62) and (E.22) (which we note are equivalent, the latter is used here), is fulfilled for all temperatures. We note that the low temperature limit above uses $\rho_B \sim e^{-\beta(E-E_0)}$, with $E_0 = \frac{E_{max}}{2}$, to ensure that the initial state is not simply the ground state. For this limit we also use $W_O = \overline{[\Delta O^2]}$, as discussed in the final section. Simulations are performed with a single realisation of the random matrix V, and thus we observe directly the self-averaging property.

$\beta \lesssim 125$. We show plots for $\beta = 100$ and $\beta = 500$ in Figs. E.1b and E.1c, respectively. For the parameters used these correspond to a high temperature, near the edge of the expected limit, and a low temperature initial state. We observe that the finite temperature form in fact works well for *all* β values. This is further discussed analytically in the final section below, where we see that the low temperature limit of our current approach is equal to the pure state result previously obtained in Ref. [17].

E.2 Gaussian, Non-Gaussian, and Mixed Contractions

Here we calculate the contributions to the long-time fluctuations of Eq. (7.47). We see that the relevant correlation function is an 8-point correlation function, which we will show below may be split into three groups: products of Gaussian contractions, products of non-Gaussian contractions, and mixed products of two Gaussian and one non-Gaussian contraction.

An example of the first form, Gaussian contractions only, is

$$\langle c_\mu(\overline{\alpha)c_\nu(\alpha}\underline{)c_\mu(\beta}\underline{)c_\nu(\beta)}c_\mu(\overline{\alpha')c_\nu(\alpha'}\underline{)c_\mu(\beta'}\underline{)c_\nu(\beta')}\rangle_V = \Lambda(\mu,\alpha)\Lambda(\nu,\alpha)\Lambda(\mu,\alpha')\Lambda(\nu,\alpha')\delta_{\alpha\beta}\delta_{\alpha'\beta'}. \tag{E.5}$$

Indeed, there are three such contractions, occurring each time between pairs of indices, that only contribute two kronecker-δ factors - $\sim \delta_{\alpha\beta}\delta_{\alpha'\beta'}, \delta_{\alpha\alpha'}\delta_{\beta\beta'}, \delta_{\alpha\beta'}\delta_{\beta\alpha'}$. Other Gaussian contractions may be defined, but may be ignored due to a reduction in the number of summations.

In a similar manner, we may define non-Gaussian contractions that do not reduce the

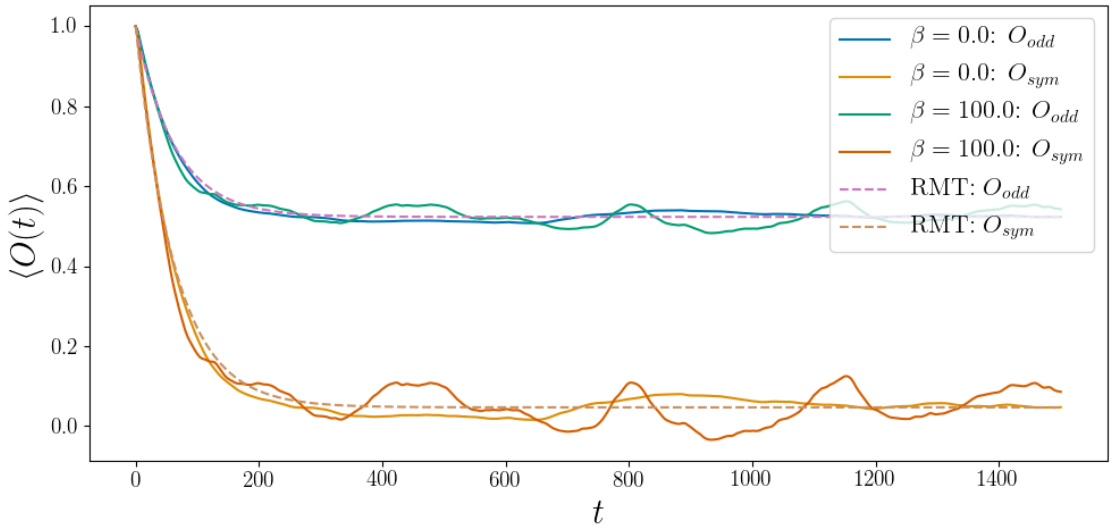

Figure E.2: Time dependence of random matrix observables O_{odd} and O_{sym}. Exact diagonalization numerics (solid lines) show time evolutions for a single realisation of the random matrix perturbation V. RMT calculation (dashed lines), show Eq. (7.37), with $\langle O(t) \rangle_0 = 1$, and $\langle O \rangle_{MC} = \overline{[O_{\alpha\alpha}]} = 0(0.5)$ for $O = O_{sym}(O_{odd})$. Parameters used are $\mathcal{N} = 500, g = 0.05, \beta = 0, 100$.

number of summations at all, such that they contribute on the same order as the Gaussian contractions above. An example is,

$$\langle c_\mu(\alpha)c_\nu(\alpha)c_\mu(\beta)c_\nu(\beta)c_\mu(\alpha')c_\nu(\alpha')c_\mu(\beta')c_\nu(\beta')\rangle_V = L_{\mu\nu}^{\alpha\alpha\beta\beta}L_{\mu\nu}^{\alpha'\alpha'\beta'\beta'}. \tag{E.6}$$

It can be easily seen that there are three non-Gaussian contractions of this form, with the other two being defined by swapping pairs of primed and unprimed indices in turn.

Finally, we see that mixed contractions may also contribute, for example,

$$\langle c_\mu(\alpha)c_\nu(\alpha)c_\mu(\beta)c_\nu(\beta)c_\mu(\alpha')c_\nu(\alpha')c_\mu(\beta')c_\nu(\beta')\rangle_V = \Lambda(\mu,\alpha)\Lambda(\nu,\alpha)L_{\mu\nu}^{\alpha'\alpha'\beta'\beta'}\delta_{\alpha\beta}. \tag{E.7}$$

We can see that there are six terms of this form that contribute only one δ factor. These are $\delta_{\alpha\beta}, \delta_{\alpha\alpha'}, \delta_{\alpha\beta'}, \delta_{\beta\alpha'}, \delta_{\beta\beta'}, \delta_{\alpha'\beta'}$.

We thus obtain that for the contribution from Gaussian contractions, $\delta_G^2(\infty)$,

$$\begin{aligned}\delta_G^2(\infty) &= \sum_{\substack{\mu\nu \\ \mu\neq\nu}} \sum_{\alpha\beta\alpha'\beta'} w_\alpha w_\beta O_{\alpha'\alpha'} O_{\beta'\beta'} \Lambda(\mu,\alpha)\Lambda(\nu,\beta)\Lambda(\mu,\alpha')\Lambda(\nu,\beta') \\ &\qquad \times (\delta_{\alpha\beta}\delta_{\alpha'\beta'} + \delta_{\alpha\alpha'}\delta_{\beta\beta'} + \delta_{\alpha\beta'}\delta_{\alpha'\beta}) \\ &= \sum_{\substack{\mu\nu \\ \mu\neq\nu}} \sum_{\alpha\beta} \Lambda(\mu,\alpha)\Lambda(\nu,\alpha)\Lambda(\mu,\beta)\Lambda(\nu,\beta)[w_\alpha^2 O_{\beta\beta}^2 + 2w_\alpha w_\beta O_{\alpha\alpha} O_{\beta\beta}]\end{aligned} \tag{E.8}$$

Similarly, for the non-Gaussian ($\delta^2_{NG}(\infty)$), and mixed ($\delta^2_{M}(\infty)$) contractions we have

$$\delta^2_{NG}(\infty) = 3\sum_{\substack{\mu\nu\\ \mu\neq\nu}}\sum_{\alpha\beta\alpha'\beta'} w_\alpha w_\beta O_{\alpha'\alpha'} O_{\beta'\beta'} L^{\alpha\beta\alpha\beta}_{\mu\nu} L^{\alpha'\beta'\alpha'\beta'}_{\mu\nu}, \tag{E.9}$$

and

$$\delta^2_{M}(\infty) = -\sum_{\substack{\mu\nu\\ \mu\neq\nu}}\sum_{\alpha\alpha'\beta'} \Lambda(\mu,\alpha)\Lambda(\nu,\alpha) L^{\alpha'\beta'\alpha'\beta'}_{\mu\nu}\left[w^2_\alpha O_{\alpha'\alpha'}O_{\beta'\beta'} + 4w_\alpha O_{\alpha\alpha} w_{\alpha'} O_{\beta'\beta'} + O^2_{\alpha\alpha} w_{\alpha'} w_{\beta'}\right], \tag{E.10}$$

respectively. In order to perform the summations over non-interacting indices in Eq. (7.47) we define coarse grained averages of observable elements $O_{\alpha\alpha}$ as in Eq. (7.23). The key assumption in writing (7.23) is that the average,

$$\overline{[O_{\alpha\alpha}]}_\mu := \sum_\alpha \Lambda(\mu,\alpha) O_{\alpha\alpha}, \tag{E.11}$$

changes slowly in energy $E_{\overline{\mu}}$ with respect to the width Γ. Similar averages over the initial state, or mixed averages must also be defined, such as

$$\begin{aligned}\sum_\alpha \Lambda(\mu,\alpha)\Lambda(\nu,\alpha) w_\alpha &= \overline{[w_\alpha]}_{\overline{\mu}} \Lambda^{(2)}(\mu,\nu)\\ \sum_\alpha \Lambda(\mu,\alpha)\Lambda(\nu,\alpha) w_\alpha O_{\alpha\alpha} &= \overline{[w_\alpha O_{\alpha\alpha}]}_{\overline{\mu}} \Lambda^{(2)}(\mu,\nu).\end{aligned} \tag{E.12}$$

Note that, $\overline{[O_{\alpha\alpha}]}_{\overline{\mu}}$ can be interpreted as a microcanonical average of the observable O.

Now, using Eqs. (7.23) and (E.12), we obtain,

$$\begin{aligned}\delta^2_G(\infty) &= \sum_{\substack{\mu\nu\\ \mu\neq\nu}}\left[\overline{[w^2_\alpha]}_{\overline{\mu}}\overline{[O^2_{\alpha\alpha}]}_{\overline{\mu}} + 2\overline{[w_\alpha O_{\alpha\alpha}]}^2_{\overline{\mu}}\right]\Lambda^{(2)}(\mu,\nu)^2,\\ \delta^2_{NG}(\infty) &= 3\sum_{\substack{\mu\nu\\ \mu\neq\nu}}\overline{[w_\alpha]}^2_{\overline{\mu}}\overline{[O_{\alpha\alpha}]}^2_{\overline{\mu}}\Lambda^{(2)}(\mu,\nu)^2,\\ \delta^2_M(\infty) &= -\sum_{\substack{\mu\nu\\ \mu\neq\nu}}\Lambda^{(2)}(\mu,\nu)^2\left[\overline{[w^2_\alpha]}_{\overline{\mu}}\overline{[O_{\alpha\alpha}]}^2_{\overline{\mu}} + 4\overline{[w_\alpha]}_{\overline{\mu}}\overline{[O_{\alpha\alpha}]}_{\overline{\mu}}\overline{[w_\alpha O_{\alpha\alpha}]}_{\overline{\mu}} + \overline{[w_\alpha]}^2_{\overline{\mu}}\overline{[O^2_{\alpha\alpha}]}_{\overline{\mu}}\right].\end{aligned} \tag{E.13}$$

E.3 Bound of dynamical term

In this section we bound third term in Eq. (7.33), showing that it's contribution is negligible. To do so, we proceed by defining,

$$A(t) = \sum_{\substack{\mu\nu\\ \mu\neq\nu}}\sum_{\alpha\beta} w_{\alpha\beta} O_{\alpha\beta} \frac{\Lambda(\mu,\alpha)\Lambda(\mu,\beta)\Lambda(\nu,\alpha)\Lambda(\nu,\beta)}{\Lambda^{(2)}(\mu,\nu)} e^{-i(E_\mu - E_\nu)t}. \tag{E.14}$$

We may now use the relation $|\sum_i a_i| \leq \sum_i |a_i|$, to write

$$\begin{aligned}
|A(t)| &\leq \sum_{\substack{\mu\nu \\ \mu\neq\nu}} \left| \sum_{\alpha\beta} w_{\alpha\beta} O_{\alpha\beta} \frac{\Lambda(\mu,\alpha)\Lambda(\mu,\beta)\Lambda(\nu,\alpha)\Lambda(\nu,\beta)}{\Lambda^{(2)}(\mu,\nu)} \right| \left| e^{-i(E_\mu - E_\nu)t} \right| \\
&\leq \sum_{\substack{\mu\nu \\ \mu\neq\nu}} \sum_{\alpha\beta} \left| w_{\alpha\beta} O_{\alpha\beta} \frac{\Lambda(\mu,\alpha)\Lambda(\mu,\beta)\Lambda(\nu,\alpha)\Lambda(\nu,\beta)}{\Lambda^{(2)}(\mu,\nu)} \right| \\
&= \sum_{\alpha\beta} |w_{\alpha\beta} O_{\alpha\beta}| \sum_{\substack{\mu\nu \\ \mu\neq\nu}} \frac{\Lambda(\mu,\alpha)\Lambda(\mu,\beta)\Lambda(\nu,\alpha)\Lambda(\nu,\beta)}{\Lambda^{(2)}(\mu,\nu)} \\
&\leq \frac{3\omega_0}{4\pi\Gamma} \sum_{\alpha} |w_{\alpha\beta} O_{\alpha\beta}| \,,
\end{aligned} \tag{E.15}$$

where we have used that,

$$\sum_{\substack{\mu\nu \\ \mu\neq\nu}} \frac{\Lambda(\mu,\alpha)\Lambda(\mu,\beta)\Lambda(\nu,\alpha)\Lambda(\nu,\beta)}{\Lambda^{(2)}(\mu,\nu)} = \omega_0 \frac{(E_\alpha - E_\beta)^2\Gamma + 12\Gamma^3}{\pi((E_\alpha - E_\beta)^2 + 4\Gamma^2)^2} \leq \frac{3\omega_0}{4\pi\Gamma}. \tag{E.16}$$

Now, using $\sum_{\alpha\beta} O_{\alpha\beta} = \sum_\alpha \sum_n^{N_O} O_{\alpha,\alpha+n}\delta_{\beta,\alpha+n}$ [17], we have

$$\begin{aligned}
\sum_{\alpha\beta} |w_{\alpha\beta} O_{\alpha\beta}| &= \sum_{\alpha,n} |w_{\alpha,\alpha+n} O_{\alpha\alpha+n}| \\
&\leq \max_{\alpha\beta}(O_{\alpha\beta}) \sum_{\alpha,n} w_{\alpha,\alpha+n}.
\end{aligned} \tag{E.17}$$

Now, we see that in the case of $w_{\alpha\beta} \sim \delta_{\alpha\beta}$, the bound simply becomes

$$|A(t)| \leq \max_{\alpha}(O_{\alpha\alpha}) \frac{3\omega_0}{4\pi\Gamma}, \tag{E.18}$$

similarly, this is the case for our application studied in the main text, where $O_{\alpha\beta} \sim \delta_{\alpha\beta}$. We note that the condition of diagonal $w_{\alpha\beta}$ correspond to a reasonable initial state in many experimental situations, since thermalization takes place typically by incoherent exchange of energy in the basis of eigenstates of H_0. For states with coherences, to bound this quantity we require that the coherences are not large on the off-diagonals defined by $\alpha, \alpha+n$, in the sense that $\sum_\alpha w_{\alpha,\alpha+n} \lesssim \mathcal{O}(1)$, so

$$|A(t)| \lesssim N_O \max_{\alpha}(O_{\alpha\alpha}) \frac{3\omega_0}{4\pi\Gamma}. \tag{E.19}$$

In this sense, 'special' initial states may be chosen that do not satisfy this bound, but they are highly atypical. Further, we note that the stronger of the two assumptions made on the form of observables, that is that we may write $\sum_{\alpha\beta} O_{\alpha\beta} = \sum_\alpha \sum_n^{N_O} O_{\alpha,\alpha+n}\delta_{\beta,\alpha+n}$, is only used above in bounding $|A(t)|$, the other terms are more general. As noted above, whilst this form is reasonable for generic local variables [17], one may of course be able to build observables that do not match this form, in which case, one may either have an additional contribution due to $A(t)$, or be able to arrive at a similar bound.

E.4 FDT in terms of Thermal Averages

In this section, we show that the FDT may be recast in terms of the thermal averages $\langle\langle\cdots\rangle\rangle_\beta$, obtained from the a fit to the decay, shown in Sec 7.6. We begin by re-expressing our finite temperature FDT in terms of the thermal averages,

$$\langle\langle A(E)\rangle\rangle_\beta := \frac{1}{Z'_\beta}\int_0^{\Delta E} dE D(E) e^{-\beta(E-E_0)} A(E), \tag{E.20}$$

with $Z'_\beta := \int_0^{\Delta E} dE D(E) e^{-\beta(E-E_0)}$, where we have introduced the low-energy cut-off E_0, which is the energy of our zero temperature pure state. The addition of this cut-off ensures that, for non-zero E_0, the initial state is not the ground state of the bath at zero temperature.

To include this thermal average, we return to Eq. (7.70), and note that,

$$\int_0^{\Delta E} dE \frac{e^{-2\beta E}}{\Gamma(E)} = Z'_{2\beta}\langle\langle D(E)^{-1}\Gamma(E)^{-1}\rangle\rangle_{2\beta}. \tag{E.21}$$

We thus obtain,

$$\delta_O^2(\infty) = \frac{W_O Z'_{2\beta}}{8\pi Z_\beta^2}\langle\langle D(E)^{-1}\Gamma(E)^{-1}\rangle\rangle_{2\beta}. \tag{E.22}$$

We note that this can be put in the same form as the infinite temperature case, $\delta_O^2(\infty) \sim \overline{\Gamma^{-1}}$, by noting that the quantity

$$C'_\beta = \frac{\langle\langle D(E)^{-1}\Gamma(E)^{-1}\rangle\rangle_{2\beta}}{\langle\langle D(E)\rangle\rangle_{2\beta}^{-1}\langle\langle\Gamma(E)^{-1}\rangle\rangle_{2\beta}} \tag{E.23}$$

depends only on the particular forms of the functions $D(E)$ and $\Gamma(E)$, and the temperature - importantly, not on N, or on the system-bath coupling strengths (for weak couplings), as both the numerator and denominator share the same dependence in N and the system-bath coupling in the thermodynamic limit. As such, we can write

$$\delta_O^2(\infty) = C'_\beta \frac{W_O Z'_{2\beta}}{8\pi Z_\beta^2\langle\langle D(E)\rangle\rangle_{2\beta}}\langle\langle\Gamma(E)^{-1}\rangle\rangle_{2\beta}, \tag{E.24}$$

and thus we recover the form of our main result, Eq. (3) of the main text, with $\chi(N) = C'_\beta \frac{W_O Z_{2\beta}}{16\pi Z_\beta^2\langle\langle D(E)\rangle\rangle_\beta}$.

For the random matrix case, where $D(E)^{-1} = \omega_0$, and $\Gamma(E) = \Gamma$ is constant, we also have,

$$\delta_O^2(\infty) = \frac{W_O Z'_{2\beta}\omega_0}{8\pi Z_\beta^2\Gamma} \tag{E.25}$$

as in this case, the thermal average $\langle\langle\cdots\rangle\rangle_\beta$ and unbiased thermal average $\langle\cdots\rangle_\beta$, can be seen to be equal.

We can check that, as required, one obtains the infinite temperature limit derived

above by sending $\beta \to 0$ by noting that for the infinite temperature case, we have

$$\delta_O^2(\infty) = \frac{W_O}{2\mathcal{N}_B^2}\int_0^{\Delta E} dE \frac{1}{4\pi\Gamma(E)}, \tag{E.26}$$

which, in terms of the infinite temperature thermal average, may be written (noting that $\lim_{\beta\to 0} Z'_\beta = 2\mathcal{N}_B$),

$$\begin{aligned}\delta_O^2(\infty) &= \frac{W_O}{4\pi\mathcal{N}_B}\langle\langle D(E)^{-1}\Gamma(E)^{-1}\rangle\rangle_0 \\ &= C'_0\frac{W_O}{4\pi\mathcal{N}_B\langle\langle D(E)\rangle\rangle_0}\langle\langle\Gamma(E)^{-1}\rangle\rangle_0.\end{aligned} \tag{E.27}$$

We finally note here that it is the measurement of a thermal average of the decay rate, and not the unbiased average, that obscures the direct measurement of $\mathcal{N}_B$, such that in general a FDT of the form of Eq. (E.27) would be observed experimentally. We thus limit our claim in cases where the energy dependence of the decay rate is important (which, as can be seen from Eq. (7.40), is implied by a non-exponential decay to equilibrium, due to multiple contributing decay rates) to the experimental verification of the finite size scaling of the Hilbert space dimension, rather than the particular value of $\mathcal{N}_B$, without additional assumptions or the numerical calculation of C'_β.

E.4.1 Low Temperature FDT

We now turn to the low temperature limit of Eq. (7.67) for which we expect to obtain the same result as the pure state case of Ref. [17], given by,

$$\delta_O^2(\infty) = \frac{\overline{[\Delta O_{\alpha\alpha}^2]}}{4\pi D(E_{\alpha_0})\Gamma}, \tag{E.28}$$

where $D(E_{\alpha_0})$ is the DOS at the initial state energy E_{α_0}, which is chosen to be in the bulk of the spectrum, and $\overline{[\Delta O_{\alpha\alpha}^2]} := \overline{[O_{\alpha\alpha}^2]} - \overline{[O_{\alpha\alpha}]}^2$. We have that in this limit,

$$\langle\langle A(E)\rangle\rangle_\infty = A(E_0), \tag{E.29}$$

so

$$C'_\infty = \frac{D(E_0)^{-1}\Gamma(E_0)^{-1}}{D(E_0)^{-1}\Gamma(E_0)^{-1}} = 1, \tag{E.30}$$

and thus,

$$\delta_O^2(\infty) = \frac{W_O}{4\pi D(E_0)}\Gamma(E_0)^{-1}, \tag{E.31}$$

which is the zero temperature limit, Eq. (E.28) when $W_0 = \overline{[\Delta O_{\alpha\alpha}^2]}$. Which can be seen to be the case for zero temperature as follows. Recalling that W_0 is defined by

$$W_O = \frac{W_\mu}{\overline{[w_\alpha^2]}} \tag{E.32}$$

where,

$$W_\mu = \overline{[w_\alpha^2]}_\mu \overline{[O_{\alpha\alpha}^2]}_\mu + 2\overline{[w_\alpha O_{\alpha\alpha}]}_\mu^2 + 3\overline{[w_\alpha]}_\mu^2 \overline{[O_{\alpha\alpha}]}_\mu^2 - \overline{[w_\alpha^2]}_\mu \overline{[O_{\alpha\alpha}]}_\mu^2 - 4\overline{[w_\alpha]}_\mu \overline{[O_{\alpha\alpha}]}_\mu \overline{[w_\alpha O_{\alpha\alpha}]}_\mu - \overline{[w_\alpha]}_\mu^2 \overline{[O_{\alpha\alpha}^2]}_\mu. \tag{E.33}$$

We see that in the zero temperature limit $w_\alpha \sim \delta_{\alpha\alpha_0}$, and thus, the averages in Eq. (E.12) contribute to a lower order as the number of summations is reduced for terms with, e.g. $w_\alpha w_\beta$, over terms with, e.g. w_α^2. This can be seen to lead to $\overline{[w_\alpha]}_\mu^2 \ll \overline{[w_\alpha^2]}_\mu$. Similarly, both terms above with mixed averages $\overline{[w_\alpha O_{\alpha\alpha}]}_\mu$ contribute on the order $\overline{[w_\alpha]}_\mu^2$, as $\overline{[w_\alpha O_{\alpha\alpha}]}_\mu = \overline{[w_\alpha]}_\mu O_\uparrow$. Using only the remaining terms, we have that,

$$W_\mu = \overline{[w_\alpha^2]}_\mu \overline{[O_{\alpha\alpha}^2]}_\mu - \overline{[w_\alpha^2]}_\mu \overline{[O_{\alpha\alpha}]}_\mu^2 = \overline{[w_\alpha^2]}_\mu \overline{[\Delta O_{\alpha\alpha}^2]}, \tag{E.34}$$

so,

$$W_O = \overline{[\Delta O^2]}, \tag{E.35}$$

as required.

We recall that until Eq. (7.67), no assumptions on the initial state or observable are made other than the ability to define the required microcanonical averages. As such, taking the low temperature limit at this point, as we have done above, does not contradict any assumptions made.

Bibliography

[1] Martin J. Klein. Thermodynamics in Einstein's thought. *Science*, 157(3788): 509–516, 1967. 1

[2] Jos Uffink. Compendium of the Foundations of Classical Statistical Physics. In *Philosophy of Physics*, pages 923–1074. 2007. ISBN 9780444515605. doi: 10.1016/B978-044451560-5/50012-9. 1, 4, 5

[3] J Von Neumann. Proof of the ergodic theorem and the H-theorem in quantum mechanics. *The European Physical Journal H*, 237:41, 2010. 1, 45, 71

[4] Erwin Schrödinger. *Statistical thermodynamics*. Dover Publications, 1989. ISBN 0486661016. 1

[5] Richard P. Feynman. Simulating physics with computers. *International Journal of Theoretical Physics*, 21(6-7):467–488, 1982. 2, 8

[6] J Zhang, G Pagano, P W Hess, A Kyprianidis, P Becker, H Kaplan, A. V. Gorshkov, Z. X. Gong, and C Monroe. Observation of a many-body dynamical phase transition with a 53-qubit quantum simulator. *Nature*, 551(7682):601–604, 2017. 2

[7] Axel Friedenauer, Hector Schmitz, Jan Tibor Glueckert, Diego Porras, and Tobias Schätz. Simulating a quantum magnet with trapped ions. *Nature Physics*, 4(10): 757–761, 2008. 2, 8

[8] Henrik P Lüschen, Pranjal Bordia, Sean S Hodgman, Michael Schreiber, Saubhik Sarkar, Andrew J Daley, Mark H Fischer, Ehud Altman, Immanuel Bloch, and Ulrich Schneider. Signatures of many-body localization in a controlled open quantum system. *Physical Review X*, 7(1):011034, 2017. 2, 3, 9

[9] Toshiya Kinoshita, Trevor Wenger, and David S Weiss. A quantum Newton's cradle. *Nature*, 440(7086):900–903, 2006. 2

[10] Yijun Tang, Wil Kao, Kuan Yu Li, Sangwon Seo, Krishnanand Mallayya, Marcos Rigol, Sarang Gopalakrishnan, and Benjamin L Lev. Thermalization near Integrability in a Dipolar Quantum Newton's Cradle. *Physical Review X*, 8(2):021030, 2018. 2, 3, 9

[11] Dmitry A Abanin, Ehud Altman, Immanuel Bloch, and Maksym Serbyn. Colloquium: Many-body localization, thermalization, and entanglement. *Reviews of Modern Physics*, 91(2):021001, 2019. 3

[12] Govinda Clos, Diego Porras, Ulrich Warring, and Tobias Schaetz. Time-Resolved Observation of Thermalization in an Isolated Quantum System. *Physical Review Letters*, 117(17):170401, 2016. 3, 9, 47, 51, 68, 71, 91

[13] C Neill, P Roushan, M Fang, Y. Chen, M Kolodrubetz, Z Chen, A Megrant, R Barends, B Campbell, B Chiaro, A Dunsworth, E. Jeffrey, J Kelly, J Mutus, P. J.J. O'Malley, C Quintana, D Sank, A Vainsencher, J Wenner, T C White, A Polkovnikov, and J M Martinis. Ergodic dynamics and thermalization in an isolated quantum system. *Nature Physics*, 12(11):1037–1041, 2016. 3, 9, 47, 71, 91

[14] S Trotzky, Y. A. Chen, A Flesch, I. P. McCulloch, U Schollwöck, J Eisert, and I Bloch. Probing the relaxation towards equilibrium in an isolated strongly correlated one-dimensional Bose gas. *Nature Physics*, 8(4):325–330, 2012. 3

[15] Hyosub Kim, Yeje Park, Kyungtae Kim, H. S. Sim, and Jaewook Ahn. Detailed Balance of Thermalization dynamics in Rydberg atom quantum simulators. *Physical Review Letters*, 120(18):180502, 2018. 3, 9, 91, 92

[16] Charlie Nation and Diego Porras. Off-diagonal observable elements from random matrix theory: Distributions, fluctuations, and eigenstate thermalization. *New Journal of Physics*, 20(10):103003, sep 2018. 3, 18, 27, 72, 75, 80, 81, 83, 84, 94, 95, 96, 101, 102, 147, 151, 153, 156, 162, 167

[17] Charlie Nation and Diego Porras. Quantum chaotic fluctuation-dissipation theorem: Effective Brownian motion in closed quantum systems. *Physical Review E*, 99(5): 052139, 2019. 3, 96, 103, 104, 106, 114, 118, 128, 130, 153, 167, 168, 171, 173

[18] Charlie Nation and Diego Porras. Ergodicity probes: using time-fluctuations to measure the Hilbert space dimension. *Quantum*, 3:207, 2019. 3, 19, 25

[19] Charlie Nation and Diego Porras. Taking snapshots of a quantum thermalization process: emergent classicality in quantum jump trajectories. *arXiv:2003.08425*, 2020. 3

[20] Sheldon Goldstein. Individualist and Ensemblist Approaches to the Foundations of Statistical Mechanics. *Monist*, 102(4):439–457, 2019. 4, 6

[21] Sheldon Goldstein. Boltzmann's Approach to Statistical Mechanics. In *In: Bricmont J., Ghirardi G., Dürr D., Petruccione F., Galavotti M.C., Zanghi N. (eds) Chance in Physics. Lecture Notes in Physics, vol 574.*, pages 39–54. Springer, Berlin, Heidelberg, 2001. doi: 10.1007/3-540-44966-3_3. 4, 6

[22] Roman Frigg. A Field Guide to Recent Work on the Foundations of Statistical Mechanics. *arXiv:0804.0399*, 2008. 5, 6

[23] Sheldon Goldstein, Joel L Lebowitz, Roderich Tumulka, and Nino Zanghi. Gibbs and Boltzmann Entropy in Classical and Quantum Mechanics. *arXiv:1903.11870*, 2019. 4, 7

[24] L. E. Reichl. *A modern course in statistical physics*. University of Texas Press, 1980. 4

[25] César R. de Oliveira and Thiago Werlang. Ergodic hypothesis in classical statistical mechanics. *Revista Brasileira de Ensino de Fisica*, 29(2):189–201, 2007. 4

[26] C E Shannon. A Mathematical Theory of Communication. *Bell System Technical Journal*, 27(3):379–423, 1948. 5

[27] Roman Frigg and Charlotte Werndl. Can Somebody Please Say What Gibbsian Statistical Mechanics Says? *The British Journal for the Philosophy of Science*, 2018. 6

[28] E. T. Jaynes. Information theory and statistical mechanics. *Physical Review*, 106 (4):620–630, 1957. 6

[29] E. T. Jaynes. Information theory and statistical mechanics. II. *Physical Review*, 108 (2):171–190, 1957. 6

[30] William C. Schieve and Lawrence P. Horwitz. *Quantum Statistical Mechanics*. 2009. ISBN 0521841461. doi: 10.1017/CBO9780511626555. 6

[31] Yichen Huang, Fernando G. S. L. Brandao, and Yong-Liang Zhang. Finite-size scaling of out-of-time-ordered correlators at late times. *Physical Review Letters*, 123:010601, 2019. 6

[32] Kerson Huang. *Statistical Mechanics, 2nd Edition*. 1987. ISBN 0471815187. doi: citeulike-article-id:712998. 7

[33] D Leibfried, R Blatt, C. Monroe, and D. Wineland. Quantum dynamics of single trapped ions. *Reviews of Modern Physics*, 75(1):281–324, 2003. 8

[34] H Haffner, C Roos, and R Blatt. Quantum computing with trapped ions. *Physics Reports*, 469(4):155–203, dec 2008.

[35] R Blatt and C F Roos. Quantum simulations with trapped ions. *Nature Physics*, 8 (4):277–284, 2012. 91

[36] Winfried K Hensinger, Austin G Fowler, Simon J Devitt, Bjoern Lekitsch, Klaus Mølmer, Christof Wunderlich, and Sebastian Weidt. Blueprint for a microwave trapped ion quantum computer. *Science Advances*, 3(2):e1601540, 2017.

[37] Colin D Bruzewicz, John Chiaverini, Robert McConnell, and Jeremy M Sage. Trapped-ion quantum computing: Progress and challenges. *Applied Physics Reviews*, 6(2):021314, 2019. 8

[38] J Q You and Franco Nori. Superconducting circuits and quantum information, 2005. ISSN 00319228. 8

[39] Jay M Gambetta, Jerry M Chow, and Matthias Steffen. Building logical qubits in a superconducting quantum computing system. *npj Quantum Information*, 3(1), 2017.

[40] P Roushan, E Lucero, John M Martinis, B Chiaro, A Megrant, K Kechedzhi, A Dunsworth, J Wenner, P Klimov, B Burkett, K Arya, A Vainsencher, J Mutus, H Neven, A Fowler, Z Chen, Y. Chen, R Barends, S V Isakov, M Giustina, T Huang, J Kelly, M Neeley, T C White, S Boixo, D Sank, B Foxen, V Smelyanskiy, R Graff, E Jeffrey, C Quintana, and C Neill. A blueprint for demonstrating quantum supremacy with superconducting qubits. *Science*, 360(6385):195–199, 2018. 91

[41] Morten Kjaergaard, Mollie E Schwartz, Jochen Braumüller, Philip Krantz, Joel I-Jan Wang, Simon Gustavsson, and William D Oliver. Superconducting Qubits: Current State of Play. *arXiv:1905.13641*, 2019. 8

[42] Juan Ignacio Cirac and Peter Zoller. How to manipulate cold atoms, 2003. ISSN 00368075. URL http://science.sciencemag.org/. 9

[43] Thilo Stöferle, Henning Moritz, Christian Schori, Michael Köhl, and Tilman Esslinger. Transition from a strongly interacting 1D superfluid to a Mott insulator. *Physical Review Letters*, 92(13):130403–130404, 2004.

[44] Immanuel Bloch, Jean Dalibard, and Wilhelm Zwerger. Many-body physics with ultracold gases. *Reviews of Modern Physics*, 80(3):885–964, 2008.

[45] Michael Schreiber, Sean S. Hodgman, Pranjal Bordia, Henrik P. Lüschen, Mark H. Fischer, Ronen Vosk, Ehud Altman, Ulrich Schneider, and Immanuel Bloch. Observation of many-body localization of interacting fermions in a quasirandom optical lattice. *Science*, 349(6250):842–845, 2015. 9, 47, 71

[46] Christian Gross and Immanuel Bloch. Quantum simulations with ultracold atoms in optical lattices. *Science*, 357(6355):995–1001, 2017. 9

[47] Philipp Hauke, Helmut G Katzgraber, Wolfgang Lechner, Hidetoshi Nishimori, and William D Oliver. Perspectives of quantum annealing: Methods and implementations. *arXic:1903.06559*, 2019. 9

[48] David P. DiVincenzo. The physical implementation of quantum computation, 2000. ISSN 00158208. 9

[49] J. Ignacio Cirac and Peter Zoller. Goals and opportunities in quantum simulation, apr 2012. ISSN 17452473. URL http://www.nature.com/articles/nphys2275. 9, 47

[50] I M Georgescu, S Ashhab, and Franco Nori. Quantum simulation. *Reviews of Modern Physics*, 86(1):153, 2014. 9, 47

[51] John Preskill. Quantum Computing in the NISQ era and beyond. *Quantum*, 2:79, 2018. 9

[52] Michael A Nielsen and Isaac L Chuang. *Quantum Computation and Quantum Information*. Cambridge University Press. ISBN 978-1-107-00217-3. 9

[53] Ehud Altman, Kenneth R Brown, Giuseppe Carleo, Lincoln D Carr, Eugene Demler, Cheng Chin, Brian DeMarco, Sophia E Economou, Mark Eriksson, Kai-Mei C Fu, Markus Greiner, Kaden R. A. Hazzard, Randall G Hulet, Alicia J. Kollar, Benjamin L Lev, Mikhail D Lukin, Ruichao Ma, Xiao Mi, Shashank Misra, Christopher Monroe, Kater Murch, Zaira Nazario, Kang-Kuen Ni, Andrew C Potter, Pedram Roushan, Mark Saffman, Monika Schleier-Smith, Irfan Siddiqi, Raymond Simmonds, Meenakshi Singh, I B Spielman, Kristan Temme, David S Weiss, Jelena Vuckovic, Vladan Vuletic, Jun Ye, and Martin Zwierlein. Quantum Simulators: Architectures and Opportunities. *arXiv:1912.06938*, 2019. 9

[54] F Verstraete, V Murg, and J I Cirac. Matrix product states, projected entangled pair states, and variational renormalization group methods for quantum spin systems. *Advances in Physics*, 57(2):143–224, 2008. 9, 42

[55] Frank Arute, Kunal Arya, Ryan Babbush, Dave Bacon, Joseph C Bardin, Rami Barends, Rupak Biswas, Sergio Boixo, Fernando G.S.L. Brandao, David A Buell, Brian Burkett, Yu Chen, Zijun Chen, Ben Chiaro, Roberto Collins, William Courtney, Andrew Dunsworth, Edward Farhi, Brooks Foxen, Austin Fowler, Craig Gidney, Marissa Giustina, Rob Graff, Keith Guerin, Steve Habegger, Matthew P Harrigan, Michael J Hartmann, Alan Ho, Markus Hoffmann, Trent Huang, Travis S Humble, Sergei V Isakov, Evan Jeffrey, Zhang Jiang, Dvir Kafri, Kostyantyn Kechedzhi, Julian Kelly, Paul V Klimov, Sergey Knysh, Alexander Korotkov, Fedor Kostritsa, David Landhuis, Mike Lindmark, Erik Lucero, Dmitry Lyakh, Salvatore Mandrà, Jarrod R. McClean, Matthew McEwen, Anthony Megrant, Xiao Mi, Kristel Michielsen, Masoud Mohseni, Josh Mutus, Ofer Naaman, Matthew Neeley, Charles Neill, Murphy Yuezhen Niu, Eric Ostby, Andre Petukhov, John C Platt, Chris Quintana, Eleanor G Rieffel, Pedram Roushan, Nicholas C Rubin, Daniel Sank, Kevin J Satzinger, Vadim Smelyanskiy, Kevin J Sung, Matthew D Trevithick, Amit Vainsencher, Benjamin Villalonga, Theodore White, Z Jamie Yao, Ping Yeh, Adam Zalcman, Hartmut Neven, and John M Martinis. Quantum supremacy using a programmable superconducting processor. *Nature*, 574(7779):505–510, 2019. 9, 25

[56] M Aidelsburger, J. L. Ville, R Saint-Jalm, S. Nascimbène, J Dalibard, and J Beugnon. Relaxation Dynamics in the Merging of N Independent Condensates. *Physical Review Letters*, 119(19):190403, 2017. 9, 91

[57] Peter Reimann. Foundation of statistical mechanics under experimentally realistic conditions. *Physical Review Letters*, 101(19):190403, 2008. 10, 23, 45, 68, 72, 92

[58] Christian Gogolin and Jens Eisert. Equilibration, thermalisation, and the emergence of statistical mechanics in closed quantum systems. *Reports on Progress in Physics*, 79(5):056001, 2016. 10, 71

[59] Marcos Rigol and Mark Srednicki. Alternatives to eigenstate thermalization. *Physical Review Letters*, 108(11):110601, 2012. 12, 45, 92

[60] H. Wilming, M. Goihl, C. Krumnow, and J. Eisert. Towards local equilibration in closed interacting quantum many-body systems. *arXiv:1704.06291*, (1):1–16, 2017. 12

[61] Sheldon Goldstein, Joel L Lebowitz, Christian Mastrodonato, Roderich Tumulka, and Nino Zangh. On the Approach to Thermal Equilibrium of Macroscopic Quantum Systems. *arXiv:0911.1724*, pages 1–19, 2009. 13, 23

[62] Sheldon Goldstein, Joel L Lebowitz, Christian Mastrodonato, Roderich Tumulka, and Nino Zanghí. Normal typicality and von Neumann's quantum ergodic theorem. In *Proceedings of the Royal Society A: Mathematical, Physical and Engineering Sciences*, volume 466, pages 3203–3224, 2010. doi: 10.1098/rspa.2009.0635. 13, 23

[63] Mark Srednicki. Chaos and quantum thermalization. *Physical Review E*, 50(2): 888–901, 1994. 13, 15, 46, 49, 92

[64] J. M. Deutsch. Quantum statistical mechanics in a closed system. *Physical Review A*, 43(4):2046–2049, 1991. 13, 18, 19, 45, 46, 47, 49, 50, 51, 69, 72, 74, 75, 101, 131

[65] J. M. Deutsch. A closed quantum system giving ergodicity. *(unpublished)*, 1991. 13, 19, 49, 51, 53, 69, 75, 101, 102, 131, 137, 139, 140, 142, 144

[66] Luca D'Alessio, Yariv Kafri, Anatoli Polkovnikov, and Marcos Rigol. From Quantum Chaos and Eigenstate Thermalization to Statistical Mechanics and Thermodynamics. *Advances in Physics*, 65(3):239–362, 2016. 13, 16, 21, 45, 59, 60, 71, 84, 92, 94

[67] Marcos Rigol, Vanja Dunjko, and Maxim Olshanii. Thermalization and its mechanism for generic isolated quantum systems. *Nature*, 452(7189):854–858, 2008. 13, 21, 46, 71, 92

[68] M Berry. Regular and irregular semiclassical wavefunctions. *Journal of Physics A: Mathematical and General*, 10(12):2083–2091, 1977. 13, 14, 52

[69] Mark Srednicki. Thermal fluctuations in quantized chaotic systems. *Journal of Physics A: Mathematical and General*, 29(4):75–79, 1996. 13, 20, 66

[70] Mark Srednicki. The approach to thermal equilibrium in quantized chaotic systems. *Journal of Physics A: Mathematical and General*, 32(3299):1163–1175, 1999. 13, 20, 49, 51, 66, 72, 75, 79, 92, 151

[71] Joshua M Deutsch. Eigenstate thermalization hypothesis. *Reports on Progress in Physics*, 81(8):082001, aug 2018. 13, 26, 92

[72] F. Borgonovi, F. M. Izrailev, Lea F Santos, and V. G. Zelevinsky. Quantum chaos and thermalization in isolated systems of interacting particles, apr

2016. ISSN 03701573. URL https://linkinghub.elsevier.com/retrieve/pii/S0370157316000831. 14, 15, 16, 17, 18, 19, 30, 45, 60, 62, 71, 92

[73] Takashi Mori, Tatsuhiko N Ikeda, Eriko Kaminishi, and Masahito Ueda. Thermalization and prethermalization in isolated quantum systems: A theoretical overview. *Journal of Physics B: Atomic, Molecular and Optical Physics*, 51(11):112001, 2018. 14, 22, 23, 45, 71, 129

[74] Amy C. Cassidy, Charles W. Clark, and Marcos Rigol. Generalized thermalization in an integrable lattice system. *Physical Review Letters*, 106(14):140405, 2011. 14

[75] Marcos Rigol, Vanja Dunjko, Vladimir Yurovsky, and Maxim Olshanii. Relaxation in a completely integrable many-body Quantum system: An Ab initio study of the dynamics of the highly excited states of 1D lattice hard-core bosons. *Physical Review Letters*, 98(5):050405, 2007. 14

[76] Kai He and Marcos Rigol. Initial-state dependence of the quench dynamics in integrable quantum systems. III. Chaotic states. *Physical Review A*, 87(4):043615, 2013. 14

[77] Michael Berry. Quantum chaology, not quantum chaos. *Physica Scripta*, 40(3): 335–336, 1989. 14

[78] Philip Pechukas. Remarks on "Quantum Chaos". *J. Phys. Chem.*, 88(21):4823–4829, 1984. 14, 16, 46

[79] Martin C Gutzwiller. Periodic orbits and classical quantization conditions. *Journal of Mathematical Physics*, 12(3):343–358, 1971. 14

[80] Anatoli Polkovnikov. Phase space representation of quantum dynamics. *Annals of Physics*, 325(8):1790–1852, 2010. 14

[81] P. O'Connor, J Gehlen, and E J. Heller. Properties of random superpositions of plane waves. *Physical Review Letters*, 58(13):1296–1299, 1987. 14

[82] Martin C. Gutzwiller. *Chaos in Classical and Quantum Mechanics*, volume 1 of *Interdisciplinary Applied Mathematics*. Springer New York, New York, NY, 1990. ISBN 978-1-4612-6970-0. doi: 10.1007/978-1-4612-0983-6.

[83] V N Prigodin. Spatial structure of chaotic wave functions. *Physical Review Letters*, 74(9):1566–1569, 1995. 14

[84] C Jarzynski. Berry's conjecture and information theory. *Physical Review E*, 56(2): 2254–2256, 1997. 15

[85] R. Balian. Random Matrices and Information Theory. *Il Nuovo Cimento B Series 10*, 57(1):183–193, 1968. 15

[86] Eugene P Wigner. Characteristic Vectors of Bordered Matrices With Infinite Dimensions. *The Annals of Mathematics*, 62(3):548, 1955. 15

[87] Eugene P. Wigner. Random Matrices in Physics. *SIAM Review*, 9(1):1–23, 1967. 15, 19

[88] Lea F Santos, Anatoli Polkovnikov, and Marcos Rigol. Entropy of isolated quantum systems after a quench. *Physical Review Letters*, 107(4):040601, 2011. 15

[89] Eduardo Jonathan Torres-Herrera, Jonathan Karp, Marco Tavora, and Lea F Santos. Realistic many-body quantum systems vs. full random matrices: Static and dynamical properties. *Entropy*, 18(10):359, 2016. 19, 92

[90] Lea F Santos and Marcos Rigol. Onset of quantum chaos in one-dimensional bosonic and fermionic systems and its relation to thermalization. *Physical Review E*, 81(3): 036206, 2010. 16

[91] Y Y Atas and E Bogomolny. Quantum Ising model in transverse and longitudinal fields: Chaotic wave functions. *Journal of Physics A: Mathematical and Theoretical*, 50(38):385102, sep 2017. 17, 18, 28, 49, 61, 68, 84

[92] Jordan Cotler, Nicholas Hunter-Jones, Junyu Liu, and Beni Yoshida. Chaos, complexity, and random matrices. *Journal of High Energy Physics*, 2017(11):048, 2017.

[93] Ivan M Khaymovich, Masudul Haque, and Paul A. McClarty. Eigenstate Thermalization, Random Matrix Theory, and Behemoths. *Physical Review Letters*, 122(7): 070601, 2019. 15

[94] M. V. Berry and M. Tabor. Level Clustering in the Regular Spectrum. *Proceedings of the Royal Society A: Mathematical, Physical and Engineering Sciences*, 356(1686): 375–394, 1977. 16

[95] Lea F Santos and Marcos Rigol. Onset of quantum chaos in one-dimensional bosonic and fermionic systems and its relation to thermalization. *Physical Review E*, 81(3): 036206, 2010. 16, 21, 46, 72

[96] V V Flambaum and F M Izrailev. Statistical theory of finite Fermi systems based on the structure of chaotic eigenstates. *Physical Review E*, 56(5):5144–5159, 1997. 16, 17

[97] V V Flambaum and F M Izrailev. Excited eigenstates and strength functions for isolated systems of interacting particles. *Physical Review E*, 61(3):2539–2542, 2000. 49, 61, 68

[98] E J Torres-Herrera, Davida Kollmar, and Lea F Santos. Relaxation and thermalization of isolated many-body quantum systems. In *Physica Scripta*, volume 2015, page 14018, 2015. doi: 10.1088/0031-8949/2015/T165/014018. 17

[99] V V Flambaum and F M Izrailev. Distribution of occupation numbers in finite Fermi systemsand role of interaction in chaos and thermalization. *Physical Review E*, 55 (1):R13–R16, 1997. 17

[100] Peter Reimann. Eigenstate thermalization: Deutsch's approach and beyond. *New Journal of Physics*, 17(5):055025, 2015. 19, 46, 50, 72, 101

[101] E. J. Torres-Herrera, Antonio M. García-García, and Lea F Santos. Generic dynamical features of quenched interacting quantum systems: survival probability, density imbalance and out-of-time-ordered correlator. *Physical Review B*, 97:060303(R), 2018. 19

[102] Mauro Schiulaz, E Jonathan Torres-Herrera, Francisco Pérez-Bernal, and Lea F Santos. Self-averaging in many-body quantum systems out of equilibrium. *arXiv:1906.11856*, 2019. 19, 153

[103] V. V. Flambaum, F. M. Izrailev, and Giulio Casati. Towards a statistical theory of finite Fermi systems and compound states: Random two-body interaction approach. *Physical Review E*, 54(2):2136–2139, 1996. 19

[104] Fausto Borgonovi, Felix M Izrailev, and Lea F Santos. Exponentially fast dynamics in the Fock space of chaotic many-body systems. *Physical Review E*, 99(1): 010101(R), 2019. 19, 72, 92

[105] Daniel Nickelsen and Michael Kastner. Modelling equilibration of local many-body quantum systems by random graph ensembles. *arXiv:1912.02043*, 2019. 19

[106] Giuseppe De Tomasi, Mohsen Amini, Soumya Bera, Ivan Khaymovich, and Vladimir Kravtsov. Survival probability in Generalized Rosenzweig-Porter random matrix ensemble. *SciPost Physics*, 6(1), 2019. 19

[107] M. Pino, J. Tabanera, and P. Serna. From ergodic to non-ergodic chaos in Rosenzweig-Porter model. *Journal of Physics A: Mathematical and Theoretical*, 52:475101, apr 2019. 19

[108] Hyungwon Kim, Tatsuhiko N Ikeda, and David A Huse. Testing whether all eigenstates obey the eigenstate thermalization hypothesis. *Physical Review E*, 90(5): 052105, 2014. 21

[109] Rubem Mondaini, Keith R Fratus, Mark Srednicki, and Marcos Rigol. Eigenstate thermalization in the two-dimensional transverse field Ising model. *Physical Review E*, 93(3):032104, 2016. 21, 46, 72, 73

[110] Ehsan Khatami, Guido Pupillo, Mark Srednicki, and Marcos Rigol. Fluctuation-dissipation theorem in an isolated system of quantum dipolar bosons after a quench. *Physical Review Letters*, 111(5):050403, 2013. 21, 72

[111] N. P. Konstantinidis. Thermalization away from integrability and the role of operator off-diagonal elements. *Physical Review E*, 91(5):052111, 2015.

[112] Wouter Beugeling, Roderich Moessner, and Masudul Haque. Off-diagonal matrix elements of local operators in many-body quantum systems. *Physical Review E*, 91 (1):012144, 2015. 46, 66, 72, 73, 92

[113] Rubem Mondaini and Marcos Rigol. Eigenstate thermalization in the two-dimensional transverse field Ising model. II. Off-diagonal matrix elements of observables. *Physical Review E*, 96(1):012157, 2017. 49, 59, 61, 68, 84

[114] Enrico M Brehm, Diptarka Das, and Shouvik Datta. Probing thermality beyond the diagonal. *Physical Review D*, 98(12):126015, 2018. 21

[115] Lea F Santos, Fausto Borgonovi, and F M Izrailev. Onset of chaos and relaxation in isolated systems of interacting spins: Energy shell approach. *Physical Review E*, 85(3):036209, 2012. 21, 49, 61, 68, 84

[116] F Pietracaprina, C Gogolin, and J Goold. Total correlations of the diagonal ensemble as a generic indicator for ergodicity breaking in quantum systems. *Physical Review B*, 95(12):125118, 2017. 21

[117] J Gemmer and G Mahler. Distribution of local entropy in the Hilbert space of bipartite quantum systems: Origin of Jaynes' principle. *European Physical Journal B*, 31(2):249–257, 2003. 22

[118] Sandu Popescu, Anthony J Short, and Andreas Winter. Entanglement and the foundations of statistical mechanics. *Nature Physics*, 2(11):754–758, 2006. 22, 72

[119] Sheldon Goldstein, Joel L Lebowitz, Roderich Tumulka, and Nino Zanghì. Canonical typicality. *Physical Review Letters*, 96(5):050403, 2006. 22

[120] Sebastian Deffner and Wojciech H Zurek. Foundations of statistical mechanics from symmetries of entanglement. *New Journal of Physics*, 18(6):63013, 2016. 22

[121] Ralf R Müller. Random matrices, free probability and the replica method. In *European Signal Processing Conference*, volume 06-10-Sept, pages 189–196, 2015. ISBN 9783200001657. URL https://core.ac.uk/download/pdf/30466091.pdf. 22, 60, 153

[122] Christian Bartsch and Jochen Gemmer. Dynamical typicality of quantum expectation values. *Physical Review Letters*, 102(11):110403, 2009. 22, 72

[123] Sho Sugiura and Akira Shimizu. Thermal pure quantum states at finite temperature. *Physical Review Letters*, 108(24):240401, 2012. 22

[124] Sho Sugiura and Akira Shimizu. Canonical thermal pure quantum state. *Physical Review Letters*, 111(1):010401, 2013.

[125] Tjark Heitmann, Jonas Richter, Dennis Schubert, and Robin Steinigeweg. Selected applications of typicality to real-time dynamics of quantum many-body systems. *arXiv:2001.05289*, 2020. 22, 23

[126] Peter Reimann. Generalization of von neumann's approach to thermalization. *Phys. Rev. Lett.*, 115:010403, Jul 2015. 23

[127] Noah Linden, Sandu Popescu, Anthony J Short, and Andreas Winter. Quantum mechanical evolution towards thermal equilibrium. *Physical Review E*, 79(6):061103, 2009. 24, 45, 72

[128] Anthony J Short. Equilibration of quantum systems and subsystems. *New Journal of Physics*, 13(5):053009, may 2011. 24, 68

[129] Anthony J Short and Terence C Farrelly. Quantum equilibration in finite time. *New Journal of Physics*, 14(1):013063, jan 2012. 24, 45, 68

[130] Peter Reimann and Michael Kastner. Equilibration of isolated macroscopic quantum systems. *New Journal of Physics*, 14:043020, 2012. 24

[131] Sheldon Goldstein, Takashi Hara, and Hal Tasaki. Time scales in the approach to equilibrium of macroscopic quantum systems. *Physical Review Letters*, 111(14): 140401, 2013. 24

[132] Artur S L Malabarba, Luis Pedro Garcia-Pintos, Noah Linden, Terence C. Farrelly, and Anthony J Short. Quantum systems equilibrate rapidly for most observables. *Physical Review E*, 90(1):012121, 2014. 24, 30, 92

[133] Peter Reimann. Typical fast thermalization processes in closed many-body systems. *Nature Communications*, 7:10821, 2016. 24, 30, 72, 92

[134] Luis Pedro García-Pintos, Noah Linden, Artur S.L. Malabarba, Anthony J Short, and Andreas Winter. Equilibration time scales of physically relevant observables. *Physical Review X*, 7(3):031027, 2017. 25, 72, 92

[135] Joseph Tindall, Carlos Sanchez Munoz, Berislav Buca, and Dieter Jaksch. Quantum Synchronisation Enabled by Dynamical Symmetries and Dissipation. *arXiv:1907.12837*, 2019. 25

[136] Berislav Buča, Joseph Tindall, and Dieter Jaksch. Non-stationary coherent quantum many-body dynamics through dissipation. *Nature Communications*, 10(1):1730, 2019. 25

[137] Carlos Sánchez Muñoz, Berislav Buča, Joseph Tindall, Alejandro González-Tudela, Dieter Jaksch, and Diego Porras. Non-stationary dynamics and dissipative freezing in squeezed superradiance. *arXiv:1903.05080*, 2019. 25

[138] Amos Chan, Andrea De Luca, and J T Chalker. Solution of a Minimal Model for Many-Body Quantum Chaos. *Physical Review X*, 8(4):041019, 2018. 25

[139] Bruno Bertini, Pavel Kos, and Tomaž Prosen. Entanglement Spreading in a Minimal Model of Maximal Many-Body Quantum Chaos. *Physical Review X*, 9(2):021033, 2019.

[140] Lei Zhang, Justin A Reyes, Stefanos Kourtis, Claudio Chamon, Eduardo R Mucciolo, and Andrei E Ruckenstein. Nonuniversal Entanglement Level Statistics in Projection-driven Quantum Circuits. *arXiv:2001.11428*, 2020. 25

[141] C Neill, P Roushan, K Kechedzhi, S Boixo, S V Isakov, V Smelyanskiy, A Megrant, B Chiaro, A Dunsworth, K Arya, R Barends, B Burkett, Y. Chen, Z Chen, A Fowler, B Foxen, M Giustina, R Graff, E Jeffrey, T Huang, J Kelly, P Klimov, E Lucero, J Mutus, M Neeley, C Quintana, D Sank, A Vainsencher, J Wenner, T C White, H Neven, and J M Martinis. A blueprint for demonstrating quantum supremacy with superconducting qubits. *Science*, 360(6385):195–199, apr 2018. 25, 71

[142] Huitao Shen, Pengfei Zhang, Yi-Zhuang You, and Hui Zhai. Information Scrambling in Quantum Neural Networks. 2019. 26

[143] P W Anderson. More Is Different. *Science*, 177(4047):393–396, 1972. 26

[144] Joris Deguet, Yves Demazeau, and Laurent Magnin. Elements about the emergence issue: A survey of emergence definitions. In *Complexus*, volume 3, pages 24–31, 2006. doi: 10.1159/000094185. URL www.karger.com/cpu.

[145] James Ladyman, James Lambert, and Karoline Wiesner. What is a complex system?, 2013. ISSN 18794912. URL https://link.springer.com/content/pdf/10.1007{%}2Fs13194-012-0056-8.pdf.

[146] Erik P Hoel. When the map is better than the territory. *Entropy*, 19(5), 2017. 26

[147] F Anzà and V Vedral. Information-theoretic equilibrium and observable thermalization. *Scientific Reports*, 7:44066, 2017. 31

[148] Udo Seifert. Stochastic thermodynamics, fluctuation theorems and molecular machines. *Reports on Progress in Physics*, 75(12):126001, 2012. 43, 115, 124, 130

[149] Juan MR Parrondo, Jordan M. Horowitz, and Takahiro Sagawa. Thermodynamics of information. *Nature Physics*, 11(2):131–139, 2015. 43, 115, 124

[150] G. E. Uhlenbeck and L. S. Ornstein. On the theory of Brownian motion. *Physical Review*, 36:823–841, 1930. 44, 117, 119

[151] Peter Reimann. Canonical thermalization. *New Journal of Physics*, 12:055027, 2010. 45, 49

[152] Tatsuhiko N Ikeda, Yu Watanabe, and Masahito Ueda. Eigenstate Randomization Hypothesis: Why Does the Long-Time Average Equal the Microcanonical Average? *Physical Review E*, 84(2):021130, 2011.

[153] David J Luitz and Yevgeny Bar Lev. Anomalous Thermalization in Ergodic Systems. *Physical Review Letters*, 117(17):170404, 2016.

[154] Naoto Shiraishi and Takashi Mori. Systematic Construction of Counterexamples to the Eigenstate Thermalization Hypothesis. *Physical Review Letters*, 119(3):030601, 2017. 45

[155] Philip Pechukas. Distribution of energy eigenvalues in the irregular spectrum. *Physical Review Letters*, 51(11):943–946, sep 1983. 46

[156] Lea F Santos and Marcos Rigol. Localization and the effects of symmetries in the thermalization properties of one-dimensional quantum systems. *Physical Review E*, 82(3):031130, 2010. 46, 72

[157] R Steinigeweg, A Khodja, H Niemeyer, Christian Gogolin, and J Gemmer. Pushing the limits of the eigenstate thermalization hypothesis towards mesoscopic quantum systems. *Physical Review Letters*, 112(13):130403, 2014.

[158] Wouter Beugeling, R Moessner, and Masudul Haque. Finite-size scaling of eigenstate thermalization. *Physical Review E*, 89(4):042112, 2014. 92

[159] Nicholas Hunter-Jones, Junyu Liu, and Yehao Zhou. On thermalization in the SYK and supersymmetric SYK models. *Journal of High Energy Physics*, 142(2), 2018. 46, 72

[160] Ch Schneider, Diego Porras, and Tobias Schaetz. Experimental quantum simulations of many-body physics with trapped ions. *Reports on Progress in Physics*, 75(2): 24401–33, 2012. 47, 91

[161] M Gring, M Kuhnert, T Langen, T Kitagawa, B Rauer, M Schreitl, I Mazets, D. Adu Smith, E Demler, and J Schmiedmayer. Relaxation and prethermalization in an isolated quantum system. *Science*, 337(6100):1318–1322, 2012. 47

[162] Adam M. Kaufman, M. Eric Tai, Alexander Lukin, Matthew Rispoli, Robert Schittko, Philipp M. Preiss, and Markus Greiner. Quantum thermalization through entanglement in an isolated many-body system. *Science*, 353(6301):794–800, 2016. 47, 71

[163] J Smith, A Lee, P Richerme, B Neyenhuis, P W Hess, P Hauke, M Heyl, D A Huse, and C Monroe. Many-body localization in a quantum simulator with programmable random disorder. *Nature Physics*, 12(10):907–911, 2016. 47

[164] Njema Frazier, B. Alex Brown, and Vladimir Zelevinsky. Strength functions and spreading widths of simple shell model configurations. *Physical Review C - Nuclear Physics*, 54(4):1665–1674, oct 1996. 49, 61, 68

[165] D. J. Thouless. Electrons in disordered systems and the theory of localization. *Physics Reports*, 13(3):93–142, 1974. 51

[166] Anatoly Dymarsky and Hong Liu. Canonical Universality. 2017. 59

[167] T. A. Brody, J. Flores, J. B. French, P. A. Mello, A. Pandey, and S. S.M. Wong. Random-matrix physics: Spectrum and strength fluctuations. *Reviews of Modern Physics*, 53(3):385–479, jul 1981. 60

[168] H. S. Camarda and P. D. Georgopulos. Statistical behavior of atomic energy levels: Agreement with random-matrix theory. *Physical Review Letters*, 50(7):492–495, feb 1983. 60

[169] Clemens Neuenhahn and Florian Marquardt. Thermalization of interacting fermions and delocalization in Fock space. *Physical Review E*, 85(6):060101, jun 2012. 68

[170] E J Torres-Herrera and Lea F Santos. Dynamics at the many-body localization transition. *Physical Review B*, 92(1):033022, 2015. 68

[171] Toru Yoshizawa, Eiki Iyoda, and Takahiro Sagawa. Numerical Large Deviation Analysis of the Eigenstate Thermalization Hypothesis. *Physical Review Letters*, 120 (20):200604, may 2018. 72

[172] Jonas Richter, Jochen Gemmer, and Robin Steinigeweg. Impact of Eigenstate Thermalization on the Route to Equilibrium. *Physical Review E*, 99(5):050104, 2018. 72, 92

[173] R Kubo. The fluctuation-dissipation theorem. *Reports on Progress in Physics*, 29 (1):255, 1966. 72, 92, 115, 117

[174] H Breuer and F Petruccione. *Theory of open quantum systems*. 2002. ISBN 0198520638. doi: 10.1093/acprof. 72

[175] Thomas Guhr, Axel Müller-Groeling, and Hans A. Weidenmüller. Random-matrix theories in quantum physics: Common concepts. *Physics Report*, 299(4-6):189–425, jun 1998. 75

[176] Fausto Borgonovi, Francesco Mattiotti, and Felix M Izrailev. Temperature of a single chaotic eigenstate. *Physical Review E*, 95(4):42135, 2017. 85, 120

[177] Fabio Anza, Christian Gogolin, and Marcus Huber. Eigenstate Thermalization for Degenerate Observables. *Physical Review Letters*, 120(15):150603, 2018. 85, 92, 167

[178] Zeeya Merali. Bending the rules Thermodynamics might operate differently in the quantu realm. Experiments are starting to put that idea to the test. *Nature*, 551: 20–22, 2017. 90, 92

[179] Immanuel Bloch, Jean Dalibard, and Sylvain Nascimbène. Quantum simulations with ultracold quantum gases. *Nature Physics*, 8(4):267–276, 2012. 91

[180] Maciej Lewenstein, Anna Sanpera, and Ver‘ onica Ahufinge. *Ultracold Atoms in Optical Lattices Simulating quantum many-body systems*, volume 1. 2015. ISBN 9788578110796. doi: 10.1017/CBO9781107415324.004. 91

[181] D Porras and J Cirac. Effective Quantum Spin Systems with Trapped Ions. *Physical Review Letters*, 92(20):207901, 2004. 91

[182] Hannes Bernien, Sylvain Schwartz, Alexander Keesling, Harry Levine, Ahmed Omran, Hannes Pichler, Soonwon Choi, Alexander S Zibrov, Manuel Endres, Markus Greiner, Vladan Vuletic, and Mikhail D Lukin. Probing many-body dynamics on a 51-atom quantum simulator. *Nature*, 551(7682):579–584, 2017. 91

[183] Thiago R. De Oliveira, Christos Charalambous, Daniel Jonathan, Maciej Lewenstein, and Arnau Riera. Equilibration time scales in closed many-body quantum systems. *New Journal of Physics*, 20(3):33032, 2018. 92

[184] Mauro Schiulaz, E Jonathan Torres-Herrera, and Lea F Santos. Thouless and Relaxation Time Scales in Many-Body Quantum Systems. *Physical Review B*, 99(17): 174313, 2019.

[185] Álvaro M. Alhambra, Jonathon Riddell, and Luis Pedro García-Pintos. Time evolution of correlation functions in quantum many-body systems. *arXiv:1906.11280*, 2019. 92

[186] V. I. Yukalov. Equilibration and thermalization in finite quantum systems. *Laser Physics Letters*, 8(7):485–507, 2011. 92

[187] J Eisert, M Friesdorf, and C Gogolin. Quantum many-body systems out of equilibrium. *Nature Physics*, 11(2):124–130, 2014. 92

[188] Marcos Rigol. Quantum quenches and thermalization in one-dimensional fermionic systems. *Physical Review A*, 80(5):053607, 2009. 92

[189] Lennart Dabelow and Peter Reimann. Perturbed relaxation of quantum many-body systems. *arXiv:1903.11881*, 2019. 92, 96, 153

[190] Peter Reimann and Lennart Dabelow. Typicality of Prethermalization. *Physical Review Letters*, 122(8):080603, 2019.

[191] Ryusuke Hamazaki. *Theoretical study on thermalization in isolated quantum systems.* PhD thesis, jan 2019. 92

[192] Phillip Weinberg and Marin Bukov. QuSpin: a Python Package for Dynamics and Exact Diagonalisation of Quantum Many Body Systems part I: spin chains. *SciPost Phys*, 2:003, 2016. 97

[193] Phillip Weinberg and Marin Bukov. QuSpin: a Python Package for Dynamics and Exact Diagonalisation of Quantum Many Body Systems. Part II: bosons, fermions and higher spins. *SciPost Phys*, 7:020, 2019. 97

[194] Albert Einstein. On the Movement of Small Particles Suspended in Stationary Liquids Required by the Molecular-Kinetic Theory of Heat. *Ann. Phys.*, 17:549–560, 1905. 115, 117

[195] Ryogo Kubo. Brownian motion and nonequilibrium statistical mechanics. *Science*, 233(4761):330–334, 1986. 115

[196] Juan P. Garrahan and Igor Lesanovsky. Thermodynamics of quantum jump trajectories. *Physical Review Letters*, 104(16):160601, 2010. 116

[197] Udo Seifert. Entropy production along a stochastic trajectory and an integral fluctuation theorem. *Physical Review Letters*, 95(4):040602, 2005. 116, 124, 130

[198] Haye Hinrichsen, Christian Gogolin, and Peter Janotta. Non-equilibrium dynamics, thermalization and entropy production. In *Journal of Physics: Conference Series*, volume 297, page 012011, 2011. doi: 10.1088/1742-6596/297/1/012011.

[199] Robert Ziener, Amos Maritan, and Haye Hinrichsen. On entropy production in nonequilibrium systems. *Journal of Statistical Mechanics: Theory and Experiment*, 2015(8):8014, 2015.

[200] Gili Bisker, Matteo Polettini, Todd R. Gingrich, and Jordan M. Horowitz. Hierarchical bounds on entropy production inferred from partial information. *Journal of Statistical Mechanics: Theory and Experiment*, (9):93210, 2017.

[201] Gonzalo Manzano, Rosario Fazio, and Édgar Roldán. Quantum Martingale Theory and Entropy Production. *Physical Review Letters*, 122(22):220602, 2019. 116

[202] J L Doob. The Brownian Movement and Stochastic Equations. *The Annals of Mathematics*, 43(2):351, 1942. 117

[203] Abolfazl Bayat, Bedoor Alkurtass, Pasquale Sodano, Henrik Johannesson, and Sougato Bose. Measurement Quench in Many-Body Systems. *Physical Review Letters*, 121(3):030601, 2018. 122

[204] Wayne Itano, D. J Heinzen, J. J. Bollinger, and D. J. Wineland. Quantum Zeno Effect. *Physical Review A*, 41(5):2295, 1990. 122

[205] A. V. Chubukov. Spontaneous dimerization in quantum-spin chains. *Physical Review B*, 43:3337–3344, Feb 1991. 128

[206] J J García-Ripoll, M A Martin-Delgado, and J I Cirac. Implementation of spin Hamiltonians in optical lattices. *Physical Review Letters*, 93(25):250405, 2004.

[207] Andreas Läuchli, Guido Schmid, and Simon Trebst. Spin nematics correlations in bilinear-biquadratic S=1 spin chains. *Physical Review B - Condensed Matter and Materials Physics*, 74(14):144426, 2006. 128

[208] Charlie Nation and Diego Porras. Non-ergodic quantum thermalization. *arXiv:1908.11773*, 2019. 153

[209] Amnon Aharony and A Brooks Harris. Absence of self-averaging and universal fluctuations in random systems near critical points. *Physical Review Letters*, 77(18): 3700–3703, 1996. 153

[210] Giorgio Parisi and Nicolas Sourlas. Scale Invariance in Disordered Systems: The Example of the Random-Field Ising Model. *Physical Review Letters*, 89(25):257204, 2002. 153